Robust Nonlinear Model Predictive Control based on Constrained Saddle Point Optimization : Stability Analysis and Application to Type 1 Diabetes

Maxime Penet

N° d'ordre : 2013-19-TH

THESE DE DOCTORAT

DOMAINE : S.T.I.C.

SPECIALITE : AUTOMATIQUE

Ecole doctorale "Mathématiques, Télécommunications, Informatique, Signal, Systèmes Electronique"

Présentée par:

Maxime PENET

Commande Prédictive Nonlinéaire Robuste par Méthode de Point Selle en Optimisation sous Contraintes : Analyse de Stabilité et Application au Diabète de Type 1

Date de soutenance : 10 Octobre 2013

Jury :

M. Mazen ALAMIR	Université de Grenoble, GIPSA-lab	Rapporteur
M. Aziz BELMILOUDI	INSA de Rennes, IRMAR	Directeur de thèse
M. Jamal DAAFOUZ	Université de Lorraine, CRAN	Rapporteur
M. Hervé GUEGUEN	Supélec, IETR	Directeur de thèse
M. Jean-Jacques LOISEAU	Ecole Centrale de Nantes, IRCCyN	Examinateur
Mme. Isabelle GUILHEM	C.H.U. de Rennes	Invitée

Remerciements

Achever cette thèse, c'est comme finir d'écrire un chapitre de ma vie. Que de par ces quelques lignes il me soit permis de remercier les personnes qui ont contribué à l'aboutissement de ces travaux.

Mes premiers remerciements iront tout naturellement à mes directeurs de thèse, Hervé Gueguen et Aziz Belmiloudi, qui, de par leur présence et leurs conseils, ont permis à ces travaux de voir le jour tels qu'ils sont aujourd'hui.

Aussi il me semble important de remercier ceux qui auront eu la lourde tâche de juger mes travaux. Ainsi, merci à mes rapporteurs, Mazen Alamir et Djamal Daafouz, et merci à mon examinateur Jean-Jacques Loiseau, pour leur relecture attentive et leurs remarques avisées.

Merci tout spécialement à Marie-Anne Lefebvre et aux médecins du C.H.U. de Rennes, Jean-Yves Poirier et Isabelle Guilhem, avec qui j'ai eu beaucoup de plaisir à travailler et grâce à qui j'ai eu l'occasion de passer de sympathiques nuits blanches.

Outre toutes ces personnes, j'aimerai remercier les membres de l'IST à Stuttgart et plus particulièrement le professeur Frank Allgöwer, Marcus Reble, Christian Breindl et Beate Spinner, pour m'avoir accueilli dans leurs locaux pour une période de cinq mois afin d'envisager l'extension formelle de notre approche de commande aux systèmes retardés.

Un merci tout spécial à mes *compagnons de souffrances*. Bien sûr j'entend par là tous mes collégues doctorants avec qui j'ai pu partager des moments qui seront autant de souvenirs. Je leur souhaite à tous le meilleur pour la suite.

Merci aussi à tous les membres du laboratoire ASH pour le temps que nous avons pu passer ensemble, tout particulièrement au moment de la pause café.

Et bien entendu, je tiens à vous remercier, vous, lecteur. J'espère que vous saurez trouver votre intérêt dans les quelques lignes qui suivent.

Tout naturellement, j'aimerai aussi remercier l'inventeur des pâtes (en particulier des spaghettis !), du fromage rapé et du café car ils ont aussi, sans le savoir, contribuer à l'avancement de mes travaux.

Très formellement, j'aimerai remercier tous ceux qui ont contribué de prés ou de loin au succès de cette thèse.

Enfin, j'aimerai remercier ma famille qui a contribué à faire de moi ce que je suis aujourd'hui et qui de par son soutien m'a permis de voir la lumière dans les endroits les plus sombres. A ce titre, je tiens à remercier tout particulièrement mon père pour m'avoir aidé à sa facon dans les moments les plus délicats.

Abstract

This thesis deals with the design of a robust and safe control algorithm to aim at an *artificial pancreas*. More precisely we will be interested in controlling the stabilizing part of a classical cure. To meet this objective, the design of a robust nonlinear model predictive controller based on the solution of a saddle point optimization problem is considered. Also, to test the controller performances in a realistic case, numerical simulations on a FDA validated testing platform are envisaged.

In a first part, we present an extension of the usual nonlinear model predictive controller designed to robustly control, in a sampled-data framework, systems described by nonlinear ordinary differential equations. This controller, which computes the best control input by considering the solution of a constrained saddle point optimization problem, is called *saddle point model predictive controller* (SPMPC). Using this controller, it is proved that the closed-loop is Ultimately Bounded and, with some assumptions on the problem structure, Input-to-State practically Stable. Then, we are interested in numerically solving the corresponding control problem. To do so, we propose an algorithm inspired from the augmented Lagrangian technique and which makes use of adjoint model.

In a second part, we consider the application of this controller to the problem of artificial blood glucose control. After a modeling phase, two models are retained. A simple one will be used to design the controller and a complex one will be used to simulate realistic virtual patients. This latter is needed to validate our control approach. In order to compute a good control input, the SPMPC controller needs the full state value. However, the sensors can only provide the value of blood glucose. That is why the design of an adequate observer is envisaged. Then, numerical simulations are performed. The results show the interest of the approach. For all virtual patients, no hypoglycemia event occurs and the time spent in hyperglycemia is too short to induce damageable consequences. Finally, the interest of extending the SPMPC approach to consider the control of time delay systems in a sampled-data framework is numerically explored.

Résumé

Cette thèse s'intéresse au développement d'un contrôleur sûre et robuste en tant que partie intégrante d'un pancréas artificiel. Plus précisément, nous sommes intéressés à contrôler la partie du traitement usuel qui a pour but d'équilibrer la glycémie du patient. C'est ainsi que le développement d'une commande prédictive nonlinéaire robuste basée sur la résolution d'un problème de point selle a été envisagé. Afin de valider les performances du contrôleur dans une situation réaliste, des simulations numériques en utilisant une plate-forme de tests validée par la FDA sont envisagées.

Dans une première partie, nous présentons une extension de la classique commande prédictive nonlinéaire dont le but est d'assurer le contrôle robuste de systèmes décrits par des équations différentielles ordinaires non linéaires dans un cadre échantillonné. Ce contrôleur, qui calcule une action de contrôle adéquate en considérant la solution d'un problème de point selle, est appelé *saddle point model predictive controller* (SPMPC). En utilisant cette commande, il est prouvé que le système converge en temps fini dans un espace borné et, en supposant une certaine structure dans le problème, qu'il est pratiquement stable entrée-état. Ensuite, nous nous sommes intéressés à la résolution numérique. Pour ce faire, nous proposons une méthode de résolution inspirée de la méthode du Langrangien augmenté et qui fait usage de modèles adjoints.

Dans un deuxième temps, nous considérons l'application de ce contrôleur au problème du contrôle artificiel de la glycémie. Après une phase de modélisation, nous avons retenu deux modèles : un modèle simple qui est utilisé pour développer la commande et un modèle complexe qui est utilisé comme un simulateur réaliste de patients. Ce dernier est nécessaire pour valider notre approche de contrôle. Afin de calculer une entrée de commande adéquate, la commande SPMPC a besoin de l'état complet du système. Or, les capteurs ne peuvent fournir qu'une valeur du glucose sanguin. C'est pourquoi le développement d'un observateur est envisagé. Ensuite, des simulations sont réalisées. Les résultats obtenus témoignent de l'intérêt de l'approche retenue. En effet, pour tous les patients, aucune hypoglycémie n'a été observée et le temps passé en état hyperglycémique est suffisamment faible pour ne pas être dommageable. Enfin, l'intérêt d'étendre l'approche de commande SPMPC au problème de contrôle de systèmes décrits par des équations différentielles retardées non linéaires dans un cadre échantillonné est formellement investigué.

Contents

Chapter 1

Stabilité et Application au Diabète de Type 1 d'une Commande SPMPC

Contents

1.1 Contexte

Le diabète de type 1 (T1DM) est une maladie auto-immune qui est à l'origine de la destruction de certaines cellules du pancréas. Ces cellules sont normalement chargées de produire de l'insuline. Il s'agit d'une hormone dont le rôle est de favoriser le stockage du sucre sanguin dans le foie, les muscles, ... afin de permettre une régulation de la glycémie sanguine autour d'une valeur de 100mg.dL^{-1}. Un patient atteint de T1DM ne peut donc plus réguler, sans traitement approprié, sa glycémie. Ceci peut entrainer de nombreuses complications en raison des risques importants d'hypo- et d'hyperglycémies, c'est-à-dire en cas de glycèmie trop basse (*i.e.* inférieure à 60mg.dL^{-1}) ou trop haute (*i.e.* supérieure à 180mg.dL^{-1}).

A ce jour, le seul traitement efficace pour gérer cette maladie consiste à régulièrement s'injecter de l'insuline. La dose à se prescrire est définie en fonction d'une mesure de la glycémie courante et, lors d'une prise de repas, en fonction d'une estimation de la quantité de sucre qui va être ingérée. Bien sûr, pour viser les meilleures performances de régulation, il faut aussi anticiper, autant que possible, sur les événements à venir (par exemple sur la pratique prévue d'un sport, etc). Ce traitement a l'avantage d'apporter un remède relativement simple à cette maladie. Si le patient diabétique se connait bien, il peut espérer vivre une vie quasi-normale. Toutefois il est difficile de maitriser le traitement dans toutes les circonstances d'autant plus s'il est mal géré ou mal accepté par le patient. Il est en particulier difficile d'estimer la quantité de sucre contenue dans un aliment ou encore de quantifier l'effet de certains phénomènes, comme par exemple une situation de stress. D'autre part, les capteurs les plus courants ne mesurent que la glycémie interstitielle ce qui induit un biais dans la mesure (voir par exemple [87]). Enfin, le fait que l'insuline est généralement injectée par voie sous-cutanée, induit un délai dans l'action de cette dernière, compliquant d'autant la gestion du traitement. Une sur-estimation ou une sous-estimation de la dose à s'injecter peut entrainer une hypo- ou une hyperglycémie avec tous les risques qui peuvent y être associés. C'est pourquoi l'automatisation de ce traitement permettrait non seulement d'améliorer le confort du patient mais aussi la qualité de son traitement et, *in fine*, ses conditions de vie.

Le projet d'un système qui permettrait une régulation artificielle de la glycémie, encore appelé le projet pancréas artificiel, a été initié dans les années 1970 par Albisser et al.[8] et Pfeiffer et al.[123], mais n'a pas encore abouti à une solution ambulatoire. Les travaux s'articulent autour de trois défis majeurs :

- le développement d'un capteur de glycémie fiable,
- le développement d'un système d'injection d'insuline efficace,
- le développement de commandes adaptées.

Une grande partie du travail présenté dans cette thèse concerne essentiellement l'analyse de cette dernière.

Les premières solutions qui ont été proposées, se basent sur des algorithmes de commande très simples, par exemple, pour des patients en soins intensifs, un correcteur PID réglé sur un modèle linéaire. Cependant le déploiement massif chez des patients diabétiques dans des conditions de vie banalisées demande le développement d'algorithmes plus évolués. Pour ce faire, plusieurs approches peuvent être envisagées. Un premier type d'approche consiste à garder un modèle linéaire mais en développant des contrôleurs robustes comme par exemple des commandes à mode glissant [3]. Un deuxième type d'approche concerne des modèles plus précis du patient en conservant le caractère non linéaire propre au problème (soit en utilisant des approches boites noires comme dans [4] ou en utilisant des approches par modèle d'état comme dans [73]).

L'approche développée dans cette thèse cherche à faire un compromis entre l'aspect non linéaire du système et la complexité du modèle. Pour ce faire une version modifiée d'un modèle non linéaire simple

est retenue et associée à un contrôleur de type commande prédictive non linéaire robuste pour prendre en compte les erreurs de modélisation.

1.2 Le diabète de type 1

1.2.1 Quelques mots sur la maladie

Chez un individu sain, la glycémie est naturellement régulée entre 80 et 120mg.dL^{-1} (avec des glycémies post-prandial d'au plus 180mg.dL^{-1}). En temps normal, cette régulation est principalement assurée par l'action combinée de deux hormones: le glucagon et l'insuline. L'insuline a une action hypoglycémiante. Elle fonctionne en se fixant sur des récepteurs appropriés qui provoque la libération d'autres protéines (GLUT) qui, à leurs tours, favorisent le transport du glucose au travers des membranes plasmiques, permettant ainsi un stockage du sucre du sanguin. *A contrario* le glucagon est une des hormones hyperglycémiantes qui permet de libérer le sucre préalablement stocké. Ces deux hormones sont sécrétées par le pancréas, plus précisément dans les ilots de Langerhans (voir fig.1.1). L'insuline est produite par des cellules dites β et le glucagon par des cellules dites α [97].

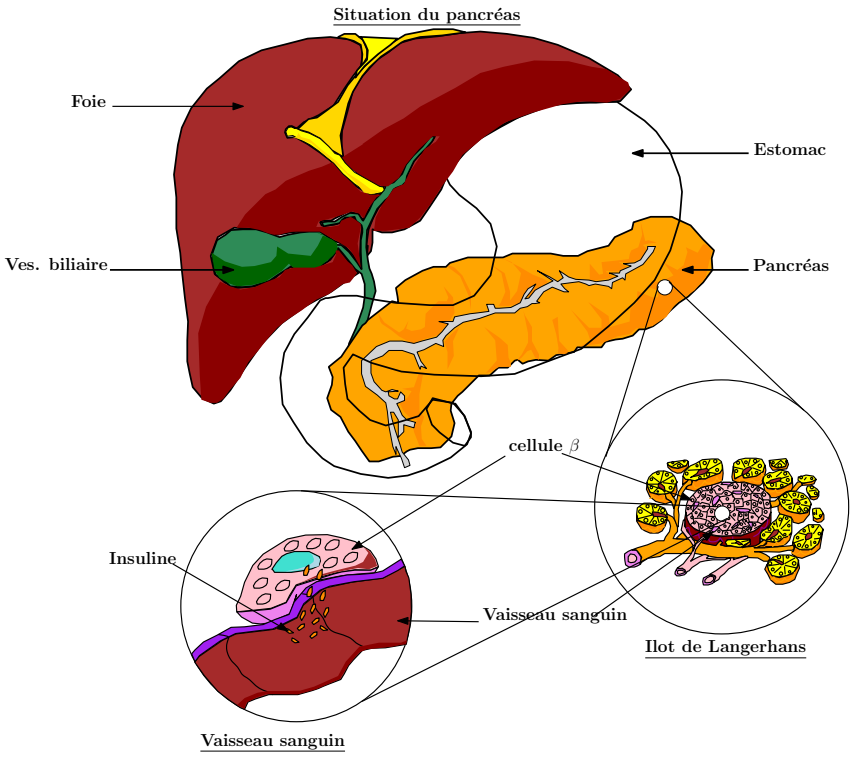

Figure 1.1: Une vue générale du métabolisme glucidique

Le diabète de type 1 est une maladie auto-immune qui va induire une destruction des cellules β. La conséquence en est claire : le pancréas d'une personne atteinte par cette maladie se retrouve dans l'incapacité de produire de l'insuline et donc celle-ci ne peut plus diminuer son taux de sucre. En effet, l'insuline est la seule hormone hypoglycémiante du corps humain. Ceci peut entrainer un grand nombre de complications : soit en raison d'hyperglycémies durables où on prend le risque d'observer des problèmes rénaux, cardiaques, ..., soit en raison d'hypoglycémies. Ces dernières étant extrêmement

dangereuses puisqu'elles peuvent rapidement entrainer des effets néfastes qui peuvent aller jusqu'à la mort du patient.

1.2.2 Modélisation d'un patient diabétique

Le problème de contrôle artificiel de la glycémie est extrêmement complexe. Cela peut sans doute partiellement s'expliquer par la complexité liée à l'aspect modélisation du métabolisme glucidique. En effet, du fait de la difficulté de réaliser des expériences à la fois sures et informatives, il est difficile d'obtenir des données pour construire et/ou identifier un modèle de patient diabétique.

Classiquement, on distingue deux grandes familles de modèles. Tout d'abord les modèles qui sont obtenus à partir d'expèriences complexes et difficilement réalisables dans un cadre simple. Dans cette catégorie, on peut trouver le modèle de Dalla-Man et al. [106]. Ce dernier a été utilisé pour développer une plate-forme de test [90] qui a été validée par la Food and Drug Administration (FDA). Cela signifie que cette plate-forme de test peut être utilisée comme un substitut à des tests sur animaux. Une deuxième famille de modèles ne modèlise que les tendances principales du métabolisme glucidique. L'exemple typique d'un modèle appartenant à cette catégorie est le modèle de Bergman [14].

D'un point de vue dévelopement d'un contrôleur, les modèles les plus précis ne sont pas forcément les plus intéressant à utiliser. En effet, leur complexité limite fortement leur utilisation. D'ailleurs, les approches qui utilisent ces modèles ont plutôt tendance à incorporer une première phase de reformulation (par exemple une phase de réduction de modèle) comme dans [102]. C'est pourquoi nous avons envisagé d'utiliser un modèle simple pour développer notre contrôleur. C'est ainsi que la commande va être développée à partir d'une version modifiée du modèle de Bergman, quant au modèle de Dalla-Man et al., il sera utilisé pour valider notre approche de contrôle. Plus concrétement, le modèle de contrôle est donné par le système d'équations différentielles suivant

$$
\begin{aligned}
&\underline{\text{Modèle du métabolisme glucose-insuline}}:\\
&\frac{dG}{dt} = -(P_1+X)G + P_1G_b + k_{gr}R_2,\\
&\frac{dX}{dt} = -P_2X + P_3(I-I_b),\\
&\frac{dI}{dt} = -k_fI + b_fU_1,\\
&\frac{dU_1}{dt} = -k_sU_1 + u,\\
&(G,X,I,U_1)(t_0) = (G_0,X_0,I_0,U_{1,0}),\\
&\underline{\text{Modèle du métabolisme gastro-intestinale}}:\\
&\frac{dR_2}{dt} = -c_2(R_2-R_1),\\
&\frac{dR_1}{dt} = -c_1(R_1-d),\\
&(R_2,R_1)(t_0) = (R_{2,0},R_{1,0}),
\end{aligned}
\tag{1.1}
$$

où P_1, G_b, k_{gr}, P_2, P_3, I_b, k_f, b_f, k_s, c_1 et c_2 sont des paramètres (strictement positifs) du modèle. L'état G représente la glycémie sanguine, l'état X l'insuline dans un compartiment distant, l'état I l'insuline sanguine, l'état U_1 l'insuline sous-cutanée et les états R_2 et R_1 des quantités de sucre dans des compartiments distants. Les entrées u et d représentent respectivement un débit d'insuline et une quantité de sucre.

1.3 Une commande prédictive par méthode d'un problème de point selle (SPMPC)

D'un point de vue contrôle, il semble qu'une approche par commande prédictive présente de nombreux avantages (voir par exemple la review [13]). L'un de ces avantages provient du fait que, lorsqu'un patient applique son traitement classique, ses décisions peuvent être interprétées mathématiquement comme la résolution d'un problème d'optimisation sous contraintes. En effet le patient cherche à réguler sa glycémie à une valeur donnée (régulation), il cherche à éviter les hypo- et les hyperglycémies (contraintes sur l'état) en s'injectant seulement de l'insuline (contraintes sur l'entrée). De plus l'aspect prédictif est intéressant puisqu'il permet d'anticiper certaines perturbations connues à l'avance, comme par exemple les perturbations de type repas.

Les techniques de contrôles prédictives reposent sur le modèle du processus qui doit être contrôlé. Toutefois, dans le cas du diabète, il est très difficile d'obtenir un bon modèle. C'est pourquoi la plupart des approches développées incorporent soit une composante robuste soit des aspects adaptatifs (comme par exemple dans [73]). Parmi toutes les approches retenues et testées jusqu'à alors, une approche de type min-max n'a pas été considérée. Il est vrai que cette approche n'est pas souvent retenue comme une alternative viable du fait des temps de calculs importants nécessaires à la résolution du problème d'optimisation sous-jacent. Pourtant, dans le cadre de la régulation artificielle de la glycémie, les constantes de temps du système sont compatibles avec une telle approche (de l'ordre de la dizaine de minutes). Dans cette thèse, nous allons nous intéresser à ce type de contrôleur.

Le problème de contrôle artificiel de la glycémie est typiquement posé dans un cadre échantillonné. En effet, le métabolisme glucidique est un processus à temps continu alors que les capteurs de glycémie fonctionnent avec des temps d'échantillonnages non négligeables devant les constantes de temps du système. La littérature concernant les résultats qui garantissent la stabilité d'un contrôleur min-max MPC dans un cadre échantillonné est très réduite. Ceci a motivé les travaux de cette thèse qui consistent à développer des outils théoriques et numériques garantissant la stabilité d'un tel système dans le cadre d'un contrôleur de type MPC robuste dont l'entrée de contrôle est donnée par la solution d'un problème de point selle contraint en l'état. L'intérêt de cette formulation par rapport à une formulation de type min-max réside dans la simplification de la partie résolution numérique tout en conservant les mêmes garanties de robustesse (sous hypothèses que le point selle est bien défini). Ce contrôleur, appelé *Saddle Point Model Predictive Control* (**SPMPC**), a pour but d'assurer,dans un cadre échantillonné, pour des systèmes décrits par des équations différentielles ordinaires non linéaires, des performances de contrôle robuste. Concrétement, on s'intéresse aux systèmes qui sont décrits par des équations du type

$$\begin{aligned} &\frac{dx}{dt} = \mathscr{G}(x,u,w), \\ &x(t_0) = x_0, \end{aligned} \tag{1.2}$$

où $\mathscr{G} : \mathbb{R}^{n_x} \times \mathbb{R}^{n_u} \times \mathbb{R}^{n_w} \to \mathbb{R}^{n_x}$ est une fonction continue, $x \in \mathbb{R}^{n_x}$ est l'état du système, $u \in \mathbb{R}^{n_u}$ est l'entrée de contrôle et $w \in \mathbb{R}^{n_w}$ représente des perturbations. Le contrôleur SPMPC fonctionne selon l'algorithme suivant

Définition 1[SPMPC]
L'algorithme de contrôle SPMPC consiste, pour un taux d'échantillonnage donné δ, un ensemble robuste invariant $\Omega_a^{f_E}$ et un horizon de prédiction $T > \delta$, à se donner une entrée de contrôle $u(t) = u_i^*(t)$ pour tout $t \in [t_i; t_{i+1}[$ où, pour un temps $t_i = t_0 + i\delta$ et une condition initiale x_i, u_i^* est donnée par la solution

du problème de point selle suivant

$$\begin{aligned}(u_i^*, w_i^*) = \arg\inf_{u\in U}\sup_{w\in W} J^{t_i}(u,w) = \arg\sup_{w\in W}\inf_{u\in U} J^{t_i}(u,w),\\ s.c.\ x(t_i+T)\in\Omega_a^{f_E}.\end{aligned} \tag{1.3}$$

où $x(s)$ est la valeur prédite de l'état à l'instant s, U et W sont deux sous-ensembles de $L^2(I)$ donnés convexes, fermés, bornés et non vides, avec I un intervalle de longueur T et $J^{t_i}(u,w)$ est donné par

$$J^{t_i}(u,w) = E(x(t_i+T)) + \int_{t_i}^{t_i+T} F(x,u,w)ds, \tag{1.4}$$

où $E : \mathbb{R}^{n_x} \to \mathbb{R}^+$ et $F : \mathbb{R}^{n_x}\times\mathbb{R}^{n_u}\times\mathbb{R}^{n_w} \to \mathbb{R}$.

Plus concrétement, nous avons prouvé, sous certaines hypothèses, que ce contrôleur permet d'assurer une convergence en temps fini dans un sous-espace d'état borné (*Ultimately Bounded*), ou, sous davantage d'hypothèses, que le système est pratiquement stable entrée-sortie (*Input-to-State practically Stable*). Ces résultats sont exprimés au travers des deux théorèmes suivant (pour plus de détails sur les hypothèses et la preuve de ces théorèmes, se référer au chapitre 3):

Théorème 2. *Sous les hypothèses 1 à 9, si les hypothèses du lemme 1 sont satisfaites et si $x(t_0) \in X_E$, alors en utilisant un contrôleur SPMPC, à chaque instant d'échantillonnage, la trajectoire d'état est "*Ultimately Bounded*" relativement à un sous-ensemble de X_E qui contient l'origine, et converge asymptotiquement dans un sous-ensemble qui contient l'origine.*

Théorème 3. *Sous les hypothèses 1 à 9, si les hypothèses du lemme 1 sont satisfaites, si $x(t_0) \in X_E$, et si il existe $a,b,\lambda \in \mathbb{R}^{*+}$ avec $a<b$ tel que $\alpha_F^0(s) \geq as^\lambda$ et $\beta_E(s) \leq bs^\lambda$, alors en utilisant un contrôleur SPMPC, à chaque instant d'échantillonnage, le système est "*Input-to-State practically Stable*".*

1.4 Résultats

L'implémentation numérique de cette commande est ensuite mise en oeuvre. Pour ce faire une méthode numérique pour résoudre les problèmes de point selle sous contraintes est présentée. Le but de cette méthode consiste à remplacer le problème d'optimisation contraint par une séquence de problèmes d'optimisations non contraints en l'état en utilisant une méthode qui s'inspire de la méthode du Lagrangien augmenté [116]. Chaque problème non contraint est ensuite résolu en utilisant une méthode de gradient conjugué. Le gradient du critère à optimiser est calculé en utilisant un modèle adjoint (pour plus de détails et pour d'autres applications biomédicales voir [10] et [11]).

Pour résoudre le problème de contrôle, les approches prédictives reposent sur l'optimisation de trajectoires d'état. Ceci implique qu'un système d'équations différentielles doit être intégré, et donc que la condition initiale du système, donné par la valeur de l'état courant, est nécessaire. Toutefois, comme leur nom l'indique, les capteurs de glucose ne fournissent qu'une mesure bruitée de la concentration en glucose sanguin. Cela implique qu'il est nécessaire d'envisager le développement d'un observateur. A ce titre, trois observateurs reposant sur des méthodologies différentes ont été envisagés, l'idée étant de comparer les différents résultats d'estimations et de valider les approches retenues dans le cas où les différents résultats d'observations sont cohérents entre eux. A la vue des résultats d'observation obtenus (cf fig.1.2), un filtre de Kalman sans biais [144] est utilisé.

L'approche SPMPC est testée en utilisant tout d'abord le modèle de contrôle comme un modèle de simulation puis en utilisant une plateforme de simulation approuvée par la FDA. Le contrôleur est testé

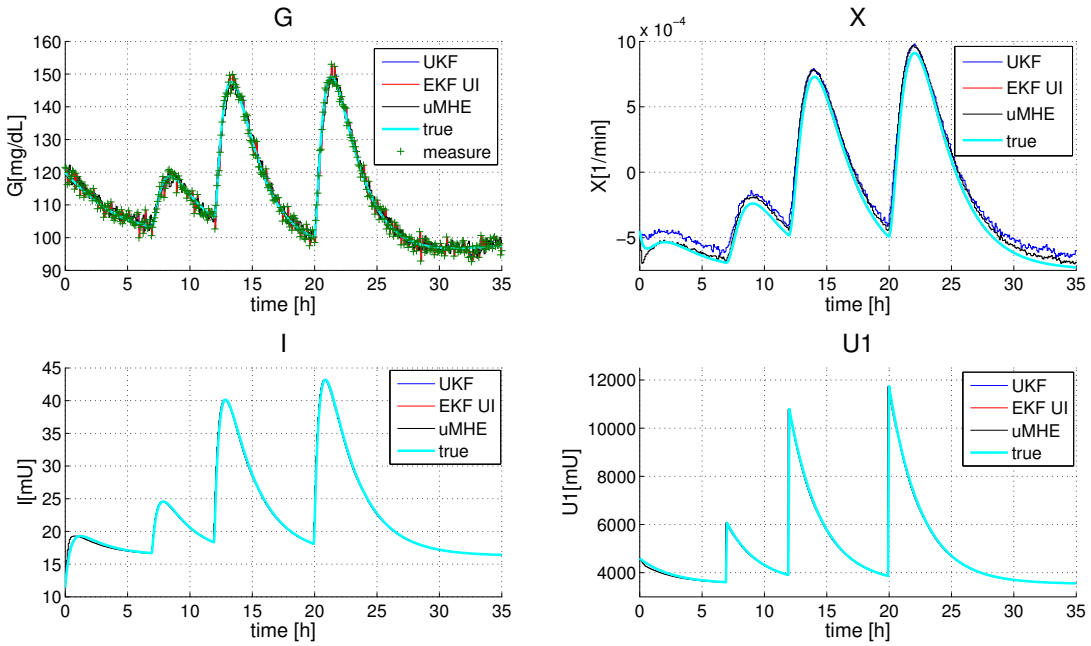

Figure 1.2: Comparaison d'un observateur de type UKF, MHE et UIEKF en partant d'une estimation initiale exacte

sur deux scénarios. Tout d'abord un scénario simple où le contrôleur a pour seul but de stabiliser la glycémie alors que le patient a initialement une glycémie haute. Avec ce scénario, l'objectif est de tester si pour rejeter une hyperglycémie, le contrôleur ne va pas induire une hypoglycémie. Ensuite un scénario consistant en une journée avec prise de trois repas est envisagé. L'idée est de tester les performances du contrôleur quand ce dernier est combiné à une cure de bolus classique (par exemple donné par le traitement usuel du patient). Plus précisément le scénario de type repas consiste en le scénario suivant

Scenario : Journée classique

$t = 0h$**:** La simulation commence. Le glucose sanguin est initialisé à 100mg.dL^{-1}. L'observateur (UKF) est branché.

$t = 2h$**:** Le contrôleur (SPMPC) est branché.

$t = 7h$**:** Le patient mange un repas de 25g en sucre.

$t = 12h$**:** Le patient mange un repas de 70g en sucre.

$t = 20h$**:** Le patient mange un repas de 80g en sucre.

$t = 35h$**:** La simulation est terminée.

Il est supposé que chaque repas est contrôlé par le patient en s'envoyant une quantité d'insuline correspondant à 75% de ce qu'il s'enverrait en temps normal (relativement à son traitement usuel). Pour mesurer les performances du contrôleur, on s'intéresse aux indicateurs suivants : $\%\, G \in [70, 140]$ le pourcentage de temps que le glucose sanguin passe dans l'intervalle $[70, 140]$mg.dL^{-1}, $\min G$ la glycémie minimale et $\max G$ la glycémie maximale. Chacun d'entre eux est évalué à partir du moment où la boucle est fermée. Les résultats de simulation pour les 10 adultes de la version d'essai du simulateur de

patient virtuel [90] sont fournis dans le tableau 9.8 du chapitre 9. Le résultat de simulation pour l'adulte 9 est visible sur la fig. 1.3. Sur cette courbe on peut voir que le contrôleur démontre de bonnes propriétés. La glycémie est stabilisée dans un intervalle sûr, on n'observe pas d'hypoglycémie et le temps passé en hyperglycémie est réduit.

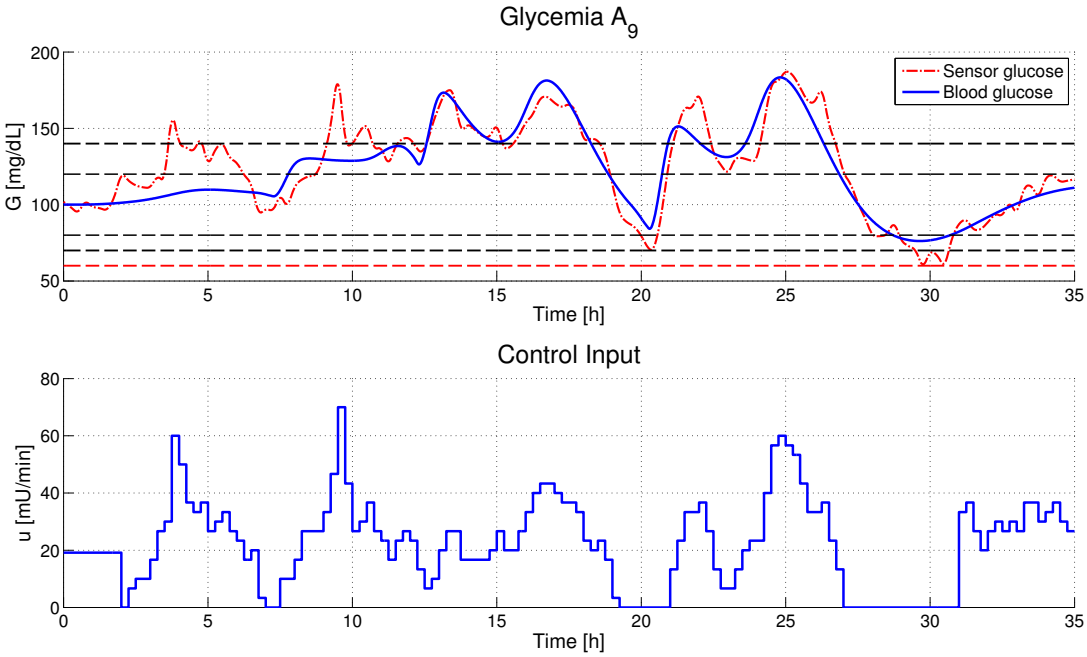

Figure 1.3: Résultat de simulation pour l'adulte 9 de la plateforme de test, cas d'une modélisation par équations différentielles ordinaires.

A la vue des résultats de contrôle positifs, l'extension de la méthodologie de contrôle SPMPC pour le contrôle des systèmes retardés est mise en oeuvre d'un point de vue numérique. L'objectif est de valider l'intérêt de cette extension en fonction des résultats de simulations obtenus dans le cadre de la régulation artificielle de la glycémie. Pour ce faire, le modèle de contrôle jusqu'à alors utilisé est reformulé en utilisant des équations différentielles retardées. Suite à quoi des simulations numériques sont réalisées en considérant un scénario consistant en une journée avec prise de trois repas. Comme précédemment, les patients virtuels sont soit donnés par le modèle de contrôle soit par la plateforme de test approuvée par la FDA. Les résultats de simulation pour les 10 adultes de la version d'essai du simulateur sont donnés dans le tableau 10.3 du chapitre 10. Le résultat de simulation pour l'adulte 9 est visible sur la fig. 1.4. On peut voir que cette fois-ci encore le contrôleur démontre de bonnes propriétés.

1.5 Conclusions et perspectives

Le problème de régulation de la glycémie pour des patients atteints de diabète de type 1 est un problème d'une grande complexité qui mélange à la fois des aspects de contrôle non linéaire dans un cadre échantillonné, de processus variant dans le temps, de limitation de possibilité d'action des actionneurs, etc. L'approche retenue a permis de prendre en compte le plus de contraintes possibles afin de rester au plus proche du système réel. Toutefois, pour que le problème reste faisable, il a fallu s'orienter vers des modèles extrêmement simples. Afin de prendre en compte cette inadéquation entre le système et le modèle, des approches robustes ont été privilégiées.

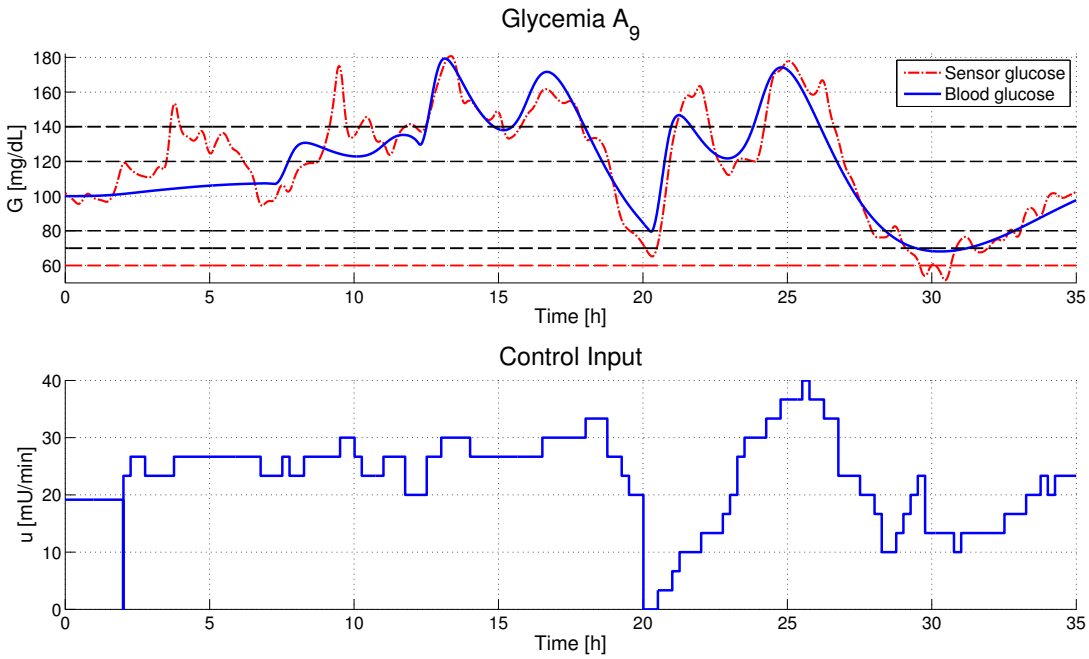

Figure 1.4: Résultat de simulation pour l'adulte 9 de la plateforme de test, cas d'une modélisation par équations différentielles retardées.

Ainsi, le dévelopement théorique et numérique d'une commande MPC non linéaire robuste basée sur la résolution d'un problème de point selle a été envisagée. Dans le cadre de l'application au diabète de type 1, cette commande a été implémentée en utilisant une version modifiée du modèle minimal de Bergman. Le problème d'optimisation correspondant a été résolu en utilisant un algorithme qui se base sur l'utilisation de modèles adjoints. Le contrôleur obtenu a ensuite été testé sur un simulateur de patients virtuels approuvé par la FDA. Les résultats de simulation montrent l'intérêt de l'approche retenue en particulier dans le cas où le patient est amené à réguler lui-même son repas. L'extension formelle pour le contrôle des systèmes décrits par des équations différentielles retardées s'est aussi montré extrêmement intéressante en montrant des résultats de contrôle tout à fait satisfaisant malgré la complexité du problème sous-jacent.

D'un point de vue perspectives, il peut être intéressant de considérer de nouvelles conditions suffisantes pour assurer la stabilité du contrôleur. Ensuite, il peut être intéressant d'étudier la stabilité théorique du contrôleur SPMPC quand ce dernier est combiné à un observateur. En effet, au cours des simulations, il a été implicitement supposé qu'un pseudo principe de séparation était applicable. Toutefois il n'existe pas de résultats généraux dans le cas non linéaire. C'est pourquoi il peut être intéressant d'étudier la stabilité du contrôleur d'un point de vue retour de sortie. Aussi, l'étude de la stabilité du contrôleur dans le cadre d'un problème de suivi de trajectoire semble pertinente.

A la vue des résultats de simulations obtenus dans le cas du contrôle d'un système à retard, il peut être intéressant d'envisager d'un point de vue théorique la stabilité de la boucle fermée.

En ce qui concerne le développement d'un pancréas artificiel, il peut être judicieux de voir comment il est possible de profiter d'un retour d'expérience afin d'obtenir de meilleures performances de contrôle. Enfin, il semble logique de désormais considérer la partie du traitement qui s'intéresse à rejeter automatiquement les perturbations de type repas. Ainsi, combiné avec notre approche SPMPC, le patient n'aurait plus à se soucier de son traitement.

Chapter 2

Introduction

Contents

2.1 Motivation and Background of the Thesis

The focus of this thesis is to consider the design of a robust nonlinear controller in a sampled-data framework. This problem comes from the need to design a controller to bring a solution to the problem of artificial blood glucose control. This problem belongs to the field of *red* biotechnology [76]. That is the field which is interested in a medical use of control.

Surprisingly enough, this field is not very developed. One reason is that, most of the time, the corresponding control problems gather many control difficulties. To quote the most relevant ones, we can mention the difficulty to model the process (which are often nonlinear, time varying, subject to delay, ...), the difficulty to obtain relevant measures (sparse and noisy measure, difficulty to design both human friendly and informative experiments, ...) or , from an even more general point of view, the difficulty to define a metric which provides a good measure of the performance of the considered algorithm. Another reason that inhibits its expansion is the difficulty to validate an approach. Indeed as in this field human lives are concerned, the error is not allowed. This leads to really demanding validation phase.

Nevertheless, the endocrinology field is currently an important subject of researches. These latter bring new insights but also some hopes for new cure. In this thesis, we will be interested in type 1 diabetes mellitus, one special field of the endocrinology field. This disease of the pancreas is an auto-immune disease which leads to the impossibility of secreting insulin. This has for consequence that a patient suffering from this disease can not regulate its blood glucose. This can be at the origin of various complications (e.g. coma or even death).

The main objective of bringing control is to design what is often called an *artificial pancreas*. The idea is to combine the existing hardware (such as the glucose sensors and the insulin pumps) with an adequate control algorithm to develop a device which mimic the behavior of an healthy pancreas. If it were to work, this would lead to a simpler cure for the millions of people suffering from diabetes [115].

To provide a potential solution, many control algorithms have already been proposed (see e.g. [165] or [13] for a review of the considered controller and the remaining challenge in this field). Among the most commonly used control strategies, it is possible to mention the PID controllers (see e.g. [109], [80] or [57]), the controllers which make use of fuzzy logic and/or neural techniques (see e.g. [168], [35] or [93]), the strategies which implement run-to-run algorithm (see e.g. [117], [24] or [119]), the sliding mode controllers (see e.g. [5] or [58]) or the MPC controllers (see e.g. [2], [156], [159], [89] or [40]).

Even if all approaches present their own advantages compared to other approaches (e.g. the PID controller can provide a good approximation of the behavior of healthy beta cells [153]), lately, it seems that the MPC approach is the more promising because of numerous attractive features. First, it is easy to interpret its behavior in terms of a classical cure. Indeed, when the patient deals with his disease, it can be seen as the patient trying to solve a constrained optimal control problem. He wants to stabilize his blood glucose to a given value (stabilization), to avoid hypoglycemia and reduce hyperglycemia (state constraints) by only injecting insulin (input constraints). Then, the predictive aspect is interesting as it enables to anticipate on known disturbances. As an example, a patient often knows in advance when and what he will eat, thus providing the controller with these informations, it becomes possible to aim at better control performances (see e.g. [168] or [1]). Finally, it can also be useful to overcome physiological delays due to the use of the subcutaneous route for both the insulin injection and the blood sugar measures [72].

The problem of controlling blood glucose is challenging in regards to various aspects. The considered system (*i.e.* the human body) is nonlinear and time varying (e.g. the diabetics are subject to the dawn phenomena which make them more insulin resistant in the early morning). The available devices favor the use of the subcutaneous route (see e.g.[139]), which implies that there is some time lag, either on the blood glucose measure or on the insulin effect. This makes the design of an efficient controller more

challenging as these aspects are detrimental for the stability of the closed-loop. Also, all patients are extremely different in the sense that for the same excitation, we can obtain very different responses. Finally, the patients are subject to various disturbances, the effects of which are hard to quantify (e.g. stress, exercise, ... see e.g. [154]).

All these facts have implied that the design of robust controllers have always been the prime concern of the community. This has lead to a massive interest in adaptive approach (see e.g. [23], [16] or [73]) and robust approach (see e.g. [5], [120], [58] or [71]). These solutions have proved to be interesting and motivate further research in this direction. So far, the design of a min-max MPC controller has not been considered. As this control approach can guarantee robust control performances and also benefits from the various advantages of predictive controller, we are interested in considering this approach.

For control purpose, we will only be interested in stabilizing blood glucose and not to reject meal effects which can be considered as a different problem. Anyway, the usual cure for type 1 diabetes is also split into two terms, the basal term to stabilize blood glucose and the bolus term to counter the sudden blood glucose increase, e.g. due to meal digestion. Also, because the glucose metabolism is a time continuous process and the measure are time discrete, we are also interested in designing a controller in a sampled-data framework.

This implies that we are particularly interested in what is usually done to consider the sampled-data aspect in control problem. The problem of controlling a time continuous dynamics using a control input which is only computed at discrete time instant is a common situation. This is typically the case when considering the digital control of a continuous time system via A/D and D/A converters (see fig. 2.1)

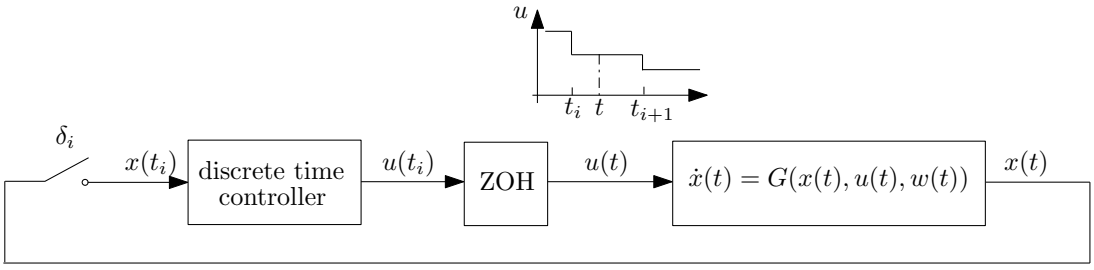

Figure 2.1: Sampled data feedback

To design a controller in this framework, many approaches can be used. Assuming that the sampling time δ is known and constant, one of the most natural approach is to globally consider the system as a discrete one. It is possible to use a discrete approximation of the continuous time model and then to design a discrete controller (see e.g. [150] or [107]). It is also possible to design a time continuous controller and then to apply a discrete approximation of this latter (see e.g. [64] or [114]).

Others approaches, which do not need a discretization step, are either considering the sampled-data aspect by introducing a time varying delay in the input (see e.g. [54] or [53]) or by embedding the mixed continuous-discrete dynamic in an equivalent jump system (see e.g. [84] or [86]).

The previous techniques are worth applying when it is assumed that the AD/DA converters are the key limiting factors and so that the control input has to remain constant in between two sampling instants. However nowadays it is not always true. Indeed the progress in microprocessor are such that they can easily work under the milli- or even micro-seconds so that now , at least for a relevant class of processes, the true limiting factor is due to the slow state measurements (e.g. because of long processing time of a chemical sensor). This implies that it is worth considering open-loop sampled-data feedback control [48]. Here the idea is to open-loop apply an input signal which is computed at each sampling instant (see fig. 2.2).

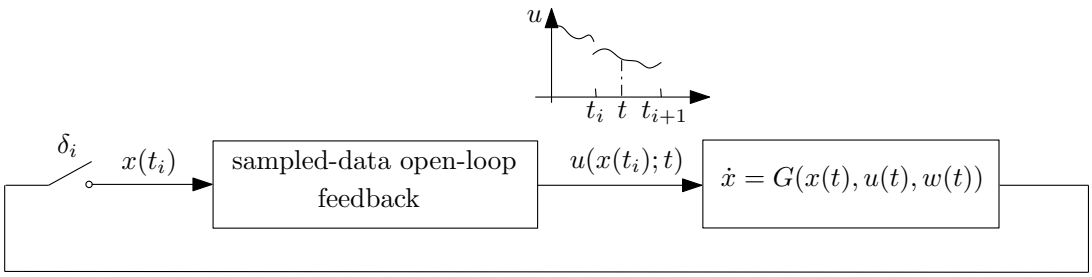

Figure 2.2: Sampled data open loop feedback

In this setting, the usual approach consists in using what is often designed as an open-loop input generators (see e.g. [108]). The idea is to combine a stabilizing state feedback with feedforward simulation (see e.g. [48]). In this regards, the predictive control approach is particularly interesting (see e.g. [50] or [47]). To better understand this assertion, let us remind some well-known facts concerning this control technique.

Model Predictive Control (MPC) is a control strategy whose aim is to ensure stability and control performances using the tool of optimization. Its principle consists in considering the control input trajectory which is given as the solution of a finite horizon optimal control problem. Concretely, at a given time t, the control problem is recast as an optimization problem with a prediction horizon of length T subject to a dynamical model of the system that has to be controlled and where the current state value $x(t)$ is the initial condition. Then the computed optimal control input trajectory $u^*(s)$ is applied in open-loop until a new measure is available at $t+\delta$. At this instant, the prediction horizon is shifted and a new optimal control problem is solved [22]. Figure 2.3 (which has been inspired from [12]) illustrates this concept in the case of a single input single output system.

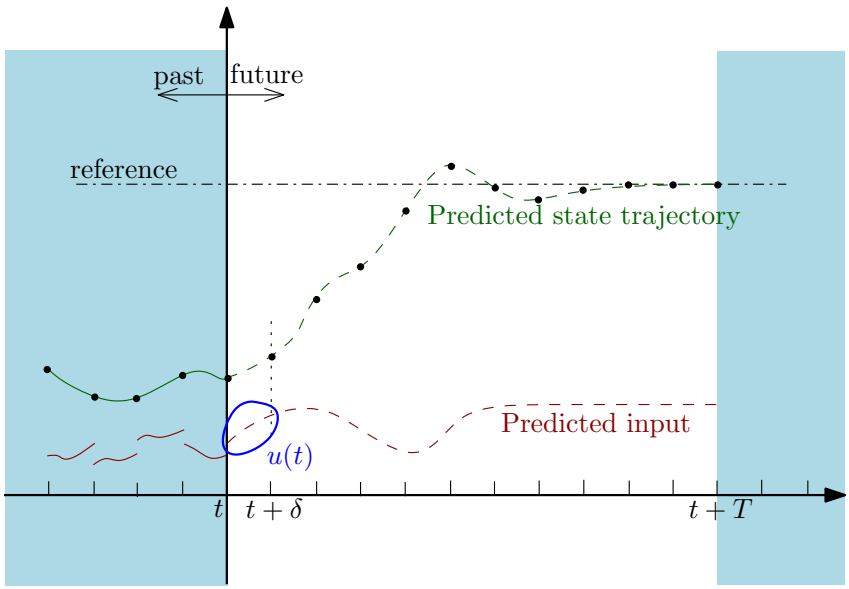

Figure 2.3: MPC strategy: only the first control move is applied in open loop

One of the main advantage of MPC is that it is easy to consider constraints on the inputs or on the states by solving a constrained optimization problem. Of course, if the plant model were to be perfect,

there would be no need to solve a new optimal control problem and the control sequence could have been applied in open loop for all $s \in [t, t+T[$. However, as it is most likely, the predicted trajectory will more or less differ from the actual plant trajectory. That is why the optimization problem is solved as often as possible in order to introduce some robustness via this *feedback* mechanism.

Because of its ability to handle constraints and to ensure a certain optimality in regards to a given criterion, the MPC control technique has rapidly found its place in industry with more and more applications, see e.g. [126]. In a sense, this success is quite surprising. Indeed, at its very beginning, in the early 1980's, there were no formal guarantee on stability of the closed-loop and/or feasibility of the optimization problem. Since then, the situation has changed and in the case of classical MPC algorithms, the necessary tools to ensure stability and feasibility, are now well understood, see e.g. [110].

One possibility to ensure stability of the closed-loop is to add a final cost in the functional that is optimized and a supplementary terminal state constraint. The final cost is simply a function of the value of the state at the end of the prediction horizon which can be interpreted as a local Lyapunov function. The terminal state constraint requires that at the end of the prediction the state has reached a given subset which satisfies some properties, e.g. to be positive invariant. The final cost and the terminal state constraint are usually computed via the design of an intermediate control law. This *final* controller can either be applied when the state has reached the terminal state as in the dual mode approach, see e.g. [112] or [146], or never be applied as in the quasi infinite approach [26].

However, even if MPC controller inherently provides some degree of robustness (see e.g. [143], [167] or [125]), it is well known that, at least for nonlinear system, the margin can be arbitrary small. This has to be understood in the sense that any discrepancy between the control model and the system leads to instability of the closed-loop [62]. From a type 1 diabetes point of view, this is of prime importance as this is nearly impossible to obtain a good model of the process. That is why, despite the supplementary computational burden, it is of prime interest to consider the design of robust MPC controller.

Many approaches have been developed to cope with robustness. The main idea behind all these algorithms comes from the game theoretic approach of the control problem [28]. The original robust stability and performance problem is transformed into a constrained game type minimax optimization one, *i.e.* the control problem is expressed as a game between the control engineer which aims at stabilizing the system and the nature which has the opposite objective. That is, by applying a useful control on the system, the first player, which plays the role of the control engineer, seeks to minimize the result of the game, *i.e* the value of a given cost functional of the game, while the second player, which plays the role of the various uncertainties, seeks to maximize the result of the game (see e.g. [10] or[79]).

Simply, the objective of robust control is to compensate for the undesirable effects of system disturbances through control actions such that a cost function achieves its minimum for the worst disturbances [10]. The different algorithms proposed to solve the robust control problem differs by their balance between the needed on line computation time and the robust performances guarantee. Roughly speaking, when it is desired to have a small on line computation time, then the controller has to give up on robustness guarantee (e.g. by assuming a structure on the disturbances). Without looking for an exhaustive enumeration of the available algorithms, it is possible to retain the following approaches.

One of the most time efficient technique consists in solving off-line the optimal control problem thanks to parametric programming (see e.g [36], [161], [30] or [38]). These control strategies are based on the property that, for a given class of control problem, the optimal solution can be parametrized. This approach leads to explicit solutions which are valid for a given subspace. Off line, one limitation of these approaches comes from the difficulty to determine the various subspaces for large dimensional system and/or long prediction horizon. Also, on line, it can be time consuming to find the active subspace and actually it can be faster to solve the optimization problem.

An other time efficient approach consists in finding an approximate solution to the original optimiza-

tion problem by not directly considering the optimization of a given cost functional but by considering the optimization of an upper bound of the optimal value of the cost functional (see e.g. [7] or [63]). This approach provides algorithms whose computation time is tractable but at the cost of the introduction of a certain conservatism in the results depending on the quality of the derived bound.

In order to ensure optimal control performances relatively to a chosen criterion and to reduce the computation time, it is possible to use a tube MPC approach (see e.g. [46], [166] or [167]). The idea is to reduce the on line computational burden to the task of solving on line a MPC control problem on the nominal model of the process. The thus obtained control input is then coupled with an auxiliary control law whose aim is to ensure that the error in the predicted trajectory remains in a robust control positive invariant set. The limitation of the method is in the computation of this auxiliary control law as it is desirable to be both simple and to provide a sufficiently big invariant set (to ensure a good robustness of the controller).

Finally, there is the family of algorithms which solves the original minimax optimization problem arising from game theoretic consideration. The aim is here to compute a sequence of control action which enables to stabilize the system under the worst disturbances (worst to be understood in the sense that they maximize the value of the game). In this category we can distinguish between the strategy which use the same criterion as in the nominal case, *i.e.* the disturbances do not appear explicitly in the criterion (see e.g. [94], [130], [51], [100] or [92]) and the strategy which explicitly introduce a negatively weighted term for the disturbances in the criterion that has be optimized (see e.g. [111], [85] or [98]). The main advantage of the minimax approach is that the robust performances are guaranteed for a well defined set of disturbances which can take various form (additive disturbances, parameter disturbances, ...) and that the problem is easier to cast. The main disadvantage comes from the heavy computational burden as the control problem is recast as a minimax optimization problem.

In the problem of artificial blood glucose control, the sampling time is in the order of the minute, implying that the computation time is not a limit. As the robustness of a minimax approach is *a priori* the best that can be expected, we will focus on this approach. Surprisingly enough, there are only few results that can be found when it comes to design a min max MPC controller in a sampled-data framework. That is why in this thesis we will be interested in considering, from a theoretical point of view, the design of a stable robust predictive controller in order to control systems described by nonlinear ordinary differential equations in a sampled-data framework. The control input will be given by the solution of a constrained saddle point optimization problem. We have chosen to consider saddle point problem instead of min-max problem in order to suppress the implicit advantage which is given to the disturbances in this latter formulation. This is at the origin of the proposed name of the method, the *saddle point MPC* (SPMPC). Then, as this controller is perfectly suited to the problem of artificial blood glucose control, its application to this control problem will be considered.

2.2 Outline of the Thesis

The thesis is structured as follows:

In part I, we present the *saddle point model predictive controller* from both a theoretical and numerical point of view. In chapter 3, it will be proved that using a final cost and a terminal state constraint, under reasonable assumptions, this controller can robustly stabilize the controlled system (to be understood in the ultimate bounded or input to state practical stability sense). Also, as the assumptions on the final cost and the terminal state constraint differ from the usual ones, a formulation to compute these elements using the tool of differential inclusion is given. In chapter 4, a numerical method based on adjoint model is given in order to solve the control problem which is formulated as a constrained sad-

dle point optimization problem. Finally, in chapter 5, the good numerical implementation and control performances of the SPMPC controller are assessed by considering the problem of robust control of a disturbed in parameters Van der Pol oscillator.

In part II, we are interested in applying the previously presented algorithm to the problem of artificial blood glucose control. In chapter 6, we will present two models of the glucose-insulin metabolism. The first one, which is quite complex, will be used for validation purpose, the second one, which only provides global trend of the process, will be used to design the controller. In chapter 7, we will study the properties of the control model in regards to its applicability with a SPMPC controller. In chapter 8, we will present some state observers. Indeed, in the problem of blood glucose control, the sole measure of the blood glucose is available meaning that the value of the remaining state has to be estimated thanks to a state observer. In chapter 9, we will consider the numerical validation of our control approach using a virtual testing platform. For a given set of virtual patient, the parameters of the control model will be identified using optimal control on the parameters. Then, the controller performances will be tested thanks to numerical simulation using both the control model and the testing platform to simulate a virtual patient. Finally in chapter 10, the possibility to extend the SPMPC approach to the control problem of time delay systems is formally investigated.

2.3 Contributions of the Thesis

The main contributions of this thesis are as follows:

Saddle point MPC to robustly control nonlinear system described by nonlinear ordinary differential equations in a sampled-data framework

- Presentation of a new MPC control scheme based on zero sum differential games,
- Theoretical proof of the stability of the closed-loop,
- Under the supplementary assumption of a quadratic stage cost, formulation of the final cost and the terminal state constraint problems in a LMI framework using differential inclusion embedding.

Numerical methods

- Proposition of a numerical algorithm inspired from the augmented Lagrangian method, based on adjoint formulation, to solve a constrained saddle point optimization problem.

Application to artificial blood glucose control

- Design of a SPMPC controller to take care of the stabilizing part of the cure,
- Numerical simulation to assess the controller performances and its good behavior when combined with the other part of the classical cure.

Saddle point MPC to robustly control nonlinear system described by nonlinear delay differential equations in a sampled-data framework

- Assuming that the stage cost is quadratic, formulation of the final cost and the terminal state constraint problems in a LMI framework using differential inclusion embedding.

This thesis has lead to the following publication

Articles

- M. Penet, H. Gueguen, and A. Belmiloudi. Saddle Point MPC Approach to Nonlinear Robust Sampled-Data Control Problem, submitted.

- M. Penet, H. Gueguen, and A. Belmiloudi. Blood Glucose Control for Type 1 Diabetes Using a Saddle Point MPC Approach, in preparation.

Conferences

- M. Penet, H. Gueguen, and A. Belmiloudi. A Robust Receding Horizon Control Approach to Artificial Glucose Control for Type 1 Diabetes, *9th IFAC Symposium on Nonlinear Control Systems (NOLCOS)*, 2013.

- M. Penet, H. Gueguen, and A. Belmiloudi. Régulation Artificielle de la Glycémie: Développement d'une commande robuste, *7e Conférence internationale d'Automatique francophone (CIFA)*, p.425-430, 2012.

- M. Penet, H. Gueguen, A. Belmiloudi, I. Guilhem, and J.Y. Poirier. A Robust Receding Horizon Approach for Blood Glucose Control in Type1 Diabetes, *5th International Conference on Advanced Technologies and Treatments for Diabetes (ATTD)*, 2012.

- M. Penet, H. Gueguen, A. Belmiloudi, I. Guilhem, and J.Y. Poirier. Régulation artificielle de la glycémie chez les patients diabétiques de type 1, *2e journée des jeunes chercheurs, Mesure, Modélisation et Simulation (MMS)*, p.71-72, 2011.

Part I

Stability and Numerical Methods

Chapter 3

Saddle point MPC: Stability properties

Contents

3.1 Introduction

Model Predictive Control (MPC) (see e.g. [22]) is a control strategy whose aim is to ensure stability and control performances using the tool of optimization. Because of its ability to handle constraints and to ensure a certain optimality in regards to a given criterion, the MPC control technique has rapidly found its place in industry with more and more applications (see e.g. [126]). It has also reached a high level of maturity in academia. In the case of classical MPC algorithms, the necessary tools to ensure stability and feasibility, are now well understood (see e.g. [110]).

Despite its widespread use, there is still huge interest in developing algorithms for various cases which differ from the classical theory but covers practically encountered situations. Among these latter, one of the main issue deals with the design of a robust MPC algorithm in a sampled-data framework for systems described by nonlinear ordinary differential equations.

This chapter aims at presenting a MPC controller which guarantees robust stability properties in a sampled-data framework. Contrary to some approaches which consider a discretization step (see e.g. [150]), the presented controller is based on the time continuous dynamics and consider that the control is updated at discrete occurrence of time. Moreover it is considered that the control input is any piecewise time-continuous function which generalizes the case of piecewise constant input (see e.g. [101, 85]) what leads to consider an open-loop sampled-data control algorithm [48].

If MPC controller provides some degree of robustness [166], this margin can sometime be small [62], and it is interesting to consider the design of robust MPC controller. Many approaches have been proposed to tackle this control issue. In [132, 27], an upper bound of the cost function instead of the cost function itself is minimized using a linear representation of the dynamics and the tool of linear matrix inequality (LMI). Another approach consists in using the MPC algorithm to control the nominal model of the process combined with an auxiliary controller. This later is designed such that the error induced by the difference between the system and the model is rejected (see e.g. [142]) or that the error remains in an invariant set as in tube MPC [167, 46]. Robustness can also be introduced in MPC by explicitly considering the disturbances in the model used for prediction. One strategy consists in minimizing the same criterion as in the nominal case leading to minimax strategy (see e.g.[94, 130, 51, 100, 92]). The approach presented here stems from the game theoretic approach of the control problem. It introduces a negatively weighted term for the disturbances in the criterion [111, 85, 98] and, assuming that pure strategies exist, searches for the saddle point of the game [10].

Despite its robust stability guarantee, the minimax approach is rarely implemented because of its heavy computational load [167]. However, sufficiently slow process which needs robust stability guarantee does exist (e.g. the problem which has motivated our work, namely the problem of artificial blood glucose control in type 1 diabetic). That is why, in this chapter we are interested in presenting a MPC strategy to consider the robust control problem of nonlinear systems subject to bounded disturbances using bounded control action. The continuous time control signals which are not *a priori* parametrized, are calculated, at discrete time instants, when the measures are available, by solving a saddle-point problem. It is proved that this *saddle point MPC* (SPMPC) stabilizes, at each sampling instant, the state trajectory in a robust positive invariant set which contains the target. To simplify the proof, the case of a constant sampling time is considered. However, it is straightforward to extend the obtained results to the varying sampling time case as long as uniform bounds on the sampling time are known.

This chapter is organized as follows. First, the required properties on the system dynamics are given and the *saddle point MPC* controller is presented. Then, under some assumptions, it is proved that the closed-loop is ultimately bounded relatively to a set which contains the origin and that the system is input-to-state practically stable (ISpS). Finally, a last section is devoted to the problem of formulating the final cost and the terminal state constraint problem using differential inclusion.

3.2 Problem statement

3.2.1 Notation and definition

The notation $\|x\|$ stands for the 2-norm of a vector $x \in \mathbb{R}^{n_x}$, *i.e.* $\|x\| = \sqrt{x^T x}$.

For a given $t_0 \in \mathbb{R}^+$, the notation t_k where $k \in \mathbb{N}^*$ stands for $t_k = t_0 + k\delta$ where $\delta \in]0; T[$ is a constant sampling time.

Let Ω be a non-empty, bounded subset of $\mathbb{R}^{n_x}$ with a sufficiently regular boundary, int(Ω) stands for the interior of Ω.

We remind the following useful definition:

a) A function $\alpha : \mathbb{R}^+ \to \mathbb{R}^+$ is of class $\mathscr{K}$ if it is continuous, strictly increasing and $\alpha(0) = 0$,

b) A function $\alpha : \mathbb{R}^+ \to \mathbb{R}^+$ is of class $\mathscr{K}^\infty$ if it is of class $\mathscr{K}$ and is unbounded,

c) A continuous function $\beta : \mathbb{R}^+ \times \mathbb{R}^+ \to \mathbb{R}^+$ is of class $\mathscr{K}\mathscr{L}$ if $s \to \beta(s,\tau)$ is of class $\mathscr{K}$ for each $\tau \geq 0$ and $\tau \to \beta(s,\tau)$ is decreasing to zero for each s.

3.2.2 System description

The system to be controlled is modeled by the following ordinary differential equation

$$\begin{aligned} &\frac{dx}{dt} = \mathscr{G}(x,u,w), \\ &x(t_0) = x_0, \end{aligned} \tag{3.1}$$

where x is the state vector, $\mathscr{G} : \mathbb{R}^{n_x} \times \mathbb{R}^{n_u} \times \mathbb{R}^{n_w} \to \mathbb{R}^{n_x}$ is a continuous function and where the control input u and the disturbances w are such that:

$$U(I) = \{u \in L^2(I),\ \|u(t)\| \leq u_M \ a.e.\ t \in I\}, \tag{3.2}$$

$$W(I) = \{w \in L^2(I),\ \|w(t)\| \leq w_M \ a.e.\ t \in I\}, \tag{3.3}$$

where u_M and w_M are known constant belonging to $\mathbb{R}^{+*}$ and $I \subset [t_0, +\infty[$ is an interval. To simplify the notation we will not further explicit the dependency on I and simply write the set of control input U and the set of disturbances W.

Remark 1. In order to avoid the problem of non differentiability of x at the discontinuous point of the couple control disturbances (u,w), we will consider the integral formulation of the differential problem (3.1), *i.e.* for a given initial data x_0 and for all $t \geq t_0$:

$$x(x_0,u,w,t_0;t) = x_0 + \int_{t_0}^{t} \mathscr{G}(x(x_0,u,w,t_0;s),u,w)ds.$$

In the sequel, $x(x_i,u,w,t_i;t)$ for $t \geq t_i$ will denote the solution (to be understood in an integral form) of the problem (3.1) with initial condition $x(t_i) = x_i$ and a given couple control disturbance (u,w).

Let us make some assumptions on the problem.

Assumption 1. For a given initial condition, the integration of (3.1) with a control input in U and a disturbance in W provides a forward complete trajectory.

Assumption 2. For all bounded x and $\tilde{x} \in \mathbb{R}^{n_x}$, for all bounded $u \in \mathbb{R}^{n_u}$ and for all bounded w and $\tilde{w} \in \mathbb{R}^{n_w}$, the function $\mathscr{G}$ is Lipschitz in x and w, *i.e.* there exists two constants L_x and L_w such that:

$$\begin{aligned} \|\mathscr{G}(x,u,w) - \mathscr{G}(\tilde{x},u,w)\| &\leq L_x \|x - \tilde{x}\|, \\ \|\mathscr{G}(x,u,w) - \mathscr{G}(x,u,\tilde{w})\| &\leq L_w \|w - \tilde{w}\|. \end{aligned} \tag{3.4}$$

Assumption 3. For all bounded $x \in \mathbb{R}^{n_x}$, for all bounded $u \in \mathbb{R}^{n_u}$ and for all bounded $w \in \mathbb{R}^{n_w}$, the function $\mathscr{G}$ verifies the following condition, there exists a constant $K > 0$ such that:

$$\|\mathscr{G}(x,u,w)\| \leq K(1 + \|x\| + \|u\| + \|w\|). \tag{3.5}$$

Theorem 1. *If $\mathscr{G} : \mathbb{R}^{n_x} \times \mathbb{R}^{n_u} \times \mathbb{R}^{n_w} \to \mathbb{R}^{n_x}$ is a continuous function which satisfies Assumptions 2 and 3, then for every integrable function u and w and initial condition $x(t_0) = x_0$ there exists a unique absolutely continuous solution of (3.1).*

Proof. Let us sketch the main idea of the proof. First, we obtain the local existence by proving that the operator $x \to Tx = x_0 + \int_{t_0}^{t} \mathscr{G}(x,u,w)ds$ is a contraction (and then has unique fixed point). Then, using the linear growth of $\mathscr{G}$ (3.5) and similar argument as in continuous case of (u,w), (see e.g. [145]), we can obtain the existence of a global solution on $[t_0; t_0 + T]$. Finally the uniqueness result can be obtained by using the Lipschitz condition on $\mathscr{G}$ and the Gronwall lemma (see appendix section 12.2). □

3.2.3 Control strategy

The control strategy aims at stabilizing the state trajectory to a given set which contains the target, that will be considered as the origin for simplicity reasons. The considered control strategy is an open-loop sampled-data robust MPC controller.

It will be moreover assumed that:

Assumption 4. The right hand side of (3.1) is differentiable and we have $\mathscr{G}(0,0,0) = 0$.

Let us recall the definition of a robust control positive invariant set (see e.g. [18]):

Definition 1 (RCPI set)**.** *A set $\Omega \subset \mathbb{R}^{n_x}$ is said to be a robust controlled positive invariant (RCPI) set for (3.1) if there exists $f : \mathbb{R}^{n_x} \to \mathbb{R}^{n_u}$ a feedback controller, which ensures the existence and uniqueness of the state trajectory and, which is such that for all $x(t_0) \in \Omega$, for all $w \in W$ and for all $t \geq t_0$, we have $x(x(t_0), f(x), w, t_0; t) \in \Omega$.*

Now let us define the retained control strategy:

Definition 2 (SPMPC)**.** *The* saddle point model predictive control *(SPMPC) consists, for a given sampling rate δ, RCPI set $\Omega_a^{f_E}$ and prediction horizon $T > \delta$, in calculating $u(t) = u_i^*(t)$ for $t \in [t_i; t_{i+1}[$ where u_i^* is computed at t_i with respect to the state x_i and the optimal disturbances w_i^*, as the optimal solution of*

$$\begin{gathered} (u_i^*, w_i^*) = \arg \inf_{u \in U} \sup_{w \in W} J^{t_i}(u,w) = \arg \sup_{w \in W} \inf_{u \in U} J^{t_i}(u,w), \\ s.t.\ x(x_i, u, w, t_i; t_i + T) \in \Omega_a^{f_E}. \end{gathered} \tag{3.6}$$

where U and W denote $U([t_i; t_i + T])$ and $W([t_i; t_i + T])$ and $J^{t_i}(u,w)$ is defined as

$$J^{t_i}(u,w) = E(x(x_i, u, w, t_i; t_i + T)) + \int_{t_i}^{t_i + T} F(x(x_i, u, w, t_i; s), u, w)ds, \tag{3.7}$$

where $E : \mathbb{R}^{n_x} \to \mathbb{R}^+$ and $F : \mathbb{R}^{n_x} \times \mathbb{R}^{n_u} \times \mathbb{R}^{n_w} \to \mathbb{R}$.

Remark 2. The considered game is symmetric between the control input u and the disturbances w. Indeed the terminal state constraint is applied to both player. If this raises some questions on the admissible class of system for which it does not restrict the class of admissible disturbances, it enables to use the useful framework of saddle point optimization.

The following assumptions are introduced.

Assumption 5. The stage cost $F : \mathbb{R}^{n_x} \times \mathbb{R}^{n_u} \times \mathbb{R}^{n_w} \to \mathbb{R}$ is continuous in all its arguments and lower bounded such that

$$F(x,u,w) \geq \alpha_F(\|x\|) - \beta_F(\|w\|), \tag{3.8}$$

where α_F and β_F are $\mathscr{K}^\infty$ functions.

Assumption 6. The function $u \in U \to J^{t_i}(u,w)$ is assumed to be convex, lower semi-continuous and Gâteaux-differentiable for all $w \in W$. The function $w \in W \to J^{t_i}(u,w)$ is assumed to be concave, upper semi-continuous and Gâteaux-differentiable for all $u \in U$.

Remark 3. The sets U and W are convex, closed, bounded and non empty. Combined with assumption 6, this implies that J^{t_i} possesses at least one saddle point (see e.g. [10]).

In the sequel we note $V(x(t_i)) = J^{t_i}(u_i^*, w_i^*)$ the value of the game, *i.e.* the value of the cost function at the saddle point. Using the definition of $V(x(t_i))$, we have for all $u \in U$ and for all $w \in W$ the following saddle point inequality:

$$J^{t_i}(u_i^*, w) \leq V(x(t_i)) \leq J^{t_i}(u, w_i^*). \tag{3.9}$$

3.3 Stability analysis

Before further proceeding, let us recall some useful definition. These latter have been adapted in order to cope with the sampling aspect.

First, let us recall the definition of ultimate bounded trajectory (see e.g. [92]).

Definition 3 (UB)**.** *The trajectory of system (3.1) is said to be ultimately bounded (UB) in a set $\mathscr{S} \subset \mathbb{R}^{n_x}$ for initial conditions in $X_E \subset \mathbb{R}^{n_x}$, if for all $x(t_0) \in X_E$, for all $w \in W$, there exists a $N \in \mathbb{N}$ such that for all $k \geq N$ $x(t_k) \in \mathscr{S}$.*

Then, let us recall the definition of ISpS trajectory (see e.g. [92]).

Definition 4 (ISpS)**.** *System (3.1) is said to be ISpS for initial conditions in $X_E \subset \mathbb{R}^{n_x}$ if there exists a $\mathscr{KL}$ function β, a $\mathscr{K}$ function γ and a non negative number D such that for each $x(t_0) \in X_E \subset \mathbb{R}^{n_x}$, for all $w \in W$, for all $k \geq 0$ it holds that at each sampling instant the state trajectory satisfies*

$$\|x(t_k)\| \leq \beta\left(\|x(t_0)\|, k\right) + \gamma\Big(\sup_{t \in [t_0, t_k]}(w)\Big) + D.$$

The main result of this chapter is that the SPMPC strategy makes the controlled system ultimately bounded (UB). The additional assumptions needed to prove this result are given below and some intermediate results on feasibility and various properties of the value function V are presented as lemmas. Particularly, the value function V, is used to define a function that, at each sampling instant, satisfies inequalities (3.32) of discrete ISpS Lyapunov functions (see e.g. [95]). Furthermore with specific assumptions on the cost functions, it is proved that the closed loop system is Input to State practical Stable (ISpS) at each sampling instant.

To prove the stability of the closed-loop trajectory, the following assumptions are made.

Assumption 7. There exists $\Omega_a^{f_E}$, a RCPI set associated with the feedback f_E, which is such that $\|f_E(x)\| \leq u_M$ for all $x \in \Omega_a^{f_E}$.

In the sequel $f_E(x(t))$ denotes the signal resulting from the application of the feedback controller f_E along the controlled state trajectory using this controller.

Assumption 8. There exists $E : \mathbb{R}^{n_x} \to \mathbb{R}^+$ such that for all $x \in \Omega_a^{f_E}$ and for all $w \in W$ we have:

$$\begin{aligned} &a_E(\|x\|) \leq E(x) \leq b_E(\|x\|), \\ &\nabla_x E(x)^T.\mathscr{G}(x, f_E(x), w) + F(x, f_E(x), w) \leq 0, \end{aligned} \tag{3.10}$$

where ∇_x stands for the gradient operator relatively to x and a_E and b_E are $\mathscr{K}^\infty$ functions.

Remark 4. If $x(t)$ is defined as the solution of the following differential equation for a given initial condition $x_0 \in \Omega_a^{f_E}$ and for all $w \in W$:

$$\begin{cases} \dfrac{dx}{dt} = \mathscr{G}(x, f_E(x), w), \\ x(t_0) = x_0, \end{cases}$$

then we have:

$$\begin{aligned} \frac{d}{dt}\left(E(x(t))\right) &= \nabla_x E(x(t))^T.\frac{dx}{dt}(t) \\ &= \nabla_x E(x(t))^T.\mathscr{G}(x(t), f_E(x(t)), w). \end{aligned}$$

Definition 5 (Feasibility)**.** *The control problem is said feasible for a given initial condition $x(t_i) \in X \subset \mathbb{R}^{n_x}$ relatively to a subset $\Omega \subset X$ if there exists at least one couple $(u, w) \in U \times W$ such that $J^{t_i}(u, w) < \infty$ and the terminal state constraint condition $x(x_i, u, w, t_i; t_i + T) \in \Omega$ holds.*

Assumption 9. For a given RCPI set Ω and a final cost $E : \mathbb{R}^{n_x} \to \mathbb{R}^+$, for all $x(t_i) \in X_E$ the saddle point problem (3.6) admits a solution, where $X_E \subset \mathbb{R}^{n_x}$ stands for the set of states such that the control problem is feasible relatively to Ω.

3.3.1 Intermediate results

The following lemma characterizes the conditions on the sampling time and the discrepancy between the optimal and the real disturbances in order for the control problem to remain feasible.

Lemma 1. *Under Assumptions 7 to 9, if $x(t_i) \in X_E$ and if*

$$\sqrt{n_x} L_w \delta \sup_{t \in [t_i; t_{i+1}]} (\|w_i^* - w_i^S\|) e^{\sqrt{n_x} L_x T} < r_i, \tag{3.11}$$

where w_i^S is a disturbances such that $x(x_i, u_i^*, w_i^S, t_i; t_{i+1}) = x(t_{i+1})$ where $x(t_{i+1})$ is the new observation at $t = t_{i+1}$ and r_i is a positive constant such that

$$\{x \in X_E / \|x - x(x_i, u_i^*, w_i^*, t_i; t_i + T)\| \leq r_i\} \subsetneq \Omega_a^{f_E}.$$

Then we have $x(t_{i+1}) \in X_E$.

Proof. Let us define the disturbance w_i^S such that:

$$w_i^S \in L^2(t_i;t_{i+1}) \text{ with } \forall t \in [t_i;t_{i+1}] \ \|w_i^S(t)\| \leq w_M, \tag{3.12}$$

and

$$x(x_i,u_i^*,w_i^S,t_i;t_{i+1}) = x(t_{i+1}). \tag{3.13}$$

It is possible to compute the value of w_i^S by solving an adequate optimization problem.

For all $t \in [t_i;t_i+T]$ let us introduce the signal $\tilde{w}$ defined as follows:

$$\tilde{w}(t) = \begin{cases} w_i^S(t) \text{ if } t \in [t_i;t_{i+1}[, \\ w_i^*(t) \text{ if } t \in [t_{i+1};t_i+T]. \end{cases} \tag{3.14}$$

Since w_i^S verifies (3.12) and $w_i^* \in W$ we have that $\tilde{w} \in W$.

Let us note $\Delta_i x(t) = x(x_i,u_i^*,w_i^*,t_i;t) - x(x_i,u_i^*,\tilde{w},t_i;t)$. As $x(x_i,u_i^*,w_i^*,t_i;t)$ is solution of (3.1) with $u(t) = u_i^*(t)$ and $w(t) = w_i^*(t)$ and $x(x_i,u_i^*,\tilde{w},t_i;t)$ is solution of (3.1) with $u(t) = u_i^*(t)$ and $w(t) = \tilde{w}(t)$, for all $t \in [t_i;t_i+T]$, we have:

$$\begin{aligned} \|\Delta_i x(t)\| &= \| \int_{t_i}^{t} \mathscr{G}(x(x_i,u_i^*,w_i^*,t_i;s),u_i^*,w_i^*) - \mathscr{G}(x(x_i,u_i^*,\tilde{w},t_i;s),u_i^*,\tilde{w})ds\|, \\ &\leq \sqrt{n_x} \int_{t_i}^{t} \|\mathscr{G}(x(x_i,u_i^*,w_i^*,t_i;s),u_i^*,w_i^*) - \mathscr{G}(x(x_i,u_i^*,\tilde{w},t_i;s),u_i^*,\tilde{w})\|ds. \end{aligned}$$

Using the triangular inequality, it is deduced that:

$$\begin{aligned} \|\Delta_i x(t)\| \leq \sqrt{n_x} \int_{t_i}^{t} &\|\mathscr{G}(x(x_i,u_i^*,w_i^*,t_i;s),u_i^*,w_i^*) - \mathscr{G}(x(x_i,u_i^*,w_i^*,t_i;s),u_i^*,\tilde{w})\|ds \\ + \sqrt{n_x} \int_{t_i}^{t} &\|\mathscr{G}(x(x_i,u_i^*,w_i^*,t_i;s),u_i^*,\tilde{w}) - \mathscr{G}(x(x_i,u_i^*,\tilde{w},t_i;s),u_i^*,\tilde{w})\|ds. \end{aligned}$$

Using the Lipschitz condition (3.4) we can deduce that:

$$\|\Delta_i x(t)\| \leq \sqrt{n_x}L_w \int_{t_i}^{t} \|w_i^* - \tilde{w}\|ds + \sqrt{n_x}L_x \int_{t_i}^{t} \|\Delta_i x(s)\|ds. \tag{3.15}$$

According to (3.14) we can deduce that it is possible to rewrite inequality (3.15) as follows:

$$\|\Delta_i x(t)\| \leq \sqrt{n_x}L_w \int_{t_i}^{t_{i+1}} \|w_i^* - w_i^S\|ds + \sqrt{n_x}L_x \int_{t_i}^{t} \|\Delta_i x(s)\|ds. \tag{3.16}$$

And then:

$$\|\Delta_i x(t)\| \leq \sqrt{n_x}L_w\delta \sup_{t\in[t_i;t_{i+1}]} (\|w_i^* - w_i^S\|) + \sqrt{n_x}L_x \int_{t_i}^{t} \|\Delta_i x(s)\|ds. \tag{3.17}$$

Using Gronwall inequality (see 12.2), inequality (3.17) becomes:

$$\|\Delta_i x(t)\| \leq \sqrt{n_x}L_w\delta \sup_{t\in[t_i;t_{i+1}]} (\|w_i^* - w_i^S\|)e^{\sqrt{n_x}L_x(t-t_i)}.$$

In particular for $t = t_i + T$ we have:

$$\|\Delta_i x(t_i+T)\| \leq \sqrt{n_x}L_w\delta \sup_{t\in[t_i;t_{i+1}]} (\|w_i^* - w_i^S\|)e^{\sqrt{n_x}L_x T}.$$

According to (3.11) we have $\sqrt{n_x}L_w\delta \sup_{t\in[t_i;t_{i+1}]}(\|w_i^* - w_i^S\|)e^{\sqrt{n_x}L_xT} < r_i$ so it is deduced that:

$$\|\Delta_i x(t_i+T)\| < r_i.$$

And so we have:

$$\|x(x_i,u_i^*,w_i^*,t_i;t_i+T) - x(x_i,u_i^*,\tilde{w},t_i;t_i+T)\| < r_i \tag{3.18}$$

The ball of center $x(x_i,u_i^*,w_i^*,t_i;t_i+T)$ and radius r_i is strictly contained in $\Omega_a^{f_E}$ (according to the definition of r_i). Using inequality (3.18), it is deduced that

$$x(x_i,u_i^*,\tilde{w},t_i;t_i+T) \in \text{int}(\Omega_a^{f_E}). \tag{3.19}$$

Let us denote $z_1 = x(x_i,u_i^*,\tilde{w},t_i;t_i+T)$. According to (3.19) and as the feedback f_E render $\Omega_a^{f_E}$ robust invariant, it is deduced that for all $t \geq 0$ we have:

$$x(z_1, f_E(x),\tilde{w},t_i+T;t_i+T+t) \in \Omega_a^{f_E}. \tag{3.20}$$

Using the definition of w_i^S we have $x(x_i,u_i^*,\tilde{w},t_i;t_{i+1}) = x(t_{i+1})$, so for all $t \in [0,T-\delta]$ we have $x(x_i,u_i^*,\tilde{w},t_i;t_{i+1}+t) = x(x_{i+1},u_i^*,\tilde{w},t_{i+1};t_{i+1}+t)$, and so it is deduced that (3.20) also holds for $x(z_2, f_E(x),\tilde{w},t_i+T;t_i+T+t)$ where $z_2 = x(x_{i+1},u_i^*,\tilde{w},t_{i+1};t_{i+1}+T)$.

Finally it is deduced that the following couple of strategies (u_{i+1},w_{i+1}) is a feasible solution:

$$u_{i+1}(t) = \begin{cases} u_i^*(t), \text{if } t \in [t_{i+1};t_i+T[, \\ f_E(x(t)), \text{if } t \in [t_i+T;t_{i+1}+T], \end{cases}$$

$$w_{i+1}(t) = \begin{cases} w_i^*(t), \text{if } t \in [t_{i+1};t_i+T[, \\ w(t), \text{if } t \in [t_i+T;t_{i+1}+T], \end{cases}$$

where w is in $L^2(t_i+T;t_{i+1}+T)$ and such that for all $t \in [t_i+T;t_{i+1}+T]$ $\|w(t)\| \leq w_M$. By construction we have $u_{i+1} \in U$ and $w_{i+1} \in W$.

The state trajectory is forward complete and absolutely continuous (see Assumption 1 and theorem 1), so it is quite clear that using (u_{i+1},w_{i+1}), the state trajectory remains bounded (the initial condition, and the couple control disturbances (u_{i+1},w_{i+1}) are bounded). Because the functional E is upper bounded by a $\mathscr{K}^\infty$ function and the functional F is continuous in all its argument, this implies that $J^{t_{i+1}}(u_{i+1},w_{i+1})$ is bounded.

Under the introduced notion of feasibility (see definition 5), this means that the problem remains feasible for the new initial condition $x(t_{i+1})$, *i.e.* if $x(t_i) \in X_E$ then $x(t_{i+1}) \in X_E$. This completes the proof. □

Remark 5. The assumption (3.11) is a sufficient condition which ensures the recursive feasibility of the control problem. This inequality can be interpreted as conditions on the sampling time δ and the control horizon T in order for the problem to remain feasible. Indeed, if we upper bound the term $\sup_{t\in[t_i;t_{i+1}]}(\|w_i^* - w_i^S\|)$, then, on line, we can think to a strategy which uses the current value of r_i to adjust the sampling time or the prediction horizon. It is important to see that the formulation of lemma 1 is highly related to our definition of feasibility and that a stronger definition of this latter will imply a simpler formulation of the former.

Lemma 2 links the discrete variations of the value function V at sampling time to the integral of the stage cost.

Lemma 2. *If the assumptions of lemma 1 hold, then we have:*

$$V(x(t_{i+1}))-V(x(t_i)) \leq -\int_{t_i}^{t_{i+1}} F(x(x_i,u_i^*,w_i^S,t_i;s),u_i^*,w_i^S)ds. \tag{3.21}$$

Proof. Let us compare the value of $J^{t_i}(u_i^*,\overline{w})$ and $J^{t_{i+1}}(\overline{u},w_{i+1}^*)$, where $\overline{u}\in U$ and $\overline{w}\in W$ are defined as follows:

$$\overline{u}(t)=\begin{cases} u_i^*(t), \text{if } t\in[t_{i+1};t_i+T[,\\ f_E(x(t)), \text{if } t\in[t_i+T;t_{i+1}+T],\end{cases}$$

and

$$\overline{w}(t)=\begin{cases} w_i^S(t), \text{if } t\in[t_i;t_{i+1}[,\\ w_{i+1}^*(t), \text{if } t\in[t_{i+1};t_i+T],\end{cases}$$

where w_i^S is defined in lemma 1. The disturbance w_{i+1}^* is well defined because of lemma 1.

First let us express $J^{t_i}(u_i^*,\overline{w})$:

$$\begin{aligned} J^{t_i}(u_i^*,\overline{w}) &= E(x(x_i,u_i^*,\overline{w},t_i;t_i+T))+\int_{t_i}^{t_i+T} F(x(x_i,u_i^*,\overline{w},t_i;s),u_i^*,\overline{w})ds,\\ &= E(x(x_i,u_i^*,w_{i+1}^*,t_i;t_i+T))+\int_{t_i}^{t_{i+1}} F(x(x_i,u_i^*,w_i^S,t_i;s),u_i^*,w_i^S)ds\\ &\quad+\int_{t_{i+1}}^{t_i+T} F(x(x_i,u_i^*,w_{i+1}^*,t_i;s),u_i^*,w_{i+1}^*)ds. \end{aligned} \tag{3.22}$$

Then let us express $J^{t_{i+1}}(\overline{u},w_{i+1}^*)$:

$$\begin{aligned} J^{t_{i+1}}(\overline{u},w_{i+1}^*) &= E(x(x_{i+1},\overline{u},w_{i+1}^*,t_{i+1};t_{i+1}+T))+\int_{t_{i+1}}^{t_{i+1}+T} F(x(x_{i+1},\overline{u},w_{i+1}^*,t_{i+1};s),\overline{u},w_{i+1}^*)ds,\\ &= E(x(x_{i+1},f_E,w_{i+1}^*,t_{i+1};t_{i+1}+T))+\int_{t_{i+1}}^{t_i+T} F(x(x_{i+1},u_i^*,w_{i+1}^*,t_{i+1};s),u_i^*,w_{i+1}^*)ds\\ &\quad+\int_{t_i+T}^{t_i+T} F(x(x_{i+1},f_E,w_{i+1}^*,t_{i+1};s),f_E,w_{i+1}^*)ds. \end{aligned} \tag{3.23}$$

It is deduced from the definition of w_i^S and theorem 1 that for all $t\in[0;T]$ the state trajectories are such that:

$$x(x_i,\overline{u},\overline{w},t_i;t_{i+1}+t)=x(x_{i+1},\overline{u},\overline{w},t_{i+1};t_{i+1}+t).$$

And so, using (3.22) and (3.23), it is deduced that:

$$\begin{aligned} J^{t_{i+1}}(\overline{u},w_{i+1}^*)-J^{t_i}(u_i^*,\overline{w}) &= -\int_{t_i}^{t_{i+1}} F(x(x_i,u_i^*,w_i^S,t_i;s),u_i^*,w_i^S)ds\\ &\quad+E(x(x_{i+1},f_E,w_{i+1}^*,t_{i+1};t_{i+1}+T))-E(x(x_{i+1},u_i^*,w_{i+1}^*,t_{i+1};t_i+T))\\ &\quad+\int_{t_i+T}^{t_{i+1}+T} F(x(x_{i+1},f_E,w_{i+1}^*,t_{i+1};s),f_E,w_{i+1}^*)ds \end{aligned} \tag{3.24}$$

Let us integrate the second inequality of Assumption 8 between t_i+T and $t_{i+1}+T$ with $w(t)=w_{i+1}^*(t)$. Using the remark 4,we obtain the following inequality:

$$\begin{aligned} &E(x(x_{i+1},f_E,w_{i+1}^*,t_{i+1};t_{i+1}+T))-E(x(x_{i+1},u_i^*,w_{i+1}^*,t_{i+1};t_i+T))\\ &+\int_{t_i+T}^{t_{i+1}+T} F(x(x_{i+1},f_E,w_{i+1}^*,t_{i+1};s),f_E,w_{i+1}^*)ds\leq 0. \end{aligned} \tag{3.25}$$

According to (3.25), the inequality (3.24) becomes:

$$J^{t_{i+1}}(\overline{u}, w_{i+1}^*) - J^{t_i}(u_i^*, \overline{w}) \leq -\int_{t_i}^{t_{i+1}} F(x(x_i, u_i^*, w_i^S, t_i; s), u_i^*, w_i^S) ds.$$

Finally using the saddle point inequalities (3.9), we can deduce that:

$$V(x(t_{i+1})) - V(x(t_i)) \leq -\int_{t_i}^{t_{i+1}} F(x(x_i, u_i^*, w_i^S, t_i; s), u_i^*, w_i^S) ds. \tag{3.26}$$

□

Lemma 3 provides an upper-bound of the value function for all states in the final set $\Omega_a^{f_E}$.

Lemma 3. *Under Assumptions 7 and 8, if $x(t_i) \in \Omega_a^{f_E}$ then $V(x(t_i)) \leq E(x(t_i))$.*

Proof. The set $\Omega_a^{f_E}$ is RCPI under the feedback controller f_E. Under Assumption 7, we have for all $x \in \Omega_a^{f_E}$ $\| f_E(x) \| \leq u_M$. As the state trajectory is forward complete and absolutely continuous, the signal $f_E(x(t))$ resulting from the application of the controller f_E along the state trajectory is in $L^2(I)$, where I is an interval of length T.

Assume that $x(t_i) \in \Omega_a^{f_E}$. To avoid possible confusion, let us introduce $f_E^{t_i} \in U$ defined as follows

$$\begin{aligned} f_E^{t_i} : [t_i; t_i + T] &\to \mathbb{R}^{n_u}, \\ t &\to f_E(x(t)). \end{aligned}$$

Using the right hand side of (3.9) with the *a priori* suboptimal control signal $u = f_E^{t_i}$ we have:

$$V(x(t_i)) \leq J^{t_i}(f_E^{t_i}, w_i^*). \tag{3.27}$$

Let us consider the inequality of Assumption 8 along a state trajectory (this makes sense because it is assumed that $x(t_i) \in \Omega_a^{f_E}$) with $w = w_i^*$. Then for all $t \in [t_i; t_i + T]$, we have:

$$\nabla E(x(x_i, f_E^{t_i}, w_i^*, t_i; t))^T . \mathscr{G}(x(x_i, f_E^{t_i}, w_i^*, t_i; t), f_E^{t_i}, w_i^*) + F(x(x_i, f_E^{t_i}, w_i^*, t_i; t), f_E^{t_i}, w_i^*) \leq 0.$$

Let us integrate this inequality between t_i and $t_i + T$, according to remark 4 we obtain:

$$-E(x(t_i)) + E(x(x_i, f_E^{t_i}, w_i^*, t_i; t_i + T)) + \int_{t_i}^{t_i+T} F(x(x_i, f_E^{t_i}, w_i^*, t_i; s), f_E^{t_i}, w_i^*) ds \leq 0. \tag{3.28}$$

Using the expression of $J^{t_i}(f_E^{t_i}, w_i^*)$, inequality (3.28) becomes:

$$J^{t_i}(f_E^{t_i}, w_i^*) - E(x(t_i)) \leq 0.$$

And so using the saddle point inequality (3.9) we deduce that $\forall x(t_i) \in \Omega_a^{f_E}$:

$$V(x(t_i)) \leq E(x(t_i)).$$

□

The previous lemmas 1, 2 and 3 consider properties of the controlled system between two successive sampling instants. From now on, they consider the complete controlled trajectory.

Lemma 4. *Under Assumptions 1 to 6, if the assumptions of lemma 1 hold, then there exists a bounded subset of X_E which contains the origin such that for all bounded $x(t_0) \in X_E$ the state trajectory reaches this subset in finite time, the state trajectory is bounded and there exists a constant $\bar{V} > 0$ such that for all bounded $x \in X_E$ we have $V(x) \leq \bar{V}$.*

Proof. We have $x(t_0) \in X_E$, so $V(x_0)$ is well defined and is finite (because the control and disturbances are bounded and the state trajectory is absolutely continuous and forward complete).

For a given $n \in \mathbb{N}^*$, for all $t \in [t_0, t_n]$, let us introduce the following notation:

$$u^*(t) = u_k^*(t) \ \forall t \in [t_k; t_{k+1}[, \ \forall k \in \{0, \dots, n-1\},$$
$$w^S(t) = w_k^S(t) \ \forall t \in [t_k; t_{k+1}[, \ \forall k \in \{0, \dots, n-1\}.$$

Let us introduce the following set:

$$\mathscr{X} = \{x \in X_E / \alpha_F(\|x\|) \leq \beta_F(w_M) + \varepsilon\},$$

where ε is a strictly positive constant.

First let us prove that for all i the value function V is positive at $x(t_i)$. Using the left hand side of the saddle point inequality (3.9) with a null disturbance signal, we have:

$$V(x(t_i)) \geq J^{t_i}(u_i^*, 0) \geq 0, \ \forall i. \tag{3.29}$$

Now let us prove that the controlled trajectory $x(x_0, u^*, w^S, t_0; t)$ reach $\mathscr{X}$ in finite time. Summing the inequality of lemma 2 and using the inequality (3.29) we have:

$$0 \leq V(x(t_n)) \leq V(x(t_0)) - \int_{t_0}^{t_n} F(x(x_0, u^*, w^S, t_0; s), u^*, w^S) ds,$$

where for all $t \in [t_i; t_{i+1}]$ we have $x(x_0, u^*, w^S, t_0; t) = x(x_i, u_i^*, w_i^S, t_i; t)$.

So it is deduced that:

$$\int_{t_0}^{t_n} F(x(x_0, u^*, w^S, t_0; s), u^*, w^S) ds \leq V(x(t_0)).$$

Using inequality (3.8) we have:

$$\int_{t_0}^{t_n} \alpha_F(\|x(x_0, u^*, w^S, t_0; s)\|) - \beta_F(\|w^S\|) ds \leq V(x(t_0)). \tag{3.30}$$

Let us prove that the state trajectory reach $\mathscr{X}$ in finite time by contradiction. Assume that the state trajectory never reach $\mathscr{X}$, *i.e.* for all $t \geq t_0$ $x(x_0, u^*, w^S, t_0; t) \notin \mathscr{X}$, then for all $s \in [t_0; t_n]$ we have:

$$\alpha_F(\|x(x_0, u^*, w^S, t_0; s)\|) - \beta_F(\|w^S\|) \geq \varepsilon.$$

And so inequality (3.30) becomes:

$$n\delta\varepsilon \leq V(x(t_0)). \tag{3.31}$$

What leads to an absurdity because this inequality holds for all n, ε is constant and $V(x(t_0))$ is finite.

This implies that the state trajectory reaches $\mathscr{X}$ in finite time.

Using lemma 1 we know that if $x(t_0)$ is a feasible initial condition then, for all $k \in \mathbb{N}$, $x(t_k)$ is also a feasible solution. This implies that if the state trajectory leaves $\mathscr{X}$ then it returns in $\mathscr{X}$ in finite time.

As the state trajectory is absolutely continuous and assumed to be forward complete, this implies that the controlled state trajectory remains bounded.

The control input and the disturbances are assumed to belongs to $U \times W$, so they are a.e. bounded. As F is assumed to be continuous in all its arguments and E is upper bounded by a $\mathscr{K}^\infty$ function, this implies that the value function V can not take an infinite value.

According to the expression of V which is a function of F and E, we deduce that for all bounded $x \in X_E$ we have $\sup_{x \in X_E} V(x) < \infty$. So, there exists a positive constant $\bar{V} < \infty$ such that for all $x \in X_E$ we have $V(x) \leq \bar{V}$. □

Lemma 5 introduces a function $\tilde{V}$ that satisfies the inequalities of discrete ISpS Lyapunov functions.

Lemma 5. *Under Assumptions 1 to 6, if the assumptions of lemma 1 hold and if $x(t_0) \in X_E$ is bounded then there exists a function $\tilde{V} : \mathbb{R}^{n_x} \to \mathbb{R}^+$ such that at each sampling instant the following inequalities hold:*

$$\begin{aligned} &\alpha_1(\|x(t_i)\|) \leq \tilde{V}(x(t_i)) \leq \alpha_2(\|x(t_i)\|) + d_1, \\ &\tilde{V}(x(t_{i+1})) - \tilde{V}(x(t_i)) \leq -\alpha_3(\|x(t_i)\|) + \sigma(w_M) + d_2, \end{aligned} \tag{3.32}$$

where $(\alpha_j)_{j=1,\ldots,3}$ are in $\mathscr{K}^\infty$, σ is in $\mathscr{K}$ and $(d_k)_{k=1,2}$ are in $\mathbb{R}^+$.

Proof. Let us prove first that the value function V can be upper bounded by a $\mathscr{K}^\infty$ function. We remind that because of lemma 4, we know that for all bounded $x \in X_E$ there exists $\bar{V} > 0$ such that the value function is uniformly bounded, *i.e.* for all $x \in X_E$ we have $V(x) \leq \bar{V}$.

First, let us assume that $x(t_i) \in \Omega_a^{f_E}$.

Using lemma 3 and Assumption 8, we have:

$$V(x(t_i)) \leq E(x(t_i)) \leq b_E(\|x(t_i)\|). \tag{3.33}$$

Let us now consider the case where $x(t_i) \notin \Omega_a^{f_E}$.

Let us call $r \in \mathbb{R}^{+*}$ a constant such that $\{x \in X_E / \|x\| \leq r\} \subset \Omega_a^{f_E}$ and note $K = \max\left(1, \dfrac{\bar{V}}{b_E(r)}\right)$.

As $x(t_i) \notin \Omega_a^{f_E}$, we have $x \notin \{x \in X_E / \|x\| \leq r\}$ what implies that $\|x(t_i)\| > r$. So it is deduced that for all $x(t_i) \notin \Omega_a^{f_E}$ we have $\dfrac{b_E(\|x(t_i)\|)}{b_E(r)} > 1$ and so finally we have:

$$V(x(t_i)) \leq \bar{V} \leq \bar{V}\frac{b_E(\|x(t_i)\|)}{b_E(r)} \leq K b_E(\|x(t_i)\|). \tag{3.34}$$

This enables us to conclude on the upper bound of V by a $\mathscr{K}^\infty$ function. Indeed, as $K \geq 1$, according to (3.33) and(3.34), for all $x(t_i) \in X_E$ we have that:

$$V(x(t_i)) \leq \beta_E(\|x(t_i)\|), \tag{3.35}$$

where

$$\beta_E(s) = K b_E(s). \tag{3.36}$$

Let us now consider the lower bound on V and the upper bound on its variations.

First as $x(t_0) \in X_E$, using lemma 1, it is deduced that, for all $i \in \mathbb{N}$, $x(t_i) \in X_E$. So, using theorem 1 , it is deduced that the state trajectory is absolutely continuous with respect to time. This implies that it is

uniformly continuous with respect to time. This means that for all $\theta > 0$, there exists $\xi(\theta) > 0$ such that for any couple control disturbance $(u,w) \in U \times W$ we have:

$$\|x(x_i,u,w,t_i;t) - x(t_i)\| \leq \theta,\ \forall t\ s.t.\ |t-t_i| \leq \xi(\theta).$$

And so using the triangular inequality it is deduced that for all t such that $|t-t_i| \leq \xi(\theta)$ we have:

$$\|x(t_i)\| - \theta \leq \|x(x_i,u,w,t_i;t)\|. \tag{3.37}$$

To further proceed, let us distinguish two cases depending on whether we have $\|x(t_i)\| > \theta$ by introducing a constant $\varepsilon > 0$ and comparing $\|x(t_i)\|$ with $\theta + \varepsilon$.

i) **Case 1: if** $\|x(t_i)\| \geq \theta + \varepsilon > \theta$**,**

In this case the left hand side of inequality (3.37) can be lower bounded as follows:

$$\underline{c}\|x(t_i)\| < \|x(t_i)\| - \theta \leq \|x(x_i,u,w,t_i;t)\|, \tag{3.38}$$

where $\underline{c} = \dfrac{\varepsilon}{\varepsilon+\theta}$.

Using inequalities (3.8) we can deduce that:

$$\begin{aligned}\int_{t_i}^{t_i+\delta} F(x(x_i,u,w,t_i;s),u,w)ds &\geq \int_{t_i}^{t_i+\delta} \alpha_F(\|x(x_i,u,w,t_i;s)\|) - \beta_F(\|w\|)ds,\\ &\geq \int_{t_i}^{t_i+r(\theta)} \alpha_F(\|x(x_i,u,w,t_i;s)\|)ds - \delta\beta_F(w_M),\end{aligned} \tag{3.39}$$

where $r(\theta) = \min(\delta, \xi(\theta))$, and then (according to (3.38)):

$$\begin{aligned}\int_{t_i}^{t_i+\delta} F(x(x_i,u,w,t_i;s),u,w)ds &\geq \int_{t_i}^{t_i+r(\theta)} \alpha_F(\underline{c}\|x(t_i)\|)ds - \delta\beta_F(w_M),\\ &\geq r(\theta)\alpha_F(\underline{c}\|x(t_i)\|) - \delta\beta_F(w_M),\\ &\geq r(\theta)\alpha_F(\frac{\underline{c}}{2}\|x(t_i)\|) - \delta\beta_F(w_M).\end{aligned} \tag{3.40}$$

In the sequel let us introduce the following $\mathscr{K}^\infty$ function:

$$\begin{aligned}\alpha_F^0(s) &= r(\theta)\alpha_F(\frac{\underline{c}}{2}s),\\ \beta_F^0(s) &= \delta\beta_F(s).\end{aligned} \tag{3.41}$$

Let us prove that the value function is lower bounded by a $\mathscr{K}^\infty$ function.

Using the definition of a saddle point (3.9) we have:

$$V(x(t_i)) \geq J^{t_i}(u_i^*, 0). \tag{3.42}$$

Using (3.8) and (3.38) it is deduced (as to obtain (3.40)) that for the couple control disturbances $(u_i^*, 0)$ we have:

$$\int_{t_i}^{t_i+\delta} F(x(x_i,u_i^*,0,t_i;s),u_i^*,0)ds \geq \alpha_F^0(\|x(t_i)\|). \tag{3.43}$$

Using the definition of $J^{t_i}(u_i^*,0)$ and inequality (3.43) we have:

$$\begin{aligned} J^{t_i}(u_i^*,0) &= E(x(x_i,u_i^*,0,t_i;t_i+T)) + \int_{t_i}^{t_i+T} F(x(x_i,u_i^*,0,t_i;s),u_i^*,0)ds, \\ &\geq \int_{t_i}^{t_i+\delta} F(x(x_i,u_i^*,0,t_i;s),u_i^*,0)ds, \\ &\geq \alpha_F^0(\|x(t_i)\|). \end{aligned} \tag{3.44}$$

So finally combining inequalities (3.42) and (3.44) it is deduced that we have:

$$V(x(t_i)) \geq \alpha_F^0(\|x(t_i)\|). \tag{3.45}$$

Finally let us compute an upper bound on the difference $V(x(t_{i+1})) - V(x(t_i))$.
Using the results of lemma 2 we have:

$$V(x(t_{i+1})) - V(x(t_i)) \leq -\int_{t_i}^{t_{i+1}} F(x(x_i,u_i^*,w_i^S,t_i;s),u_i^*,w_i^S)ds.$$

And so using the inequalities (3.40) it is deduced that we have:

$$V(x(t_{i+1})) - V(x(t_i)) \leq -\alpha_F^0(\|x(t_i)\|) + \beta_F^0(w_M). \tag{3.46}$$

ii) **Case 2: if** $\|x(t_i)\| \leq \theta + \varepsilon$**,**

In this case we can not state on the sign of $\|x(t_i)\| - \theta$. However it is possible to rewrite inequality (3.37) as follows:

$$0 < \|x(t_i)\| + \varepsilon \leq \|x(x_i,u,w,t_i;t)\| + \theta + \varepsilon.$$

We have:

$$\|x(t_i)\| + \varepsilon \geq (1 + \frac{\varepsilon}{\varepsilon+\theta})\|x(t_i)\| \geq \frac{\varepsilon}{\varepsilon+\theta}\|x(t_i)\|.$$

So if $\|x(t_i)\| \leq \theta + \varepsilon$ we have:

$$\underline{c}\|x(t_i)\| \leq \|x(x_i,u,w,t_i;t)\| + \theta + \varepsilon. \tag{3.47}$$

Let us add and subtract $r(\theta)\alpha_F(\theta+\varepsilon)$ on the right hand side of (3.39). We can deduce that:

$$\begin{aligned} \int_{t_i}^{t_i+\delta} F(x(x_i,u,w,t_i;s),u,w)ds \geq \int_{t_i}^{t_i+r(\theta)} &\alpha_F(\|x(x_i,u,w,t_i;s)\|) + \alpha_F(\theta+\varepsilon)ds \\ &- \delta\beta_F(w_M) - r(\theta)\alpha_F(\theta+\varepsilon). \end{aligned}$$

Using the properties of $\mathscr{K}$ function (item 12 of proposition 2, see 12.1) we have:

$$\begin{aligned} \int_{t_i}^{t_i+\delta} F(x(x_i,u,w,t_i;s),u,w)ds \geq \int_{t_i}^{t_i+r(\theta)} &\alpha_F(\frac{1}{2}(\|x(x_i,u,w,t_i;s)\| + \theta + \varepsilon))ds \\ &- \delta\beta_F(w_M) - r(\theta)\alpha_F(\theta+\varepsilon). \end{aligned}$$

And so finally using inequality (3.47), it is deduced that we have:

$$\begin{aligned} \int_{t_i}^{t_i+\delta} F(x(x_i,u,w,t_i;s),u,w)ds &\geq \int_{t_i}^{t_i+r(\theta)} \alpha_F(\frac{\underline{c}}{2}\|x(t_i)\|)ds - \delta\beta_F(w_M) - r(\theta)\alpha_F(\theta+\varepsilon), \\ &\geq r(\theta)\alpha_F(\frac{\underline{c}}{2}\|x(t_i)\|) - \delta\beta_F(w_M) - r(\theta)\alpha_F(\theta+\varepsilon). \end{aligned}$$

So finally, with the same steps as in case i), the following inequalities are deduced:

$$\begin{aligned} &\alpha_F^0(\|x(t_i)\|) \leq V(x(t_i)) + r(\theta)\alpha_F(\theta+\varepsilon), \\ &V(x(t_{i+1})) - V(x(t_i)) \leq -\alpha_F^0(\|x(t_i)\|) + \beta_F^0(w_M) + r(\theta)\alpha_F(\theta+\varepsilon). \end{aligned} \tag{3.48}$$

Conclusion

Let us define the function $\tilde{V}(x(t_i)) = V(x(t_i)) + r(\theta)\alpha_F(\theta+\varepsilon)$. From (3.45) and (3.46) in case one, (3.48) in case two and (3.35), it is deduced that

$$\begin{aligned} &\alpha_F^0(\|x(t_i)\|) \leq \tilde{V}(x(t_i)) \leq \beta_E(\|x(t_i)\|) + r(\theta)\alpha_F(\theta+\varepsilon), \\ &\tilde{V}(x(t_{i+1})) - \tilde{V}(x(t_i)) \leq -\alpha_F^0(\|x(t_i)\|) + \beta_F^0(w_M) + r(\theta)\alpha_F(\theta+\varepsilon), \end{aligned} \tag{3.49}$$

where $r(\theta) = \min(\delta, \xi(\theta))$, α_F is defined in (3.8), α_F^0 and β_F^0 are defined in (3.41) and β_E is defined in (3.36).

So finally we have defined a function $\tilde{V}(x(t_i))$ such that there exists three $\mathscr{K}^\infty$ functions $\alpha_1 = \alpha_F^0$, $\alpha_2 = \beta_E$ and $\alpha_3 = \alpha_F^0$, one $\mathscr{K}$ function $\sigma = \beta_F^0$ and two non negative constants $d_1 = r(\theta)\alpha_F(\theta+\varepsilon)$ and $d_2 = r(\theta)\alpha_F(\theta+\varepsilon)$ which verify inequalities (3.32). □

3.3.2 Main results

Now we are in position to prove the required properties on the closed-loop trajectory. First, at each sampling instant the state trajectory is proved to be UB. This result is adapted from the proof of robust stability of min-max discrete MPC controllers (see e.g. [94]) thanks to the function $\tilde{V}$ of lemma 5. Then supplementary assumptions on the previously introduced $\mathscr{K}$ and $\mathscr{K}^\infty$ functions leads to ISpS results.

Theorem 2. *Under Assumptions 1 to 6, if the assumptions of lemma 1 hold and if $x(t_0) \in X_E$ is bounded, then under the SPMPC controller, at each sampling instant, the state trajectory is UB relatively to a subset of X_E which contains the origin, and is asymptotically stabilized to a bounded subset which contains the origin.*

Proof. The proof can be obtained by proceeding in three steps. First, the function $\tilde{V}$ defined in lemma 5 is used to define a set Θ that is proved invariant. Then, a parametrized set of supersets Θ_λ are introduced and used to prove the UB property. Finally the trajectories are proved to asymptotically reach the set Θ.

In the sequel the variable θ, $r(\theta)$ and ε and the functions β_E, α_F, α_F^0 and β_F^0 are the same as introduced in the proof of lemma 5.

(i) **Prove that there exists a subset $\Theta \subsetneq X_E$ which is invariant under the considered control law,**

Using the function $\tilde{V}$ of lemma 5, let us prove that there exists $b \in \mathscr{K}$ and $c \in \mathbb{R}^+$ such that the set $\Theta = \{x \in X_E / \tilde{V}(x) \leq b(w_M) + c\} \subsetneq X_E$ is invariant at each sampling instant, *i.e.* if $x(t_i) \in \Theta$ then for all $k \in \mathbb{N}$ $x(t_{i+k}) \in \Theta$.

Using the properties of $\mathscr{K}$ function (item 11 of proposition 2, see 12.1), we have:

$$\beta_E(\|x(t_i)\|) + r(\theta)\alpha_F(\theta+\varepsilon) \leq \beta_E(\|x(t_i)\| + \theta + \varepsilon) + r(\theta)\alpha_F(\|x(t_i)\| + \theta + \varepsilon). \tag{3.50}$$

According to the right hand side of the first inequality of (3.49) and inequality (3.50), we have:

$$\tilde{V}(x(t_i)) \leq \beta_E^0(\|x(t_i)\| + \theta + \varepsilon), \tag{3.51}$$

where

$$\beta_E^0(s) = \beta_E(s) + r(\theta)\alpha_F(s). \tag{3.52}$$

Since $\beta_E^0 \in \mathscr{K}^\infty$, its inverse function exists, and then (3.51) becomes:

$$\|x(t_i)\| + \theta + \varepsilon \geq (\beta_E^0)^{-1}(\tilde{V}(x(t_i))). \tag{3.53}$$

Let $\gamma(.)$ be a given $\mathscr{K}^\infty$ function and let us consider the following $\mathscr{K}^\infty$ function:

$$\underline{\alpha_F^0}(s) = \min(\alpha_F^0(\frac{s}{2}), \gamma(\frac{s}{2})).$$

Using the properties of $\mathscr{K}^\infty$ functions (item 12 of property 2, see 12.1) and inequality (3.53) we have:

$$\begin{aligned} \alpha_F^0(\|x(t_i)\|) + \gamma(\theta+\varepsilon) &\geq \underline{\alpha_F^0}(\|x(t_i)\| + \theta + \varepsilon) \\ &\geq \underline{\alpha_F^0} \circ (\beta_E^0)^{-1}(\tilde{V}(x(t_i))). \end{aligned} \tag{3.54}$$

Using inequalities (3.49) we have:

$$\tilde{V}(x(t_{i+1})) \leq \tilde{V}(x(t_i)) - \alpha_F^0(\|x(t_i)\|) + \beta_F^0(w_M) + r(\theta)\alpha_F(\theta+\varepsilon).$$

Adding and subtracting $\gamma(\theta+\varepsilon)$ on the right hand side of the previous inequality and using inequality (3.54) it is deduced that we have:

$$\tilde{V}(x(t_{i+1})) \leq (id - \underline{\alpha_F^0} \circ (\beta_E^0)^{-1})(\tilde{V}(x(t_i))) + \gamma(\theta+\varepsilon) + \beta_F^0(w_M) + r(\theta)\alpha_F(\theta+\varepsilon). \tag{3.55}$$

As a composition of two $\mathscr{K}^\infty$ functions, $\underline{\alpha_F^0} \circ (\beta_E^0)^{-1}$ is a $\mathscr{K}^\infty$ function, it is deduced that there exists a $\mathscr{K}^\infty$ function ϑ which verifies the following inequality (item 13 of property 3, see 12.1):

$$\vartheta(s) \leq \underline{\alpha_F^0} \circ (\beta_E^0)^{-1}(s). \tag{3.56}$$

and which is such that $s - \vartheta(s)$ is a $\mathscr{K}$ function.

To simplify the notation, let us introduce the following function:

$$\rho(s) = \gamma(s) + r(\theta)\alpha_F(s). \tag{3.57}$$

Using the functions defined in (3.56) and (3.57), (3.55) becomes:

$$\tilde{V}(x(t_{i+1})) \leq (id - \vartheta)(\tilde{V}(x(t_i))) + \rho(\theta+\varepsilon) + \beta_F^0(w_M). \tag{3.58}$$

Assume that $x(t_i) \in \Theta$, then we have that $\tilde{V}(x(t_i)) \leq b(w_M) + c$. As $id - \vartheta \in \mathscr{K}$, and so is increasing, it is deduced that (3.58) becomes:

$$\tilde{V}(x(t_{i+1})) \leq (id - \vartheta)(b(w_M) + c) + \rho(\theta+\varepsilon) + \beta_F^0(w_M). \tag{3.59}$$

Let us choose:

$$\begin{aligned} b &= (\vartheta)^{-1} \circ (2\beta_F^0) \in \mathscr{K}^\infty, \\ c &= (\vartheta)^{-1} \circ (2\rho)(\theta+\varepsilon) \in \mathbb{R}^+. \end{aligned} \tag{3.60}$$

Using (3.60) and item 12 of property 2 (see 12.1, in the special case when $\theta_1 = \theta_2$) we deduce that:

$$b(w_M) + c \geq (\vartheta)^{-1}\left(\beta_F^0(w_M) + \rho(\theta+\varepsilon)\right). \tag{3.61}$$

So finally using (3.61), (3.59) becomes:

$$\tilde{V}(x(t_{i+1})) \leq b(w_M) + c.$$

This implies that $x(t_{i+1}) \in \Theta$. Thus it is possible to show that if $x(t_i) \in \Theta$, then for all $k \in \mathbb{N}$, we have $x(t_{i+k}) \in \Theta$. This proves that the introduced set Θ is invariant.

(ii) **Let us prove now that the state trajectory is UB relatively to Θ_λ.**

Let us introduce the following set:

$$\Theta_\lambda = \{x \in X_E / \tilde{V}(x) \leq b(w_M) + c + \lambda\},$$

where $\lambda > 0$.

First it is proved that Θ_λ is invariant at each sampling time, using the same proof as for Θ. Indeed the only point which changes is inequality (3.59) which becomes:

$$\tilde{V}(x(t_{i+1})) \leq (id - \vartheta)(b(w_M) + c + \lambda) + \rho(\theta + \varepsilon) + \beta_F^0(w_M). \tag{3.62}$$

Using item 10 of property on $\mathscr{K}$ functions (see 12.1), inequality (3.62) becomes:

$$\tilde{V}(x(t_{i+1})) \leq (id - \vartheta)(b(w_M) + c) + (id - \vartheta)(\lambda) + \rho(\theta + \varepsilon) + \beta_F^0(w_M).$$

And so finally we conclude that if we have $\tilde{V}(x(t_i)) \leq b(w_M) + c + \lambda$ then we have:

$$\tilde{V}(x(t_{i+1})) \leq b(w_M) + c + \lambda,$$

what proves that Θ_λ is invariant.

Let us introduce the following notation:

$$V_l = b(w_M) + c > 0,$$
$$V_{l,\lambda} = b(w_M) + c + \lambda > V_l.$$

Let us prove the set Θ_λ is reached in finite time.

Inequality (3.58) can be rewritten:

$$\tilde{V}(x(t_{i+1})) - \tilde{V}(x(t_i)) \leq -\vartheta(\tilde{V}(x(t_i))) + \beta_F^0(w_M) + \rho(\theta + \varepsilon), \tag{3.63}$$

and inequality (3.61):

$$\vartheta(V_l) \geq \beta_F^0(w_M) + \rho(\theta + \varepsilon). \tag{3.64}$$

So, from (3.63) it comes:

$$\tilde{V}(x(t_{i+1})) - \tilde{V}(x(t_i)) \leq -\vartheta(\tilde{V}(x(t_i))) + \vartheta(V_l). \tag{3.65}$$

Assume that for all $k \geq 0$, $x(t_{i+k}) \notin \Theta_\lambda$ then, as $\vartheta \in \mathscr{K}$, we have:

$$-\vartheta(\tilde{V}(x(t_i))) \leq -\vartheta(V_{l,\lambda}). \tag{3.66}$$

It is then deduced from (3.65) that:

$$\tilde{V}(x(t_{i+1})) - \tilde{V}(x(t_i)) \leq -\vartheta(V_{l,\lambda}) + \vartheta(V_l),$$

and recursively that for all $k \geq 0$:

$$V_{l,\lambda} \leq \tilde{V}(x(t_{i+k})) \leq \tilde{V}(x(t_i)) - k(\vartheta(V_{l,\lambda}) - \vartheta(V_l)).$$

As $\vartheta \in \mathscr{K}$, for $\lambda > 0$ small enough, we have $\vartheta(V_{l,\lambda}) - \vartheta(V_l) > 0$. As the value of $\tilde{V}(x(t_i))$ is bounded, the previous inequality leads to falsify the assumption. So it exists N such that $x(t_{i+N}) \in \Theta_\lambda$.

So, for some $\lambda > 0$ small enough, the set $\Theta_\lambda^- \subset \mathbb{R}^{n_x}$ is such that for all initial condition $x(t_0) \in X_E$, there exists $N \in \mathbb{N}$, such that, for all $w \in W$, for all $k \geq N$, $x(t_k) \in \Theta_\lambda^-$ (convergence in finite time and invariance property). The state trajectory is then UB in the set Θ_λ^-.

(iii) **Finally, prove that the state trajectory asymptotically converges toward Θ.**

First, it is straightforward to prove that the previous conclusion also holds for all sets Θ_λ where $\lambda \leq \bar{\lambda}$. Let us then introduce the following strictly decreasing sequence $(\lambda_n)_{n\in\mathbb{N}}$ that converges toward 0 defined as follows:

$$\lambda_n = \frac{\bar{\lambda}}{2^n}.$$

Since the sequence Θ_{λ_n} is strictly decreasing in the sense of the inclusion, we have:

$$\Theta = \bigcap_{n\in\mathbb{N}} \Theta_{\lambda_n}$$

So, it is deduced that the state trajectory is asymptotically stabilized in Θ. □

Now, let us prove that under supplementary assumptions on the stage cost F and the final cost E, the system is ISpS at each sampling instant.

Theorem 3. *Under Assumptions 1 to 6, if the assumptions of lemma 1 hold and if $x(t_0) \in X_E$ is bounded, if there exists $a,b,\lambda \in \mathbb{R}^{*+}$ with $a < b$ such that $\alpha_F^0(s) \geq as^\lambda$ and $\beta_E(s) \leq bs^\lambda$ then under the SPMPC controller, at each sampling instant, the system is ISpS.*

Proof. Using lemma 5 to only consider sampling instant, the idea of the proof is inspired from the proof in the full discrete setting (see e.g. [95]).

Using the assumptions on α_F^0 and β_E, the inequalities (3.49) of lemma 5 become:

$$\begin{aligned} &a\|x(t_i)\|^\lambda \leq \tilde{V}(x(t_i)) \leq b\|x(t_i)\|^\lambda + r(\theta)\alpha_F(\theta+\varepsilon), \\ &\tilde{V}(x(t_{i+1})) - \tilde{V}(x(t_i)) \leq -a\|x(t_i)\|^\lambda + \beta_F^0(\|w_M\|) + r(\theta)\alpha_F(\theta+\varepsilon). \end{aligned} \tag{3.67}$$

To simplify the notation, let d denotes $d = r(\theta)\alpha_F(\theta+\varepsilon)$.

The right hand-side of the first inequality of (3.67) is used to get a lower bound of $\|x(t_i)\|^\lambda$ that leads to:

$$\tilde{V}(x(t_i)) - a\|x(t_i)\|^\lambda \leq \left(1 - \frac{a}{b}\right)\tilde{V}(x(t_i)) + \frac{a}{b}d. \tag{3.68}$$

Let us introduce $\tau = \dfrac{a}{b} \in]0;1[$, since it is assumed that $a < b$.

Using (3.68), the second inequalities of (3.67) becomes:

$$\begin{aligned} \tilde{V}(x(t_{i+1})) &\leq \tilde{V}(x(t_i)) - a\|x(t_i)\|^\lambda + \beta_F^0(\|w_M\|) + d, \\ &\leq (1-\tau)\tilde{V}(x(t_i)) + \beta_F^0(\|w_M\|) + (1+\tau)d. \end{aligned}$$

And so we have:

$$\begin{aligned} \tilde{V}(x(t_{i+1})) &\leq (1-\tau)^{i+1}\tilde{V}(x(t_0)) + \left(\beta_F^0(\|w_M\|) + (1+\tau)d\right)\sum_{k=0}^{i}(1-\tau)^k, \\ &\leq (1-\tau)^{i+1}\tilde{V}(x(t_0)) + \left(\beta_F^0(\|w_M\|) + (1+\tau)d\right)\frac{1}{\tau}(1-(1-\tau)^{i+1}). \end{aligned} \tag{3.69}$$

Combining (3.69) with the left hand side of the first inequality of (3.67), when $i = 0$, we have:

$$\begin{aligned} \tilde{V}(x(t_{i+1})) &\leq (1-\tau)^{i+1}(b\|x(t_0)\|^\lambda + d) + (\beta_F^0(\|w_M\|) + (1+\tau)d)\frac{1}{\tau}(1-(1-\tau)^{i+1}), \\ &\leq (1-\tau)^{i+1}b\|x(t_0)\|^\lambda + \frac{1}{\tau}\beta_F^0(\|w_M\|) + \left(1+\frac{1}{\tau}\right)d. \end{aligned} \tag{3.70}$$

Combining (3.70) with the right hand side of the first inequality of (3.67) we have:

$$a\|x(t_{i+1})\|^{\lambda} \leq (1-\tau)^{i+1} b\|x(t_0)\|^{\lambda} + \frac{1}{\tau}\beta_F^0(\|w_M\|) + \left(1+\frac{1}{\tau}\right) d. \tag{3.71}$$

Furthermore, using the convexity property of the function $s \to s^{1/\lambda}$, $\forall x,y,z \geq 0$ we have:

$$(x+y+z)^{\frac{1}{\lambda}} \leq (3x)^{\frac{1}{\lambda}} + (3y)^{\frac{1}{\lambda}} + (3z)^{\frac{1}{\lambda}}. \tag{3.72}$$

So combining (3.72) and (3.71) we deduce the following inequality:

$$\begin{aligned} \|x(t_{i+1})\| &\leq \left(\frac{3}{a}((1-\tau)^{i+1} b\|x(t_0)\|^{\lambda})\right)^{\frac{1}{\lambda}} + \left(\frac{3}{a\tau}\beta_F^0(\|w_M\|)\right)^{\frac{1}{\lambda}} + \left(\frac{3}{a}(1+\frac{1}{\tau})d\right)^{\frac{1}{\lambda}} \\ &\leq \left(\frac{3}{a}((1-\tau)^{i+1} b)\right)^{\frac{1}{\lambda}} \|x(t_0)\| + \left(\frac{3}{a\tau}\beta_F^0(\|w_M\|)\right)^{\frac{1}{\lambda}} + \left(\frac{3}{a}(1+\frac{1}{\tau})d\right)^{\frac{1}{\lambda}}. \end{aligned} \tag{3.73}$$

To conclude, we have found a $\mathscr{KL}$ function $\beta((x_0,i)) = \left(\frac{3}{a}((1-\tau)^{i+1} b)\right)^{\frac{1}{\lambda}} \|x_0\|$, a $\mathscr{K}$ function $\gamma(s) = \left(\frac{3}{a\tau}\beta_F^0(s)\right)^{\frac{1}{\lambda}}$ and a non negative constant $D = \left(\frac{3}{a}(1+\frac{1}{\tau})d\right)^{\frac{1}{\lambda}}$ such that:

$$\|x(t_i)\| \leq \beta((x(t_0),i)) + \gamma(\|w_M\|) + D.$$

According to definition 4, this proves that at each sampling instant the system is ISpS. □

So far, we have presented a SPMPC controller and have proved that under some assumptions this controller ensure good stability properties of the closed-loop system. To ensure these properties, one of the central issue is to satisfy Assumptions 7 and 8. These assumptions deal with the existence of a final cost E and the existence of a robust controlled positive invariant set $\Omega_a^{f_e}$. The aim of the next section is to present algorithms to compute these elements for a given control problem.

3.4 Formulation of the final cost and the terminal state constraint

3.4.1 Formulation of the problem

One of the key issue with MPC controller is the stability property of the closed-loop. To ensure good properties of the controller, one of the classical method consists in adding a final cost and a terminal set constraint in the optimization problem, see e.g. [26]. As for NMPC, it has been proved that by adding a final cost and a terminal state constraint in the optimization problem, the SPMPC controller ensures good stability properties. Using what is classically done in the framework of a NMPC controller (see e.g. [110]), the aim of this section is to present algorithms to compute these elements in the framework of the here presented controller.

To do so, we will assume that the system dynamic is described by (3.1) (possibly to be understood in an integral form). In the sequel it is assumed that the assumptions 1 to 4 are satisfied. Also, we will consider a quadratic stage cost

$$F(x,u,w) = \|x\|_R^2 + \|u\|_\alpha^2 - \|w\|_Q^2, \tag{3.74}$$

where R, α and Q are symmetric definite positive matrices (it is clear that F satisfies Assumption 5 with $\alpha_F(\|x\|) = \lambda_{min}(R)\|x\|^2$ and $\beta_F(\|w\|) = \lambda_{max}(Q)\|w\|^2$).

To solve the final cost problem, we are interested in computing a control input f_E which locally stabilizes the system. Practically, this controller won't be applied to the system. Indeed, in the previously presented control strategy, we have retained a quasi-infinite strategy [26]. This means that the final controller is just used to provide an upper bound on the value function V but will never be really applied to control the system. This implies that we are not interested in finding efficient controller but more in finding a simple one. That is why we will look for a simple linear state feedback. The main advantage of this choice is that, using an adequate local formulation of the system dynamic, it becomes possible to search for a quadratic final cost. As for the terminal state constraint, it will be chosen as a level set of E. More precisely, the final cost, the terminal state constraint and the corresponding controller will be chosen as follows:

$$\begin{aligned} &E(x) = x^T S x,\ x \in \mathbb{R}^{n_x}, \\ &f_E(x) = Kx,\ x \in \mathbb{R}^{n_x}, \\ &\Omega_a^{f_E} = \{x \in X_E / E(x) \leq \gamma\}, \end{aligned} \tag{3.75}$$

where $S \in \mathbb{R}^{n_x,n_x}$ is a symmetric definite positive matrix, $K \in \mathbb{R}^{n_x,n_u}$ and $\gamma \in \mathbb{R}^{+*}$ will be chosen such that all the supplementary constraints on the state and on the control input are satisfied within the corresponding subspace.

In this section, we will present two algorithms to compute a final cost and a terminal state constraint based on differential inclusion representation. The concept of differential inclusion is a generalization of the concept of differential equation (see e.g. [17]) where the derivatives is no longer equal to a function but belongs to a given set. The first algorithm will rely on a local polytopic linear differential inclusion (LDI) embedding of the full nonlinear disturbed dynamics (3.1). The second algorithm will assume that a linear representation of (3.1) through introduction of a norm bounded differential inclusion is possible. In both cases, the idea is to recast the original problem of computing a final cost and a RCPI set using linear matrix inequalities. Thus, using usual LMI solvers, e.g. the Matlab toolbox [55], the original problem will be solved. Also, in order to simplify the computation, we will consider strict inequalities for the inequalities (3.10). Of course, the thus obtained final cost will then satisfy Assumption 8. Finally, in a last part the previously presented algorithm will be adjusted in order to take into account supplementary constraints on the control input and on the state.

This section is organized as follows. First an algorithm to compute a final cost through a polytopic LDI is presented. Then an algorithm to compute a final cost through a norm bounded LDI is presented. Finally, an algorithm to compute the parameter γ which defines the terminal state constraint is presented for the two previous algorithms.

3.4.2 Formulation via Polytopic Linear Differential Inclusion

First, we will be interested in representing (locally) the original differential equation (3.1) via a polytopic linear differential inclusion (PLDI). This corresponds to the special case of a differential inclusion where the derivative belongs to a set which is described by a convex set of finite vertices and each vertex is described by a linear function. To solve the final cost and the terminal state constraint computation problem, we will be interested in controlling this PLDI. Because it is assumed that the considered control problem satisfies Assumption 4, then a local PLDI embedding is possible (see e.g. [19]).

Many papers have dealt with the problem of controlling such a LDI, see e.g. [75] and the references therein. Even if it is well known that for a PLDI a convex hull Lyapunov function provides controller

which show better performances (see e.g. [74]), for simplicity reasons, we will focus on the problem of finding a common (quadratic) Lyapunov function (and a corresponding controller) for all vertices. By doing so, the final cost will simply be equal to this Lyapunov function and the terminal state constraint will be defined as a level-set of the final cost. The main drawback of this approach is that the subset corresponding to the terminal state constraint will be possibly small.

In the sequel, let us assume that, locally, the full nonlinear system (3.1) is embedded in the following PLDI:

$$\frac{dx}{dt} \in \text{co}\{A_i x + B_{1,i} w + B_{2,i} u,\ i = 1,\dots,N\}, \tag{3.76}$$

where co$\{.\}$ denotes the convex hull of a set, for all $i \in \{1,\dots,N\}$ the matrices A_i, $B_{1,i}$ and $B_{2,i}$ are given constant, $x \in \mathbb{R}^{n_x}$ is the state, $w \in \mathbb{R}^{n_w}$ is the disturbance, $u \in \mathbb{R}^{n_u}$ is the control input and $N > 0$ is the number of vertices of the PLDI.

As we consider a PLDI it is possible to express $\frac{dx}{dt}$ as follows:

$$\frac{dx}{dt} = \sum_{i=1}^{N} \beta_i(t) \left(A_i x + B_{1,i} w + B_{2,i} u\right), \tag{3.77}$$

where for all $t \geq 0$, $\beta_i(t) \geq 0$, for all $i = 1,\dots,N$, and $\sum_{i=1}^{N} \beta_i(t) = 1$.

According to (3.74) and the expression of the derivative given by (3.77), the second inequality of Assumptions 8 becomes:

$$\sum_{i=1}^{N} \beta_i(t) (\nabla_x E(x)^T \left(A_i x + B_{1,i} w + B_{2,i} f_E(x)\right) + \|x\|_R^2 + \| f_E(x)\|_\alpha^2 - \|w\|_Q^2) < 0. \tag{3.78}$$

Using the final controller f_E and the final cost E given by (3.75), inequality (3.78) can be rewritten as follows:

$$\sum_{i=1}^{N} \beta_i(t) \left(2x^T S\left((A_i + B_{2,i}K)x + B_{1,i} w\right) + x^T R x + x^T K^T \alpha K x - w^T Q w\right) < 0. \tag{3.79}$$

Inequality (3.79) has to hold everywhere on the PLDI. This implies that this inequality holds if and only if it holds for all family of $(\beta_i)_{i\in\{1,\dots,N\}}$. So for all $i \in \{1,\dots,N\}$ we have to solve in S and K the following inequalities:

$$2x^T S\left((A_i + B_{2,i}K)x + B_{1,i} w\right) + x^T \left(R + K^T \alpha K\right) x - w^T Q w < 0.$$

And then to solve

$$\begin{pmatrix} x \\ w \end{pmatrix}^T \left(\begin{pmatrix} 2S(A_i + B_{2,i}K) & SB_{1,i} \\ * & -Q \end{pmatrix} + \begin{pmatrix} R + K^T \alpha K & 0 \\ 0 & 0 \end{pmatrix} \right) \begin{pmatrix} x \\ w \end{pmatrix} < 0. \tag{3.80}$$

Since the matrices R and α are symmetric definite positive, we have:

$$\begin{pmatrix} R + K^T \alpha K & 0 \\ 0 & 0 \end{pmatrix} = \begin{pmatrix} R^{\frac{1}{2}} & K^T \alpha^{\frac{1}{2}} \\ 0 & 0 \end{pmatrix} \begin{pmatrix} I_{n_x} & 0 \\ 0 & I_{n_u} \end{pmatrix} \begin{pmatrix} R^{\frac{1}{2}} & 0 \\ \alpha^{\frac{1}{2}} K & 0 \end{pmatrix},$$

where I_n stands for the n-dimensional identity matrix (the exponent $\frac{1}{2}$ indicates that we consider the square root of the corresponding matrix).

If the matrix in the inequality (3.80) were to be semi-definite negative then this inequality would be true for all x and for all w and so in particular for the subsets we are interested in. So instead of considering the inequality (3.80), let us search for S and K such that the following condition holds:

$$\begin{pmatrix} 2S(A_i+B_{2,i}K) & SB_{1,i} \\ * & -Q \end{pmatrix} + \begin{pmatrix} R^{\frac{1}{2}} & K^T\alpha^{\frac{1}{2}} \\ 0 & 0 \end{pmatrix} \begin{pmatrix} I_{n_x} & 0 \\ 0 & I_{n_u} \end{pmatrix} \begin{pmatrix} R^{\frac{1}{2}} & 0 \\ \alpha^{\frac{1}{2}}K & 0 \end{pmatrix} < 0. \tag{3.81}$$

Let us factorize the previous inequalities as follows (since $S^T = S$):

$$\begin{aligned} &\begin{pmatrix} S & 0 \\ 0 & I_{n_w} \end{pmatrix} \left(\begin{pmatrix} 2(A_i+B_{2,i}K)S^{-1} & B_{1,i} \\ * & -Q \end{pmatrix} \right. \\ &\left. - \begin{pmatrix} S^{-1}R^{\frac{1}{2}} & S^{-1}K^T\alpha^{\frac{1}{2}} \\ 0 & 0 \end{pmatrix} \begin{pmatrix} -I_{n_x} & 0 \\ 0 & -I_{n_u} \end{pmatrix} \begin{pmatrix} R^{\frac{1}{2}}S^{-1} & 0 \\ \alpha^{\frac{1}{2}}KS^{-1} & 0 \end{pmatrix} \right) \begin{pmatrix} S & 0 \\ 0 & I_{n_w} \end{pmatrix} < 0. \end{aligned} \tag{3.82}$$

As S is assumed to be symmetric definite positive, this, in turn, is equivalent to the following matrix inequality:

$$\begin{pmatrix} 2(A_i+B_{2,i}K)S^{-1} & B_{1,i} \\ * & -Q \end{pmatrix} - \begin{pmatrix} S^{-1}R^{\frac{1}{2}} & S^{-1}K^T\alpha^{\frac{1}{2}} \\ 0 & 0 \end{pmatrix} \begin{pmatrix} -I_{n_x} & 0 \\ 0 & -I_{n_u} \end{pmatrix} \begin{pmatrix} R^{\frac{1}{2}}S^{-1} & 0 \\ \alpha^{\frac{1}{2}}KS^{-1} & 0 \end{pmatrix} < 0. \tag{3.83}$$

Using the Schur complement, the previous inequality is equivalent to the following inequality:

$$\begin{pmatrix} 2(A_i+B_{2,i}K)S^{-1} & B_{1,i} & S^{-1}R^{\frac{1}{2}} & S^{-1}K^T\alpha^{\frac{1}{2}} \\ * & -Q & 0 & 0 \\ * & * & -I_{n_x} & 0 \\ * & * & * & -I_{n_u} \end{pmatrix} < 0. \tag{3.84}$$

By introducing the notation $\overline{S} = S^{-1}$ and $Y = K\overline{S}$, it is finally deduced that the solution of an inequality on a vertex is given by the solution in $\overline{S}$ and Y of the following LMI (for all $i = 1, \ldots, N$):

$$D_i = \begin{pmatrix} \mathscr{M}_i(\overline{S},Y) & B_{1,i} & \overline{S}R^{\frac{1}{2}} & Y^T\alpha^{\frac{1}{2}} \\ * & -Q & 0 & 0 \\ * & * & -I_{n_x} & 0 \\ * & * & * & -I_{n_u} \end{pmatrix} < 0. \tag{3.85}$$

where $\mathscr{M}_i(\overline{S},Y) = A_i\overline{S} + \overline{S}A_i^T + B_{2,i}Y + Y^TB_{2,i}^T$.

And so, using the usual tool to solve LMI, it is possible to solve the final cost and the terminal state constraint problem by solving the following LMI:

$$\operatorname{diag}(D_1, \ldots, D_N) < 0.$$

3.4.3 Formulation via Norm Bounded Differential Inclusion

In the previous section, we have assumed that the full nonlinear system can be described thanks to a PLDI. One difficulty when practically using this algorithm is that the number of vertices can be too large in order to obtain an easy to use embedding. That is why, in this section, we will consider an other formulation based on a norm bounded differential inclusion (NLDI) embedding.

Assume that the nonlinear system (3.1) can be embedded in a NLDI representation, then the differential equation can be rewritten as the following linear time varying system (see e.g. [19]):

$$\frac{dx}{dt} = (A+\Delta A(t,x))x + (B_1+\Delta B_1(t,x))w + (B_2+\Delta B_2(t,x))u + \Delta f(t,x), \tag{3.86}$$

where $\Delta A(t,x) = M\Delta(t,x)N_A$, $\Delta B_1(t,x) = M\Delta(t,x)N_{B_1}$, $\Delta B_2(t,x) = M\Delta(t,x)N_{B_2}$, where the matrices A, B_1, B_2, M, N_A, N_{B_1} and N_{B_2} have adequate dimensions and are known and constants. The matrix $\Delta(t,x)$ and the vector $\Delta f(t,x)$ are assumed to satisfy the following relations (for all t and for all x)

$$\begin{aligned} &\|\Delta f(t,x)\| \leq \|Wx\|, \\ &\Delta(t,x)^T\Delta(t,x) \leq I, \end{aligned} \tag{3.87}$$

where the matrix W is known and constant.

Using (3.86), the second inequality of Assumption 8 can be rewritten as follows:

$$\begin{aligned} \nabla_x E(x)^T \left((A+M\Delta(t,x)N_A)x + (B_1+M\Delta(t,x)N_{B_1})w + (B_2+M\Delta(t,x)N_{B_2})f_E(x) + \Delta f(x)\right) \\ + \|x\|_R^2 + \|f_E(x)\|_\alpha^2 - \|w\|_Q^2 < 0. \end{aligned} \tag{3.88}$$

According to (3.75), the previous inequality becomes:

$$\begin{aligned} &2x^TS((A+B_2K)x+B_1w) + x^T(R+K^T\alpha K)x - w^TQw \\ &+ 2x^TSM\Delta(t,x)N_Ax + 2x^TSM\Delta(t,x)N_{B_1}w + 2x^TSM\Delta(t,x)N_{B_2}Kx \\ &+ 2x^TS\Delta f(t,x) < 0. \end{aligned} \tag{3.89}$$

So,

$$\begin{aligned} \begin{pmatrix} x \\ w \end{pmatrix}^T \Bigg(\begin{pmatrix} 2S(A+B_2K) & SB_1 \\ * & -Q \end{pmatrix} + \begin{pmatrix} R+K^T\alpha K & 0 \\ 0 & 0 \end{pmatrix} \\ + 2\begin{pmatrix} SM\Delta(t,x) \\ 0 \end{pmatrix} \begin{pmatrix} N_A+N_{B_2}K & N_{B_1} \end{pmatrix} \Bigg) \begin{pmatrix} x \\ w \end{pmatrix} + 2x^TS\Delta f(t,x) < 0. \end{aligned} \tag{3.90}$$

The idea is now to suppress the term $\Delta(t,x)$ and $\Delta f(t,x)$ of the previous matrix inequality. To do so let us express some inequalities by using the following inequality $\pm 2uv \leq u^TSu + v^TS^{-1}v$ for any symmetric definite positive matrix S. We have for all $\varepsilon > 0$ and $\varepsilon_0 > 0$[1]:

$$\begin{aligned} &2\begin{pmatrix} x \\ w \end{pmatrix}^T \begin{pmatrix} SM\Delta(t,x) \\ 0 \end{pmatrix} \begin{pmatrix} (N_A+N_{B_2}K) & N_{B_1} \end{pmatrix} \begin{pmatrix} x \\ w \end{pmatrix} \leq \\ &\qquad \varepsilon \begin{pmatrix} x \\ w \end{pmatrix}^T \begin{pmatrix} SM\Delta(t,x) \\ 0 \end{pmatrix} \begin{pmatrix} \Delta(t,x)^TM^TS & 0 \end{pmatrix} \begin{pmatrix} x \\ w \end{pmatrix} \\ &\qquad + \frac{1}{\varepsilon} \begin{pmatrix} x \\ w \end{pmatrix}^T \begin{pmatrix} (N_A+N_{B_2}K)^T \\ N_{B_1}^T \end{pmatrix} \begin{pmatrix} (N_A+N_{B_2}K) & N_{B_1} \end{pmatrix} \begin{pmatrix} x \\ w \end{pmatrix}, \\ &2x^TS\Delta f(t,x) \leq \varepsilon_0 x^TS^TSx + \frac{1}{\varepsilon_0}\|\Delta f(t,x)\|^2. \end{aligned} \tag{3.91}$$

[1] ε and ε_0 will be chosen appropriately later (when solving the corresponding matrices inequalities).

Since $\Delta(t,x)^T\Delta(t,x) \leq I$ and $\|\Delta f(t,x)\| \leq \|Wx\|$, we can deduce that:

$$\begin{aligned}
&2\begin{pmatrix} x \\ w \end{pmatrix}^T \begin{pmatrix} SM\Delta(t,x) \\ 0 \end{pmatrix} \begin{pmatrix} (N_A + N_{B_2}K) & N_{B_1} \end{pmatrix} \begin{pmatrix} x \\ w \end{pmatrix} \\
&\quad \leq \frac{1}{\varepsilon}\begin{pmatrix} x \\ w \end{pmatrix}^T \begin{pmatrix} (N_A + N_{B_2}K)^T(N_A + N_{B_2}K) & (N_A + N_{B_2}K)^T N_{B_1} \\ * & N_{B_1}^T N_{B_1} \end{pmatrix} \begin{pmatrix} x \\ w \end{pmatrix} \\
&\quad + \varepsilon x^T SMM^T Sx, \\
&2x^T S\Delta f(x) \leq \varepsilon_0 x^T SSx + \frac{1}{\varepsilon_0} x^T W^T Wx.
\end{aligned} \tag{3.92}$$

Using (3.92), inequality (3.90) becomes:

$$\begin{aligned}
&\begin{pmatrix} x \\ w \end{pmatrix}^T \left(\begin{pmatrix} 2S(A + B_2K) + \varepsilon SMM^T S + \varepsilon_0 SS & SB_1 \\ * & -Q \end{pmatrix} \right. \\
&\qquad \left. + \begin{pmatrix} T(K,\varepsilon,\varepsilon_0) & \frac{1}{\varepsilon}(N_A + N_{B_2}K)^T N_{B_1} \\ \frac{1}{\varepsilon}N_{B_1}^T(N_A + N_{B_2}K) & \frac{1}{\varepsilon}N_{B_1}^T N_{B_1} \end{pmatrix} \right) \begin{pmatrix} x \\ w \end{pmatrix} < 0,
\end{aligned} \tag{3.93}$$

where $T(K,\varepsilon,\varepsilon_0) = R + K^T\alpha K + \frac{1}{\varepsilon_0}W^T W + \frac{1}{\varepsilon}(N_A + N_{B_2}K)^T(N_A + N_{B_2}K)$

Also, we have

$$\begin{aligned}
&\begin{pmatrix} T(K,\varepsilon,\varepsilon_0) & \frac{1}{\varepsilon}(N_A + N_{B_2}K)^T N_{B_1} \\ \frac{1}{\varepsilon}N_{B_1}^T(N_A + N_{B_2}K) & \frac{1}{\varepsilon}N_{B_1}^T N_{B_1} \end{pmatrix} \\
&= P^T \begin{pmatrix} I_{n_x} & 0 & 0 & 0 \\ 0 & I_{n_u} & 0 & 0 \\ 0 & 0 & \frac{1}{\varepsilon_0}I_{n_x} & 0 \\ 0 & 0 & 0 & \frac{1}{\varepsilon}I_{n_w} \end{pmatrix} P,
\end{aligned} \tag{3.94}$$

where P is defined as follows:

$$P = \begin{pmatrix} R^{\frac{1}{2}} & 0 \\ \alpha^{\frac{1}{2}}K & 0 \\ W & 0 \\ (N_A + N_{B_2}K) & N_{B_1} \end{pmatrix}. \tag{3.95}$$

By introducing the notation $\overline{S} = S^{-1}$ and $Y = K\overline{S}$ and using the Schur complement, it is deduced that the solution is given by the solution in $\overline{S}$, Y, ε and ε_0 to the following LMI:

$$\begin{pmatrix} \mathscr{M}(\overline{S},Y) & B_1 & \overline{S}R^{\frac{1}{2}} & Y^T\alpha^{\frac{1}{2}} & \overline{S}W^T & Y^T N_{B_2}^T + \overline{S}N_A^T \\ * & -Q & 0 & 0 & 0 & N_{B_1}^T \\ * & * & -I_{n_x} & 0 & 0 & 0 \\ * & * & * & -I_{n_u} & 0 & 0 \\ * & * & * & * & -\varepsilon_0 I_{n_x} & 0 \\ * & * & * & * & * & -\varepsilon I_{n_w} \end{pmatrix} < 0. \tag{3.96}$$

where $\mathscr{M}(\overline{S},Y) = A\overline{S} + \overline{S}A^T + B_2Y + Y^T B_2^T + \varepsilon MM^T + \varepsilon_0 I_{n_x}$.

And so, using the usual tool to solve LMI, it is possible to solve the final cost and the terminal state constraint problem.

One advantage of the norm bounded formulation compared to the polytopic formulation is that in this case we have only one LMI to solve (to be compared to N LMIs with the polytopic formulation). However, this is at a non negligible cost, as this formulation is generally harder to get and the results are generally more conservative. This can be interpreted in regards to the result mentioned in [91] which suggests, under some assumptions, that a PLDI can be over bounded by a NLDI.

3.4.4 Formulation to consider state and input constraints

Formulation through a supplementary matrix inequality

In the two previous parts, we have been mainly interested in computing an adequate final cost and a corresponding final controller. Concerning the terminal state constraint, we have just said that it can be chosen as a level set of the final cost. In this part, we will give more details on how to choose an adequate level set such that the state constraints and the control input constraints are satisfied within the corresponding level set. The idea of this part is to use the same idea as in [29] where a method to compute a final cost and a terminal state constraint for NMPC controller is presented. The aim is to slightly modify the previous LMIs to consider the constraints. In this part, the constraints are assumed to be given as box constraints, *i.e.*:

$$\begin{aligned} -\overline{x} \leq x \leq \overline{x}, \\ -\overline{u} \leq u \leq \overline{u}, \end{aligned} \tag{3.97}$$

where $\overline{x} > 0$ and $\overline{u} > 0$ are given vector of constants of adequate dimension.

In the case where $u = Kx$, where K is a constant gain matrix, the previous state and input constraints define a region in the state space defined as follows:

$$D = \{x \in \mathbb{R}^{n_x},\ (c_j + d_j K)x \leq 1,\ j = 1, \ldots, r\}, \tag{3.98}$$

where c_i and d_i are adequately chosen constant vectors and r is the number of constraints.

If it is desired that for all $x \in \Omega_a^{f_E}$ the constraints (3.97) are satisfied, then it is sufficient to define the level set $\mathscr{E}(\gamma) = \{x \in \mathbb{R}^{n_x},\ x^T S x \leq \gamma\}$ such that:

$$\mathscr{E}(\gamma) \subset D. \tag{3.99}$$

Using the results presented in [29], this implies that we have to search for a γ such that the following condition holds

$$(c_j + d_j K)(\gamma S^{-1})(c_j + d_j K)^T < 1,\ j = 1, \ldots, r. \tag{3.100}$$

Using the Schur complement, this can be translated in the following matrix inequality:

$$\begin{pmatrix} \frac{1}{\gamma} & c_j \overline{S} + d_j Y \\ * & \overline{S} \end{pmatrix} \geq 0,\ j = 1, \ldots, r. \tag{3.101}$$

Adding (3.101) to the LMI used to compute the final cost then we can determine a terminal state constraint such that for all $x \in \Omega_a^{f_E}$ the constraints (3.97) are satisfied.

Formulation through a LMI

We have presented the matrix inequality that has to be added in order to consider the supplementary constraints (3.97). According to what has been done in [29], it is desired to compute γ directly. The idea is to use the new variable $\overline{S}^0 = \gamma\overline{S}$ and $Y^0 = \gamma Y$. In this case the LMI (3.101) becomes:

$$\begin{pmatrix} 1 & c_j\overline{S}^0 + d_jY^0 \\ * & \overline{S}^0 \end{pmatrix} \geq 0,\ j = 1,\dots,r. \tag{3.102}$$

We can now adjust the LMI to compute the final cost.

First concerning the polytopic case, the LMI on a vertex, previously given by (3.85), is changed as follows:

$$D_i = \begin{pmatrix} \mathscr{M}_i(\overline{S},Y) & \gamma B_{1,i} & \overline{S}^0R^{\frac{1}{2}} & Y^{0,T}\alpha^{\frac{1}{2}} \\ * & -\gamma Q & 0 & 0 \\ * & * & -\gamma I_{n_x} & 0 \\ * & * & * & -\gamma I_{n_u} \end{pmatrix} < 0. \tag{3.103}$$

where $\mathscr{M}_i(\overline{S},Y) = A_i\overline{S}^0 + \overline{S}^0A_i^T + B_{2,i}Y^0 + Y^{0,T}B_{2,i}^T$.

In this case, we can directly solve in γ, $\overline{S}^0$ and Y^0 to compute a final cost, a final controller and a terminal state constraint which satisfy the constraints.

Then, for the norm bounded case, we also need the following change of variable $\varepsilon^0 = \gamma\varepsilon$ and $\varepsilon_0^0 = \gamma\varepsilon_0$. The LMI, previously given by (3.96), is changed as follows:

$$\begin{pmatrix} \mathscr{M}(\overline{S}^0,Y^0) & \gamma B_1 & \overline{S}^0R^{\frac{1}{2}} & Y^{0,T}\alpha^{\frac{1}{2}} & \overline{S}^0W^T & Y^{0,T}N_{B_2}^T + \overline{S}^0N_A^T \\ * & -\gamma Q & 0 & 0 & 0 & \gamma N_{B_1}^T \\ * & * & -\gamma I_{n_x} & 0 & 0 & 0 \\ * & * & * & -\gamma I_{n_u} & 0 & 0 \\ * & * & * & * & -\varepsilon_0^0 I_{n_x} & 0 \\ * & * & * & * & * & -\varepsilon^0 I_{n_w} \end{pmatrix} < 0. \tag{3.104}$$

where $\mathscr{M}(\overline{S}^0,Y^0) = A\overline{S}^0 + \overline{S}^0A^T + B_2Y^0 + Y^{0,T}B_2^T + \varepsilon^0MM^T + \varepsilon_0^0I_{n_x}$.

In this case, we can directly solve in γ, $\overline{S}^0$, Y^0, ε^0 and ε_0^0 to compute a final cost, a final controller and a terminal state constraint which satisfy the constraints.

Possibly, there are several solutions to the previous LMIs. That is why it is interesting to introduce a criterion to discriminate the one which is better. As previously mentioned, one issue when searching for a final cost with a simple quadratic Lyapunov function instead of a quadratic hull is that the terminal state constraint is possibly small. This has for consequence that the set of feasible initial state X_E may be quite small. Thus, it can be interesting to retain the solution which maximizes the volume of the corresponding level set. This leads to consider the following optimization problem:

$$\begin{array}{l} \underline{\text{PLDI formulation:}} \\ \min\limits_{\gamma,\overline{S}^0,Y^0} \log\det(\overline{S}^0)^{-1} \\ \text{s.t. LMIs (3.102) and (3.103)} \\ \underline{\text{NLDI formulation:}} \\ \min\limits_{\gamma,\overline{S}^0,Y^0,\varepsilon^0,\varepsilon_0^0} \log\det(\overline{S}^0)^{-1} \\ \text{s.t. LMIs (3.102) and (3.104)} \end{array} \tag{3.105}$$

Finally to compute a final cost and a terminal state constraint for a given control problem, depending on the chosen embedding, we have to solve one of the optimization problem (3.105).

3.5 Conclusion

In this chapter we have considered the extension of a MPC controller to the problem of robust control of nonlinear systems described by ordinary differential equations in a sampled-data framework. This has lead to the presentation of an open-loop sampled-data robust nonlinear predictive controller, that we have called a *saddle point MPC* controller. The robust control problem is solved at each sampling instant by considering the solution of a constrained saddle point optimization problem and then by applying the usual predictive algorithm. Then, it has been proved, that if some assumptions are satisfied, then this controller ensures UB, respectively ISpS, property of the controlled system. As for the usual stability result of NMPC controller, the main assumptions needed to derive these results deal with the existence of a final cost and a terminal state constraint. As the needed property to compute these elements slightly differ from the usual case, we have also considered two possible formulations based on differential inclusion embedding to compute them.

If this approach theoretically shows interesting properties, it is not clear whether it is practically interesting to use it. Indeed, to solve the robust control problem, we have to solve a constrained saddle point optimization problem (given by (3.6)). This can be at the origin of some difficulties as such an optimization problem is quite unusual from a control point of view. The next chapter will be interested in presenting robust control problems and numerical methods to solve the corresponding saddle point problem using gradient based algorithm and adjoint model formulation.

Chapter 4

Robust Control Problem and Numerical Resolution

Contents

4.1 Introduction

In chapter 3, we have presented a variant of the classical MPC, the *saddle point MPC* controller, which can robustly stabilized nonlinear system in a sampled-data framework. It has been proved that under some assumptions, a system controlled thanks to this controller is ultimately bounded (respectively input-to-state practically stable at each sampling instant). To compute the optimal control input, at each sampling instant we have to solve a state-constrained saddle point optimization problem given by (3.6). In regards to usual MPC algorithm, this optimization problem is quite unusual. This implies that it is of prime importance to consider the numerical aspect. Indeed, the SPMPC controller can only be a viable controller if it is possible to solve the corresponding optimization problem at each sampling instant.

The objective of this chapter is to present numerical methods to solve a given state-constrained saddle point optimization problem. To do so, we intend to use optimization algorithms designed to solve an state-unconstrained problem. That is why in a first step we will recast the original constrained optimization problem in a state-unconstrained optimization problem by modifying, according to the constraints, the functional that has to be optimized. The idea is to begin by characterizing the optimal solution. Then, on the basis of this characterization, the corresponding state-unconstrained saddle point optimization problem is solved using usual gradient-based algorithm. In order to express the derivatives of the criterion needed to build a numerical method, an adjoint model will be introduced.

This chapter is organized as follows. First we will consider the problem of solving a state-unconstrained robust control problem. We begin to characterize the optimal solution. Then, using this characterization, a numerical method, based on conjugate gradient, is formally presented. In a second step, the more realistic case of a state-constrained robust control problem is envisaged. To find the solution, we propose an algorithm which consists in introducing a modified functional, according to the constraints, to substitute the original state-constrained optimization problem by a sequence of state-unconstrained optimization problems. Finally, a method based on adjoint model is given to express the derivatives of the functional that has to be optimized.

4.2 State-unconstrained Robust Control Problem

The control input of a SPMPC controller is given by the solution of a state-constrained saddle point optimization problem given by (3.6). To solve this optimization problem, we intend to use numerical methods for state-unconstrained optimization problems. That is why in this section we will consider a state-unconstrained robust control problem whose solution is given by the solution of a state-unconstrained saddle point optimization problem. To solve this problem, we will first characterize the optimal condition and then present a numerical method based on conjugate gradient algorithm.

4.2.1 Formulation of a state-unconstrained control problem and optimality conditions

Let us consider a state-unconstrained robust control problem whose solution is supposedly given by the solution of the following saddle point problem

$$\begin{aligned}(u^*,w^*) = \arg \inf_{u\in U_{ad}} \sup_{w\in W_{ad}} J(u,w) = \arg \sup_{w\in W_{ad}} \inf_{u\in U_{ad}} J(u,w),\\ s.t.\ \text{the following system,}\end{aligned} \tag{4.1}$$

$$\begin{aligned}&\frac{dx}{dt} = \mathscr{G}(x,u,w),\\ &x(\tau_0) = y \text{ (be given in } X_E),\end{aligned} \tag{4.2}$$

where $x(t) \in \mathbb{R}^{n_x}$, $X_E \subset \mathbb{R}^{n_x}$ is a feasibility space, $u(t) \in \mathbb{R}^{n_u}$ is the control input, interpreted as the control vector of the first player, and $w(t) \in \mathbb{R}^{n_w}$ stands for the disturbances, interpreted as the *control* vector of the second player. The function $\mathscr{G}$ is assumed to satisfy assumptions 1, 2, 3 and 4. The control and the disturbance sets U_{ad} and W_{ad} are assumed to be given non-empty, closed, convex and bounded subspace of $L^2(I)$ where I is an interval of length T. The given cost functional $J(u,w) := J(x;u,w)$ is assumed to be sufficiently regular.

Assume that the nonlinear control problem (4.1) admits an optimal solution $(u^*, w^*) \in U_{ad} \times W_{ad}$, the necessary conditions for this optimum are given by (see e.g. [10])

$$\begin{aligned} &\int_{t_0}^{t_0+T} \left(\frac{\partial J}{\partial u}(u^*,w^*)^T (u-u^*) \right) ds \geq 0, \ \forall u \in U_{ad}, \\ &\int_{t_0}^{t_0+T} \left(\frac{\partial J}{\partial w}(u^*,w^*)^T (w-w^*) \right) ds \leq 0, \ \forall w \in W_{ad}. \end{aligned} \tag{4.3}$$

In order to solve numerically (4.1), it is necessary to derive the gradient of J with respect to the control (u,w). For this, we suppose that the operator $\mathscr{F} : (u,w) \to \mathscr{F}(u,w)$ of (4.2) is continuously differentiable on $U_{ad} \times W_{ad}$ and its derivative $\omega = \mathscr{F}'(u,w).(g,q)$ at point (u,w) in direction (g,q) is the unique solution of

$$\begin{aligned} &\frac{d\omega}{dt} = \nabla_x \mathscr{G}(x,u,w)\omega + \nabla_u \mathscr{G}(x,u,w)g + \nabla_w \mathscr{G}(x,u,w)q, \\ &\omega(\tau_0) = 0, \end{aligned} \tag{4.4}$$

where ∇_x stands for the gradient operator relatively to x, ∇_u stands for the gradient operator relatively to u and ∇_w stands for the gradient operator relatively to w. These equations will be used to obtain the adjoint model needed to express the derivatives of the criterion.

To simplify the notation, in the sequel we note $x = \mathscr{F}(u,w)$.

Before further proceeding, it is worth mentioning that, in the unconstrained case, the gradient of J can be calculated by introducing an adjoint model in the same way as for what is done in the state-constrained case in the coming section 4.3.3.

4.2.2 A Gradient-based Optimization Method

Now that we have characterized the optimal solution of (4.1), we can present a numerical algorithm in order to solve the corresponding optimization problem.

To optimize a differentiable function, many techniques are available. Among them, some use the gradient of the objective function to generate descent direction. The classical example belonging to this class of algorithms is the steepest descent method, which is often very slow, or the Newton method, which may not converge at all. There is also the powerful conjugate gradient algorithm [148]. This optimization method is particularly interesting for large dimensional optimization problems as it can, theoretically, minimize a positive definite quadratic function of n variables in at most n steps.

The good properties of conjugate gradient algorithm can be resumed as a good convergence speed, at least faster than simple steepest descent, and good stability properties, at least better than Newton methods. Furthermore, the conjugate gradient method do not need any information on the second order derivatives of the function that has to be optimized.

Conjugate Gradient Algorithm

The classical conjugate gradient method is presented in the case of the optimization problem given by (4.1). The iterates of conjugate gradient to solve this optimization problem are obtained as follows:

$$\begin{aligned} u^{(k+1)} &= u^{(k)} + \gamma^{(k)} d_u^{(k)}, \\ w^{(k+1)} &= w^{(k)} - \delta^{(k)} d_w^{(k)}, \end{aligned} \tag{4.5}$$

where $\gamma^{(k)}$ and $\delta^{(k)}$ are step length which are computed by carrying out some line search (see e.g. [116] or [34]) and $d_u^{(k)}$ and $d_w^{(k)}$ are descent direction given by (4.11). Let us present a possible algorithm to solve this problem. If we note $\tilde{\mathscr{H}}(\gamma) = J(u^{(k)} + \gamma d_u^{(k)}, w^{(k)})$ and $\tilde{\mathscr{R}}(\delta) = J(u^{(k)}, w^{(k)} - \delta d_w^{(k)})$, then it is possible to express the line search problem as the following optimization problem:

$$\begin{aligned} \gamma^{(k)} &= \arg\min_{\gamma \geq 0} \tilde{\mathscr{H}}(\gamma), \\ \delta^{(k)} &= \arg\max_{\delta \geq 0} \tilde{\mathscr{R}}(\delta). \end{aligned} \tag{4.6}$$

In order to solve the line search problem, the usual algorithms need to evaluate the value of the criterion J for various value of the step length. This implies that it it is needed to integrate various trajectories which are virtually useless. This task can be time consuming. That is why, from the numerical computational viewpoint, it is more efficient to compute admissible step length only approximately, e.g. by using a first order Taylor development. Let us briefly explain how this algorithm work.

It is possible to express the approximated effect of a given step length (γ, δ) on the state trajectory by considering a first order Taylor development as follows

$$\begin{aligned} \mathscr{F}(u^{(k)} + \gamma d_u^{(k)}, w^{(k)}) &\approx \mathscr{F}(u^{(k)}, w^{(k)}) + \gamma \frac{\partial \mathscr{F}}{\partial u}(u^{(k)}, w^{(k)}).d_u^{(k)}, \\ \mathscr{F}(u^{(k)}, w^{(k)} - \delta d_w^{(k)}) &\approx \mathscr{F}(u^{(k)}, w^{(k)}) - \delta \frac{\partial \mathscr{F}}{\partial w}(u^{(k)}, w^{(k)}).d_w^{(k)}, \end{aligned} \tag{4.7}$$

where $\frac{\partial \mathscr{F}}{\partial u}(u^{(k)}, w^{(k)})$ is given by $\omega(u^{(k)}, w^{(k)}, d_u^{(k)}, 0)$ and $\frac{\partial \mathscr{F}}{\partial w}(u^{(k)}, w^{(k)})$ is given by $\omega(u^{(k)}, w^{(k)}, 0, d_w^{(k)})$.

The main interest of these approximate formulation is that we do not need to integrate supplementary trajectories to evaluate the influence of a given step length what is computationally efficient. In addition if the functional J is quadratic, then, using (4.7), it is possible to give a formula to evaluate the value of $\gamma^{(k)}$ and $\delta^{(k)}$ solution of (4.6).

Let us assume that J is given as follows

$$J(u,w) = \int_I \left(\|\mathscr{F}(u,w)\|_R^2 + \|u\|_\alpha^2 - \|w\|_Q^2 \right) ds, \tag{4.8}$$

where R, α and Q are given symmetric definite positive matrices.

Using (4.7), the function $\tilde{\mathscr{H}}$ and $\tilde{\mathscr{R}}$ can be approximated by

$$\begin{aligned} \mathscr{H}(\gamma) &= \int_I \left(\|\mathscr{F}(u^{(k)}, w^{(k)}) + \gamma \frac{\partial \mathscr{F}}{\partial u}(u^{(k)}, w^{(k)}).d_u^{(k)}\|_R^2 + \|u^{(k)} + \gamma d_u^{(k)}\|_\alpha^2 - \|w^{(k)}\|_Q^2 \right) ds, \\ \mathscr{R}(\delta) &= \int_I \left(\|\mathscr{F}(u^{(k)}, w^{(k)}) - \delta \frac{\partial \mathscr{F}}{\partial w}(u^{(k)}, w^{(k)}).d_w^{(k)}\|_R^2 + \|u^{(k)}\|_\alpha^2 - \|w^{(k)} - \delta d_w^{(k)}\|_Q^2 \right) ds. \end{aligned} \tag{4.9}$$

The function $\mathscr{H}$ and $\mathscr{R}(\delta)$ are quadratic polynomial whose derivatives are given by

$$\begin{aligned}
\frac{\partial \mathscr{H}}{\partial \gamma} &= 2\int_I \left(\gamma\left(\|\frac{\partial \mathscr{F}}{\partial u}(u^{(k)},w^{(k)}).d_u^{(k)}\|_R^2 + \|d_u^{(k)}\|_\alpha^2\right)\right. \\
&\quad \left. + \left(\mathscr{F}(u^{(k)},w^{(k)})^T R\frac{\partial \mathscr{F}}{\partial u}(u^{(k)},w^{(k)}).d_u^{(k)} + u^{(k)T}\alpha d_u^{(k)}\right)\right) ds, \\
\frac{\partial \mathscr{R}}{\partial \delta} &= 2\int_I \left(\delta\left(\|\frac{\partial \mathscr{F}}{\partial w}(u^{(k)},w^{(k)}).d_w^{(k)}\|_R^2 + \|d_w^{(k)}\|_Q^2\right)\right. \\
&\quad \left. - \left(\mathscr{F}(u^{(k)},w^{(k)})^T R\frac{\partial \mathscr{F}}{\partial w}(u^{(k)},w^{(k)}).d_w^{(k)} + w^{(k)T} Q d_w^{(k)}\right)\right) ds.
\end{aligned} \tag{4.10}$$

Using this approximate formulation of (4.6), it becomes straightforward to solve the line search problem.

The search direction $d_u^{(k)}$ and $d_w^{(k)}$ are given as follows

$$d_\rho^{(k)} = \begin{cases} -\dfrac{\partial J}{\partial \rho}(u^{(k)},w^{(k)}) & \text{if } k=0 \\ -\dfrac{\partial J}{\partial \rho}(u^{(k)},w^{(k)}) + \beta_\rho^{(k)} d_\rho^{(k-1)} & \text{if } k\geq 1 \end{cases}, \tag{4.11}$$

where $\beta_\rho^{(k)}$ is a scalar and ρ stands for u or w.

Well known conjugate gradient methods include Fletcher-Reeves method (FR) and the Polak-Ribiére-Polyak (PRP) (see e.g. [10]). In these methods, the parameter $\beta_\rho^{(k)}$ is given by:

$$\beta_\rho^{(k),(FR)} = \frac{\|\frac{\partial J}{\partial \rho}(u^{(k)},w^{(k)})\|^2}{\|\frac{\partial J}{\partial \rho}(u^{(k-1)},w^{(k-1)})\|^2}, \quad \beta_\rho^{(k),(PRP)} = \frac{\frac{\partial J}{\partial \rho}(u^{(k)},w^{(k)})^T y_\rho^{(k-1)}}{\|\frac{\partial J}{\partial \rho}(u^{(k-1)},w^{(k-1)})\|^2}, \tag{4.12}$$

where $y_\rho^{(k-1)} = \dfrac{\partial J}{\partial \rho}(u^{(k)},w^{(k)}) - \dfrac{\partial J}{\partial \rho}(u^{(k-1)},w^{(k-1)})$.

There also exists hybrid method which were developed in order to benefit from the various advantages of each coefficient. For instance, because of the good numerical behavior of the PRP method and the good convergence of the FR method, the first hybrid conjugate gradient algorithm was introduced in [6], where the parameters $\beta_\rho^{(k)}$ is computed as follows:

$$\beta_\rho^{(k),(TS)} = \begin{cases} \beta_\rho^{(k),(PRP)} & \text{if } 0\leq \beta_\rho^{(k),(PRP)} \leq \beta_\rho^{(k),(FR)} \\ \beta_\rho^{(k),(FR)} & \text{otherwise} \end{cases}, \tag{4.13}$$

Restart Procedure

As previously mentioned, the conjugate gradient method has the important property that it can theoretically minimize a positive definite quadratic function of n variables in n steps. The problem is that practically this result is rarely verified, e.g. because of numerical approximation. Also, the robust control problem has no reason to be recast as a quadratic problem. A possibility to recover the good convergence rate of the method is to introduce a restart procedure, *i.e.* to use a different descent direction whenever some conditions are met. In the sequel, let us remind some classical restart algorithms.

The simplest restart procedure is to use a steepest descent every r iterations (see e.g. [31]). The idea is that near the solution, if the function to be minimized is sufficiently smooth, it is possible to make a Taylor development of f at the second order. So, when the solution has entered this *quadratic* region,

some huge progress can be envisaged by simply applying a restart with a steepest descent. The main limitation of this method is that it is not clear how often this restart should be applied in order to become efficient.

It can be proved that the conjugate gradient methods yields descent direction which are orthogonal (see e.g. [148] or [116]). The lost in the convergence rate is due to the lost of orthogonality between two successive descent direction. That is why in [113] a restart procedure by a steepest descent algorithm is envisaged whenever the orthogonality between two successive descent direction is too low, *i.e.* whenever:

$$\frac{\frac{\partial J}{\partial \rho}(u^{(k)},w^{(k)})^T \frac{\partial J}{\partial \rho}(u^{(k+1)},w^{(k+1)})}{\|\frac{\partial J}{\partial \rho}(u^{(k+1)},w^{(k+1)})\|^2} \geq \nu, \tag{4.14}$$

where ρ stands either for u or w and ν is a chosen positive constant (classically $\nu = 0.1$).

Finally, it is also possible to envisage more advanced restart algorithms which do not use a steepest descent as restart directions. Among them it is possible to quote the Beale-Powell restart procedure (or any modification of this latter as presented in [33]) which computes the restart direction as a sum of the steepest descent, the previous descent direction and a third component, e.g. one of the previous descent direction.

4.3 State-constrained Robust Control Problem

4.3.1 Formulation of a state-constrained robust control problem

From a more realistic point of view, the problem of robust control is formulated as a state-constrained optimization problem, e.g. in (3.6) a terminal state constraint is needed in order to ensure the stability of the closed-loop. That is why in the sequel we are interested in the following state-constrained saddle point optimization problem

$$\begin{aligned}(u^*,w^*) = &\arg \inf_{u\in U_{ad}} \sup_{w\in W_{ad}} J(u,w) = \arg \sup_{w\in W_{ad}} \inf_{u\in U_{ad}} J(u,w),\\ &s.t.\ \text{system (4.2)},\\ &\text{with } c(x)\geq 0,\end{aligned} \tag{4.15}$$

where U_{ad} and W_{ad} are assumed to be given non-empty, closed, convex and bounded subspace of $L^2(I)$ where I is an interval of length T. The function c is real valued and assumed to be sufficiently regular. The cost function J is given defined as follows:

$$J(u,w) = E(x(\tau_0+T)) + \int_{\tau_0}^{\tau_0+T} F(x,u,w)ds, \tag{4.16}$$

It is assumed that the stage cost F satisfy assumption 5 and that the final cost E satisfy assumption 8.

4.3.2 Formulation in state-unconstrained optimization problems

Motivation

In order to solve the state-constrained optimization problem given by (4.15), we are interested in using the same algorithms as for the state-unconstrained optimization problem given by (4.1). To do so, we need an algorithm to substitute the original state-constrained optimization problem by a sequence of state-unconstrained ones. In this part, we propose a method which has been inspired by the augmented

Lagrangian technique. This latter, which is a mixed between a simple penalty method (as for the logarithmic barrier method, see e.g. [69]) and a Lagrangian algorithm (see e.g. [116]), is often used as it tends to yield less ill conditioned optimization problems than does a simple penalty methods.

Before further proceeding, let us briefly recall how this method works (for more details see e.g. [116]).

The augmented Lagrangian method

The augmented Lagrangian algorithm is a method which combines a quadratic penalty function with an explicit *Lagrange multiplier* which is a supplementary variable that has to be estimated. Let us remind how this algorithm works to handle an inequality constraint with the following simple minimization example

$$\begin{aligned} &\min_{x} f(x) \\ &s.t.\ c(x) \geq 0, \end{aligned} \tag{4.17}$$

where $x \in \mathbb{R}^n$, $f : \mathbb{R}^n \to \mathbb{R}$ and $c : \mathbb{R}^n \to \mathbb{R}$ are sufficiently smooth.

First the problem is recast using a slack variable s:

$$\begin{aligned} &\min_{x,s} f(x) \\ &s.t.\ c(x) - s = 0,\ s \geq 0, \end{aligned} \tag{4.18}$$

Then we define the augmented Lagrangian in term of the equality constraint $c(x) - s = 0$:

$$\begin{aligned} &\min_{x,s} f(x) - \lambda\,(c(x) - s) + \frac{1}{2\mu}(c(x) - s)^2 \\ &s.t.\ s \geq 0, \end{aligned} \tag{4.19}$$

where λ is a Lagrangian multiplier and μ stands for a strictly positive constant.

We can see that this problem is convex in s, so without any constraint we had the minimizer in s is given by:

$$s = c(x) - \mu\lambda\,. \tag{4.20}$$

If $s < 0$ then the optimal value of s is 0, so finally we have:

$$s = \max(c(x) - \mu\lambda, 0) \tag{4.21}$$

This implies that the slack variable s can be substitute. The augmented Lagrangian method for inequality constraints consists in modifying the function f as follows [116]

$$\tilde{f}(x) = f(x) + \Psi^{\mu}(c(x), \lambda), \tag{4.22}$$

where

$$\Psi^{\mu}(z,\lambda) = \begin{cases} -\lambda z + \frac{1}{2\mu} z^2 & \text{if } z - \mu\lambda \leq 0 \\ -\frac{\mu}{2}\lambda^2 & \text{if } z - \mu\lambda \geq 0 \end{cases}, \tag{4.23}$$

with $(z,\lambda) \in \mathbb{R}^2$.

Then, to solve the original constrained optimization problem, we introduce a sequence of unconstrained problems for which it costs more and more to violate the constraints. To do so, the variable μ in

the quadratic penalty function is defined by a sequence μ^κ which decreased toward 0, e.g. by using the following recurrence formula

$$\mu^{(\kappa+1)} = r\mu^{(\kappa)} \tag{4.24}$$

where r is a constant in $]0;1[$ and κ stands for an iterate on the outer loop.

Nota bene: It is clear, for c sufficiently regular, that the function $(x,\lambda) \to \Psi^\mu(c(x),\lambda)$ is continuous. Indeed if $c(x) - \mu\lambda = 0$, then we have:

$$-\lambda c(x) + \frac{1}{2\mu}c(x)^2 = -\frac{\mu}{2}\lambda^2 \tag{4.25}$$

Moreover formally this function is differentiable and we have (according to (4.23)):

$$\nabla_x \Psi^\mu(c(x),\lambda) = \begin{cases} \nabla_x c(x)\left(-\lambda + \frac{1}{\mu}c(x)\right) & \text{if } c(x) - \mu\lambda \leq 0, \\ 0 & \text{if } c(x) - \mu\lambda \geq 0, \end{cases} \tag{4.26}$$

and

$$\frac{\partial \Psi^\mu}{\partial \lambda}(c(x),\lambda) = \begin{cases} -c(x) & \text{if } c(x) - \mu\lambda \leq 0, \\ -\mu\lambda & \text{if } c(x) - \mu\lambda \geq 0. \end{cases} \tag{4.27}$$

Formulation of a state-unconstrained sub-problem

In order to consider the state-constraints in the optimization problem (4.15), we propose an algorithm based on the previously augmented Lagrangian techniques. To provide a solution of the original state-constrained optimization problem, we introduce a sequence of state-unconstrained optimization problems by considering a strictly positive variable μ which converges toward 0 in an outer loop, e.g. using the formula (4.24). Each subproblem is given by

$$\begin{aligned} (u^*,\tilde{w}^*) = &\arg \inf_{u\in U_{ad}} \sup_{\tilde{w}\in\tilde{W}_{ad}} \mathscr{L}_A^\mu(u,\tilde{w}) = \arg \sup_{\tilde{w}\in\tilde{W}_{ad}} \inf_{u\in U_{ad}} \mathscr{L}_A^\mu(u,\tilde{w}), \\ &s.t. \text{ system (4.2).} \end{aligned} \tag{4.28}$$

where the sets U_{ad} and $\tilde{W}_{ad}$ are assumed to be given non-empty, closed, convex and bounded subspace of $L^2(I)$ where I is an interval of length T and where the functional $\mathscr{L}_A^\mu$ is defined by

$$\mathscr{L}_A^\mu(u,\tilde{w}) = J(u,w) + \int_{\tau_0}^{\tau_0+T} \Psi^\mu(c(x),\lambda)ds, \tag{4.29}$$

where Ψ is given by (4.23), $c : \mathbb{R}^{n_x} \to \mathbb{R}$, for all s, $\lambda(s) \in \mathbb{R}$ and $\tilde{w} = (w^T, \lambda^T)^T$.

As the saddle point optimization problem (4.28) is state-unconstrained, it is possible to solve it using what has been previously presented. According to (4.3), the optimality conditions are given by:

$$\begin{aligned} &\int_{\tau_0}^{\tau_0+T} \left(\frac{\partial \mathscr{L}_A^\mu}{\partial u}(u^*,\tilde{w}^*)^T(u-u^*)\right) ds \geq 0, \ \forall u \in U_{ad}, \\ &\int_{\tau_0}^{\tau_0+T} \left(\frac{\partial \mathscr{L}_A^\mu}{\partial \tilde{w}}(u^*,\tilde{w}^*)^T(\tilde{w}-\tilde{w}^*)\right) ds \leq 0, \ \forall \tilde{w} \in \tilde{W}_{ad}. \end{aligned} \tag{4.30}$$

In order to solve the state-unconstrained saddle point problem (4.28), we need to calculate the derivatives $\frac{\partial \mathscr{L}_A^\mu}{\partial u}$ and $\frac{\partial \mathscr{L}_A^\mu}{\partial \tilde{w}}$. In the next part we will be interested in presenting a method based on adjoint model to solve this issue.

4.3.3 Adjoint Model and Optimality Conditions

The Fréchet derivatives of $\mathscr{L}_A^\mu$ at point $(u,\tilde{w})$ in direction (g,q) is given by

$$\mathscr{L}_A^{\mu\prime}(u,\tilde{w}).(g,q) = J'(u,w).(g,q) + \int_{\tau_0}^{\tau_0+T} \Psi^{\mu\prime}(c(x),\lambda).(g,q)ds, \tag{4.31}$$

where $J'(f,w).(g,q)$ and $\Psi^{\mu\prime}(c(x),\lambda).(g,q)$ are given by

$$\begin{aligned} J'(u,w).(g,q) &= \nabla_x E(x(\tau_0+T))^T \omega(\tau_0+T) \\ &+ \int_{\tau_0}^{\tau_0+T} \left(\nabla_x F(x,u,w)^T \omega(s) + \nabla_u F(x,u,w)^T g + \nabla_w F(x,u,w)^T q_w\right) ds, \\ \Psi^{\mu\prime}(c(x),\lambda).(g,q) &= \nabla_x \left(\Psi^\mu(c(x),\lambda)\right)^T \omega + \left(\frac{\partial \Psi^\mu}{\partial \lambda}(c(x),\lambda)\right)^T q_\lambda, \end{aligned} \tag{4.32}$$

where $q=(q_w,q_\lambda)$, $\nabla_x\left(\Psi^\mu(c(x),\lambda)\right)$ and $\dfrac{\partial \Psi^\mu}{\partial \lambda}(c(x),\lambda)$ are given by (4.26) and (4.27), respectively.

Multiplying (4.4) by a sufficiently regular function $\tilde{x}$ and integrating by time, we can deduce that

$$\begin{aligned} &\int_{\tau_0}^{\tau_0+T} \tilde{x}^T \left(\nabla_x \mathscr{G}(x,u,w)\omega + \tilde{x}^T \nabla_u \mathscr{G}(x,u,w) g + \tilde{x}^T \nabla_w \mathscr{G}(x,u,w) q_w\right) ds \\ &\qquad = \tilde{x}^T(\tau_0+T)\omega(\tau_0+T) - \int_{\tau_0}^{\tau_0+T} \left(\frac{d\tilde{x}^T}{dt}\ \omega\right) ds. \end{aligned} \tag{4.33}$$

Then

$$\begin{aligned} &\int_{\tau_0}^{\tau_0+T} \left(\omega^T \left(\nabla_x \mathscr{G}(x,u,w)^T \tilde{x} + \nabla_x\left(\Psi^\mu(c(x),\lambda)\right) + \nabla_x F(x,u,w) + \frac{d\tilde{x}}{dt}\right)\right) ds \\ &+ \omega(\tau_0+T)^T \left(\nabla_x E(x(\tau_0+T)) - \tilde{x}(\tau_0+T)\right) \\ &+ \int_{\tau_0}^{\tau_0+T} \left(g^T \left(\nabla_u \mathscr{G}(x,u,w)\right)^T \tilde{x} + q_w^T \left(\nabla_w \mathscr{G}(x,u,w)\right)^T \tilde{x}\right) ds \\ &\qquad = \int_{\tau_0}^{\tau_0+T} \left(\omega^T \left(\nabla_x\left(\Psi^\mu(c(x),\lambda)\right) + \nabla_x F(x,u,w)\right)\right) ds \\ &\qquad + \omega(\tau_0+T)^T \nabla_x E(x(\tau_0+T)). \end{aligned} \tag{4.34}$$

Assume now that $\tilde{x}$ is the unique solution of the following adjoint model

$$\begin{aligned} -\frac{d\tilde{x}}{dt} &= \nabla_x \mathscr{G}(x,u,w)^T \tilde{x} + \nabla_x F(x,u,w) + \nabla_x\left(\Psi^\mu(c(x),\lambda)\right), \\ \tilde{x}(\tau_0+T) &= \nabla_x E(x(\tau_0+T)), \end{aligned} \tag{4.35}$$

According to (4.35), (4.34) becomes

$$\begin{aligned} &\int_{\tau_0}^{\tau_0+T} \left(\tilde{x}^T \nabla_u \mathscr{G}(x,u,w) g + \tilde{x}^T \nabla_w \mathscr{G}(x,u,w) q_w\right) ds \\ &\qquad = \int_{\tau_0}^{\tau_0+T} \left(\left(\nabla_x\left(\Psi^\mu(c(x),\lambda)\right) + \nabla_x F(x,u,w)\right)^T \omega\right) ds \\ &\qquad + \nabla_x E(x(\tau_0+T))^T \omega(\tau_0+T). \end{aligned} \tag{4.36}$$

And so (4.31) becomes

$$\begin{aligned}\mathscr{L}_A^{\mu\prime}(u,\tilde{w}).(g,q) = \int_{\tau_0}^{\tau_0+T} \Big(g^T \Big((\nabla_u \mathscr{G}(x,u,w))^T \tilde{x} + \nabla_u F(x,u,w) \Big) \\ + q_w^T \Big((\nabla_w \mathscr{G}(x,u,w))^T \tilde{x} + \nabla_w F(x,u,w) \Big) + q_\lambda \left(\frac{\partial \Psi^\mu}{\partial \lambda}(c(x),\lambda) \right) \Big)\, ds.\end{aligned} \tag{4.37}$$

So, we can deduce the following expression of the gradient of the modified cost functional (in a weak sense)

$$\begin{aligned}\frac{\partial \mathscr{L}_A^\mu}{\partial u}(u,\tilde{w}) &= \nabla_u \mathscr{G}(x,u,w)^T \tilde{x} + \nabla_u F(x,u,w), \\ \frac{\partial \mathscr{L}_A^\mu}{\partial \tilde{w}}(u,\tilde{w}) &= \begin{pmatrix} \nabla_w \mathscr{G}(x,u,w)^T \tilde{x} + \nabla_w F(x,u,w) \\ \frac{\partial \Psi^\mu}{\partial \lambda}(c(x),\lambda) \end{pmatrix},\end{aligned} \tag{4.38}$$

where x is the solution of (4.2) with inputs (u,w) and $\tilde{x}$ is the solution of the adjoint problem (4.35) corresponding to (u,w,x).

We can now give an algorithm to resolve the states-constrained saddle point problem (4.15).

4.3.4 State-constrained saddle point solver

To solve the state-constrained saddle point optimization problem (4.15), the first step consists in introducing a modified functional according to the results presented in section 4.3.2. Then according to the results presented in section 4.2, we can use a conjugate gradient algorithm to solve the corresponding optimization problem.

The solver is based on a conjugate gradient with hybrid coefficient (4.13). The interest of using a restart will be evaluated by checking the orthogonality between two successive value of the gradient according to (4.14). Because in the sequel the functional J is assumed to be quadratic, the step length will be computed using the approximate formulation given by (4.9).

In order to give a better overview of the envisaged numerical methods, let us introduce the following algorithms. The first algorithm (algorithm 1) shows how a given state-unconstrained problem can be solved and the second one (algorithm 2) shows how the solution of the original state-constrained problem is deduced from the solution of a sequence of state-unconstrained optimization problems.

The various trajectories are integrated using Runge-Kutta 54 method (see e.g. [32]).

4.4 Conclusion

In this chapter we have presented an algorithm to solve state-constrained saddle point optimization problems. To do so we have first considered the problem of solving a given state-unconstrained saddle point optimization problem using conjugate gradient technique. Then, to solve the state-constrained optimization problem, we have proposed an algorithm which consists in modifying the functional that has to be optimized according to the constraints. All this has been done in order to replace the original state-constrained optimization problem by a sequence of state-unconstrained optimization problems. This strategy has been inspired from the well known augmented Lagrangian technique. Also, a technique based on adjoint model has been presented to express the derivatives of the cost functional.

The solution of the SPMPC controller is given as the solution of a state-constrained saddle point optimization problem. So using the result presented in this chapter, we can consider the problem of applying this controller to a concrete control problem. This is the objective of the next chapter where

Algorithm 1 Saddle point optimization problem (4.28) thanks to conjugate gradient algorithm

Require: $y \in X_E$, $u^{(0)} \in U_{ad}$, $\tilde{w}^{(0)} \in \tilde{W}_{ad}$, $N_{max} \in \mathbb{R}^{+*}$, $\varepsilon_u \in \mathbb{R}^{+*}$, $\varepsilon_{\tilde{w}} \in \mathbb{R}^{+*}$,

k=0,
while ($k \leq N_{max}$) **and not** ($\frac{\|u^{(k)}-u^{(k-1)}\|}{\|u^{(k-1)}\|} \leq \varepsilon_u$ **and** $\frac{\|\tilde{w}^{(k)}-\tilde{w}^{(k-1)}\|}{\|\tilde{w}^{(k-1)}\|} \leq \varepsilon_{\tilde{w}}$) **do**
  Resolution of (4.2) (based on$(u^{(k)}, \tilde{w}^{(k)})$) gives $x^{(k)}$,
  Resolution of (4.35) (based on $(u^{(k)}, \tilde{w}^{(k)})$ and $x^{(k)}$) gives $\tilde{x}^{(k)}$,
  Evaluate the gradient of $\mathscr{L}_A^{\mu}$ at $(u^{(k)}, \tilde{w}^{(k)})$ using equations (4.38) and $x^{(k)}$ and $\tilde{x}^{(k)}$,
  Compute the descent direction $d_u^{(k)}$ and $d_{\tilde{w}}^{(k)}$ according to formula (4.11) in which J plays the role of $\mathscr{L}_A^{\mu}$ and, if needed, a given coefficient $\beta^{(k)}$,
  If $k \geq 1$ consider the need for a restart,
  Resolution of (4.4) (based on $(u^{(k)}, \tilde{w}^{(k)})$, $x^{(k)}$, $\tilde{x}^{(k)}$, $d_u^{(k)}$ and $d_{\tilde{w}}^{(k)}$) gives $\omega^{(k)}$,
  Compute the step length $\gamma^{(k)}$ and $\delta^{(k)}$ by solving (4.6)
  Determine $(u^{(k+1)}, \tilde{w}^{(k+1)})$ according to (4.5),
  $k := k+1$,
end while
return $(u_\mu^*, \tilde{w}_\mu^*) = (u^{(k+1)}, \tilde{w}^{(k+1)})$ and $x_\mu^* = x^{(k+1)} = \mathscr{F}(u^{(k+1)}, w^{(k+1)})$.

Algorithm 2 Solving a state-constrained robust control problem thanks to a sequence of state-unconstrained optimization problems

Require: $y \in X_E$, $\mu^{(0)} \in \mathbb{R}^{+*}$, $u^{(0)} \in U_{ad}$, $\tilde{w}^{(0)} \in \tilde{W}_{ad}$, $N_{max} \in \mathbb{N}^{+*}$, $r \in]0,1[$,

$\kappa = 0$,
while $\kappa \leq N_{max}$**and not** ($c(x) \geq 0$) **do**
  Express the functional $\mathscr{L}_A^{\mu^{(\kappa)}}$ according to (4.29),
  Solve (4.28) using **algorithm 1** gives $(u_{\mu^{(\kappa)}}^*, \tilde{w}_{\mu^{(\kappa)}}^*)$,
  Set $u^{(0)} := u_{\mu^{(\kappa)}}^*$ and $\tilde{w}^{(0)} := \tilde{w}_{\mu^{(\kappa)}}^*$,
  $\mu^{(\kappa+1)} := r\mu^{(\kappa)}$,
  $\kappa := \kappa+1$,
end while
return $(u^*, \tilde{w}^*) = (u_{\mu^{(\kappa+1)}}^*, \tilde{w}_{\mu^{(\kappa+1)}}^*)$.

the here presented numerical method will be implemented to test the SPMPC control performances on a classical control problem.

Chapter 5

Illustration of the SPMPC Approach

Contents

5.1 Introduction

In chapter 3 we have presented from a theoretical point of view a *saddle point model predictive controller*. When using this controller, the control input is given by the solution of a state-constrained saddle-point optimization problem. As for the usual MPC algorithm, this control input is computed each time a new measure is made available. Then, in chapter 4, we have proposed a numerical method which can be used to solve the corresponding optimization problem.

The objective of this chapter is to test the good numerical implementation and control performances on a concrete control example. The problem of controlling a disturbed in parameters Van der Pol oscillator using a SPMPC controller is envisaged. Because of the relative simplicity of this example, we will show how to formulate the final cost and the terminal state constraint problem using both a polytopic and a norm bounded differential inclusion. Then it will be shown how the results of chapter 4 can be used to express the derivatives of the criterion that has to be optimized. Finally the controller is tested in order to stabilize the system at the origin.

This chapter is organized as follows. First, under constraints on the state, the final cost and the terminal state constraint will be computed. Then, in order to use the algorithm presented in chapter 4, we will express the adjoint model and the derivatives of the criterion. Finally, the controller performances will be assessed via numerical simulation.

5.2 A disturbed in parameters Van der Pol Oscillator

In order to illustrate our approach, we consider the following Van der Pol oscillator:

$$\begin{aligned} &\frac{dx_1}{dt} = x_2, \\ &\frac{dx_2}{dt} = -x_1 - \frac{1}{2}x_2(1-x_1^2) + x_1 u, \\ &x(t_0) = x_0. \end{aligned} \tag{5.1}$$

where $x = \begin{pmatrix} x_1 \\ x_2 \end{pmatrix}$ is the state and u is the control input.

This example is taken from [39], where the solution of the corresponding Hamilton Jacobi Bellman equation is computed and given by $u^* = -x_1 x_2$. The control aim is to stabilize the system at the origin which is a stable but uncontrollable equilibrium point.

It is considered that the system parameters are disturbed leading to the following version of the Van der Pol oscillator:

$$\begin{aligned} &\frac{dx_1}{dt} = (1+w_1)x_2, \\ &\frac{dx_2}{dt} = -(1+w_2)x_1 - \frac{1}{2}x_2(1-x_1^2) + x_1 u, \\ &x(t_0) = x_0, \end{aligned} \tag{5.2}$$

where for all t we have $(w_1(t), w_2(t)) \in [-0.1, 0.1] \times [-0.1, 0.1]$. For control purpose, the control is assumed to be bounded as follows, for all $t \geq t_0$ u is such that $u(t) \in [-10, 10]$.

The stage cost F is chosen quadratic (3.74) with the following matrices:

$$R = I_2,\ Q = 0.8 I_2,\ \alpha = 10^{-6}.$$

In order to use the algorithm presented in chapter 3, the final cost is chosen quadratic and the terminal state constraint is chosen as a level set of the final cost.

5.3 Computation of the final cost

To compute an adequate final cost and terminal state constraint which satisfy assumptions 7 and 8, we are interested in finding the larger invariant set contained in $(x_1, x_2) \in [-0.3, 0.3] \times [-0.3, 0.3]$. To do so, we are interested in embedding the original dynamics in a differential inclusion.

It is clear that the controller given by the solution of the Hamilton Jacobi equation is better than a simple linear state feedback. That is why it has been chosen to use this controller as a final controller. That is f_E is chosen as follows

$$f_E(x) = -x_1 x_2. \tag{5.3}$$

Remark 6. For all combination of $(x_1, x_2) \in [-0.3, 0.3] \times [-0.3, 0.3]$, we have that $f_E(x) \in [-10, 10]$.

As we have chosen not to compute the final controller simultaneously with the final cost, the differential inclusion will not be formulated using (5.2) but using the following differential equations:

$$\begin{aligned} \frac{dx_1}{dt} &= (1+w_1)x_2, \\ \frac{dx_2}{dt} &= -(1+w_2)x_1 - \frac{1}{2}x_2(1+x_1^2), \\ x(t_0) &= x_0. \end{aligned} \tag{5.4}$$

Due to the retained form of the final controller, in order to use (3.105), we have to set $Y = 0$ and $\alpha = 0$.

Because it is not trivial to determine which one of the PLDI or the NLDI representation provides the largest terminal state constraint, we will consider the computation of the final cost in both cases. The method which provides the larger terminal set, according to the criterion (3.105), will be retained.

5.3.1 Computation via a PLDI embedding

The disturbed and controlled with $f_E(x)$ Van der Pol oscillator (5.4) can be expressed as follows:

$$\begin{aligned} \frac{dx}{dt} &= \begin{pmatrix} 0 & 1 \\ -1 & -\frac{1}{2}(1+x_1^2) \end{pmatrix} x + \begin{pmatrix} x_2 & 0 \\ 0 & -x_1 \end{pmatrix} w, \\ x(t_0) &= x_0. \end{aligned} \tag{5.5}$$

We search for a local embedding which is only valid for all $(x_1, x_2) \in [-0.3, 0.3] \times [-0.3, 0.3]$. Thus, the following PLDI embedding is easily deduced from the previous differential equations (see e.g. [91]):

$$\frac{dx}{dt} = \sum_{i=1}^{8} \beta_i(t) \left(A_i x + B_{1,i} w \right), \tag{5.6}$$

where

$$\begin{aligned} A_i &= \begin{pmatrix} 0 & 1 \\ -1 & -\frac{1}{2} \end{pmatrix}, \ \forall i \in \{1,3,5,7\}, \\ A_i &= \begin{pmatrix} 0 & 1 \\ -1 & -\frac{1.09}{2} \end{pmatrix}, \ \forall i \in \{2,4,6,8\}, \end{aligned} \tag{5.7}$$

and

$$\begin{aligned} B_{1,i} &= \begin{pmatrix} -0.3 & 0 \\ 0 & 0.3 \end{pmatrix}, \ \forall i \in \{1,2\}, \\ B_{1,i} &= \begin{pmatrix} -0.3 & 0 \\ 0 & -0.3 \end{pmatrix}, \ \forall i \in \{3,4\}, \\ B_{1,i} &= \begin{pmatrix} 0.3 & 0 \\ 0 & 0.3 \end{pmatrix}, \ \forall i \in \{5,6\}, \\ B_{1,i} &= \begin{pmatrix} 0.3 & 0 \\ 0 & -0.3 \end{pmatrix}, \ \forall i \in \{7,8\}, \end{aligned} \tag{5.8}$$

Then, using what has been presented in chapter 3, it is deduced that the matrix S in the final cost and the parameter γ in the terminal state constraint are given as follows

$$\begin{aligned} S &= \begin{pmatrix} 2.24 & 0.56 \\ 0.56 & 2.25 \end{pmatrix}, \\ \gamma &= 0.15. \end{aligned} \tag{5.9}$$

The value of the objective function of the optimization problem (3.105) at the optimal solution is

$$\log\det\left(\bar{S}_0\right)^{-1} = -5.33. \tag{5.10}$$

5.3.2 Computation via a NLDI embedding

Because of the simple structure of the disturbed Van der Pol oscillator (5.4), it is possible to embed it in a norm bounded differential inclusion. Indeed, it can be rewritten as follows

$$\frac{dx}{dt} = \begin{pmatrix} 0 & 1 \\ -1 & -\frac{1}{2} \end{pmatrix} x + \begin{pmatrix} x_2 & 0 \\ 0 & -x_1 \end{pmatrix} w + \begin{pmatrix} 0 \\ -\frac{1}{2}x_1^2 x_2 \end{pmatrix} \tag{5.11}$$

We search for a local embedding which is only valid for all $(x_1, x_2) \in [-0.3, 0.3] \times [-0.3, 0.3]$. So it is deduced that we have (5.4) is locally embedded in the following NLDI

$$\frac{dx}{dt} = Ax + M\Delta(t,x)N_{B_1}w + \Delta f(t,x), \tag{5.12}$$

where

$$\begin{aligned} M &= \sqrt{0.3}\begin{pmatrix} 1 & 0 \\ 0 & 1 \end{pmatrix}, \ N_{B_1} = \sqrt{0.3}\begin{pmatrix} 1 & 0 \\ 0 & -1 \end{pmatrix}, \\ \Delta(t,x) &= \frac{1}{0.3}\begin{pmatrix} x_2 & 0 \\ 0 & x_1 \end{pmatrix}, \ \Delta f(t,x) = \begin{pmatrix} 0 \\ -\frac{1}{2}x_1^2 x_2 \end{pmatrix}. \end{aligned} \tag{5.13}$$

Also, because the final cost and the terminal state constraint are computed in order to find the larger invariant set contained in $[-0.3, 0.3] \times [-0.3, 0.3]$, then we are sure that within this set we have

$$\Delta(t,x)^T \Delta(t,x) \leq I_2.$$

Also, we have $\|\Delta f(t,x)\| \leq \|Wx\|$ where:

$$W = \frac{0.15}{\sqrt{2}} I_2 \tag{5.14}$$

Then, using what has been presented in chapter 3, it is deduced that the matrix S in the final cost and the parameter γ of the terminal state constraint are given as follows

$$\begin{aligned} S &= \begin{pmatrix} 37.89 & 5.56 \\ 5.56 & 37.99 \end{pmatrix}, \\ \gamma &= 2.91. \end{aligned} \tag{5.15}$$

The value of the objective function of the optimization problem (3.105) at the optimal solution is

$$\log\det\left(\overline{S}_0\right)^{-1} = -5.11. \tag{5.16}$$

5.3.3 Choice of the final cost and terminal state constraint

It can be seen that both methods provide a terminal state constraint with a slightly equivalent volume (see fig.5.1).

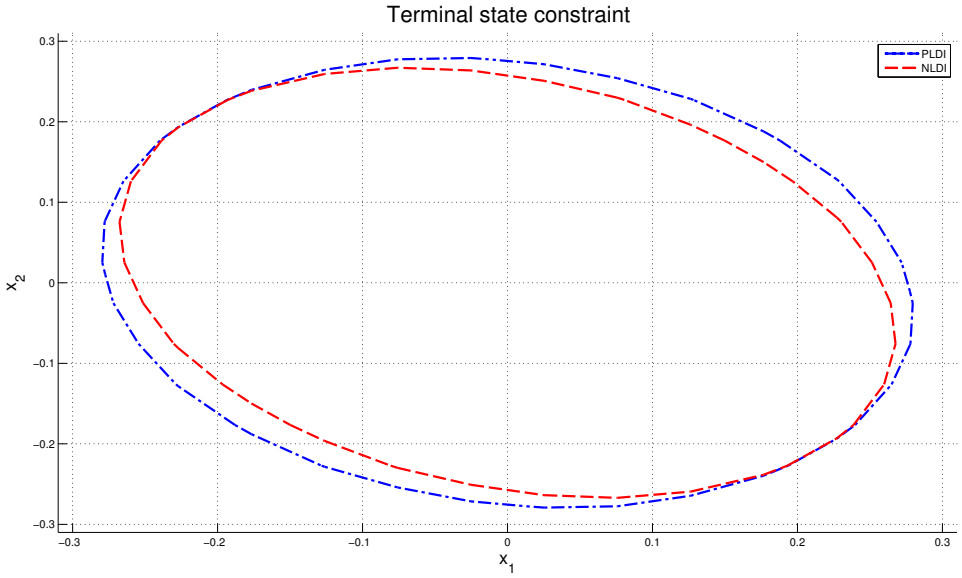

Figure 5.1: Comparison of the terminal state constraint obtained by a PLDI and a NLDI embedding.

Because the PLDI embedding provides a larger terminal subset, the SPMPC controller will be implemented using a final cost and a terminal state constraint given by

$$\begin{aligned} E(x) &= x^T S x, \\ \Omega_a^{f_e} &= \{x \in \mathbb{R}^{n_x} / E(x) \leq \gamma\}, \end{aligned}$$

where S and γ are given by (5.9).

5.4 Stabilization of a disturbed Van der Pol oscillator

5.4.1 Robust control problem

According to definition 2, at each sampling instant, the robust control problem is given by the solution of the optimization problem given by (3.6). To consider the terminal state constraint using the algorithm

presented in chapter 4, we introduce the following modified functional:

$$\mathscr{L}_A^{t_i,\mu}(u,\tilde{w}) = J^{t_i}(u,w) + \Psi^{\mu}(\gamma - x(x_i,u,w;t_i+T)^T Sx(x_i,u,w;t_i+T),\lambda_\Omega). \tag{5.17}$$

According to (4.35), to obtain the appropriate optimality system (necessary conditions), which corresponds to the identification of the gradient of $\mathscr{L}_A^{t_i,\mu}$ that is necessary to develop a numerical scheme in order to solve the saddle point problem, we introduce the adjoint system as follows:

$$\begin{aligned} -\frac{d\tilde{x}_1}{dt} &= (-(1+w_2)+x_1x_2+u)\tilde{x}_2 + R_{1,1}x_1, \\ -\frac{d\tilde{x}_2}{dt} &= (1+w_1)\tilde{x}_1 - \frac{1}{2}\tilde{x}_2(1-x_1^2) + R_{2,2}x_2, \\ \tilde{x}(t_0+T) &= 2Sx(x_i,u,w;t_i+T) + \nabla_x\left(\Psi^{\mu}(C,\lambda_\Omega)\right), \end{aligned} \tag{5.18}$$

where $C = \gamma - x(x_i,u,w;t_i+T)^T Sx(x_i,u,w;t_i+T))$ and $\nabla_x(\Psi^{\mu}(C,\lambda_\Omega))$ is defined as follows

$$\nabla_x(\Psi^{\mu}(C,\lambda_\Omega)) = \begin{cases} -2(-\lambda_\Omega + \frac{1}{\mu}C)Sx(x_i,u,w;t_i+T), \text{if } C \le \mu\lambda_\Omega, \\ 0, \text{if } C \ge \mu\lambda_\Omega, \end{cases}, \tag{5.19}$$

According to (4.38), the following expression of the derivatives of $\mathscr{L}_A^{t_i,\mu}$ are deduced:

$$\begin{aligned} \frac{\partial \mathscr{L}_A^{t_i,\mu}}{\partial u}(u,\tilde{w}) &= \tilde{x}_2x_1 + 2\alpha u, \\ \frac{\partial \mathscr{L}_A^{t_i,\mu}}{\partial \tilde{w}}(u,\tilde{w}) &= \begin{pmatrix} \tilde{x}_1x_2 - Q_{1,1}w_1 \\ -\tilde{x}_2x_1 - Q_{2,2}w_2 \\ \frac{\partial \Psi^{\mu}}{\partial \lambda}(C,\lambda_\Omega) \end{pmatrix}, \end{aligned} \tag{5.20}$$

where

$$\frac{\partial \Psi^{\mu}}{\partial \lambda}(C,\lambda_\Omega) = \begin{cases} -C, \text{if } C \le \mu\lambda_\Omega, \\ -\mu\lambda_\Omega, \text{if } C \ge \mu\lambda_\Omega, \end{cases}. \tag{5.21}$$

5.4.2 Numerical simulation

For simulation purpose it has been assumed that full state information is provided to the controller. The sampling time has been set to $\delta = 0.25$ and the control horizon is set to $T = 6$. In order to test the benefit of using a robust controller, the performances of the SPMPC controller has been compared to the one of a NMPC controller. The disturbances are given as follows

$$w_1(t) = w_2(t) = 0.1\sin(3t). \tag{5.22}$$

The system trajectory and the corresponding control input can be seen on fig.5.2. It can be seen that in this case a classical NMPC controller provides a stable closed-loop but the control performances are poorer. This has to be understood in the sense that when using a SPMPC controller the state follows a trajectory along which the influence of the disturbances are minimized (see fig.5.3). However, in order to obtain these performances, the computation time has been increased.

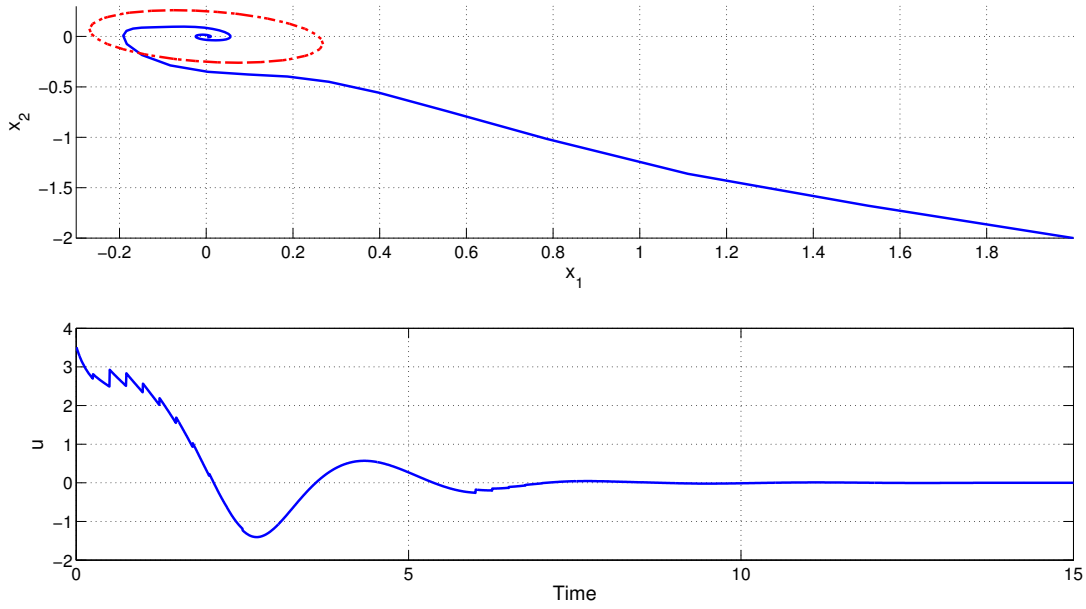

Figure 5.2: State trajectory and Control Input with a SPMPC controller, parametric disturbances

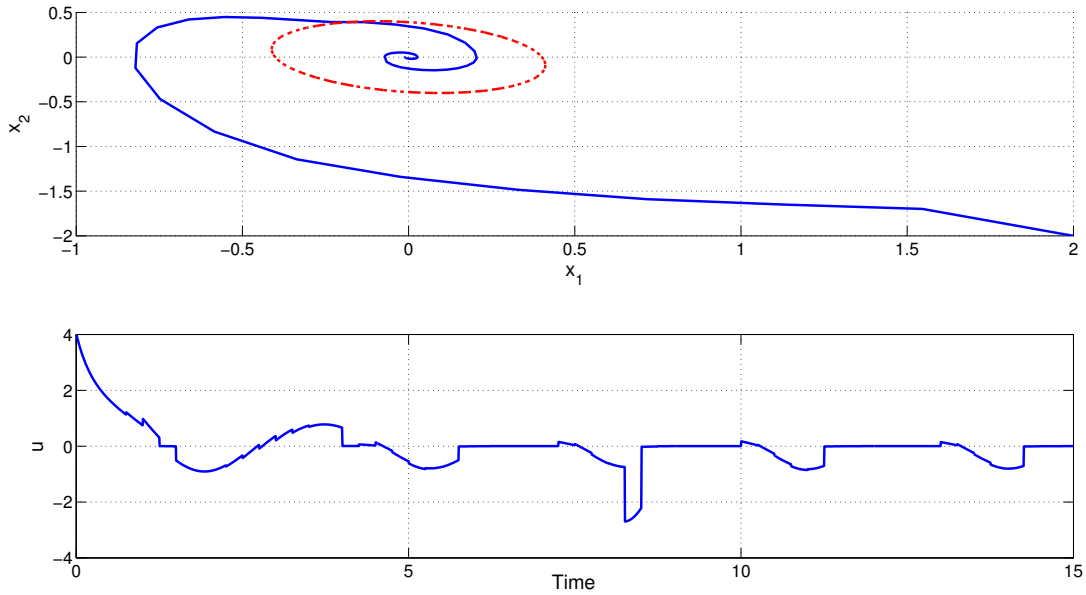

Figure 5.3: State trajectory and Control Input with a NMPC controller, parametric disturbances

5.5 Conclusion

In this chapter the implementation of the SPMPC controller to stabilize a disturbed in parameters Van der Pol oscillator has been considered. Through the numerical simulation, the controller robust performances have been shown. To numerically solve the control problem we have used the numerical methods presented in chapter 4. It has been shown that these methods can efficiently solve the corresponding state-constrained optimization problem at each sampling instant.

Now, that the feasibility and the interest of the controller has been shown on a simple example, we will be interested in testing it on a more realistic case. The remaining part of this thesis will be interested in applying a SPMPC controller to the problem of artificial blood glucose control.

Part II

Applications to Type 1 Diabetes Mellitus

Chapter 6

Modeling Type 1 Diabetes Mellitus

Contents

6.1 Introduction

Diabetes is a group of diseases marked by high levels of blood glucose resulting from defects in insulin production, insulin action or both [52]. For healthy people, glucose is regulated within narrow range *i.e.* in the interval $[60;120]\text{mg.dL}^{-1}$ [37]. This regulation is mostly made possible by the combined action of two hormones: the insulin and the glucagon. The first one enables to lower the value of blood glucose by favoring the storage of glucose in liver and fat and the second one has an opposite effect.

When this disease is not correctly treated, *i.e.* when the blood glucose remains too high or too low, this can lead to various complications including heart disease and stroke, hypertension, blindness and eye problems, kidney disease or nervous system disease [52] ... Thus the control of blood glucose to safe concentrations (also called euglycemia) is the prime concern of diabetics.

There are two main type of diabetes. Type 2 diabetes (approximately 90% of prognosed diabetes), which was often called non insulin dependent diabetes, usually begins as insulin resistance, *i.e.* a disorder in which the cells do not use insulin properly. As the need for insulin rises, the pancreas gradually loses its ability to produce it. Type 1 diabetes (approximately 5% of prognosed diabetes), which was often called insulin dependent diabetes, is developed when the immune system has destroyed the pancreatic β cells, which are normally responsible for insulin secretion [52]. In this thesis, we are only interested in type 1 diabetes. Let us give two reasons that motivate this choice. Because these patients are fully insulin dependent, they are more in a position to possess a glucose sensor and an insulin pump which are parts of a complete artificial pancreas. Also, these patients are easier to model because we do not need a model to describe the insulin and glucagon secretion. Indeed, in type 1 diabetic, the insulin secretion is non existing and the glucagon production can be neglected.

In order to live a normal life, patients who suffer from type 1 diabetes require exogenous insulin which is delivered either by injection or by *continuous* subcutaneous infusion using an insulin pump. An extensive long-term study [37] has demonstrated that intensive diabetes therapy (*i.e.* the cure which consists in regular insulin injection guided by frequent blood glucose monitoring) reduces the complication of type 1 diabetes.

However, despite the availability of glucose sensors which regularly provide glucose measure (each 1 to 5 minutes depending on the device), euglycemia still remains a difficult goal to achieve. In fact this is not surprising as, in the every day life, it seems complicated, if not impossible, to control one's insulin injection at such a high rate. That is why there has been considerable interest in developing an *artificial pancreas* [115], [121]. The aim is to use the sensor information to automatically adjust, in real-time, the insulin injection to aim at a better glucose control.

Lately, it seems that the MPC approach is the more promising because of numerous attractive features. First, it is easy to interpret its behavior in terms of a classical cure. Indeed, when the patient deals with his disease, it can be seen as the patient trying to solve a constrained optimal control problem. He wants to stabilize his blood sugar to a given value (stabilization), to avoid hypoglycemia and reduce hyperglycemia (state constraints) by only injecting insulin (input constraint). Then, the predictive aspect is interesting as it enables to anticipate on known disturbances. As an example, a patient often knows in advance when and what he will eat, thus providing the controller with these informations, it becomes possible to aim at better control performances. Finally, it can also be useful to overcome physiological delay due to the use of the sub-cutaneous route for both the insulin injection and the blood sugar measures [72], [87].

As its name tends to suggest, the MPC control techniques relies on a prediction given by a model of the process that has to be controlled. So, to obtain the best control performances, it is of prime importance to derive a good model of a patient suffering from type 1 diabetes. This issue has lead to several research and many models describing this disease have been published. In this section we aim at describing some

of the various available one and to explain why we have decided to focus on two specific models: the Dalla-Man et al. model and a modified version of the minimal model of Bergman.

The dynamics of the glucose-insulin metabolism have been studied extensively. Several models can be used depending if the purpose is to provide a realistic simulation of a patient suffering from type 1 diabetes or to provide a model in order to design a controller. These models range from simple transfer function (see e.g. [122] or [156]) to more complex models which are based on a detailed knowledge of the patient's internal metabolic behavior (see e.g. the minimal model of Bergman [14], the Dalla Man et al. model [106], the Hovorka model [73] or the Sorensen model [151]). An overview of some classical models is available, e.g., in [105] or [162].

To design a control algorithm which can ensure euglycemia in a type 1 diabetic, we have retained two models. The first one, the model of Dalla Man et al. [106], is a simulation model. It is assumed to be closed to the patient's true internal metabolic behavior. It will be used as a realistic virtual patient to assess the controller performances. It will be used in the framework of a simulation platform approved by the Food and Drug Administration (FDA) (Uva/Padova T1DM metabolic simulator the distributed version [90]). The second model will be used to design the controller, therefore it will be chosen simpler. We will use a modified version of the minimal model of Bergman [14]. This latter, which has often been used for control purpose, provides a good global trend of the glucose-insulin metabolism. However, because of is simplicity, it can not be considered as an accurate model of the real patient metabolism. This explains the need for a virtual testing platform to test the controller performances.

This chapter is organized as follows. First a short discussion on the structure of the available models is done. Then, the model of Dalla-Man et al. is presented. Assuming that it is closed to the internal metabolic behavior, this gives us the opportunity to have a rough overview of how the glucose-insulin metabolism works (at least for the parts we are interested in). Next, the minimal model of Bergman is presented. The objective is to show that it can be seen as an approximation of the true process and that, despite its simplicity, it retains the most important aspect of the glucose-insulin metabolism. Finally the section is concluded by a short discussion.

6.2 Forewords on the available models

In order to design a controller for artificial blood glucose control for a type 1 diabetic patient, the first step consists in modeling the glucose-insulin metabolism. It is possible to use black box model, *i.e.* to only use an input output formulation, or a gray box model, *i.e.* to introduce a knowledge of the metabolism in the model [96]. Generally the input-output formulation is simpler but suffers from a lack of insight of the true metabolic process. That is why, even if gray box models suffer from several problems such as the difficulty to estimate individual parameters, we will focus on this latter class of model.

The gray box models are usually derived using a knowledge of the physiology and metabolic processes. Each metabolic function is treated as a separate compartment with its own dynamic. Then, the various subprocesses are linked thanks to a variable which either stands for a concentration or a quantity of a given molecule, hormones, ... Adapted from [162], the scheme 6.1 present the elements of the glucose metabolism which are usually considered.

The main differences between the various available models lie in the compartments which are considered and the way each of them is described. As an example, the effect of exercise is often not modeled because of the difficulty to quantify its effect. An other example, the glucose kinetics can be modeled either globally as in the minimal model of Bergman [14] or by splitting the variable glucose into the glucose production part and the glucose disposal part as in the Hovorka model [73].

Despite the difficulty to validate a given model, some of them are known to be more accurate than

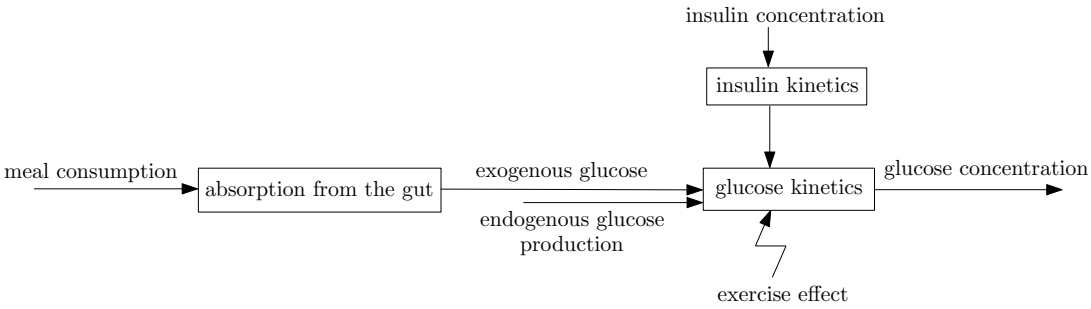

Figure 6.1: Representation of the glucose-insulin system

others. The main reason is that they consider the glucose-insulin metabolism with more details. This can be illustrated by considering the Sorensen model [151]. With its 19 differential equations and its 44 parameters, this model divides the body into 6 compartments (see the corresponding flow diagram on fig. 6.2) and is quite close to the true human metabolism. This is in opposition to the minimal model of Bergman which models the glucose-insulin metabolism only from a (simple) functional point of view (no consideration on fine details such as the existence of different type of glucose, ...).

In the next section, we will present more in depth a model close to the human metabolism and a simpler model. The former, the model of Dalla-Man et al. [106], will be used for validation purpose and the latter, the minimal model of Bergman, will be used for control design purpose.

6.3 The Dalla man et al. model

The model of Dalla-Man et al. [106] is known to be a model close to the patient's internal metabolic behavior. It has been designed using complex experiments, e.g. using the double tracer protocol. This has given the possibility to model the glucose-insulin metabolism in an accurate way using several compartments which interact among them. More details on how this model has been derived and identified can be found in [129].

From a control point of view, the overall model can be seen as a MISO (multiple input single output) system with two inputs (insulin injection and sugar consumption) and one output (blood glucose). This model has been implemented in a virtual testing platform [90] which has been approved by the FDA. This has the huge interest that it can be used as a substitute to test on animals. To give a *simple* overview of the glucose-insulin metabolism, the bloc structure of the overall model is summed up in fig.6.3 (inspired by [129]).

Globally, its structure is divided into three main parts. One is for insulin, one is for glucose and one is for meal. The insulin and the meal parts interact with the glucose part and determine how the blood glucose value evolves. Roughly speaking, if the insulin quantity increases then the blood glucose value decreases and if a meal is consumed then the blood glucose value increases. Let us now describe the various sub-models corresponding to the various compartments.

6.3.1 Gastro-intestinal subsystem

The gastro-intestinal subsystem describes the glucose transfer in the blood due to the digestion of a meal. This subsystem takes a sugar quantity as input (the sugar quantity in the ingested meal) and provides a

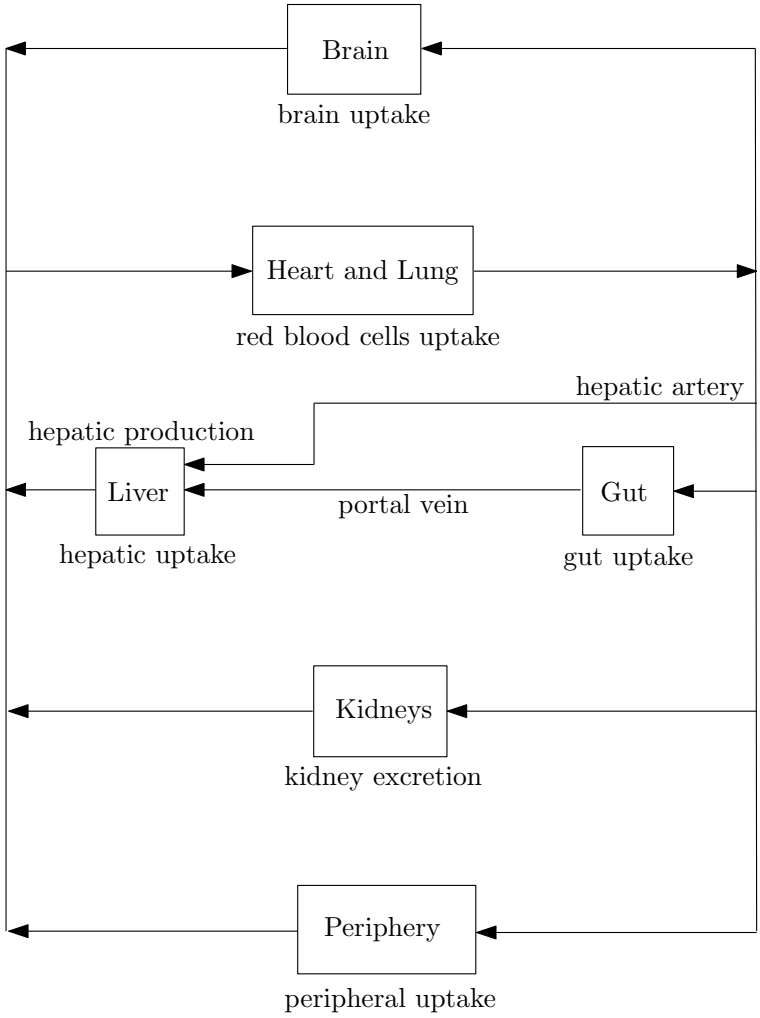

Figure 6.2: Flow diagram of the Sorensen model

glucose flow as output. The gastro-intestinal subsystem is modeled by the following set of equations

$$\begin{aligned}
\frac{dQ_{sto1}}{dt} &= -k_{gri}Q_{sto1} + d(t),\\
\frac{dQ_{sto2}}{dt} &= -k_{empt}(t,Q_{sto})Q_{sto2} + k_{gri}Q_{sto1},\\
\frac{dQ_{gut}}{dt} &= k_{empt}(t,Q_{sto})Q_{sto2},\\
R_a &= \frac{fk_{abs}}{BW}Q_{gut}.
\end{aligned}$$

where $d(t)$ mg.min^{-1} is a glucose input (*i.e.* the sugar content of a given meal), BW is the patient body weight. This model is nonlinear because of the parameter $k_{empt}(t,Q_{sto})$ which models the fact that the rate of gastro-emptying depends on the quantity of food in the stomach. The full expression of k_{empt} can be found in [106]. The rate of appearance in the blood R_a mg.kg^{-1}.min^{-1} is given as a fix percentage f of the glucose in gut Q_{gut} mg.

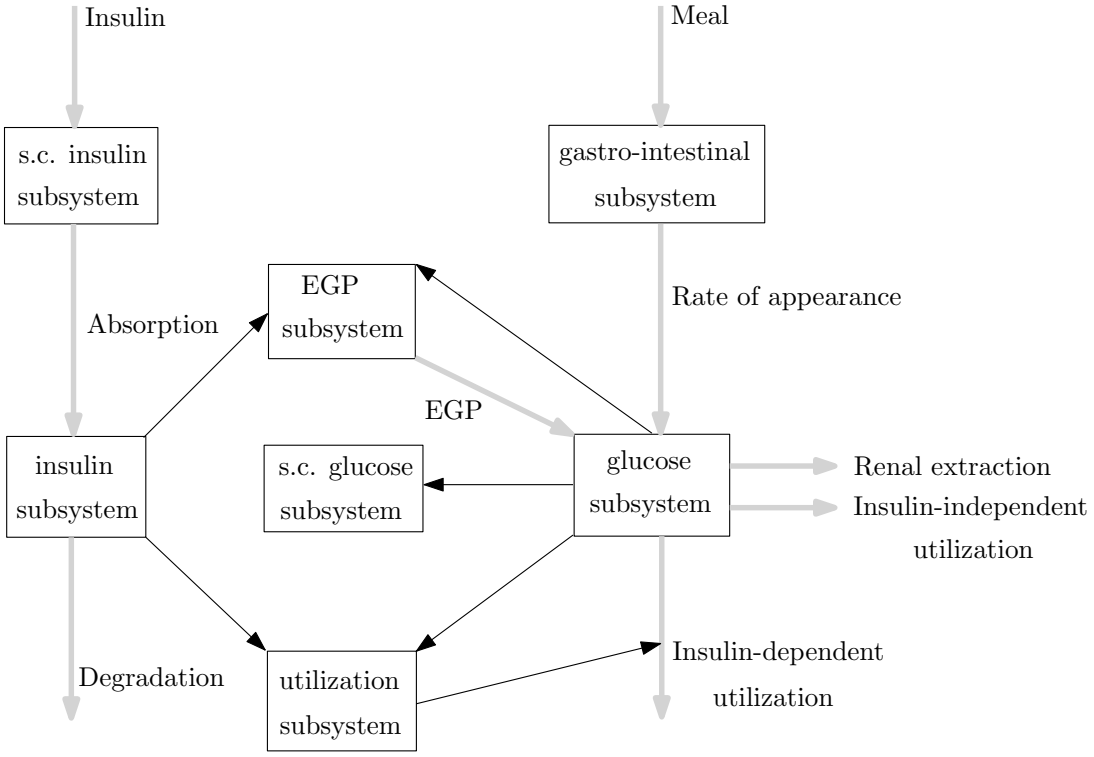

Figure 6.3: Dalla Man et al. model: structure of the model

6.3.2 Glucose subsystem

The glucose subsystem describes the dynamic of the blood glucose G when influenced by insulin and glucose flow input. The system of differential equations which governs the blood glucose evolution G mg.dL^{-1} is given by

$$\begin{aligned}
\frac{dG_p}{dt} &= -k_1 G_p + k_2 G_t + EGP + R_a - U_{ii} - E, \\
\frac{dG_t}{dt} &= k_1 G_p - k_2 G_t - U_{id}, \\
G &= \frac{1}{V_G} G_p,
\end{aligned}$$

where G_p mg.kg^{-1} is the plasma glucose and G_t mg.kg^{-1} stands for the glucose value in the tissue. The value of the blood glucose does not only depend on the action of insulin U_{id} and the rate of appearance due to a meal consumption R_a but also on the glucose in tissue G_t (e.g. in the muscles), the endogenous rate of production EGP (mainly coming from the liver), an insulin independent utilization U_{ii} (e.g. the sugar needed for the nervous system or the brain) and a renal extraction E (only active when the plasma glucose is greater than a given threshold, e.g. 300 mg.dL^{-1}). The various expression of EGP, U_{ii}, U_{id} and E can be found in [106].

6.3.3 Insulin subsystem

The insulin flow s, coming from the subcutaneous compartment enters the bloodstream and is then degraded in the liver and in the periphery. The insulin concentration in blood stream I is given by

$$\begin{aligned}\frac{dI_p}{dt} &= -(m_2+m_4)I_p + m_1 I_l + s,\\ \frac{dI_l}{dt} &= -(m_1+m_3)I_l + m_2 I_p,\\ I &= \frac{1}{V_I} I_p,\end{aligned}$$

where I_p is the plasma insulin and I_l is the *liver* insulin. V_I is the distribution volume of insulin.

6.3.4 Subcutaneous insulin subsystem

In the project of designing an *artificial pancreas*, the subcutaneous way seems more desirable to inject insulin [139]. This implies that there is a time-lag between the injection of the insulin and the moment when it reaches the blood stream. Concretely this means that insulin is not immediately active. Generally speaking there are several possibilities to model this phenomenon. It is possible to use a diffusion process model described by partial differential equations or to use a simple filter. This latter choice has been retained in the model of Dalla-Man et al., where this sub-system is described with a second order filter as follows

$$\begin{aligned}\frac{dS_1}{dt} &= -(k_{a1}+k_d)S_1 + u,\\ \frac{dS_2}{dt} &= k_d S_1 - ka2 S_2,\\ s &= k_{a1} S_1 + k_{a2} S_2,\end{aligned}$$

where u pmol.kg^{-1}.min^{-1} is the injected insulin flow, S_1 pmol.kg^{-1} stands for polymeric insulin in the subcutaneous tissue and S_2 pmol.kg^{-1} stands for monomeric insulin in the subcutaneous tissue.

6.3.5 Subcutaneous glucose subsystem

Most of the available sensors do not directly measure blood glucose but only plasma glucose. This subsystem has been added to explicitly consider that the subcutaneous glucose G_M mg.dL^{-1} is highly correlated with plasma glucose but its rate of variation is subject to some filtering. This is described by the following equation

$$\begin{aligned}\frac{dG_M}{dt} &= -\frac{1}{\tau_d}(G_M - G),\\ G_{sensor} &= G_M + \varepsilon,\end{aligned}$$

where G_{sensor} is the measure given by the sensors, τ_d is the diffusion time constant, and ε is the sensor noise driven by a Johnson distribution (see [20]).

From a model point of view this subsystem is useless in the sense that the sensor is not part of the glucose metabolism. However, from a control point of view, it is crucial as the controller has to show robustness against the non negligible measurement noise. It is also important because the dynamic of the sensor is not negligible compared to the one of the glucose metabolism.

6.3.6 Discussion

The model of Dalla-Man et al. consists in 13 states, 25 patient-dependent parameters and 5 patient-independent parameters (see [106]). This model has been identified on a data base of 204 healthy subjects using complex experiments. Then, the obtained model have been modified in order to cover the distinctive features of a patient suffering from type 1 diabetes. The main advantage of this model is that by remaining close to a patient internal metabolic behavior, the simulated behavior are quite realistic. The main disadvantage is that this model is really complex, implying that a direct design of a controller is unattractive. Thus, the controller which use this model for design purpose often includes some steps in order to simplify it (see e.g. [102] where the model is first linearized and discretized before to be used for control purpose). Furthermore, it is nearly impossible to adjust the model parameters for a given patient. Of course this point is a major drawback as it is well known that there is a wide variety of patients physiology and so it is highly probable to meet a patient whose behavior is different from one of those contained in the original database. All these points imply that the Dalla-Man et al. is a good validation model but, at least for what we intend to do, a not so good control model. That is why in the sequel, we will introduce an other simpler model which can be used to design a controller. Then, the control strategy will be validated using the Dalla-Man et al. model.

6.4 The modified minimal model of Bergman

All human beings are different. If this assertion is easily verifiable via a comparison of our phenotype, this also holds when dealing with our internal metabolic behavior. If this remark seems simplistic, in fact it is of prime importance when dealing with artificial blood glucose control. Indeed, when looking for an *artificial pancreas*, we are interested in the metabolism of a specific patient. So, in order to aim at good control performances, it seems unavoidable to consider this phenomenon in the design phase. A possibility is to adjust the parameters of the control model using identification tools. Thus the model can provide a more reliable prediction of the future value of blood glucose. The main problem is that it is really difficult to identify a nonlinear process . This is exacerbated when human is in the loop as the experiments have to satisfy some heavy constraints in order to remain human friendly. That is why it seems more reasonable to retain control model which are easier to identify. We translate this need as the problem of searching for a control model with few states and parameters. Practically, this implies that we are not interested in choosing the Dalla-Man et al. model for control design purpose, and so that a simpler model has to be found.

The main issue is now to identify the thin frontier between a simple but adequate model and a simplistic model. This question is not trivial at all, especially as it is really difficult to validate a model *in vivo*. Instead of claiming that the model we have retained is sufficient to describe the glucose-insulin metabolism, let us enumerate what we were looking for. We think that an adequate model has to satisfy the following point:

- being nonlinear (human metabolism is clearly a nonlinear process),
- being time continuous (even if the control input can not be adjusted in continuous time, it seems important to consider the continuous time aspect of human metabolism),
- possessing a minimal number of parameters (for identification purpose),
- providing a good global trend of glucose-insulin dynamic.

It can seem surprising that despite the existence of linear models (e.g. [59]), we focus on keeping the nonlinear aspect, especially as we stress on the need for simplicity. This choice has been made because the true glucose-insulin is a highly nonlinear process. Furthermore it has been often suggested (e.g. in [99]) that a nonlinear controller can provide better control performances.

These requirements have made us choose the well-known minimal model of Bergman [15]. This time continuous nonlinear model is said to be minimal in the sense that it has few parameters. Since it originally describes the glucose-insulin dynamic in response to a glucose resistance test, it provides an acceptable trend of the glucose-insulin dynamic. Furthermore this model has been extensively used for control design purpose (see e.g. [118] or [16]). Even if this does not prove that this model is well adapted for control purpose, at least it tends to show that it is not a really bad idea to work with it.

6.4.1 The original minimal model of Bergman

The original minimal model of Bergman (see e.g. [14], [15] or [105]) has been developed to provide a model of the glucose-insulin metabolism of an healthy subject in response to a glucose tolerance test. One of the main concern in its design was that it has to be as simple as possible. According to this model, the glucose metabolism is described by the following set of equations

$$\begin{aligned} \frac{dG}{dt} &= -(P_1 + X)G + P_1 G_b + R_a, \\ \frac{dX}{dt} &= -P_2 X + P_3(I - I_b), \\ \frac{dI}{dt} &= \gamma \max(0, G - G_{Th})t - k_f(I - I_b), \end{aligned} \tag{6.1}$$

where P_1, G_b, P_2, P_3, I_b, γ, G_{Th} and k_f are positive parameters. The state G mg.dL^{-1} stands for the blood glucose concentration. The state X min^{-1} stands for the insulin in a remote compartment. It mimics the time-lag of the insulin consumption on glucose. The state I mU stands for the blood insulin. The input R_a stands for a glucose flow in the blood.

In this model, the behavior of the healthy pancreas is divided into two terms. There is the constant flux of insulin $k_f I_b$, whose aim is to stabilize blood glucose, and there is the corrective term $\gamma \max(0, G - G_{Th})t$, whose aims is to reject sudden disturbances (e.g. to minimize an increase of the blood glucose in case of a glucose injection) and which is only active when blood glucose grows beyond a given threshold G_{Th}.

In order to ease the comparison between the Dalla-Man et al. model and the minimal model of Bergman, it can be interesting to interpret the term $-P_1 G$ as an insulin independent glucose utilization, the term $-XG$ as an insulin dependent glucose utilization, and the term $P_1 G_b$ as an endogenous glucose production. Also it is interesting to consider the state product XG from a chemical point of view. It can be interpreted as the fact that to initiate the reaction of glucose storage, one *molecule* of glucose has to interact with one *molecule* of insulin.

As mentioned, a type 1 diabetic can not secrete insulin at all. This means that this model has to be modified in order to take into account the specificity of the disease. Furthermore this model does not possess a digestion model. Indeed in the experience of Bergman only pure glucose was injected in the blood. That is why this model has to be completed with a gastro-intestinal model. All these issue will be considered in the sequel and will lead to what we will call the modified minimal model of Bergman.

6.4.2 Gastro-intestinal subsystem

Let us begin with a fact: *in a normal day a normal person eats*. This is at the origin of a sudden blood glucose value increase as, through the digestion process, sugar enters the blood stream. Due to the amplitude of this phenomenon, to aim at better control performances, it is desired to anticipate on these events. To do so, the patient can provide the control algorithm the meal time and the corresponding sugar content. However, from a control point of view, what really matters is the glucose flow induced by the digestion of the meal. That is why it is desired to add a digestion model. In the same spirit as for the minimal model of Bergman, our choice has been guided by simplicity. That is why we have retained a simple linear model as suggested in [163]. The retained gastro-intestinal subsystem is given by

$$\begin{aligned} \frac{dR_1}{dt} &= -c_1(R_1 - d), \\ \frac{dR_2}{dt} &= -c_2(R_2 - R_1), \\ R_a &= k_{gr} R_2, \end{aligned} \tag{6.2}$$

where R_1 and R_2 stand for the sugar in a remote compartment, d mg is the meal sugar content and R_a mg.dL^{-1}.min^{-1} is the rate of appearance in the blood.

6.4.3 Glucose subsystem

The glucose subsystem is simply given by the first two equations of the original minimal model of Bergman (6.1), that is

$$\begin{aligned} \frac{dG}{dt} &= -(P_1 + X)G + P_1 G_b + R_a, \\ \frac{dX}{dt} &= -P_2 X + P_3(I - I_b). \end{aligned} \tag{6.3}$$

6.4.4 Insulin subsystem

In type 1 diabetes the secretion of insulin from the pancreas is negligible. To cover his need in insulin, a patient mainly count on insulin injection. That is why the insulin subsystem of the minimal model of Bergman has to be adjusted. According to what has been done in [49], the insulin subsystem becomes

$$\frac{dI}{dt} = -k_f I + s, \tag{6.4}$$

where s is the insulin flow coming from the subcutaneous compartment.

6.4.5 Subcutaneous insulin subsystem

The use of a subcutaneous way of action for insulin injection is at the origin of a diffusion process. To aim at good control performances, it seems unavoidable to model this phenomenon. Searching for simplicity, a simple first order model has been chosen

$$\begin{aligned} \frac{dU_1}{dt} &= -k_s U_1 + u, \\ s &= b_f U_1, \end{aligned} \tag{6.5}$$

where U_1 mU is the *subcutaneous* insulin, k_s and b_f are positive parameters and u mU.min^{-1} is the injected insulin flow.

6.4.6 The modified minimal model of Bergman

Finally, the control model is given by the combination of the sub-models 6.2, 6.3, 6.4 and 6.5 according to the scheme 6.4.

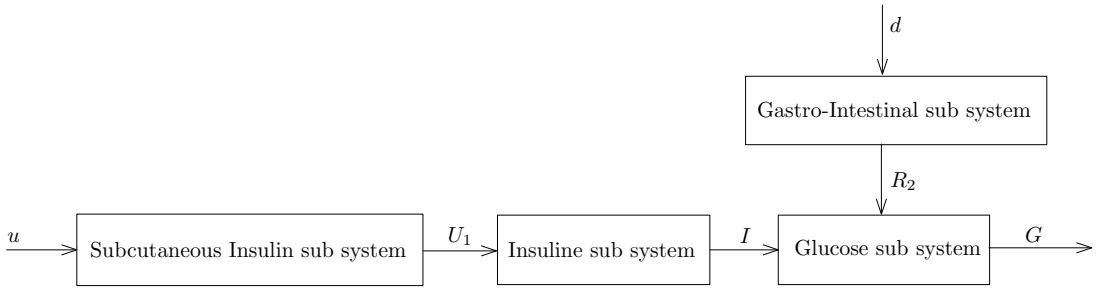

Figure 6.4: Modified minimal model of Bergman: interconnection between subsystems

The final model consists in 6 states and 11 (positive) parameters given as follows:

$$
\begin{aligned}
&\underline{\text{Glucose-insulin sub-model}}:\\
&\frac{dG}{dt} = -(P_1 + X)G + P_1 G_b + k_{gr} R_2,\\
&\frac{dX}{dt} = -P_2 X + P_3 (I - I_b),\\
&\frac{dI}{dt} = -k_f I + b_f U_1,\\
&\frac{dU_1}{dt} = -k_s U_1 + u,\\
&(G, X, I, U_1)(t_0) = (G_0, X_0, I_0, U_{1,0}),\\
&\underline{\text{Gastro-intestinal sub-model}}:\\
&\frac{dR_2}{dt} = -c_2 (R_2 - R_1),\\
&\frac{dR_1}{dt} = -c_1 (R_1 - d),\\
&(R_2, R_1)(t_0) = (R_{2,0}, R_{1,0}).
\end{aligned}
\tag{6.6}
$$

The Dalla-Man et al. model and the modified minimal model of Bergman share a common structure. This can be seen by comparing the structure of the two models respectively given by fig.6.3 and fig.6.5. The modified minimal model of Bergman considers the same three components of the glucose-insulin metabolism, namely the absorption from the gut (given by the state $R_1$and R_2), the insulin kinetics (given by the state I and U_1) and the glucose kinetics (given by the state G and X). The main difference is that, for each compartment, the model is extremely simple. Thus, only global trends are modeled.

6.5 Conclusion

In this chapter, we have presented some of the models which are available to describe the glucose-insulin metabolism. We have been particularly interested in two models: the Dalla-Man et al. model, which is rather complex but is known to be accurate, and a modified minimal model of Bergman, which provides rough blood glucose trend but possesses a simple structure. At that point, let us remind that one difficulty

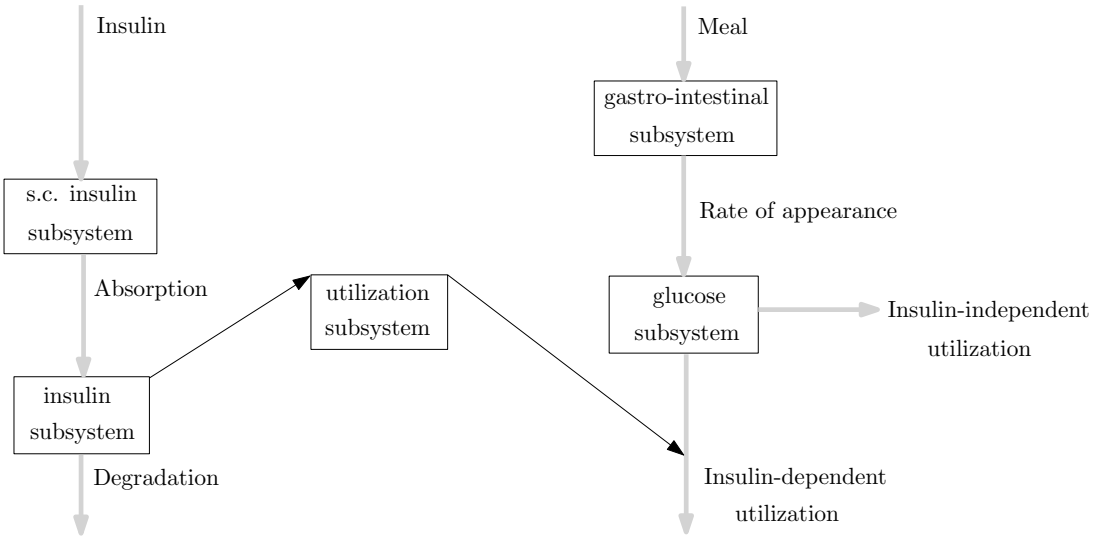

Figure 6.5: Modified minimal model of Bergman: structure of the model

with artificial blood glucose control is the inter-patient variability. We have suggested that this problem can be, at least partially, solved by identifying the parameters of the model for each patient. However, this task is limited to simple model. Concretely, using simple experiment, it is unrealistic to identify the Dalla-Man et al. model. This point raises a question. Is this better to design a controller with an accurate model of the glucose metabolism but which can not be identified or to design a controller with a model which only provides rough trend but which can be identified ? In this thesis, we have assumed that the second choice is the more interesting. Then, to compensate for the known simplicity of the control model, we will consider the design of a SPMPC controller. The Dalla-Man et al. model will be used in the framework of a testing platform [90] to assess the controller performances.

To design the controller, we have to verify whether the modified minimal model of Bergman satisfy the needed assumptions in order to be sure that the closed-loop is stable and whether the control problem is well-posed. This is the objective of the next chapter.

Chapter 7

Model Analysis and Controller Design

Contents

7.1 Introduction

In chapter 6, we have been interested in modeling the glucose-insulin metabolism. In order to obtain models, some assumptions have been made (e.g. assuming that the process is stationary or that the effect of all hormones but insulin is negligible). In regards to the true metabolism, these assumptions are quite simplistic. So, in order to ensure good control performances, the design of a robust controller seems unavoidable. In the sequel, the design of the previously presented SPMPC controller is envisaged.

Let us more precisely motivate our controller choice:

- To obtain a model suitable for control purpose, some dynamics of the glucose-insulin metabolism have been neglected (e.g. the effect of adrenaline in a situation of stress). It can be interesting to design a controller which is robust against these dynamics by introducing the adequate disturbances in the model that has to be controlled.

- The retained models in chapter 6 are stationary. However, human metabolism is a time varying process, e.g. in type 1 diabetics, the dawn phenomena implies a sudden insulin resistance in the early morning. We can model these phenomenon thanks to time varying parameters. If the variations are bounded (what is obviously the case as we consider a biological process), the time varying parameters can be expressed as the sum between a nominal parameter and a bounded time varying disturbance. By using a SPMPC controller, it is possible to ensure control performances for disturbed parameters. Thus, by introducing adequate bounds on the parameter disturbances, we will design a controller which consider this aspect and so that will guarantee control performances despite this phenomenon.

- It is difficult to identify a nonlinear time continuous model with discrete noisy measurement. This is even more critical when the control problem is concerned with human beings. Indeed, the patient welfare is the most important issue. This strongly restricts the scope of available experiments to obtain data for identification purpose. Practically, this implies that the parameters will be known relatively to a non negligible bound. By introducing adequate bounds on parameter disturbances, using a SPMPC controller, we can use this information to mitigate the influence of a potentially badly identified model.

- The up to date technology implies that the sensors sampling-time is not negligible compared to the metabolism time constant (depending on the sensor, a measure is available each 1 to 5 minutes). This means that the control problem has to be cast in a sampled-data framework. The SPMPC controller is a sampled-data controller, so by using this controller, this point is not a big issue.

- The up to date hardware favors the choice of the subcutaneous way to deliver the cure, implying that, before insulin becomes active, there is some time lag. This point is handled by the combined use of a state space model which has a memory of the past via the actual value of the state and a predictive control approach which computes the adequate control action by considering state trajectories.

- The control objective is asymmetric, e.g. if a blood glucose of 200mg.dL^{-1} is not too dangerous, a blood glucose of 0mg.dL^{-1}, means that the patient is dead. A SPMPC controller solves the robust control problem by considering an optimization problem. So, to take the asymmetric control objective into account, it is possible either to optimize an asymmetric cost function (as what has been done in [89]) or to consider a state-constrained optimization problem to ensure that blood glucose remains in a safe interval.

- When consuming a meal, the blood glucose grows faster than the time needed for insulin to become active. This implies that if it is desired to have a good control of meals either they are treated by the patient himself or an anticipatory behavior is needed. In both cases the SPMPC controller is well suited because the problem will be recast in a variational form and the predictive aspect enables to anticipate on known disturbances.

At that point, it seems quite clear that the SPMPC approach provides a potential answer to many difficulties surrounding the problem of artificial blood glucose control. The robust aspect of the controller can cope with the problem of neglected dynamics, time-varying metabolism and potentially badly identified parameters. Also, the predictive approach can give an answer to the need for anticipatory behavior. The asymmetric objective can be handled via introduction of a constrained optimization problem or by using an asymmetric cost function. In the remaining part of this thesis, we will be interested in applying this control technique using the modified minimal model of Bergman given by the system of differential equations (6.6).

In this chapter, we will study the properties of the modified minimal model of Bergman. First, we will be interested in testing its consistency. To do so, we will search for the conditions on the parameters and on the inputs in order for the state to keep its physiological meaning. Also, we will be interested in verifying that the model is both observable and controllable. Then the properties of the model in regards to its applicability for control purpose are studied. We will begin to verify whether the control problem is well-posed. The first step will consist in formulating the control problem in a variational form. It will then be verified whether the retained control model satisfy the needed assumptions of theorem 1 and 2. Finally, a PLDI embedding is provided in order to compute the final cost and the terminal state constraint. Also the adjoint model and the expression of the gradient of the criterion are given.

7.2 Consistency of the modified minimal model of Bergman

In this section we are interested in presenting some general properties satisfied by the modified minimal model of Bergman. We will begin to search for the condition on the parameters and on the inputs in order for the state to satisfy a kind of invariance property. Then, we will show that this model is observable. Also, under the assumptions that the initial condition of the gastro-intestinal sub-model and the meal consumption profile are perfectly known, it will be proved that the glucose-insulin sub-model is controllable.

7.2.1 Invariance property

When considering the problem of artificial blood glucose control, we are interested in a biological process. This has for consequence that some states, which have a physiological meaning, have to satisfy some properties for all time instant. As an example a concentration or a quantity has to remain always positive. In this section we will be interested in looking for the conditions that the parameters of the model and the inputs have to satisfy in order for the state to keep its physiological meaning.

To do so let us consider the following theorem which will prove that if the initial condition of the system satisfies some bounds, if the parameters of the model are positive and if the inputs are bounded then the state is bounded for all time instant.

Theorem 4. *Assume that the parameters of the model are given and positive, and for all $t \geq t_0$ the control input $u(t) \in [\underline{u}, \overline{u}]$, and the meal input $d(t) \in [\underline{d}, \overline{d}]$. Then, for a given data $(\underline{G}, \underline{X}, \underline{I}, \underline{U}_1, \underline{R}_2, \underline{R}_1) \in$*

$\mathbb{R}^{+*}\times\mathbb{R}\times\mathbb{R}^{+}\times\mathbb{R}^{+}\times\mathbb{R}^{+}\times\mathbb{R}^{+}$ *and* $(\overline{G},\overline{X},\overline{I},\overline{U}_1,\overline{R}_2,\overline{R}_1)\in\mathbb{R}^{+*}\times\mathbb{R}\times\mathbb{R}^{+}\times\mathbb{R}^{+}\times\mathbb{R}^{+}\times\mathbb{R}^{+}$ *such that*

$$
\begin{aligned}
&(\underline{G},\underline{X},\underline{I},\underline{U}_1,\underline{R}_2,\underline{R}_1)\leq(\overline{G},\overline{X},\overline{I},\overline{U}_1,\overline{R}_2,\overline{R}_1),\\
&\underline{u}=\frac{k_sk_f}{b_f}\max\left(\frac{b_f}{k_f}\underline{U}_1,\underline{I},\left(I_b+\frac{P_2}{P_3}\underline{X}\right),\left(I_b+\frac{P_2}{P_3}\left(-P_1+\frac{P_1G_b+k_{gr}\overline{R}_2}{\overline{G}}\right)\right)\right),\\
&\overline{u}=\frac{k_sk_f}{b_f}\min\left(\frac{b_f}{k_f}\overline{U}_1,\overline{I},\left(I_b+\frac{P_2}{P_3}\overline{X}\right),\left(I_b+\frac{P_2}{P_3}\left(-P_1+\frac{P_1G_b+k_{gr}\underline{R}_2}{\underline{G}}\right)\right)\right),\\
&\underline{d}=\max\left(\underline{R}_1,\underline{R}_2\right),\\
&\overline{d}=\min\left(\overline{R}_1,\overline{R}_2\right),\\
&0\leq\underline{u}\leq\overline{u},\\
&0\leq\underline{d}\leq\overline{d},
\end{aligned}
$$

we have that if $(\underline{G},\underline{X},\underline{I},\underline{U}_1,\underline{R}_2,\underline{R}_1)\leq(G,X,I,U_1,R_2,R_1)(t_0)\leq(\overline{G},\overline{X},\overline{I},\overline{U}_1,\overline{R}_2,\overline{R}_1)$ *then for all* $t\geq t_0$ $(\underline{G},\underline{X},\underline{I},\underline{U}_1,\underline{R}_2,\underline{R}_1)\leq(G,X,I,U_1,R_2,R_1)(t)\leq(\overline{G},\overline{X},\overline{I},\overline{U}_1,\overline{R}_2,\overline{R}_1)$.

Proof. • **Let us consider the state** U_1**.**

Denote $\tilde{U}_1=U_1-\underline{U}_1$. Using the differential equation on U_1 we deduce that $\tilde{U}_1$ evolves via the following differential equation:

$$\frac{d\tilde{U}_1}{dt}=-k_s\tilde{U}_1+u-k_s\underline{U}_1. \tag{7.1}$$

Let us introduce $\tilde{U}_1^-=\max(0,-\tilde{U}_1)$, we have $\tilde{U}_1^-\geq 0$. Multiplying (7.1) by $-\tilde{U}_1^-$, we have

$$-\tilde{U}_1^-\frac{d\tilde{U}_1}{dt}=-\tilde{U}_1{}^-(-k_s\tilde{U}_1+u-k_s\underline{U}_1). \tag{7.2}$$

Since $-\tilde{U}_1^-\dfrac{d\tilde{U}_1}{dt}=\dfrac{1}{2}\dfrac{d|\tilde{U}_1^-|^2}{dt}$ (see e.g. [60]), by integrating (7.2) we obtain

$$\int_{t_0}^{t}\frac{1}{2}\frac{d|\tilde{U}_1^-|^2}{dt}ds=\int_{t_0}^{t}-k_s|\tilde{U}_1^-|^2-(u-k_s\underline{U}_1)\tilde{U}_1^-ds. \tag{7.3}$$

Because it is assumed that $u\geq k_s\underline{U}_1$, and that the parameters are positive, it is deduced that

$$\int_{t_0}^{t}\frac{1}{2}\frac{d|\tilde{U}_1^-|^2}{dt}ds\leq 0 \tag{7.4}$$

and then

$$0\leq|\tilde{U}_1^-|^2(t)\leq|\tilde{U}_1^-|^2(t_0). \tag{7.5}$$

As $U_1(t_0)\geq\underline{U}_1$, this implies that $|\tilde{U}_1^-|^2(t_0)=0$ and then $U_1(t)\geq\underline{U}_1$ for all $t\geq t_0$.

Using the same method (by taking for $\tilde{U}_1$ the value $\tilde{U}_1=\overline{U}_1-U_1$) and the fact that $u\leq k_s\overline{U}_1$ and $U_1(t_0)\geq\underline{U}_1$ we can deduce that $U_1(t)\leq\overline{U}_1$, for all $t\geq t_0$.

• **Consider now the states** X **and** I**.**

According to the positivity of the parameters and the assumptions on the initial condition $\underline{I}\leq I(t_0)\leq\bar{I}$, and on the control input $\dfrac{k_sk_f}{b_f}\underline{I}\leq u\leq\dfrac{k_sk_f}{b_f}\bar{I}$, using the same method as for U_1, we have $\underline{I}\leq I(t)\leq\bar{I}$, for all $t\geq t_0$.

In the same way, by using the assumptions on the initial condition $\underline{X} \leq X(t_0) \leq \overline{X}$, and on the control input $\frac{k_s k_f}{b_f}\left(I_b + \frac{P_2}{P_3}\underline{X}\right) \leq u \leq \frac{k_s k_f}{b_f}\left(I_b + \frac{P_2}{P_3}\overline{X}\right)$, we can deduce that $\underline{X} \leq X(t) \leq \overline{X}$, for all $t \geq t_0$. So we omit the details.

- **Let us consider the state R_1 and R_2.**

According to the positivity of the parameters and the assumptions on the initial condition $(\underline{R}_2, \underline{R}_1) \leq (R_2, R_1)(t_0) \leq (\overline{R}_2, \overline{R}_1)$, and on the meal input $\underline{d} \leq d \leq \overline{d}$, using the same method as for U_1, we have $(\underline{R}_2, \underline{R}_1) \leq (R_2, R_1)(t) \leq (\overline{R}_2, \overline{R}_1)$, for all $t \geq t_0$.

- **Finally, consider the state G.**

Let us introduce $\tilde{G} = G - \underline{G}$ and $\tilde{G}^- = \max(0, -\tilde{G})$, using the differential equation on G and the same method as for U_1 we have:

$$\int_{t_0}^{t} \frac{1}{2}\frac{d|\tilde{G}^-|^2}{dt} ds = \int_{t_0}^{t} -(P_1 + X)|\tilde{G}^-|^2 - (-(P_1 + X)\underline{G} + P_1 G_b + k_{gr} R_2)\tilde{G}^- ds. \tag{7.6}$$

According to the positivity of the parameters and the assumptions on the initial condition $(\underline{X}, \underline{R}_2) \leq (X, R_2)(t_0)$, on the meal input $\underline{d} \leq d$ and on the control input $u \geq \frac{k_s k_f}{b_f}\left(I_b + \frac{P_2}{P_3}\underline{X}\right)$, it is deduced that

$$\int_{t_0}^{t} \frac{1}{2}\frac{d|\tilde{G}^-|^2}{dt} ds \leq \int_{t_0}^{t} -(-(P_1 + X)\underline{G} + P_1 G_b + k_{gr}\underline{R}_2)\tilde{G}^- ds. \tag{7.7}$$

Since $u \leq \frac{k_s k_f}{b_f}\left(I_b + \frac{P_2}{P_3}\left(-P_1 + \frac{P_1 G_b + k_{gr}\underline{R}_2}{\underline{G}}\right)\right)$, and as the parameters are positive, it is deduced from inequality (7.7) that

$$\int_{t_0}^{t} \frac{1}{2}\frac{d|\tilde{G}_1^-|^2}{dt} ds \leq 0 \tag{7.8}$$

and then

$$0 \leq |\tilde{G}^-|^2(t) \leq |\tilde{G}^-|^2(t_0). \tag{7.9}$$

As $G(t_0) \geq \underline{G}$, this implies that $|\tilde{G}^-|^2(t_0) = 0$ and then $G(t) \geq \underline{G}$ for all $t \geq t_0$. Using similar arguments as bellow we can deduce also that $G(t) \leq \overline{G}$, for all $t \geq t_0$. □

Remark 7. The previous results can be used to deduce that if the parameters of the model are positive, if the control input is such that $u \geq \max\left(0, \frac{k_s k_f}{b_f}\left(I_b - \frac{P_1 P_2}{P_3}\right)\right)$ and the meal input is such that $d \geq 0$, then the state keeps their physiological meaning, *i.e.* if at $t = t_0$ we have $(G, X, I, U_1, R_2, R_1)(t_0) \in \mathbb{R}^{+*} \times \mathbb{R} \times \mathbb{R}^+ \times \mathbb{R}^+ \times \mathbb{R}^+ \times \mathbb{R}^+$ then we have $(G, X, I, U_1, R_2, R_1)(t) \in \mathbb{R}^{+*} \times \mathbb{R} \times \mathbb{R}^+ \times \mathbb{R}^+ \times \mathbb{R}^+ \times \mathbb{R}^+$ for all $t \geq t_0$. Because the only constraint on the control input is that $u \geq 0$, the set of parameter is guaranteed to be coherent if we have $P_3 I_b \leq P_1 P_2$.

7.2.2 Observability and Controllability properties

Let us verify that the modified minimal model (6.6) is both observable and controllable. To do so, let us consider the following proposition.

Proposition 1. *Assume that the parameters of the model (6.6) are given and strictly positive, if the control input u and the meal input d are known and given then the modified minimal model of Bergman is almost everywhere locally observable and if the initial condition* $(R_{2,}, R_1)(t_0)$ *and the meal consumption profile d are known and given then this model is controllable for all* $G \neq 0$.

Proof. In order to simplify the presentation, let us write (6.6) as follows:

$$\begin{aligned}
\frac{dx_1}{dt} &= -P_1 x_1 - x_1 x_2 + k_{gr} x_5 + P_1 G_b \\
\frac{dx_2}{dt} &= -P_2 x_2 + P_3 x_3 - P_3 I_b \\
\frac{dx_3}{dt} &= -k_f x_3 + b_f x_4 \\
\frac{dx_4}{dt} &= -k_s x_4 + u \\
\frac{dx_5}{dt} &= -c_2 x_5 + c_2 x_6 \\
\frac{dx_6}{dt} &= -c_1 x_6 + c_1 d \\
y &= x_1,
\end{aligned} \tag{7.10}$$

where y stands for the model output.

- **Let us begin to verify that the modified minimal model of Bergman is observable.**

It is assumed that the control input u and the meal input d are known and given, so, to verify if this model is observable, we will consider the rank of the matrix (see e.g.[78])

$$\Omega = \begin{pmatrix} \nabla_x h(x) \\ \nabla_x L_{\mathscr{G}} h(x) \\ \nabla_x L^2_{\mathscr{G}} h(x) \\ \nabla_x L^3_{\mathscr{G}} h(x) \\ \nabla_x L^4_{\mathscr{G}} h(x) \\ \nabla_x L^5_{\mathscr{G}} h(x) \end{pmatrix} \tag{7.11}$$

where the Lie derivatives are defined as follows

$$L^k_{\mathscr{G}} h(x) = \begin{cases} \displaystyle\sum_{i=1}^{n_x} \frac{\partial h}{\partial x_i} \mathscr{G}_i(x) & \text{if } k = 1 \\ L_{\mathscr{G}} \left(L^{k-1}_{\mathscr{G}} h(x) \right) & \text{if } k > 1 \end{cases}, \tag{7.12}$$

and where the function $\mathscr{G}$ and h are given by

$$\mathscr{G}(x) = \begin{pmatrix} -P_1 x_1 - x_1 x_2 + k_{gr} x_5 + P_1 G_b \\ -P_2 x_2 + P_3 x_3 - P_3 I_b \\ -k_f x_3 + b_f x_4 \\ -k_s x_4 + u \\ -c_2 x_5 + c_2 x_6 \\ -c_1 x_6 + c_1 d \end{pmatrix}, \; h(x) = x_1. \tag{7.13}$$

It is shown that the matrix Ω is almost everywhere full rank, thus proving that the modified minimal model of Bergman is almost everywhere locally observable. For more details see in the appendix the section 12.4.

- **Let us verify that the modified minimal model of Bergman is controllable.**

It is assumed that the initial condition $(x_5, x_6)(t_0)$ and the meal consumption profile d are known and given. So we can integrate the gastro-intestinal sub-system. In the sequel, we substitute the term $k_{gr}x_5$ in the glucose-insulin sub-model by the known rate of appearance $R_a = k_{gr}x_5$. This leads to consider the controllability of the following model

$$\begin{aligned}
\frac{dx_1}{dt} &= -P_1x_1 - x_1x_2 + P_1G_b + R_a \\
\frac{dx_2}{dt} &= -P_2x_2 + P_3x_3 - P_3I_b \\
\frac{dx_3}{dt} &= -k_fx_3 + b_fx_4 \\
\frac{dx_4}{dt} &= -k_sx_4 + u
\end{aligned} \tag{7.14}$$

To test the controllability, let us consider the rank of the matrix (see e.g.[78])

$$\mathscr{R} = \begin{pmatrix} g(x) & \mathrm{ad}_f g(x) & \mathrm{ad}_f^2 g(x) & \mathrm{ad}_f^3 g(x) \end{pmatrix}, \tag{7.15}$$

where the Lie bracket are defined as follows

$$\mathrm{ad}_f^k g(x) = \begin{cases} \nabla_x(g(x))\, f(x) - \nabla_x(f(x))\, g(x) & \text{if } k = 1 \\ \nabla_x\left(\mathrm{ad}_f^{k-1} g(x)\right) f(x) - \nabla_x(f(x))\, \mathrm{ad}_f^{k-1} g(x) & \text{if } k > 1 \end{cases}. \tag{7.16}$$

and where the function f and g stands for

$$f(x) = \begin{pmatrix} -P_1x_1 - x_1x_2 + P_1G_b + R_a \\ -P_2x_2 + P_3x_3 - P_3I_b \\ -k_fx_3 + b_fx_4 \\ -k_sx_4 \end{pmatrix}, \; g(x) = \begin{pmatrix} 0 \\ 0 \\ 0 \\ 1 \end{pmatrix}. \tag{7.17}$$

We have

$$\mathscr{R} = \begin{pmatrix} 0 & 0 & 0 & -P_3b_fx_1 \\ 0 & 0 & -P_3b_f & -P_3b_f(P_2 + k_f + k_s) \\ 0 & b_f & b_f(k_f + k_s) & b_f(k_f^2 + k_s^2 + k_fk_s) \\ 1 & -k_s & -k_s^2 & -k_s^3 \end{pmatrix} \tag{7.18}$$

Because all the parameters are assumed to be given strictly positive, it is deduced that the matrix $\mathscr{R}$ is full rank for all $x_1 \neq 0$ thus proving that the modified minimal model of Bergman is locally controllable for all $x_1 \neq 0$. □

Remark 8. Practically, the fact that the model is not controllable when $G = 0$ is not a big issue. Indeed, in this case, the patient has absolutely no sugar in the blood meaning that he is dead, such that it might be useless to envisage control action then.

Now that we have verified that the modified minimal of Bergman is consistent, let us consider the design of a SPMPC controller.

7.3 Controller design

So far, we have been interested in studying general properties satisfied by the modified minimal model of Bergman. Now let us consider some properties which are desirable when using a SPMPC controller. To do so, we will begin to express the control problem using a variational formulation. Then, we will verify whether the control problem is well-posed. To do so, we will verify if it satisfies assumptions 2 and 3. Next, we will be interested in proposing an adequate PLDI embedding which can be used to compute a final cost and a terminal state constraint which satisfy assumptions 7 and 8. Finally, the necessary tools to numerically solve the control problem using adjoint model will be introduced.

7.3.1 Control problem

For control purpose, we have chosen to only consider the global trend of the glucose-insulin metabolism. This has lead us to model this phenomenon thanks to the modified minimal model of Bergman to which a simple gastro-intestinal sub-model has been added. For convenience, let us remind the equation of the model

$$\begin{aligned}
&\underline{\text{Glucose-insulin sub-model}}:\\
&\frac{dG}{dt} = -(P_1+X)G + P_1G_b + k_{gr}R_2,\\
&\frac{dX}{dt} = -P_2X + P_3(I-I_b),\\
&\frac{dI}{dt} = -k_fI + b_fU_1,\\
&\frac{dU_1}{dt} = -k_sU_1 + u,\\
&(G,X,I,U_1)(t_0) = (G_0,X_0,I_0,U_{1,0}),
\end{aligned} \tag{7.19}$$

$$\begin{aligned}
&\underline{\text{Gastro-intestinal sub-model}}:\\
&\frac{dR_2}{dt} = -c_2(R_2-R_1),\\
&\frac{dR_1}{dt} = -c_1(R_1-d),\\
&(R_2,R_1)(t_0) = (R_{2,0},R_{1,0}).
\end{aligned} \tag{7.20}$$

For control purpose, it is assumed that the meal consumption profile d and the initial condition $(R_2,R_1)(t_0)$ are known and given. That is why it is possible to integrate (7.20) to obtain the state trajectory $R_2(t)$ for all $t \geq t_0$. Let us call $R_a(t) = k_{gr}R_2(t)$ the rate of appearance. Then, for control purpose we consider the following model

$$\begin{aligned}
&\frac{dG}{dt} = -(P_1+X)G + P_1G_b + R_a(t),\\
&\frac{dX}{dt} = -P_2X + P_3(I-I_b),\\
&\frac{dI}{dt} = -k_fI + b_fU_1,\\
&\frac{dU_1}{dt} = -k_sU_1 + u,\\
&(G,X,I,U_1)(t_0) = (G_0,X_0,I_0,U_{1,0}).
\end{aligned} \tag{7.21}$$

In the sequel, the *nominal model* corresponds to (7.21) where all the parameters are assumed to be perfectly known. The trajectory generated by the nominal model for a given initial condition $(G_0, X_0, I_0, U_{1,0})$, a given rate of appearance $R_a(t)$ and a given insulin flow $u(t)$ is called *nominal trajectory*.

To obtain the variational problem, we begin to write the nominal model when disturbed both in states and parameters. This leads to the following disturbed system

$$\begin{aligned}
&\frac{d(x_1+G)}{dt} = -(\overline{p}_1+P_1)(x_1+G-G_b) - (x_2+X)(x_1+G) + (R_a(t)+r_a(t)),\\
&\frac{d(x_2+X)}{dt} = -(\overline{p}_2+P_2)(x_2+X) + (\overline{p}_3+P_3)(x_3+I-I_b),\\
&\frac{d(x_3+I)}{dt} = -(\overline{k}_f+k_f)(x_3+I) + (\overline{b}_f+b_f)(x_4+U_1),\\
&\frac{d(x_4+U_1)}{dt} = -(\overline{k}_s+k_s)(x_4+U_1) + (u+f),\\
&(x_1+G, x_2+X, x_3+I, x_4+U_1)(t_0) = (x_{1,0}+G_0, x_{2,0}+X_0, x_{3,0}+I_0, x_{4,0}+U_{1,0}),
\end{aligned} \tag{7.22}$$

where u and $R_a(t)$ are the inputs such that the variable G, X, I and U_1 describe a desired nominal trajectory issued from the nominal model (7.21). The control input f is a disturbance of the nominal input u which has been introduced in order to reject the state disturbance $(x_i)_{i\in\{1,\dots,4\}}$ despite the parameters disturbances $(\overline{p}_1, \overline{p}_2, \overline{p}_3, \overline{k}_f, \overline{b}_f, \overline{k}_s)^T$ and the rate of appearance disturbance r_a. In the sequel we note $w = (\overline{p}_1, \overline{p}_2, \overline{p}_3, \overline{k}_f, \overline{b}_f, \overline{k}_s, r_a)^T$.

To use the previously presented control algorithm, let us introduce the following variational model which is obtained by subtracting the nominal model (7.21) from the disturbed model (7.22)

$$\begin{aligned}
&\frac{dx_1}{dt} = -\overline{p}_1(x_1+G-G_b) - (P_1+X)x_1 - Gx_2 - x_1x_2 + r_a(t),\\
&\frac{dx_2}{dt} = -\overline{p}_2(x_2+X) + \overline{p}_3(x_3+I-I_b) - P_2x_2 + P_3x_3,\\
&\frac{dx_3}{dt} = -\overline{k}_f(x_3+I) + \overline{b}_f(x_4+U_1) - k_fx_3 + b_fx_4,\\
&\frac{dx_4}{dt} = -\overline{k}_s(x_4+U_1) - k_sx_4 + f,\\
&(x_1, x_2, x_3, x_4)(t_0) = (x_{1,0}, x_{2,0}, x_{3,0}, x_{4,0}).
\end{aligned} \tag{7.23}$$

Now that we have expressed the control problem using a variational formulation, let us consider the problem of verifying that the control problem is well-posed, *i.e.* let us verify that the model (7.23) satisfies assumptions 2 and 3.

7.3.2 Well-posed Primal Problem

Lemma 6. *For all bounded x and $\tilde{x}$ in $\mathbb{R}^{n_x}$, for all bounded f in $\mathbb{R}^{n_u}$ and for all bounded w and $\tilde{w}$ in $\mathbb{R}^{n_w}$, if the nominal state $(G,X,I,U_1)(t)$ is bounded for all $t \geq t_0$, then the model (7.23) satisfies assumption 2 and 3.*

Proof. Let us introduce the following notation:

$$\begin{aligned}\mathscr{G}(x,f,w) &= \begin{pmatrix} g_1(x,f,w) \\ g_2(x,f,w) \\ g_3(x,f,w) \\ g_4(x,f,w) \end{pmatrix}, \\ &= \begin{pmatrix} -\overline{p}_1(x_1+G-G_b)-(P_1+X)x_1-Gx_2-x_1x_2+r_a \\ -\overline{p}_2(x_2+X)+\overline{p}_3(x_3+I-I_b)-P_2x_2+P_3x_3 \\ -\overline{k}_f(x_3+I)+\overline{b}_f(x_4+U_1)-k_fx_3+b_fx_4 \\ -\overline{k}_s(x_4+U_1)-k_sx_4+f \end{pmatrix},\end{aligned} \tag{7.24}$$

where $w = (\overline{p}_1, \overline{p}_2, \overline{p}_3, \overline{k}_f, \overline{b}_f, \overline{k}_s, r_a)^T$.

Lipschitz assumption

First let us prove that the disturbed control model (7.23) satisfies assumption 2.

- Let us show that there exists a constant L_x such that we have $\|\mathscr{G}(x,f,w)-\mathscr{G}(\tilde{x},f,w)\| \leq L_x\|x-\tilde{x}\|$.

Let us begin to express the different component of the vector $\mathscr{G}(x,f,w)-\mathscr{G}(\tilde{x},f,w)$:

$$\begin{aligned} g_1(x,f,w)-g_1(\tilde{x},f,w) &= -(\overline{p}_1+P_1)(x_1-\tilde{x}_1)-G(x_2-\tilde{x}_2)-x_1x_2-\tilde{x}_1\tilde{x}_2, \\ g_2(x,f,w)-g_2(\tilde{x},f,w) &= -(\overline{p}_2+P_2)(x_2-\tilde{x}_2)+(\overline{p}_3+P_3)(x_3-\tilde{x}_3), \\ g_3(x,f,w)-g_3(\tilde{x},f,w) &= -(\overline{k}_f+k_f)(x_3-\tilde{x}_3)+(\overline{b}_f+b_f)(x_4-\tilde{x}_4), \\ g_4(x,f,w)-g_4(\tilde{x},f,w) &= -(\overline{k}_s+k_s)(x_4-\tilde{x}_4). \end{aligned} \tag{7.25}$$

Let us consider $\|g_1(x,f,w)-g_1(\tilde{x},f,w)\|$. We have

$$\begin{aligned}\|g_1(x,f,w)-g_1(\tilde{x},f,w)\| &= \|-(\overline{p}_1+P_1)(x_1-\tilde{x}_1)-G(x_2-\tilde{x}_2)-x_1x_2-\tilde{x}_1\tilde{x}_2\| \\ &= \|-(\overline{p}_1+P_1+x_2)(x_1-\tilde{x}_1)-(G+\tilde{x_1})(x_2-\tilde{x}_2)\| \\ &\leq |\overline{p}_1+P_1+x_2|\|x_1-\tilde{x}_1\|+|G+\tilde{x_1}|\|x_2-\tilde{x}_2\|.\end{aligned} \tag{7.26}$$

The next step consists in finding an upper-bound which is independent of the specific value of $\overline{p}_1$, x_2, G and $\tilde{x}_1$. Since the disturbances, the nominal state and the state are assumed to be bounded, we consider the new upper-bound which consider the (well-defined) supremum $\sup|\overline{p}_1+P_1+x_2|$ and $\sup|G+\tilde{x}_1|$

$$\|g_1(x,f,w)-g_1(\tilde{x},f,w)\| \leq (\sup|\overline{p}_1+P_1+x_2|)\|x_1-\tilde{x}_1\|+(\sup|G+\tilde{x}_1|)\|x_2-\tilde{x}_2\|. \tag{7.27}$$

Similarly, we have

$$\begin{aligned} \|g_2(x,f,w)-g_2(\tilde{x},f,w)\| &\leq (\sup|\overline{p}_2+P_2|)\|x_2-\tilde{x}_2\|+(\sup|\overline{p}_3+P_3|)\|x_3-\tilde{x}_3\|, \\ \|g_3(x,f,w)-g_3(\tilde{x},f,w)\| &\leq (\sup|\overline{k}_f+k_f|)\|x_3-\tilde{x}_3\|+(\sup(|\overline{b}_f+b_f|)\|x_4-\tilde{x}_4\|, \\ \|g_4(x,f,w)-g_4(\tilde{x},f,w)\| &\leq (\sup|\overline{k}_s+k_s|)\|x_4-\tilde{x}_4\|. \end{aligned} \tag{7.28}$$

So it is deduced that

$$\begin{aligned} \|g_1(x,f,w)-g_1(\tilde{x},f,w)\| &\leq K_1\left(\|x_1-\tilde{x}_1\|+\|x_2-\tilde{x}_2\|\right), \\ \|g_2(x,f,w)-g_2(\tilde{x},f,w)\| &\leq K_2\left(\|x_2-\tilde{x}_2\|+\|x_3-\tilde{x}_3\|\right), \\ \|g_3(x,f,w)-g_3(\tilde{x},f,w)\| &\leq K_3\left(\|x_3-\tilde{x}_3\|+\|x_4-\tilde{x}_4\|\right), \\ \|g_4(x,f,w)-g_4(\tilde{x},f,w)\| &\leq K_4\|x_4-\tilde{x}_4\|, \end{aligned} \tag{7.29}$$

where $K_1 = \max(\sup|\overline{p}_1 + P_1 + x_2|, \sup|G + \tilde{x}_1|)$, $K_2 = \max(\sup|\overline{p}_2 + P_2|, \sup|\overline{p}_3 + P_3|)$, $K_3 = \max(\sup|\overline{k}_f + k_f|, \sup(|\overline{b}_f + b_f|)$ and $K_4 = \sup|\overline{k}_s + k_s|$.

We have

$$\|\mathscr{G}(x, f, w) - \mathscr{G}(\tilde{x}, f, w)\| \leq \sum_{i=1}^{4} \|g_i(x, f, w) - g_i(\tilde{x}, f, w)\|. \tag{7.30}$$

Let us introduce the following constant

$$L_x = \max(K_1, K_2 + K_3, K_3 + K_4) \tag{7.31}$$

So, using (7.30) and (7.29) it is deduced that we have

$$\|\mathscr{G}(x, f, w) - \mathscr{G}(\tilde{x}, f, w)\| \leq L_x \|x - \tilde{x}\|. \tag{7.32}$$

- Now let us show that there exists a constant L_w such that we have $\|\mathscr{G}(x, f, w) - \mathscr{G}(x, f, \tilde{w})\| \leq L_w \|w - \tilde{w}\|$.

Let us begin to express the different component of the vector $\mathscr{G}(x, f, w) - \mathscr{G}(x, f, \tilde{w})$

$$\begin{aligned}
g_1(x, f, w) - g_1(x, f, \tilde{w}) &= -(x_1 + G - G_b)(\overline{p}_1 - \tilde{\overline{p}}_1) + (r_a - \tilde{r}_a), \\
g_2(x, f, w) - g_2(x, f, \tilde{w}) &= -(x_2 + X)(\overline{p}_2 - \tilde{\overline{p}}_2) + (x_3 + I - I_b)(\overline{p}_3 - \tilde{\overline{p}}_3), \\
g_3(x, f, w) - g_3(x, f, \tilde{w}) &= -(x_3 + I)(\overline{k}_f - \tilde{\overline{k}}_f) + (x_4 + U_1)(\overline{b}_f - \tilde{\overline{b}}_f), \\
g_4(x, f, w) - g_4(x, f, \tilde{w}) &= -(x_4 + U_1)(\overline{k}_s - \tilde{\overline{k}}_s).
\end{aligned} \tag{7.33}$$

As the state is bounded, it is deduced that we have

$$\begin{aligned}
\|g_1(x, f, w) - g_1(x, f, \tilde{w})\| &\leq k_1(\|\overline{p}_1 - \tilde{\overline{p}}_1\| + \|r_a - \tilde{r}_a\|), \\
\|g_2(x, f, w) - g_2(x, f, \tilde{w})\| &\leq k_2(\|\overline{p}_2 - \tilde{\overline{p}}_2\| + \|\overline{p}_3 - \tilde{\overline{p}}_3\|), \\
\|g_3(x, f, w) - g_3(x, f, \tilde{w})\| &\leq k_3(\|\overline{k}_f - \tilde{\overline{k}}_f\| + \|\overline{b}_f - \tilde{\overline{b}}_f\|), \\
\|g_4(x, f, w) - g_4(x, f, \tilde{w})\| &\leq k_4\|\overline{k}_s - \tilde{\overline{k}}_s\|,
\end{aligned} \tag{7.34}$$

where $k_1 = \max(1, \sup|x_1 + G - G_b|)$, $k_2 = \max(\sup|x_2 + X|, \sup|x_3 + I - I_b|)$, $k_3 = \max(\sup|x_3 + I|, \sup|x_4 + U_1|)$ and $k_4 = \sup|x_4 + U_1|$.

Let us introduce the following constant

$$L_w = \max(k_1, k_2, k_3, k_4) \tag{7.35}$$

Using (7.33) it is deduced that we have

$$\|\mathscr{G}(x, f, w) - \mathscr{G}(x, f, \tilde{w})\| \leq L_w \|w - \tilde{w}\|. \tag{7.36}$$

Linear Growth assumption

Then, let us prove that the disturbed control model (7.23) satisfy assumption 3. Since the state and the nominal state are assumed to be bounded, it is deduced that we have

$$\begin{aligned}
\|g_1(x, f, w)\| &\leq c_1(\|x_1\| + \|x_2\| + \|\overline{p}_1\| + \|r_a\|), \\
\|g_2(x, f, w)\| &\leq c_2(\|\overline{p}_2\| + \|\overline{p}_3\| + \|x_2\| + \|x_3\|), \\
\|g_3(x, f, w)\| &\leq c_3(\|\overline{k}_f\| + \|\overline{b}_f\| + \|x_3\| + \|x_4\|), \\
\|g_4(x, f, w)\| &\leq c_4(\|\overline{k}_s\| + \|x_4\| + \|f\|).
\end{aligned} \tag{7.37}$$

where $c_1 = \max(\sup|x_1 + G - G_b|, \sup|P_1 + X|, \sup|G + x_1|, 1)$, $c_2 = \max(\sup|x_2 + X|, \sup|x_3 + I - I_b|, P_2, P_3)$, $c_3 = \max(\sup|x_3 + I|, \sup|x_4 + U_1|, k_f, b_f)$ and $c_4 = \max(\sup|x_4 + U_1|, k_s, 1)$.

Let us introduce the following constant

$$c = \max(c_1, c_2 + c_3, c_3 + c_4). \tag{7.38}$$

Using (7.37) it is deduced that we have

$$\|\mathscr{G}(x, f, w)\| \leq c(\|x\| + \|f\| + \|w\|). \tag{7.39}$$

□

Now that it has been shown that the robust control problem is well-posed, let us introduce the necessary tools needed to solve it.

7.3.3 Formulation of a PLDI embedding

The final cost will be computed assuming that the meal effect is negligible at the end of the prediction horizon. This implies that to formulate an adequate differential inclusion embedding we consider the following control model

$$\begin{aligned}
\frac{dx_1}{dt} &= -\overline{p}_1(x_1 + G - G_b) - (P_1 + X)x_1 - Gx_2 - x_1x_2, \\
\frac{dx_2}{dt} &= -\overline{p}_2(x_2 + X) + \overline{p}_3(x_3 + I - I_b) - P_2x_2 + P_3x_3, \\
\frac{dx_3}{dt} &= -\overline{k}_f(x_3 + I) + \overline{b}_f(x_4 + U_1) - k_fx_3 + b_fx_4, \\
\frac{dx_4}{dt} &= -\overline{k}_s(x_4 + U_1) - k_sx_4 + f, \\
(x_1, x_2, x_3, x_4)(t_0) &= (x_{1,0}, x_{2,0}, x_{3,0}, x_{4,0}).
\end{aligned} \tag{7.40}$$

To apply the algorithm presented in chapter 3, the simpler possibility is to use a PLDI embedding of (7.40). To do so, the idea is to see that the only nonlinearity in the state comes from the product x_1x_2. Furthermore, as it has been previously shown, we know that the state is bounded for bounded inputs. Concretely, in the case of the state x_1, this means that there exists $\underline{x}_1 < \overline{x}_1$ such that if we have $x_1(t_0) \in [\underline{x}_1, \overline{x}_1]$ then for all $t \geq t_0$ we have $x_1(t) \in [\underline{x}_1, \overline{x}_1]$. So using x_1 as a *parameter*, it should be straightforward to design an adequate embedding by first considering a linear parameter variant representation of (7.40) and then to use classical results (see e.g. [91]) to build an PLDI embedding. However, because of the disturbances on the parameters, we also have nonlinearities arising from the product state/ parameter disturbances. To simplify the problem, the idea is to enlarge the space of admissible disturbances, such that all the disturbances which are not linked to x_1 appear as additive disturbances.

Let us exemplify this approach with the term $\overline{p}_2(x_2 + X)$. We know that the state x_2 is bounded, *i.e.* there exists $\underline{x}_2$ and $\overline{x}_2$ with $\underline{x}_2 < \overline{x}_2$ such that for all $t \geq t_0$ we have $x_2(t) \in [\underline{x}_2, \overline{x}_2]$. Let us call $X_2 = \max(|\underline{x}_2|, |\overline{x}_2|)$ and assume that X is non null and constant then for all t we have:

$$\overline{p}_2(x_2 + X) \leq \overline{p}_2X\left(1 + \frac{X_2}{|X|}\right). \tag{7.41}$$

So if the disturbance $\overline{p}_2$ originally belongs to $[a,b]$ then we consider the *new* disturbance $\overline{p}_2\left(1+\frac{X_2}{|X|}\right)$ which belongs to the interval $\left[a\left(1+\frac{X_2}{|X|}\right),b\left(1+\frac{X_2}{|X|}\right)\right]$. Thus, it is possible to suppress the nonlinearity in the term $\overline{p}_2(x_2+X)$ by considering the new term $\overline{p}_2X\left(1+\frac{X_2}{|X|}\right)$ which provides worst disturbances.

Assuming that G, X, I and U_1 are given non null constant such that $I-I_b$ is non null, we introduce the following new additive disturbances to suppress the nonlinearity state/ parameter disturbances

$$\begin{aligned}
\overline{\overline{p}}_2 &= \overline{p}_2\left(1+\frac{X_2}{|X|}\right),\\
\overline{\overline{p}}_3 &= \overline{p}_3\left(1+\frac{X_3}{|I-I_b|}\right),\\
\overline{\overline{k}}_f &= \overline{k}_f\left(1+\frac{X_3}{|I|}\right),\\
\overline{\overline{b}}_f &= \overline{b}_f\left(1+\frac{X_4}{|U_1|}\right),\\
\overline{\overline{k}}_s &= \overline{k}_s\left(1+\frac{X_4}{|U_1|}\right).
\end{aligned} \tag{7.42}$$

Using the previous reformulation of the disturbances to transform multiplicative disturbances into additive disturbances, the variational model (7.40) becomes

$$\begin{aligned}
\frac{dx_1}{dt} &= -\overline{p}_1(x_1+G-G_b)-(P_1+X)x_1-Gx_2-x_1x_2,\\
\frac{dx_2}{dt} &= -\overline{\overline{p}}_2X+\overline{\overline{p}}_3(I-I_b)-P_2x_2+P_3x_3,\\
\frac{dx_3}{dt} &= -\overline{\overline{k}}_fI+\overline{\overline{b}}_fU_1-k_fx_3+b_fx_4,\\
\frac{dx_4}{dt} &= -\overline{\overline{k}}_sU_1-k_sx_4+f,\\
(x_1,x_2,x_3,x_4)(t_0) &= (x_{1,0},x_{2,0},x_{3,0},x_{4,0}).
\end{aligned} \tag{7.43}$$

Using matrix notation, it is possible to rewrite (7.43) as follows

$$\frac{dx}{dt} = A(x_1)x+B_1(x_1)w+B_2f, \tag{7.44}$$

where w stands for the vector of disturbances and

$$\begin{aligned}
A(x_1) &= \begin{pmatrix} -(P_1+X) & -(G+x_1) & 0 & 0\\ 0 & -P_2 & P_3 & 0\\ 0 & 0 & -k_f & b_f\\ 0 & 0 & 0 & -k_s \end{pmatrix}, B_2 = \begin{pmatrix} 0\\0\\0\\1 \end{pmatrix},\\
B_1(x_1) &= \begin{pmatrix} -(x_1+G-G_b) & 0 & 0 & 0 & 0 & 0\\ 0 & -X & I-I_b & 0 & 0 & 0\\ 0 & 0 & 0 & -I & U_1 & 0\\ 0 & 0 & 0 & 0 & 0 & -U_1 \end{pmatrix}.
\end{aligned} \tag{7.45}$$

As we have for all $t \geq t_0$ $x_1(t) \in [\underline{x_1}, \overline{x_1}]$, it is possible to use (7.44) to express (7.43) with a PLDI formulation, *i.e.* (7.43) is locally embedded in the following PLDI

$$\frac{dx}{dt} = \sum_{k=1}^{4} \beta_k(t) \left(A_k x + B_{1,k} w + B_2 f\right), \tag{7.46}$$

where $A_1 = A_2 = A(\underline{x}_1)$, $A_3 = A_4 = A(\overline{x}_1)$, $B_{1,1} = B_{1,3} = B_1(\underline{x}_1)$, $B_{1,2} = B_{1,4} = B_1(\overline{x}_1)$, for all $k \in \{1, \ldots, 4\}$ and for all t $\beta_k(t) \geq 0$ and $\sum_{k=1}^{4} \beta_k(t) = 1$.

Thus, assuming that the stage cost F is quadratic, using the algorithm presented in chapter 3, it is possible to compute a final cost $E(x) = x^T S x$ and a terminal state constraint $\Omega_a^{f_E} = \{x \in X_E / x^T S x \leq \gamma\}$ associated to a final controller $f_E(x) = Kx$.

Remark 9. To compute a PLDI embedding which can be used to compute a final cost and a terminal state constraint that can be used to design a stabilizing SPMPC controller, we have introduced additive disturbances. It is important to see that this embedding is valid for (7.40) because the thus obtained disturbances are strictly larger than the original disturbances.

7.3.4 Adjoint model and Gradient of the Criterion

In this section, the necessary tools to solve a sub-problem via adjoint model are introduced. In order to consider that hypoglycemia are more dangerous than hyperglycemia, we add the supplementary state constraint $x_1 \geq \underline{x}_1$ in the optimization problem (3.6). Similarly to the results presented in chapter 4, to consider both the terminal state constraint and the supplementary inequality constraint, we introduce the following modified functional

$$\mathscr{L}_A^{t_i,\mu}(f, \tilde{w}) = J^{t_i}(f, w) + \int_{t_i}^{t_i+T} (\Psi^{\mu}(x_1 - \underline{x}_1, \lambda_c))\, ds + \Psi^{\mu}(\gamma - \|x(t_i+T)\|_S^2, \lambda_\Omega), \tag{7.47}$$

where $\tilde{w} = (w^T, \lambda_c, \lambda_\Omega)^T$ and J^{t_i} is given as follows

$$J^{t_i}(f, w) = \|x(x(t_i), f, w, t_i; t_i+T)\|_S^2 + \int_{t_i}^{t_i+T} \left(\|x(x(t_i), f, w, t_i; s)\|_R^2 + \|f\|_\alpha^2 - \|w\|_Q^2\right) ds. \tag{7.48}$$

Let us assume that the initial condition of (7.43) is perfectly known. According to (4.4), let us introduce ω the Fréchet derivatives in direction (g, q) of the operator solution $(f, w) \to x(x(t_i), f, w, t_i; .)$ given as the solution of the following differential equation

$$\begin{aligned}
\frac{d\omega_1}{dt} &= -q_{P_1}(x_1 + G - G_b) - (P_1 + \overline{p}_1 + X + x_2)\omega_1 - (G + x_1)\omega_2 + q_{r_a}, \\
\frac{d\omega_2}{dt} &= -q_{P_2}(x_2 + X) + q_{P_3}(x_3 + I - I_b) - (P_2 + \overline{p}_2)\omega_2 + (P_3 + \overline{p}_3)\omega_3, \\
\frac{d\omega_3}{dt} &= -q_{k_f}(x_3 + I) + q_{b_f}(x_4 + U_1) - (k_f + \overline{k}_f)\omega_3 + (b_f + \overline{b}_f)\omega_4, \\
\frac{d\omega_4}{dt} &= -q_{k_s}(x_4 + U_1) - (k_s + \overline{k}_s)\omega_4 + g, \\
\omega(t_i) &= 0.
\end{aligned} \tag{7.49}$$

According to (4.35), to obtain the appropriate necessary optimality system conditions, which corresponds to the identification of the gradient of $\mathscr{L}_A^{t_i,\mu}$ that is necessary to develop a numerical scheme in

order to solve the saddle point problem, we introduce the adjoint system as follows

$$\begin{aligned}
-\frac{d\tilde{x}_1}{dt} &= -(\overline{p}_1+P_1+X)\tilde{x}_1 - x_2\tilde{x}_2 + R_{1,1}x_1 + \nabla_x\left(\Psi^\mu(C_c,\lambda_c)\right),\\
-\frac{d\tilde{x}_2}{dt} &= -(x_1+G)\tilde{x}_1 - (\overline{p}_2+P_2)\tilde{x}_2 + R_{2,2}x_2,\\
-\frac{d\tilde{x}_3}{dt} &= (\overline{p}_3+P_3)\tilde{x}_2 - (\overline{k}_f+k_f)\tilde{x}_3 + R_{3,3}x_3,\\
-\frac{d\tilde{x}_4}{dt} &= (\overline{b}_f+b_f)\tilde{x}_3 - (\overline{k}_s+k_s)\tilde{x}_4 + R_{4,4}x_4,\\
\tilde{x}(t_i+T) &= 2Sx(x_i,f,w,t_i;t_i+T) + \nabla_x\left(\Psi^\mu(C_\Omega,\lambda_\Omega)\right),
\end{aligned} \tag{7.50}$$

where $C_c = x_1 - \underline{x}_1$ and $C_\Omega = \gamma - \|x(t_i+T)\|_S^2$, and

$$\nabla_x\left(\Psi^\mu(C_\rho,\lambda_\rho)\right) = \begin{cases} (-\lambda_\rho + \frac{1}{\mu}C_\rho), \text{if } C_\rho \le \mu\lambda_\rho, \\ 0, \text{if } C_\rho \ge \mu\lambda_\rho, \end{cases}, \tag{7.51}$$

where ρ stands either for c or Ω.

According to (4.38), the following expression of the derivatives of $\mathscr{L}_A^{t_i,\mu}$ are deduced:

$$\begin{aligned}
\frac{\partial \mathscr{L}_A^{t_i,\mu}}{\partial f}(f,w) &= \tilde{x}_4 + \alpha f,\\
\frac{\partial \mathscr{L}_A^{t_i,\mu}}{\partial w}(f,w) &= \begin{pmatrix}
-\tilde{x}_1(x_1+G-G_b) - Q_{1,1}\overline{p}_1\\
-\tilde{x}_2(x_2+X) - Q_{2,2}\overline{p}_2\\
\tilde{x}_2(x_3+I-I_b) - Q_{3,3}\overline{p}_3\\
-\tilde{x}_3(x_3+I) - Q_{4,4}\overline{k}_f\\
\tilde{x}_3(x_4+U_1) - Q_{5,5}\overline{b}_f\\
-\tilde{x}_4(x_4+U_1) - Q_{6,6}\overline{k}_s\\
\tilde{x}_1 - Q_{7,7}r_a\\
\frac{\partial\Psi^\mu}{\partial\lambda}(C_c,\lambda_c)\\
\frac{\partial\Psi^\mu}{\partial\lambda}(C_\Omega,\lambda_\Omega)
\end{pmatrix}
\end{aligned} \tag{7.52}$$

where x is the solution of (7.43) with initial condition $x(t_i)$ under the influence of the couple control disturbances (f,w) and $\tilde{x}$ is the solution of (7.50) and where

$$\frac{\partial\Psi^\mu}{\partial\lambda}(C_\rho,\lambda_\rho) = \begin{cases} -C_\rho, \text{if } C_\rho \le \mu\lambda_\rho, \\ -\mu\lambda_\rho, \text{if } C_\rho \ge \mu\lambda_\rho, \end{cases}, \tag{7.53}$$

where ρ stands either for c or Ω.

7.4 Conclusion

In this chapter we have studied the properties of the retained control model in regards to its applicability with a SPMPC controller. First we have studied some general properties satisfied by the control model. We have begun to show that if the initial condition is bounded, if the parameters of the model are positive and if the inputs satisfy some bounds, then the state is bounded for all time instant. From this properties, the conditions on the input in order for the state to keep their physiological meaning have been deduced. Also it has been shown that the nominal model is almost everywhere observable and controllable. In a

second part, we have been interested in testing if the control problem is well-posed. To do so, we have begun to express the control problem in a variational form and then it has been verified that the control model satisfies assumptions 2 and 3. Then, the design of the SPMPC controller has been envisaged by considering the design of a PLDI embedding which can be used to compute an adequate final cost and a terminal state constraint. Also, according to the results presented in chapter 4, we have been interested in the numerical implementation by considering an adjoint model formulation to solve the corresponding saddle point optimization problem.

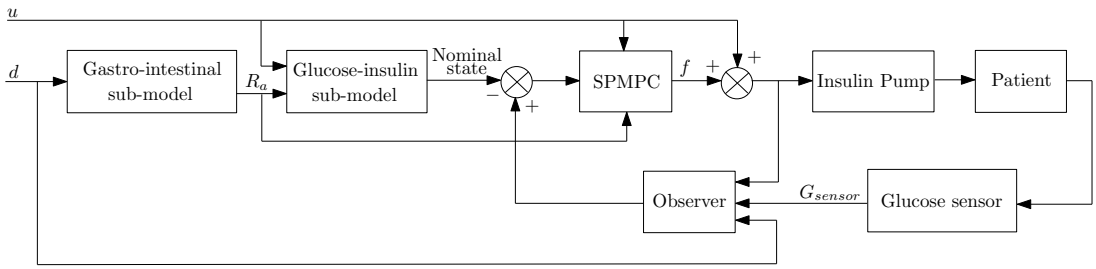

Figure 7.1: Structure of the control scheme

Let us mention that, concretely, we have chosen the nominal model to be a steady state of the system. This has been done because the simple structure of the modified minimal model of Bergman enables a simple computation of the corresponding control input u_{eq}. For a more general case, a control problem has to be solved.

Now it just remains to test, through numerical simulations, the controller performances. Before further proceeding, we have to consider the problem of designing a state observer. Indeed, from a control point of view, the knowledge of the full initial condition is needed at each sampling instant. However, practically, the sensors can only provide the value of the blood glucose G, implying that a state observer is needed. This leads to consider the control problem according to the structure given by fig.7.1. The model used in the SPMPC bloc is the disturbed model (7.23) and the model used in the observer bloc is the modified minimal model of Bergman (6.6). The objective of the next chapter is to present some observers to solve this issue.

Chapter 8

Observer

Contents

8.1 Introduction

To solve the problem of artificial blood glucose control, the design of a SPMPC controller on the modified minimal model of Bergman is envisaged. By solving a constrained saddle point optimization problem on a finite prediction horizon subject to a dynamical model of the system that has to be controlled and where the current state value is the initial condition, this controller provides the control input that has to be applied in order to robustly stabilize the system. However, from a practical point of view, the sensors can only provide a (noisy) measure of the blood glucose. This implies that the value of the remaining states has to be inferred on the basis of the measurement, the insulin and the meal inputs. This task will be done by a state observer.

The task of estimating the state is crucial in regards to the expectable control performances. Indeed, if we begin to compute an optimal control sequence for an erroneous initial condition, then the system trajectory will strongly differ from the predicted trajectory what can possibly lead to instability of the closed-loop. That is why it is of prime importance to assess if an observer provides a *good* state estimate. To try to solve this issue, our idea consists in designing multiple observers, which are based on different methodologies, and to compare their relative state estimate. In case the estimate provided by all observers are comparable, then we will assume that the observers performances are satisfactory. However, for control purpose, we will use only one of them.

We will consider the design of three observers. Two of them will be designed using the complete modified minimal model of Bergman. The first one is an Unscented Kalman filter (UKF) (see e.g. [144]) and the second one is a Moving Horizon Estimator (MHE) (see e.g. [133]). For these observers, it will be assumed that the meal times and the meal contents are perfectly known, e.g. they can be provided by the patient at the moment when the corresponding event occurs. The third observer will be designed using only the glucose-insulin sub-model. The idea of this observer will be to treat the rate of appearance (which is given by the term $k_{gr}R_2$ in the modified minimal model of Bergman (6.6)) as an unknown input that has to be estimated at the same time that the state is estimated. To do so the design of an Unknown Input Observer based on an Extended Kalman Filter (UIEKF) is envisaged (see e.g. [61] or [141]). This choice has been done for validation purpose. Indeed, it seems legitimate to think that the retained gastro-intestinal sub-model is too simple in regards to the true digestion process. So we can wonder if this has some consequence in the process of estimating the state G, X, I and U_1. By comparing the state of the UIEKF with the ones given by the UKF and MHE, it will be possible to verify whether the simplicity of the digestion model do deteriorate the estimation of the remaining states. However, because for this observer this input can not only model a glucose flow due to meal consumption but also all kind of unknown dynamics, it is not intended to directly use it to detect a meal consumption.

Because the system dynamic is time continuous and the measurement are discrete, the various observers will have to work in a sampled-data framework. It is worth noticing that one advantage to have retained an (open-loop) sampled-data control strategy is that it becomes possible to consider a different sampling rate on the input $T_{s,i}$ (measurement rate) and on the output $T_{s,o}$ (control update rate), under the only condition that the latter is a multiple of the former. In the process of estimating the state, we have decided to use the nominal form of the control model (see section 7.3.1). The state of the disturbed model is then deduced by subtracting from the estimated state the (known) value of the nominal state.

This chapter is organized as follows. First, the various observers are briefly presented. Then, their respective performances are tested using the control model for simulation purpose. Finally, this chapter is concluded.

8.2 Some nonlinear observers

In this section let us briefly recall how an unscented Kalman filter, a moving horizon estimator and an unknown input observer based on an extended Kalman filter work.

To design the two Kalman filters (UKF and UIEKF) it will be assumed that the model is additively disturbed. These disturbances are different from the one introduced for control purpose in chapter 3 as, in the framework of these observers, the noise is assumed to be given stochastic (classically assumed to be given Gaussian). To design the MHE observer, even if it is possible to work with more complex disturbances, it will also be assumed that the model is additively disturbed. This choice has been done in order to use the previously presented Kalman filter to determine the arrival cost needed to ensure the good convergence property of the observer.

8.2.1 State observer via Unscented Kalman Filter

In 1960, R.E. Kalman published his famous paper describing a recursive solution to the discrete data filtering problem [83]. The Kalman filter is a simple set of equations which provides a minimum mean squared state error estimate for linear systems. This filter can be used for many tasks ranging from simple state estimator to information fusion (see e.g. [152]). Because of its huge success to solve the estimate problem in the linear case, many attempts have been done to extend its use to the nonlinear case. The most common approach is to use the so called Extended Kalman Filter (EKF) (see e.g. [136] or [137]) which is based on the linearization of the nonlinear model. Some difficulties with this approach can arise, e.g. because of the nontrivial task of computing Jacobian matrices. Moreover the resulting filter can be unstable.

Generally speaking, Kalman filter works on mean and covariance of the true probability distribution of the state (which may be non Gaussian). In the EKF, the idea is to use a linearization of the model in order to make the assumption that if the probability distribution of the state were to be Gaussian then it would remain Gaussian for all further time instant, making it sufficient to estimate the first two momentum of the distribution. This approach is awkward as in general, there is no reason that through a nonlinear process a Gaussian distribution remains Gaussian. In order to take this fact into account, the Unscented Kalman Filter (UKF) has been developed (see e.g. [82]). The idea remains to design an algorithm which only estimates the first two momentum of the distribution law. Based on a set of symmetrically distributed sampled points (called sigma points), the main idea is to parametrize the mean and covariance of the true probability distribution of the state and then to approximate this latter (at least at the second order). As a consequence, such a filter do not require any linearization step. Up to today, UKF is a vast subject of research and one of the main issue deals with the design of methods which enable to choose the best set of sigma points under various assumptions (see e.g. [56], [152] or [41]).

In the sequel we will remind the UKF equations in the continuous-discrete setting on the basis of the work presented in [144] and [152]. The retained formulation of the filter corresponds to what is called the additive Unscented Kalman Filter in [68].

To derive the observer equations, we assume in this section that the noise on the process and on the measures are additive, that is for $t \in [t_{k-1}, t_k]$

$$\begin{aligned} &\frac{dx}{dt} = \mathscr{G}(x,u) + w(t), \\ &x(t_{k-1}) = x_{k-1}, \\ &y_k = h(x(x_{k-1}, u, w; t_k)) + r_k, \end{aligned} \tag{8.1}$$

where $x_{k-1} \in \mathbb{R}^{n_x}$ is the initial condition, $x \in \mathbb{R}^{n_x}$ is the state, $y_k \in \mathbb{R}^{n_y}$ is the measurement, w is a white

noise process with variance Q and r_k is a zero mean Gaussian measurement noise with covariance matrix R.

The objective is as follows. For a given state estimate $\hat{x}_{k-1}$ at $t = t_{k-1}$ with mean m_{k-1} and covariances $\mathscr{P}_{k-1}$, the input $u(t)$ for $t \in [t_{k-1}; t_k[$ and the measure y_k at $t = t_k$, the objective is to estimate at $t = t_k$ the mean and covariance of the state of (8.1). To do so, let us introduce the following unscented transform denoted $UT(m_{k-1}, \mathscr{P}_{k-1})$ which generates $2n_x + 1$ *sigma points* $\mathscr{X}_i$ with the associated weights W_i

$$\begin{aligned} \mathscr{X}_0(t_{k-1}) &= m_{k-1} & W_0 &= \tfrac{\lambda}{n_x+\lambda}, \\ \mathscr{X}_i(t_{k-1}) &= m_{k-1} + (\sqrt{(n_x+\kappa)\mathscr{P}_{k-1}})_i & W_i &= \tfrac{1}{2(n_x+\lambda)}, \\ \mathscr{X}_{n_x+i}(t_{k-1}) &= m_{k-1} - (\sqrt{(n_x+\lambda)\mathscr{P}_{k-1}})_{n_x+i} & W_{n_x+i} &= \tfrac{1}{2(n_x+\lambda)}, \end{aligned}$$

where $i = \{1, \ldots, n_x\}$, $\lambda = \alpha^2(n_x + \kappa) - n_x$ is a scaling parameter, α and κ are (positive) parameters of the method, $(\sqrt{(n_x+\kappa)\mathscr{P}_{k-1}})_i$ stands for the i^{th} column of the matrix $(\sqrt{(n_x+\kappa)\mathscr{P}_{k-1}})$ and where $(\sqrt{(n_x+\kappa)\mathscr{P}_{k-1}})$ stands for the square root of $(n_x+\kappa)\mathscr{P}_{k-1}$. Let us introduce the following variable

$$\begin{aligned} & w_m = [W_0, \ldots, W_{2n_x}]^T, \\ & W = (I_{2n_x+1} - [w_m, \ldots, w_m])\mathrm{diag}\,(W_0^c, W_1, \ldots, W_{2n_x})\,(I_{2n_x+1} - [w_m, \ldots, w_m])^T, \\ & \mathscr{X}(t_k) = [\mathscr{X}_0(t_k), \ldots, \mathscr{X}_{2n_x}(t_k)], \\ & h(\mathscr{X}(t_k)) = [h(\mathscr{X}_0(t_k)), \ldots, h(\mathscr{X}_{2n_x}(t_k))], \end{aligned} \tag{8.2}$$

where $W_0^c = W_0 + 1 - \alpha^2 + \beta$, I_n stands for the n dimensional identity matrix and β is a (positive) parameter of the method.

In terms of the unscented transform UT the UKF equations are quite similar to the classical Kalman filter equation. They can be divided in one prediction and one correction step

- *Time update:* Compute the vector of sigma points $\mathscr{X}(t_{k-1})$ using $UT(m_{k-1}, \mathscr{P}_{k-1})$ and compute their propagation, *i.e.* for $i \in \{1, \ldots, 2n_x + 1\}$ compute

$$\mathscr{X}_i(t_k|t_{k-1})^* := \mathscr{X}_i(t_{k-1}) + \int_{t_{k-1}}^{t_k} \mathscr{G}(\mathscr{X}_i, u)ds. \tag{8.3}$$

  Compute the predicted mean and covariance as follows

$$\begin{aligned} & m_{k|k-1} := w_m \mathscr{X}(t_k|t_{k-1})^*, \\ & \mathscr{P}_{k|k-1} := \mathscr{X}(t_k|t_{k-1})^{*T} W \mathscr{X}(t_k|t_{k-1})^* + Q. \end{aligned} \tag{8.4}$$

  Then, compute the following new set of sigma point

$$\mathscr{X}(t_k|t_{k-1}) := UT(m_{k|k-1}, \mathscr{P}_{k|k-1}). \tag{8.5}$$

  Finally compute the expected output as follows

$$\begin{aligned} & Y_{k|k-1} := h(\mathscr{X}(t_k)), \\ & y_{k|k-1} := w_m Y_{k|k-1}. \end{aligned} \tag{8.6}$$

- *Measurement update:* Compute the following variance and covariance

$$\begin{aligned} & \mathscr{P}_{yy,k} := Y_{k|k-1}^T W Y_{k|k-1} + R, \\ & \mathscr{P}_{xy,k} := \sum_{i=0}^{2n_x} W_i^{(c)} (\mathscr{X}_i(t_k|t_{k-1}) - m_{k|k-1})(Y_{i,k|k-1} - y_{k|k-1})^T, \end{aligned} \tag{8.7}$$

where $W_i^{(c)} = W_i$ if $i > 0$ and $W_0^c = W_0 + 1 - \alpha^2 + \beta$.

Then update the estimated mean m_k and covariance $\mathscr{P}_k$ using the filter gain K_k as follows

$$\begin{aligned} K_k &= \mathscr{P}_{xy,k}\mathscr{P}_{yy,k}^{-1}, \\ m_k &= m_{k|k-1} + K_k(y_k - y_{k|k-1}), \\ \mathscr{P}_k &= \mathscr{P}_{k|k-1} - K_k\mathscr{P}_{yy,k}K_k^T. \end{aligned} \tag{8.8}$$

The estimated state $\hat{x}_k$ at $t = t_k$ has mean m_k and covariance $\mathscr{P}_k$.

8.2.2 State observer via Moving Horizon Estimator

Kalman filters are known to be efficient but they suffer from a major drawback, it is not easy to consider constraints on the state, e.g. to consider that a concentration or a quantity is always positive. As observer are often used to estimate unmeasured concentration, many attempts have been done to solve this issue. Some strategies consist in adjusting the existing algorithm (see e.g. [77] to consider state constraints when using an UKF). Others strategies consist in developing *new* algorithm in a more adequate framework. One of the most natural possibility is to recast the original estimation problem as a series of constrained optimal control problem (see e.g. [133]) where the initial condition is the control. Each time a new measurement is available, an optimization problem is solved to compute the initial condition which provides the best fit in regards to the past data. The problem is that when time goes by, the number of stored measures increased, making it longer and longer to solve the optimization problem and also increasing the need for memory. That is why this strategy has been refined by introducing a receding approach. Only a finite number of past measures is stored, thus ensuring that the need for memory is controlled and that the computation time remains reasonable. This kind of observer is called a Moving Horizon Observer (MHE). The idea is to minimize an *estimation* cost function, subject to various constraints, defined on a sliding window involving a finite number of past samples. These observers have been used for time continuous measurement (see e.g. [127] or [124]) as well as for time discrete measurement (see e.g. [133] or [70]).

To estimate the state at $t = t_k$ using a MHE observer, we are given a set of N measurements where $N \in \mathbb{N}^*$. We consider that the system of nonlinear ordinary differential equations and the discrete measure $y(t_k)$ are additively disturbed. That is for $t \in [t_{k-N}, t_k]$

$$\begin{aligned} &\frac{dx}{dt} = \mathscr{G}(x,u) + w, \\ &x(t_{k-N}) = x_{k-N}, \\ &y(t_i) = h(x(x_{k-N}, u, w; t_i)) + v_i,\ i \in \{k-N, \ldots, k\}, \end{aligned} \tag{8.9}$$

where $x \in \mathbb{R}^{n_x}$ is the state vector, $x_{k-N} \in \mathbb{R}^{n_x}$ is the unknown initial state that has to be estimated, $u \in \mathbb{R}^{n_u}$ is the control input, $w \in \mathbb{R}^{n_w}$ is a (bounded) disturbance, $y(t_k) \in \mathbb{R}^{n_y}$ is a measurement vector and $v_k \in \mathbb{R}^{n_v}$ is a (bounded) measurement noise vector.

The objective of this observer is to derive for each $i \in \{k-N, \ldots, k\}$ the estimate of $x(x_{k-N}, u, w; t_i)$ and the corresponding disturbances w and v_i. The measurements and the inputs are collected within the sliding window $[t_{k-N}; t_k]$. The estimate problem is cast as the problem of minimizing the following cost function each time a new measurement is made available

$$J^{t_k}(x_{k-N}, w) = \|x_{k-N} - \hat{x}_{k-N}\|^2_{\mathscr{P}_k} + \sum_{i=k-N}^{k} \|v_i\|^2_{R_k} + \int_{t_{i-1}}^{t_i} \|w\|^2_{Q_k} ds, \tag{8.10}$$

where the matrices $\mathscr{P}_k$, R_k and Q_k are assumed to be positive definite. The term $\|x_{k-N} - \hat{x}_{k-N}\|^2_{\mathscr{P}_k}$, which is often called arrival cost, penalizes the distance from the initial condition x_{k-N} to some *a priori* estimate $\hat{x}_{k-N}$ which incorporates the past information $(y(t_j))_{j\in\{0,\dots,k-N-1\}}$. The term $\|v_i\|^2_{R_k}$ penalizes the measurement noise and the term $\int_{t_{i-1}}^{t_i} \|w\|^2_{Q_k} ds$ penalizes the noise on the model.

In a stochastic setting, $\mathscr{P}_k$ can be interpreted as the inverse of the covariance matrix corresponding to the state estimate $\hat{x}_{k-N}$. This means that if we are confident in the estimate $\hat{x}_{k-N}$, then the corresponding covariance matrix will be small and its inverse will be large. Thus, it implies that in the optimization problem it will be costly to estimate a different state value x_{k-N}. As for R_k, it can be interpreted as the inverse of the measurement noise covariance matrix and Q_k as the inverse of the model noise covariance matrix [70].

One of the main issue with MHE observer is to compute an adequate arrival cost. When computing this term the idea is to have a first guess which is not too bad and not too numerically demanding. Classically a Kalman filter (either EKF or UKF) is used (see e.g. [127]) . In the sequel, we will compute the arrival cost using the previously presented UKF. An other main issue with MHE observer comes from the computational burden [9]. Indeed to obtain a state estimate it is needed to solve on-line a constrained optimization problem. Many approaches have been introduced to solve these optimization problems (see e.g. [70], [169] or [157]). In our case, we intend to use the numerical method presented in chapter 4. For more details see section 8.3.1.

8.2.3 Unknown input and state observer via Extended Kalman Filter.

In the modeling part we have retained a really simple model for the gastro-intestinal subsystem. Indeed, a real digestion process is far more complex than a simple couple of linear differential equations. In particular, the digestion process depends on the ingested quantity, the type of consumed sugar (e.g. the digestion process between bread and orange juice is clearly different due to the different nature of carbohydrates). That is why, it is interesting to design an observer which is independent from the digestion model and which can estimate both an unknown input (corresponding to the rate of appearance $R_a = k_{gr}R_2$) and the state. The aim of this observer, which is designed using only the glucose-insulin sub-model, is that it can be used to verify whether the use of a simple gastro-intestinal sub-model is detrimental when it comes to estimate the state of the glucose-insulin sub-model.

Many algorithms are available to meet this purpose (see e.g. [147], [155] or [160]). As we have soon be interested in using a Kalman filter to estimate the state, we intend to use a continuous-discrete unknown input observer based on the use of an Extended Kalman Filter (see e.g. [141]).This observer has been developed based on what has been done in the linear case using a linear Kalman filter (see e.g. [61]).

The steps to estimate both the state and the unknown input are similar to the ones of a classical Kalman filter, *i.e.* a prediction and a correction step. The only thing that change is that there is a supplementary prediction and correction step for the unknown input that has to be estimated (see fig. 8.1 which has been inspired from [141]). A good explanation of the different meaning of the equation in a stochastic setting and a convergence proof in the linear case can be found in [61]. Here, we will simply recall the different equations of the filter.

We are interested in estimating the state value $\hat{x}_k$, the corresponding covariance $\mathscr{P}_k$ and the unknown input d_k at $t = t_k$ using an iterative observer , *i.e.* under the assumption that we are given the estimate $\hat{x}_{k-1}$ of the state, a corresponding covariance matrix $\mathscr{P}_{k-1}$ and an estimate of the unknown input d_{k-1} at $t = t_{k-1}$. To do so, for $t \in [t_{k-1}, t_k]$, let us consider the following setting which is related to our estimation

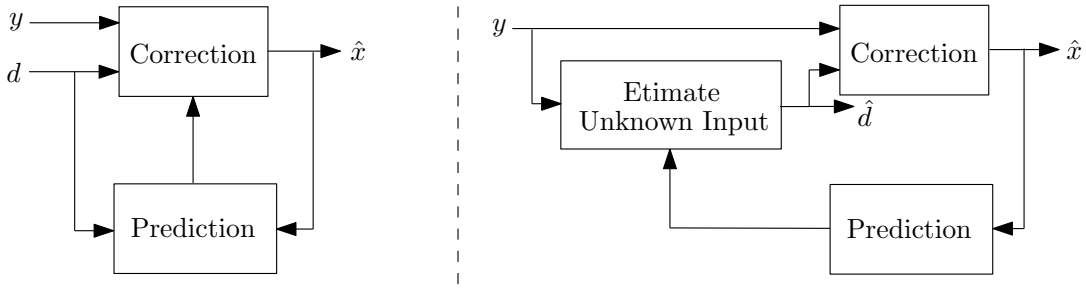

Block diagram of Kalman Filter Block diagram of unknown input observer

Figure 8.1: Comparison of the bloc diagram of Kalman Filter and unknown input observer

problem

$$\begin{aligned} &\frac{dx}{dt} = \mathscr{G}(x,u) + Fd_k + w, \\ &x(t_{k-1}) = x_{k-1}, \\ &y(t_k) = Cx(x_{k-1},u,w,d_k;t_k) + v_k, \end{aligned} \tag{8.11}$$

where $x \in \mathbb{R}^{n_x}$ is the state, $y(t_k) \in \mathbb{R}^{n_y}$ is the measured output, $d_k \in \mathbb{R}^{n_d}$ is the unknown input that has to be estimated and which is assumed to be piecewise constant, $F \in \mathbb{R}^{n_x \times n_d}$ is a given matrix, w is a white noise process with covariance matrix Q and v_k is a white noise process with covariance matrix R.

The set of equations of the filter are given as follows

- *Prediction:* When we begin to solve the estimation problem, we do not know the value of d_k. So, to make a prediction on $[t_{k-1},t_k]$, we use the value of the last estimate of the disturbance d_{k-1}. To obtain the predicted state value $\hat{x}_{k|k-1} = \hat{x}(\hat{x}_{k-1},u,d_{k-1};t_k)$ and the predicted covariance matrix $\mathscr{P}_{k|k-1} = \mathscr{P}(\mathscr{P}_k,u,d_{k-1};t_k)$, we integrate the following set of equation for $t \in [t_{k-1};t_k]$

$$\begin{aligned} &\frac{d\hat{x}}{dt} = \mathscr{G}(\hat{x},u) + Fd_{k-1}, \\ &\frac{d\mathscr{P}}{dt} = A(t)\mathscr{P} + \mathscr{P}A(t)^T + Q, \\ &\hat{x}(t_{k-1}) = \hat{x}_{k-1}, \\ &\mathscr{P}(t_{k-1}) = \mathscr{P}_{k-1}, \end{aligned} \tag{8.12}$$

  where $A(t) = \nabla_x(\mathscr{G}(\hat{x},u) + Fd_{k-1})$.

- *Estimate Unknown Input:* To estimate the unknown input d_k, we use the following set of equations

$$\begin{aligned} &\tilde{R}_k := C\mathscr{P}_{k|k-1}C^T + R, \\ &M_k := \left((C\bar{F_k})^T\tilde{R}_k^{-1}(C\bar{F_k})\right)^{-1}(C\bar{F_k})^T\tilde{R}_k^{-1}, \\ &d_k := M_k(y(t_k) - C\hat{x}_{k|k-1}), \end{aligned} \tag{8.13}$$

  where $\bar{F_k} = (\exp(A(t_k)) - I)A(t_k)^{-1}F$ if $A(t_k)$ is not singular.

- *Correction:* We obtain the estimated state $\hat{x}_k$ and the estimated covariance matrix $\mathscr{P}_k$ using the following set of equation

$$\begin{aligned}
&\hat{x}_k^- := \hat{x}_{k|k-1} + \bar{F_k} d_k,\\
&L_k := \mathscr{P}_{k|k-1} C^T \tilde{R}_k^{-1},\\
&\mathscr{P}_{d,k} := \left((C\bar{F_k})^T \tilde{R}_k^{-1} (C\bar{F_k})\right)^{-1},\\
&\mathscr{P}_k^- := \mathscr{P}_{k|k-1} + \bar{F_k}\mathscr{P}_{d,k}\bar{F_k^T} - \bar{F_k}\mathscr{P}_{d,k}(C\bar{F_k})^T L_k^T - L_k(C\bar{F_k})\mathscr{P}_{d,k}\bar{F_k^T},\\
&\hat{x}_k := \hat{x}_k^- + L_k(y(t_k) - C\hat{x}_k^-),\\
&\mathscr{P}_k := \mathscr{P}_k^- - L_k(\tilde{R}_k - \bar{F_k}\mathscr{P}_{d,k}\bar{F_k^T})L_k^T.
\end{aligned} \tag{8.14}$$

8.3 Validation on the modified minimal model of Bergman

8.3.1 Numerical methods

To solve the problem of estimating the state using an UKF or an UIEKF observer, we simply need to integrate some differential equations, e.g. using the Dormand-Prince method (see e.g. [32]). When using a MHE observer, we also need to solve a minimization problem whose cost function is given by (8.10). Let us briefly show how the numerical methods presented in chapter 4 can be used to solve this problem. Let us write the additively disturbed version of (6.6) as follows

$$\begin{aligned}
\frac{dx_1}{dt} &= -P_1(x_1 - G_b) - x_1x_2 + k_{gr}x_5 + w_1,\\
\frac{dx_2}{dt} &= -P_2x_2 + P_3(x_3 - I_b) + w_2,\\
\frac{dx_3}{dt} &= -k_f x_3 + b_f x_4 + w_3,\\
\frac{dx_4}{dt} &= -k_s x_4 + u + w_4,\\
\frac{dx_5}{dt} &= -c_2(x_5 - x_6) + w_5,\\
\frac{dx_6}{dt} &= -c_1(x_6 - d) + w_6,\\
x(t_{k-N}) &= x_{k-N},\\
y(t_i) &= Cx(x_{k-N}, u, w; t_i) + v_i,
\end{aligned} \tag{8.15}$$

where $C = [1\ 0\ 0\ 0\ 0\ 0]$, $(w_j)_{j\{1,\dots,6\}}$ is the model noise, v_i is the measurement noise, u is an insulin input assumed to be known and d is a glucose input assumed to be known. The objective is to estimate the value of x_{k-N}, $(w_j)_{j\in\{1,\dots,6\}}$ and v_i for all $i \in \{k-N,\dots,k\}$.

First we rewrite (8.10) by substituing the term v_i by $y(t_i) - Cx(x_{k-N}, u, w; t_i)$

$$J^{t_k}(x_{k-N}, w) = \|x_{k-N} - \hat{x}_{k-N}\|^2_{\mathscr{P}_k} + \sum_{i=k-N}^{k} \|y(t_i) - Cx(x_{k-N}, u, w; t_i)\|^2_{R_k} + \int_{t_{i-1}}^{t_i} \|w\|^2_{Q_k} ds, \tag{8.16}$$

Then, similarly to (4.35), to obtain the appropriate optimality system (necessary conditions), which corresponds to the identification of the gradient of J^{t_k} given by (8.16) that is necessary to develop a

numerical scheme in order to solve the minimization problem, we introduce the adjoint system as follows

$$\begin{aligned}
-\frac{d\tilde{x}_1}{dt} &= -(P_1 + x_2)\tilde{x}_1, \\
-\frac{d\tilde{x}_2}{dt} &= -x_1\tilde{x_1} - P_2\tilde{x}_2, \\
-\frac{d\tilde{x}_3}{dt} &= P_3\tilde{x}_2 - k_f\tilde{x}_3, \\
-\frac{d\tilde{x}_4}{dt} &= b_f\tilde{x}_3 - k_s\tilde{x}_4, \\
-\frac{d\tilde{x}_5}{dt} &= k_{gr}\tilde{x}_1 - c_2\tilde{x}_5, \\
-\frac{d\tilde{x}_6}{dt} &= c_2\tilde{x}_5 - c_1\tilde{x}_6, \\
\tilde{x}(t_k) &= 0, \\
\tilde{x}(\tilde{x}(t_{i-1});t_i) &= \tilde{x}(t_i) - C^T R_k(y(t_i) \\
&\qquad - Cx(x_{k-N}, u, w; t_i)) \ \ \forall i \in \{k-N+1, \ldots, k\},
\end{aligned} \tag{8.17}$$

According to (4.38), the following expression of the derivatives of J^{t_k} are deduced

$$\frac{\partial J^{t_k}}{\partial x_{k-N}}(x_{k-N}, w) = \tilde{x}(t_{k-N}) + \mathscr{P}_k(x_{k-N} - \hat{x}_{k-N}) - C^T R_k(y(t_{k-N}) - Cx_{k-N}),$$

$$\frac{\partial J^{t_k}}{\partial w}(x_{k-N}, w) = \begin{pmatrix}
\tilde{x}_1 + \sum_{i=1}^{6} Q_{1,i} w_i \\
\tilde{x}_2 + \sum_{i=1}^{6} Q_{2,i} w_i \\
\tilde{x}_3 + \sum_{i=1}^{6} Q_{3,i} w_i \\
\tilde{x}_4 + \sum_{i=1}^{6} Q_{4,i} w_i \\
\tilde{x}_5 + \sum_{i=1}^{6} Q_{5,i} w_i \\
\tilde{x}_6 + \sum_{i=1}^{6} Q_{6,i} w_i
\end{pmatrix}, \tag{8.18}$$

where $\tilde{x}$ is the solution of (8.17).

8.3.2 Numerical simulation

To test the good numerical implementation and performances of the various observer, we simulate a virtual patient given by an additively disturbed modified minimal of Bergman. The noise on the model is given by a Gaussian noise $w \approx \mathscr{N}(0, Q)$. The matrix Q has been chosen diagonal

$$Q = \operatorname{diag}(q_1, q_2, q_3, q_4, q_5, q_6). \tag{8.19}$$

Because in this case we have access to the true state value, it is possible to check whether the three observer converge toward the *true* state. To simulate the virtual patient, we consider the set of parameters given in table 8.1 and the variables $(q_i)_{i\in\{1,\ldots,6\}}$ according to table 8.2.

Name	Value	Unit
P_1	3.17×10^{-3}	min^{-1}
P_2	1.53×10^{-2}	min^{-1}
P_3	6.41×10^{-7}	$\text{L.mU}^{-1}\text{.min}^{-1}$
k_f	3.85×10^{-2}	min^{-1}
b_f	1.77×10^{-4}	$\text{L}^{-1}\text{min}^{-1}$
k_s	5.54×10^{-3}	min^{-1}
c_1	2.5×10^{-2}	min^{-1}
c_2	2.5×10^{-2}	min^{-1}
k_{gr}	3.13×10^{-3}	$\text{dL}^{-1}\text{.min}^{-1}$
G_b	82	mg.dl^{-1}
I_b	24.3	mU

Table 8.1: Set of parameters used to simulate a virtual patient.

q_1	q_2	q_3	q_4	q_5	q_6
$0.1P_1G_{eq}$	$0.1P_2X_{eq}$	$0.1k_fI_{eq}$	$0.1k_sU_{1,eq}$	1×10^{-10}	1×10^{-10}

Table 8.2: Chosen value of the components of Q.

To simulate that only sampled noisy measurement are available, the measured output is given by $G(kT_{ech}) + v_k$ where $T_{ech} = 5\text{min}$ and $v_k \approx \mathcal{N}(0,5)$. The first guess to initialize the observers is either set to the equilibrium point of the model which is given by a blood glucose value of $G_{eq} = 100\text{mg.dl}^{-1}$ or set to the exact initial condition. The horizon of the MHE observer is set to 6 past data.

The observers is tested by considering the following scenario

$t = 0h$**:** The simulation is initialized. The initial blood glucose is set at 100mg.dl^{-1}. The observer (UKF) is switched on.

$t = 7h$**:** The patient eats a meal of 25g.

$t = 12h$**:** The patient eats a meal of 70g.

$t = 20h$**:** The patient eats a meal of 80g.

$t = 35h$**:** The simulation is ended.

In order to study the influence of the noise on the measure, the simulation is run 100 times. The observer performances are compared thanks to the computation of the mean root mean square (RMS) of the relative error between the estimated state and the true state[1]

$$\text{RMS} = \sqrt{\sum_{k=0}^{420} \left(\frac{\|x(t_k) - \hat{x}(t_k)\|}{\|x(t_k)\|} \right)^2}, \tag{8.20}$$

where x stands for the true value of the state and $\hat{x}$ stands for the estimated value of the state. This definition of the RMS has a sense because we have $x_1 > 0$ for all $t \geq t_0$.

[1]The number 420 comes from the following computation $\frac{T_{\text{end experiment}}}{T_{ech}}$ where $T_{\text{end experiment}} = 35 \times 60$ min and $T_{ech} = 5\text{min}$.

Observer	UKF	uMHE	UIEKF
RMS	1.5397	1.9193	1.4322

Table 8.3: RMS of the three observer for equilibrium starting point.

Observer	UKF	uMHE	UIEKF
RMS	1.5675	1.8868	1.4191

Table 8.4: RMS of the three observer for exact starting point.

A simulation example, when the observer initial condition is set to the equilibrium starting point, can be seen on fig.8.2. The mean RMS for the three observers is given on table 8.3. A simulation example when the observer initial condition is set to the exact initial condition can be seen on fig.8.3. The corresponding mean RMS for the three observers is given on table 8.4.

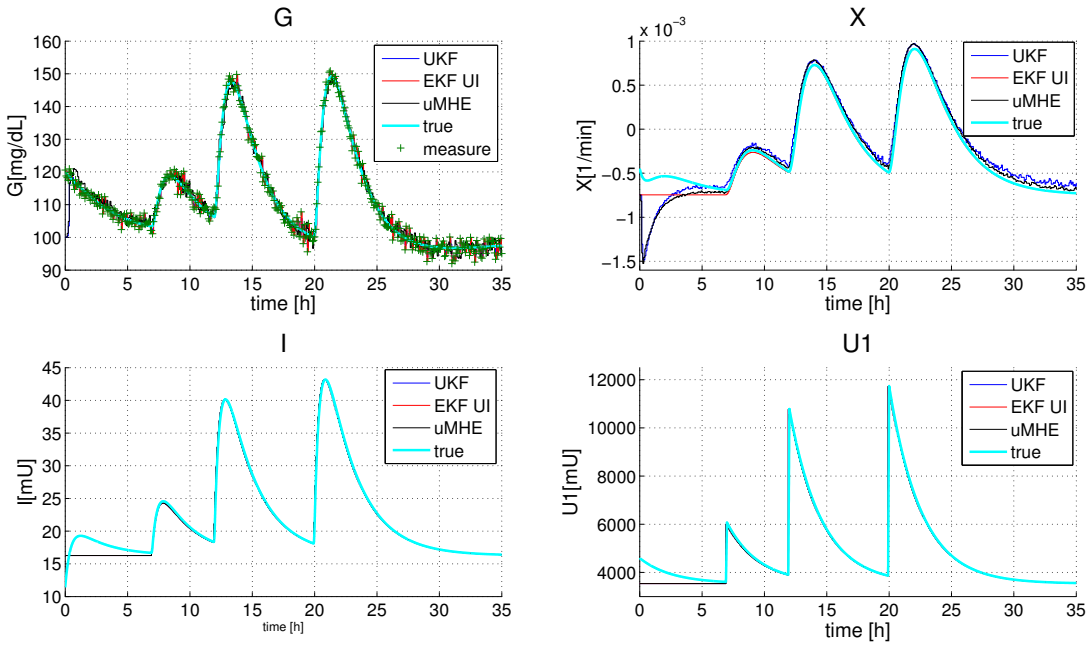

Figure 8.2: Comparison of the UKF, uMHE and UIEKF observer, equilibrium starting point

All of the three designed observers converge toward the true state. Furthermore, it can be seen that none of them show better convergence results than the two others. Because it is difficult to give a sense to the estimated unknown input when using the UIEKF observer, we do not intend to use this approach to estimate the state of the system. That is why, in the sequel, we will only retain the Unscented Kalman Filter. This choice has been done because this observer is less computationally expensive than a MHE observer.

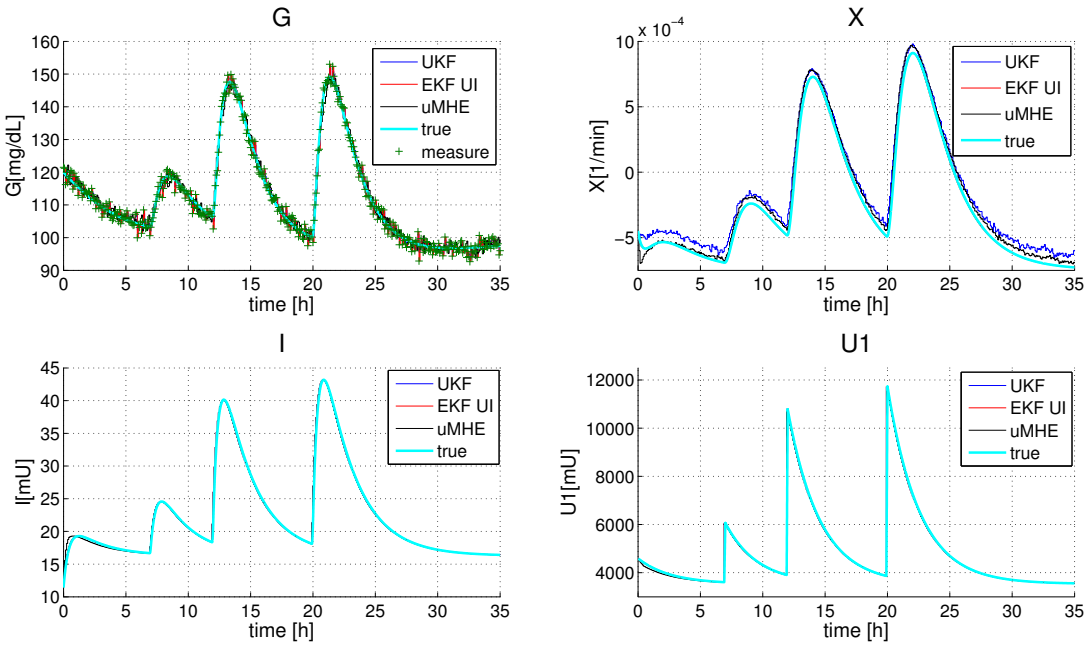

Figure 8.3: Comparison of the UKF, uMHE and UIEKF observer, exact starting point

8.4 Conclusion

In this chapter we have considered that the measure can not provide the full state information and so that the state of the system (6.6) has to be estimated. When dealing with this problem, one of the difficulty is to assess on the quality of the estimate. To solve this issue, we have considered the design of three different observers. It has been shown that the three observers converge toward the true state of the system with similar performances. Because it is difficult to give a sense to the estimated unknown input when using the UIEKF observer, we have retained the simplest approach (from a computational point of view), *i.e.* the UKF observer.

At that point, we have all the necessary tools to solve the problem of artificial blood glucose control. That is why, in the next chapter, we will be interested in considering the application of the SPMPC controller from a numerical simulation point of view. The controller performances will be assessed using both the control model and the testing platform to simulate virtual patients.

Chapter 9

Numerical Simulation on a Virtual Patient

Contents

9.1 Introduction

In chapter 3 we have considered a SPMPC controller which ensures robust control performances by repeatedly solving a constrained saddle point optimization problem. It has been proved that if the disturbances on the model belong to a given set, then the state of the system is stabilized in finite time in a bounded subset. Also, under some assumptions on the criterion, it has been proved that the system is input-to-state practically stable. Then, in chapter 4, we have proposed numerical methods to solve a state-constrained saddle point problem.

This thesis has been motivated by the problem of artificial blood glucose control. That is why, in a second part we have considered the application of the previously presented controller in order to bring a solution to this problem. Thus, in chapter 6, we have been interested in the modeling aspect. This has lead us to consider two models. One, the model of Dalla-Man et al., which can be considered as a complex model, is used for validation purpose while the other, the modified minimal model of Bergman, is used to design the controller. Then, in chapter 7, we have been interested in studying some properties of this latter. One of the main point was to verify that the control model satisfies all the necessary properties needed to use theorem 2. Finally, because the sensors can only provide a measure of blood glucose, in chapter 8, it has been necessary to consider the design of a state observer.

In this chapter we are interested in validating the retained control strategy as a viable alternative for artificial blood glucose control. To do so, we will consider numerical simulations using both the control model and the Dalla-Man et al. model to simulate virtual patients. This latter will be used in the framework of the UVA-Padova testing platform [90]. It has been validated by the Food and Drug Administration as a substitute to test on animals. From a pragmatic point of view, the validation using a testing platform was absolutely necessary in regards to the relative simplicity of the retained control model. Indeed, it seems quite clear that the human metabolism can hardly be modeled by such a simple system of ordinary differential equations. The simulation will be undergone on the trial version of the platform and will concern all of the 10 adults. For each adult, a set of parameters will be identified using optimal control technique. Before further proceeding let us recall that the classical cure of a type 1 diabetic can be split in two parts: the basal term which objective is to stabilize blood glucose in a safe interval (usually set to $[70, 140]\text{mg.dL}^{-1}$) and the bolus part which consists in injecting important quantity of insulin in a short lapse of time to counter sudden blood glucose increase, e.g. due the consumption of a meal. For control purpose we will only be interested in controlling the basal component of the cure (see e.g. [37]), *i.e.* the stabilizing part of the cure. Let us briefly explain this choice. Generally speaking, a patient can quite easily handle meals effect such that in term of quality of the usual cure the introduction of control will only bring minor benefits in regards to the introduced risk. That is why it is considered that the objective of the controller is restrained to use the numerous measures provided by the sensor in order to bring more safety in the cure by dynamically adjusting the basal value of the patient.

To validate the approach we have to consider simulation scenarios which are both challenging and realistic. Indeed, as previously mentioned, it is assumed that the bolus cure is handled thanks to an other algorithm (e.g. by the patient himself). So, the various scenarios have to be designed according to this complementary algorithm. To assess the controller performances we will consider two different scenarios. The first one will consist in stabilizing the blood glucose to a safe value when it is initially quite high (overnight type scenario). This scenario is introduced in order to test whether the controller is safe in regards to hypoglycemia when it has to stabilize a high blood glucose value. The second scenario will consist in a day with three meals. This scenario is considered in order to test whether the controller can be efficiently combined with a bolus cure.

This chapter is organized as follows. First, the identification procedure to obtain a set of parameters for each patient is briefly presented. Then, simulation concerning the two aforementioned scenarios are

undergone using the modified minimal model of Bergman to simulate a virtual patient. Finally, the same experiments are undergone using the virtual testing platform.

9.2 Identification procedure

9.2.1 Motivation and Identification procedure

The problem of artificial blood glucose control has been tackled using a model predictive controller. When using such an approach, the model of the process is of prime importance and has strong influence on the expectable controller performances. For control purpose, we have retained a simple nonlinear model which provides a rough global trend of the process. This has enabled us to easily consider the design of the controller. There is an other advantage in this choice. As the model has only few parameters, the identification of an adequate model for a given patient with simple and safe experiments is rendered possible. This is particularly interesting as this enables us to consider the inter-patient variability. That is why, even if in this thesis we focus on the control aspect, we have some interest in identifying the parameters of the model. In this section, an identification technique based on optimal control on the parameters is presented. The retained methodology is somewhat simple but sufficient to provide *admissible* parameters.

Now, let us describe the identification procedure. Assuming that a first set of parameters is given (e.g. using Matlab toolbox), the identification procedure will consist in estimating separately the glucose-insulin sub-model and the gastro-intestinal sub-model. This choice has been done in order to avoid compensatory effect through the gastro-intestinal sub-model. Indeed, in the control model, the meal input d can induce an increase in the blood glucose value with more dynamics than an increase due to a variation of the value of the state X. So, if both sub-models were to be identified simultaneously, we will take the risk that the gastro-intestinal sub-model will be used to explain others dynamics that have been neglected in the model. In order to converge to an admissible set of parameters, the procedure is implemented recursively, *i.e.*, for given parameters of the gastro-intestinal sub-model, the parameters of the glucose insulin are identified, then using these new parameters, the parameters of the gastro-intestinal sub-model are identified, and so on until the parameters converge. The identification procedure is summed up in fig. 9.1.

9.2.2 Numerical methods

Formulation of a general identification problem

The problem of identifying the model parameters will be handled as a control problem on the parameters. The identification problem will be cast as a minimization problem. The aim is to find the parameters such that the error between the measured output during an experiment and the simulated output is minimized. That is, to obtain the model parameters, we are interested in solving the following optimization problem:

$$\begin{aligned} &p^* = \arg\min_{p\in\mathbb{R}^{n_p}} J(p), \\ &s.t.\ (3.1) \text{ with } x(T_{start}) = x_0 \text{ is known}, \end{aligned} \tag{9.1}$$

where p is the vector of parameters that has to be identified and the functional $J(p)$ is given as follows:

$$J(p) = p^T \alpha p + \int_{T_{start}}^{T_{end}} \left(\|y - y_{obs}\|_R^2 \right) ds, \tag{9.2}$$

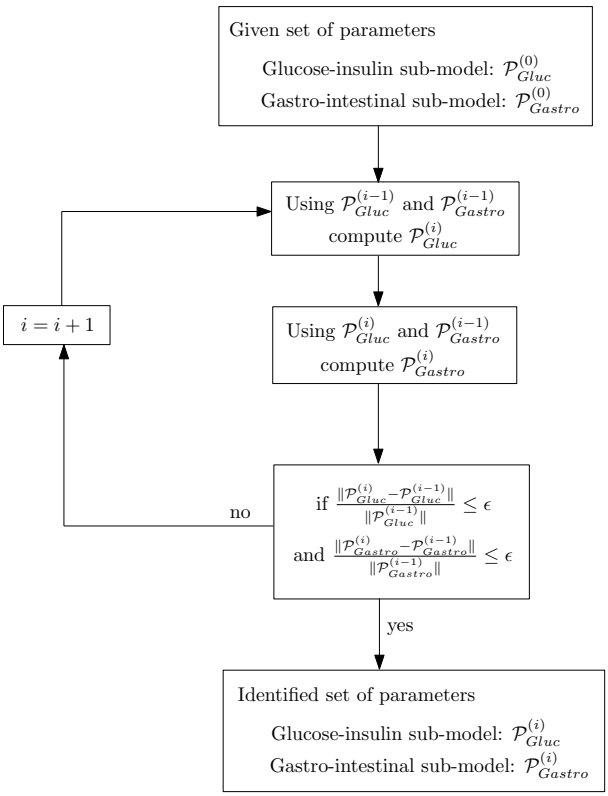

Figure 9.1: Identification procedure

where y_{obs} is the measured output, y is the simulated output, T_{start} and T_{end} stand for the time value at the beginning and at the end of the experiment respectively, α and R are given definite symmetric positive matrices.

This optimization problem will be solved using the results presented in chapter 4. To identify the model parameters of (6.6) it is assumed that the sole value of blood glucose is available.

Formulation for the glucose-insulin sub-model

To identify the parameters of the glucose-insulin sub-model, we consider the optimization problem given by (9.1), where the vector of parameters p that has to be identified is given by

$$p = \begin{pmatrix} P_1 & P_2 & P_3 & k_f & b_f & k_s & G_b \end{pmatrix}^T. \tag{9.3}$$

According to (4.35), to obtain the appropriate optimality system (necessary conditions), which corresponds to the identification of the gradient of $J(p)$ that is necessary to develop a numerical scheme in

order to solve the minimization problem (9.1), we introduce the adjoint system as follows

$$\begin{aligned}
-\frac{d\tilde{x}_1}{dt} &= -(P_1+x_2)\tilde{x}_1 + R(x_1 - x_{1,obs}),\\
-\frac{d\tilde{x}_2}{dt} &= -x_1\tilde{x}_1 - P_2\tilde{x}_2,\\
-\frac{d\tilde{x}_3}{dt} &= P_3\tilde{x}_2 - k_f\tilde{x}_3,\\
-\frac{d\tilde{x}_4}{dt} &= b_f\tilde{x}_3 - k_s\tilde{x}_4,\\
-\frac{d\tilde{x}_5}{dt} &= k_{gr}\tilde{x}_1 - c_2\tilde{x}_5,\\
-\frac{d\tilde{x}_6}{dt} &= c_2\tilde{x}_5 - c_1\tilde{x}_6,\\
\tilde{x}(T_{end}) &= 0,
\end{aligned} \tag{9.4}$$

where $x_{1,obs}$ stands for the measured output and x_1 stands for the simulated output.

According to (4.38), the following expression of the derivative of $J(p)$ is deduced

$$\frac{\partial J}{\partial p}(p) = \begin{pmatrix}
-\int_{T_{start}}^{T_{end}} \tilde{x}_1(x_1 - G_b)ds + \alpha_{1,1}P_1\\
-\int_{T_{start}}^{T_{end}} \tilde{x}_2 x_2 ds + \alpha_{2,2}P_2\\
\int_{T_{start}}^{T_{end}} \tilde{x}_2(x_3 - I_b)ds + \alpha_{3,3}P_3\\
-\int_{T_{start}}^{T_{end}} \tilde{x}_3 x_3 ds + \alpha_{4,4}k_f\\
\int_{T_{start}}^{T_{end}} \tilde{x}_3 x_4 ds + \alpha_{5,5}b_f\\
-\int_{T_{start}}^{T_{end}} \tilde{x}_4 x_4 ds + \alpha_{6,6}k_s\\
-\int_{T_{start}}^{T_{end}} P_1\tilde{x}_1 ds + \alpha_{7,7}G_b
\end{pmatrix}. \tag{9.5}$$

Formulation for the gastro-intestinal sub-model

To identify the parameters of the glucose-insulin sub-model, we consider the optimization problem given by (9.1), where the vector p is chosen as follows

$$p = \begin{pmatrix} k_{gr} & c_2 & c_1 \end{pmatrix}^T. \tag{9.6}$$

In this case, the adjoint model is also given by (9.4). According to (4.38), the derivative of $J(p)$ is given by

$$\frac{\partial J}{\partial p}(p) = \begin{pmatrix}
\int_{T_{start}}^{T_{end}} \tilde{x}_1 x_5 ds + \alpha_{1,1}k_{gr}\\
-\int_{T_{start}}^{T_{end}} \tilde{x}_5(x_5 - x_6)ds + \alpha_{2,2}c_2\\
-\int_{T_{start}}^{T_{end}} \tilde{x}_6(x_6 - d)ds + \alpha_{3,3}c_1
\end{pmatrix}. \tag{9.7}$$

Adult	P_1	P_2	P_3	k_f	b_f	k_s	G_b	I_b
1	3.2×10^{-3}	1.53×10^{-2}	1.26×10^{-6}	3.85×10^{-2}	1.77×10^{-4}	6.5×10^{-3}	76.7	25.3
2	1.29×10^{-2}	5.2×10^{-3}	1.46×10^{-6}	1.1×10^{-2}	4.93×10^{-4}	5.64×10^{-2}	80.3	28.6
3	1.14×10^{-2}	1.14×10^{-2}	4.48×10^{-6}	1.04×10^{-2}	6.17×10^{-4}	6.42×10^{-2}	89.1	31.8
4	7.27×10^{-3}	1.94×10^{-2}	1.16×10^{-5}	1.08×10^{-2}	5.67×10^{-4}	5.58×10^{-2}	83.4	18.9
5	8.67×10^{-3}	8.67×10^{-3}	1.50×10^{-6}	5.80×10^{-2}	4.81×10^{-4}	1.06×10^{-2}	92.4	29.5
6	4.51×10^{-3}	1.34×10^{-2}	4.82×10^{-6}	8.41×10^{-3}	2.64×10^{-4}	3.9×10^{-2}	85	26.9
7	6.11×10^{-3}	1.87×10^{-2}	1.23×10^{-5}	4.22×10^{-2}	3.34×10^{-4}	9.1×10^{-3}	85.4	23
8	2.81×10^{-3}	2.29×10^{-2}	1.59×10^{-6}	3.88×10^{-2}	4.50×10^{-4}	1.24×10^{-2}	89.2	25.3
9	3.8×10^{-3}	5.33×10^{-3}	5.46×10^{-7}	6.65×10^{-2}	9.34×10^{-4}	1.37×10^{-2}	75.6	30
10	7.14×10^{-3}	9.3×10^{-3}	1.50×10^{-6}	5.02×10^{-2}	5.11×10^{-4}	1.11×10^{-2}	91.2	32.6

Table 9.1: Parameters value for the adults of the simulator, glucose-insulin sub-model

9.2.3 Identification results

To obtain the data necessary to identify the parameters of the model, we have considered the simulation scenario which consists in a day with three meals as the one given given in section 8.3. These data have been generated using the testing platform [90]. It has been assumed that the blood glucose is measured each minute. Also, to simplify the problem, we have considered that a non noisy measure of the blood glucose was available. Of course this assumption is unrealistic when considering real patient data.

The matrices of the criterion (9.2) are chosen as follows

$$\begin{aligned} &\underline{\text{For the glucose-insulin sub-model}}:\\ &R=1,\\ &\alpha=0.1\text{diag}\left(\frac{1}{P_1^{(0)}},\frac{1}{P_2^{(0)}},\frac{1}{P_3^{(0)}},\frac{1}{k_f^{(0)}},\frac{1}{b_f^{(0)}},\frac{1}{k_s^{(0)}},\frac{1}{G_b^{(0)}}\right), \end{aligned} \tag{9.8}$$

$$\begin{aligned} &\underline{\text{For the gastro-intestinal sub-model}}:\\ &R=1,\\ &\alpha=0.1\text{diag}\left(\frac{1}{k_{gr}^{(0)}},\frac{1}{c_1^{(0)}},\frac{1}{c_2^{(0)}}\right), \end{aligned} \tag{9.9}$$

where $P_1^{(0)}$, $P_2^{(0)}$, $P_3^{(0)}$, $k_f^{(0)}$, $b_f^{(0)}$, $k_s^{(0)}$, $G_b^{(0)}$, $k_{gr}^{(0)}$, $c_1^{(0)}$ and $c_2^{(0)}$ correspond to the value of the first set of identified parameters.

The comparison between the measured output used to identify the parameters and the simulated output for adult 7 is shown on fig. 9.2 and for adult 10 on fig. 9.3. On these figures it can be seen that the global trend of the glucose metabolism is respected. However, the quality of the identification results can vary from satisfactory as for adult 7 to debatable as for adult 10. It is assumed that by introducing time varying parameters we can make up for the gap between the output of the identified model and the simulated value.

The parameters obtained for the 10 adults of the testing platform are summed up in table 9.1 and 9.2.

Remark 10. According to the results presented in section 7.2.1, for all adults, it is deduced that the state keeps its physiological meaning (*i.e.* it evolves in $\mathbb{R}^{+*}\times\mathbb{R}\times\mathbb{R}^{+}\times\mathbb{R}^{+}\times\mathbb{R}^{+}\times\mathbb{R}^{+}$) simply if we

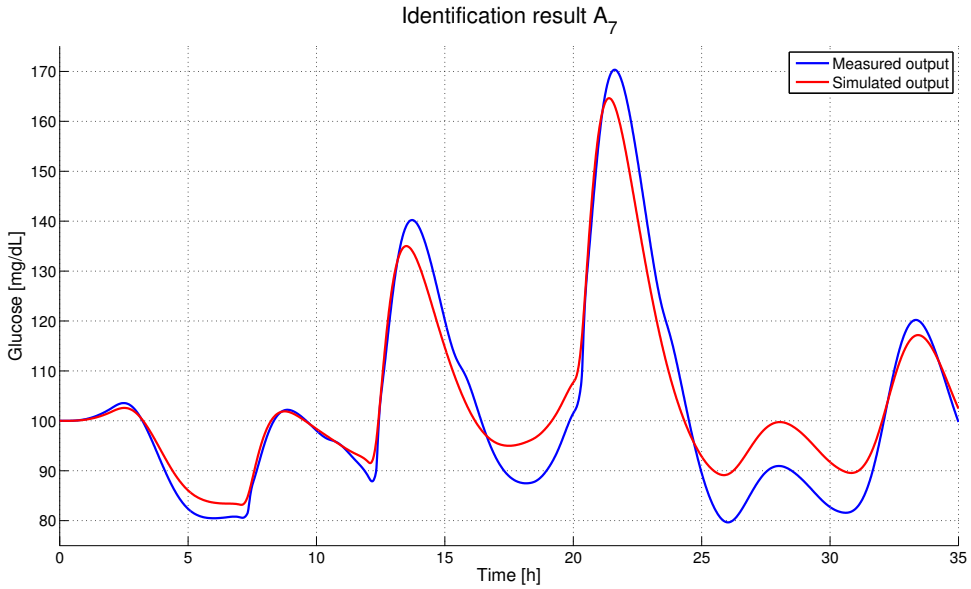

Figure 9.2: Comparison between the data used for identification purpose and simulated output for adult 7

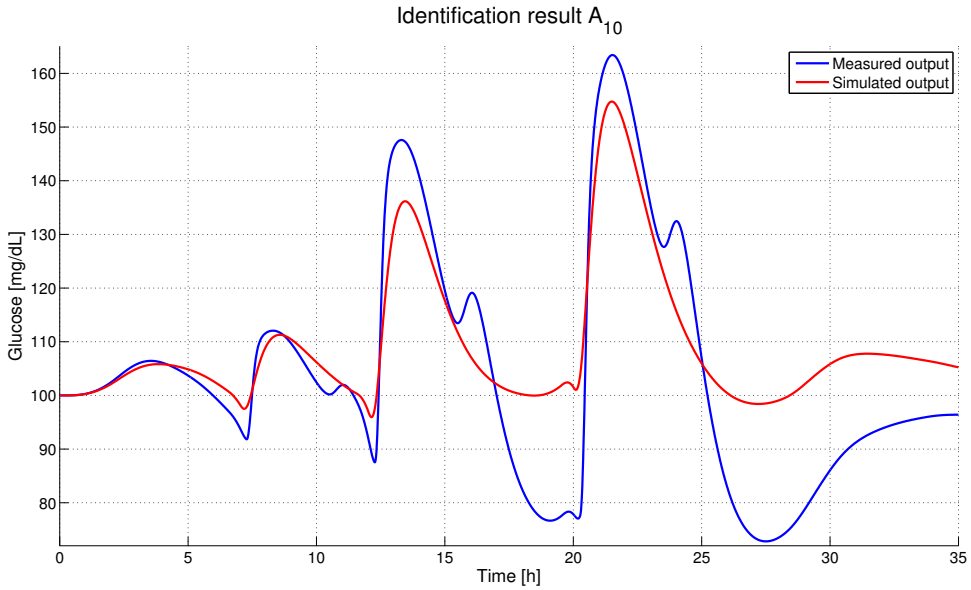

Figure 9.3: Comparison between the data used for identification purpose and simulated output for adult 10

have $u \geq 0$ and $d \geq 0$. Concretely, this does not set any supplementary conditions on the inputs as they correspond to an injected flow and a quantity respectively.

Adult	k_{gr}	c_2	c_1
1	1×10^{-3}	2.39×10^{-2}	9.95×10^{-2}
2	4×10^{-3}	6×10^{-3}	9.26×10^{-2}
3	4.5×10^{-3}	5.6×10^{-3}	9.25×10^{-2}
4	4.2×10^{-3}	9.1×10^{-3}	9.47×10^{-2}
5	3.2×10^{-3}	6.6×10^{-3}	9.32×10^{-3}
6	4×10^{-3}	8.7×10^{-3}	9.35×10^{-2}
7	3×10^{-3}	8.6×10^{-3}	9.34×10^{-2}
8	5×10^{-4}	7.9×10^{-3}	9.33×10^{-2}
9	1.8×10^{-3}	7.4×10^{-3}	9.33×10^{-2}
10	3.7×10^{-3}	8.3×10^{-3}	9.35×10^{-2}

Table 9.2: Parameters value for the adults of the simulator, gastro-intestinal sub-model

9.3 Simulation Scenarios and Controller Setting

Now that the parameters of the model of each adult have been identified, it becomes possible to consider the numerical simulation. To do so, we will consider two kind of virtual patient. The first series will be given by the control model. With this series, the aim is to test the controller performances in case the model of the process is nearly perfect. The second series will be given by the adult of the testing platform [90]. In this case the objective is to test the controller robustness against neglected dynamics.

To test the controller performances, two scenarios will be considered. The first one aims at testing the controller performances when it works alone. The second scenario is introduced in order to test the controller performances when combined with a classical bolus cure.

One difficulty when dealing with control techniques which are based on the optimization of a criterion is to tune this latter in order to obtain the *best* control performances. The more simple and common approach consists in trial and error techniques. That is, numerous simulations for various criterion are done and the one which leads to the best control performances is retained. Problem of this approach is that it can not be used when dealing with more realistic case. Indeed, when human is in the loop, we are more interested in ensuring control performances at first try rather than failing because the first tuning was too aggressive. That is why, for each virtual patient, we will consider the same *default* setting.

9.3.1 Simulation Scenarios

Let us begin to present the two scenarios that have been chosen to test the controller performances.

Overnight scenario

To begin with, we are interested in testing the controller performances when it works *alone*. By this assertion we mean that it is desired to test whether the controller can efficiently stabilize a high initial blood glucose without inducing an hypoglycemia. To do so, let us envisage the following scenario

Scenario 1: Overnight

$t = 0h$**:** The simulation is initialized. The initial blood glucose is set at 200mg.dl^{-1}. The observer (UKF) is switched on.

$t = 2h$**:** The controller is switched on.

$t = 24h$**:** The simulation is ended.

This scenario has been called overnight scenario because it can be interpreted as an evening/ night situation of a classical life. Indeed, after dinner, before sleeping, the blood glucose value can be quite high (e.g. because of a miscalculation in the bolus) despite a negligible rate of appearance, *i.e.* $R_a \approx 0$. Thus, during the night, the objective of the controller is to stabilize the blood glucose to a safer value without needing to consider meals effects because the patient is assumed to sleep and so is non active.

With this scenario, to assess the controller performances, we are interested in % $G \in [70;140]$ the percentage of time spent in the interval $[70;140]\text{mg.dL}^{-1}$ (which corresponds to a safe blood glucose), in % $G \in [80;120]$ the percentage of time spent in the interval $[80;120]\text{mg.dL}^{-1}$ (which corresponds to tight blood glucose control) and in $\min G$ the minimal value of blood glucose during the complete experiments. All these metrics are computed when the loop is closed.

Classical day scenario

Then we are interested in testing the controller performances when combined with a classical bolus cure. This point is of prime importance as a complete cure consists in the combination of a basal and a bolus component. As we have been interested in considering only one component, we have to verify that the controller will not over react when combined with the other algorithm. To do so, let us envisage the following scenario

Scenario 2: Classical day

$t = 0h$**:** The simulation is initialized. The initial blood glucose is set at 100mg.dl^{-1}. The observer (UKF) is switched on.

$t = 2h$**:** The controller is switched on.

$t = 7h$**:** The patient eats a meal of 25g.

$t = 12h$**:** The patient eats a meal of 70g.

$t = 20h$**:** The patient eats a meal of 80g.

$t = 35h$**:** The simulation is ended.

The information concerning the meal size and the injected bolus are provided to the controller when the corresponding event occurs (no anticipatory behavior).

Some variations of this scenario are envisaged depending on the way the bolus part of the cure is handled. In a first variation, it is assumed that each meal are self regulated via injection of 75% of the optimal bolus (according to the insulin to carbohydrate ratio determined by the physician). In a second variation, it will be assumed that no boluses are injected.

With this scenario, to assess the controller performances, we introduce the following metrics: % $G \in [70;140]$ the percentage of time spent in the interval $[70;140]\text{mg.dL}^{-1}$, $\min G$ the minimal value of blood glucose during the complete experiment and $\max G$ the maximal value of blood glucose during the complete experiment. All metrics are computed when the loop is closed.

In its first variation, the objective of the scenario is to test whether the controller can be efficiently combined with a classical bolus cure. If it does then this means that the here presented SPMPC controller is a potential candidate to design an artificial pancreas. In its second variation, the objective is to test the controller robustness in face to major disturbances and also if it can be used to generate the bolus part of the cure.

9.3.2 Controller Settings

The tuning of the controller is a problem in itself. Indeed, as we consider human beings, a simple and safe tuning has to be available for all patients at first try. In order to consider a somewhat realistic case, the same default tuning is used for all adults. The idea is to test whether, in lack of any control experience for a given patient, we can design a safe controller.

First, let us consider the setting of the controller objective. For all adults, the objective will be to stabilize blood glucose at $G_{eq} = 100\text{mg.dL}^{-1}$. In this case, the nominal control input is given by $u = u_{eq}$ where

$$u_{eq} = \frac{k_s k_f}{b_f}\left(I_b - \frac{P_2 P_1 (G_{eq} - G_b)}{P_3 G_{eq}}\right). \tag{9.10}$$

The prediction horizon T of the SPMPC controller has been set to 5h. To consider the asymmetric control objective, the constraint $G \geq 80\text{mg.dL}^{-1}$ has been added in the optimization problem. The matrix R, α and Q are chosen as follows:

$$R = \text{diag}\left(\frac{1}{G_{eq}}, 0, \frac{1}{I_{eq}}, 0\right),\ Q = \text{diag}\left(\frac{1}{P_1}, \frac{1}{P_2}, \frac{1}{P_3}, \frac{1}{k_f}, \frac{1}{b_f}, \frac{1}{k_s}\right),\ \alpha = \frac{1}{u_{eq}}, \tag{9.11}$$

where $I_{eq} = I_b - \dfrac{P_2 P_1 (G_{eq} - G_b)}{P_3 G_{eq}}$.

The matrix R only weight the blood glucose and the blood insulin which corresponds to the two *natural* state of the system. The uncertainties on the parameters are given by variations of 50% around the nominal value of the corresponding parameters.

The disturbed model, the adjoint model, the final cost and the terminal state constraint are defined according to the results of chapter 7.

9.4 Simulation results with the modified model of Bergman

First, to validate the implementation and the performances of the control methodology, let us consider the control of the modified minimal model of Bergman in case this model is also used for patient simulation purpose.

For simulation purpose, it is assumed that the meals are uniformly consumed in 15min. The sampling time on the blood glucose G is set to 5min and the sampling time on the control input u is set to 15min. For control purpose, a noisy blood glucose value is provided for the observer, *i.e.*:

$$G_{sensor,k} = G_k + v_k, \tag{9.12}$$

where $v_k \approx \mathcal{N}(0,5)$.

9.4.1 Scenario 1: Overnight

The table 9.3 sums up the simulation results for all adults. It can be seen that for all adults the results are satisfactory. The blood glucose is efficiently and rapidly stabilized. Also, no hypoglycemia event has to be deplored.

Adult	% $G \in [70;140]$	% $G \in [80;120]$	$\min G$ mg.dL^{-1}
1	83	76	92
2	95	91	94
3	95	90	93
4	91	88	90
5	94	88	92
6	88	84	92
7	90	87	91
8	85	83	94
9	87	81	91
10	93	86	92

Table 9.3: Simulation results for scenario 1, using the control model as patient simulator

Adult	% $G \in [70;140]$	$\min G$ mg.dL^{-1}	$\max G$ mg.dL^{-1}
1	88	92	169
2	87	95	175
3	96	90	150
4	92	90	177
5	91	92	158
6	86	88	209
7	95	83	155
8	100	91	115
9	94	93	148
10	87	92	187

Table 9.4: Simulation results for scenario 2 variation 1, using the control model as patient simulator

9.4.2 Scenario 2: Classical day

Variation 1**:** 75% **of bolus injected**

The simulation results for all adults can be seen in table 9.4. It can be seen that the blood glucose is well controlled. For all adults, no hypoglycemia event is detected. Also, the time spent in hyperglycemia is negligible. Furthermore, as it can be seen with the simulation result for adult 9 on fig.9.4, the controller shows an interesting behavior. The blood glucose is stabilized thanks to small variation of the basal insulin what is quite safe from a cure point of view.

Variation 2**: no bolus injected**

The table 9.5 sums up the simulation results for all adults. Once again the results are quite satisfactory. The simulation result for adult 9 can be seen on fig.9.5. It is interesting to see that the controller naturally works under a basal/ bolus strategy. By this assertion we mean that the blood glucose is stabilized thanks to the injection of a nearly constant insulin flow (basal behavior), while the effects of meals are rejected thanks to the injection of a more important dose of insulin (bolus behavior).

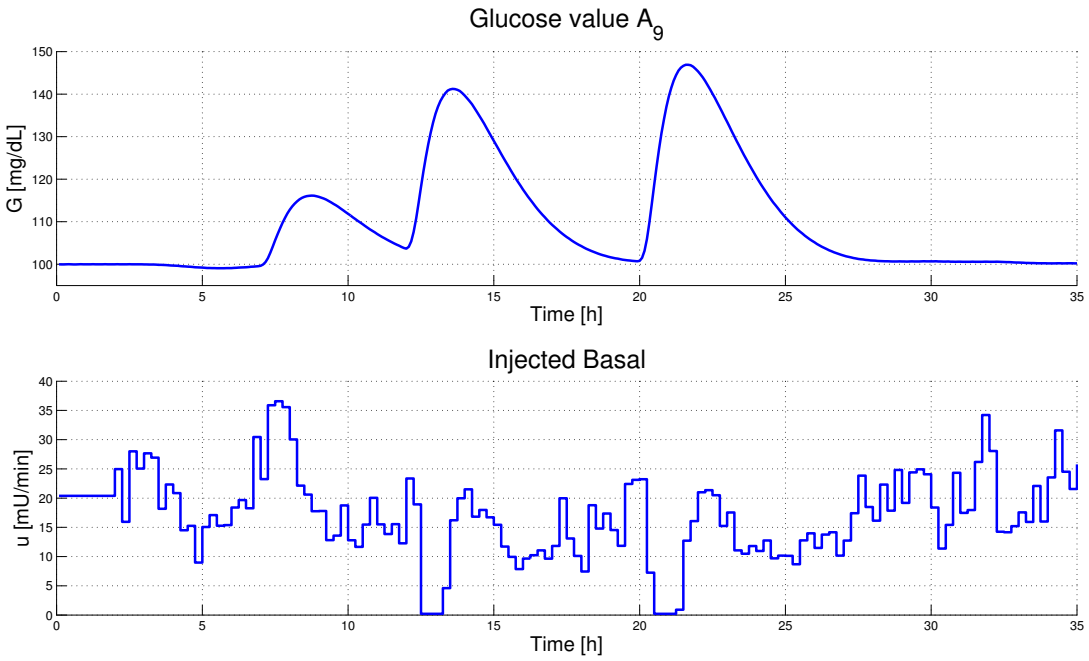

Figure 9.4: Simulation result for adult 9 with scenario 2 variation1, using the control model as patient simulator

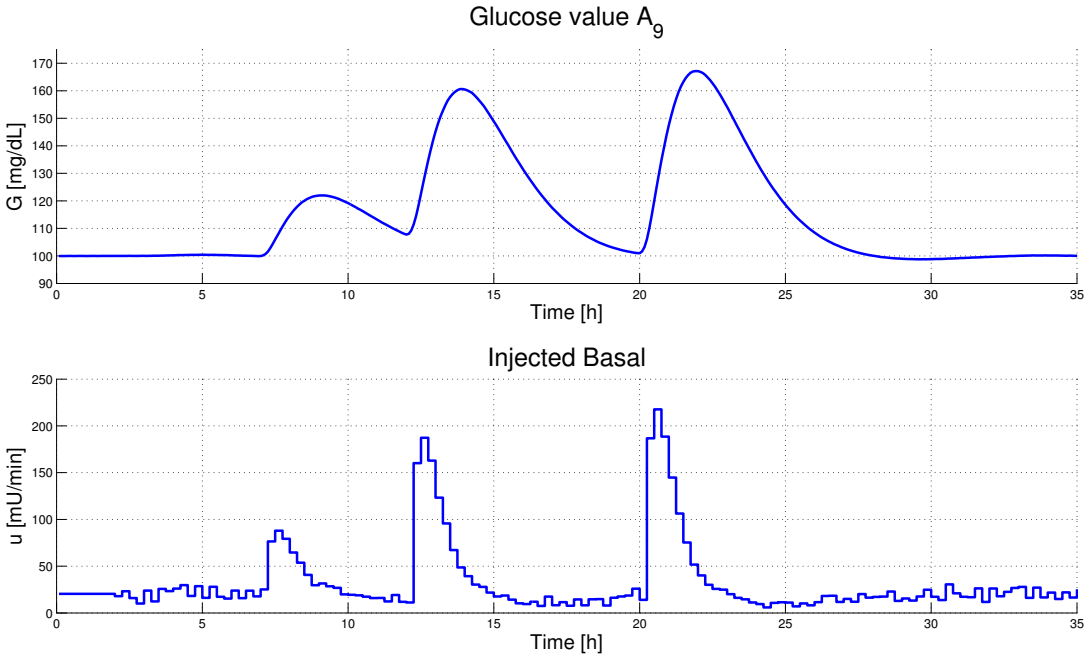

Figure 9.5: Simulation result for adult 9 with scenario 2 variation2, using the control model as patient simulator

Scenario 2 variation 1 bis: time varying parameters

Finally we have considered a last variation of the second scenario. As we have implemented the virtual patient, it is possible to consider time varying parameters. By doing so the aim is not to mimic some

Adult	% $G \in [70;140]$	$\min G$ mg.dL^{-1}	$\max G$ mg.dL^{-1}
1	85	92	176
2	82	91	195
3	86	92	189
4	83	89	228
5	84	93	188
6	79	88	242
7	88	80	189
8	100	95	119
9	84	94	173
10	81	93	223

Table 9.5: Simulation results for scenario 2 variation 2, using the control model as patient simulator

Adult	% $G \in [70;140]$	$\min G$ mg.dL^{-1}	$\max G$ mg.dL^{-1}
1	84	98	173
2	84	100	183
3	96	93	147
4	90	85	186
5	90	100	161
6	80	90	218
7	87	85	177
8	100	98	111
9	89	93	154
10	86	100	190

Table 9.6: Simulation results for scenario 2 variation 1bis, using the control model with time varying parameters as patient simulator

realistic phenomena (e.g. the dawn phenomena) but more to test the controller behavior when the process is time-varying. For a parameter with nominal value p_{nom}, to simulate the virtual patient, we have considered the time varying parameter $p(t)$ given by

$$p(t) = p_{nom}\left(1+\frac{0.5}{3}(sin(0.25t)+sin(0.5t)+sin(t))\right).$$

The simulation results are summed up in table 9.6. In this case, the results are comparable to the one given by table 9.4. These results are interesting as they show the robust performances of the retained control approach. The simulation result for adult 9 can be seen on fig. 9.6. It is interesting to see that the profile of injected insulin is comparable to the one given by the first variation of scenario 2 (see fig. 9.4).

9.4.3 Discussion

It can be seen that using a SPMPC controller the blood glucose is safely stabilized. Indeed, for all scenarios and for all adults, no hypoglycemic event occurs and the time spent in hyperglycemia is too short to induce any damages. It has been shown, with the first variation of the second scenario, that the controller can be efficiently combined with a classical bolus cure. Also, with the second variation of the

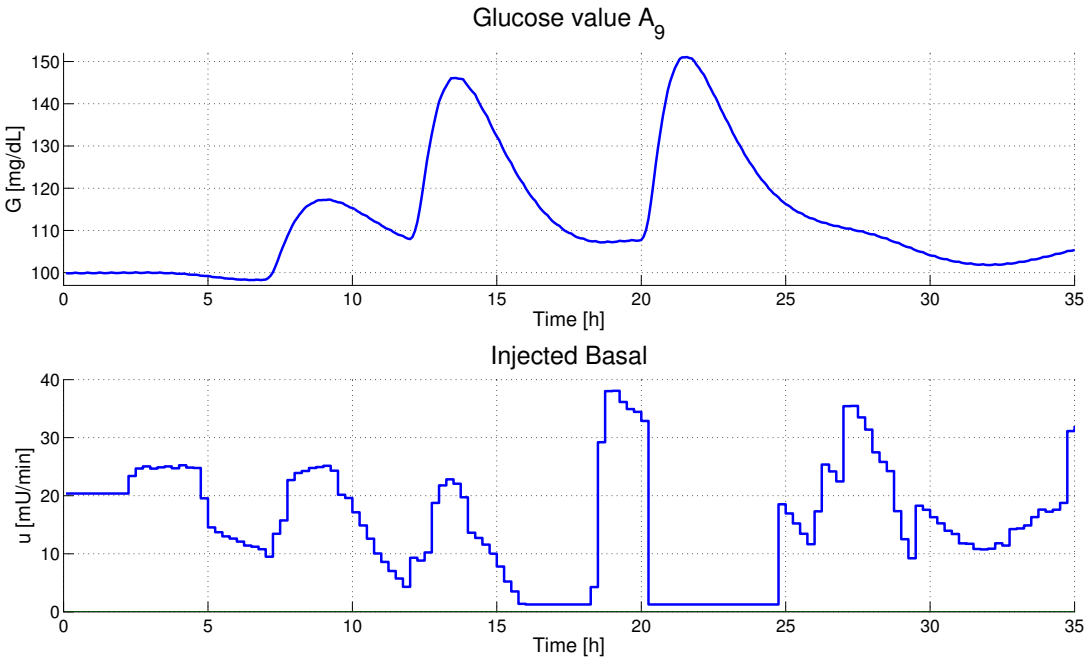

Figure 9.6: Simulation result for adult 9 with scenario 2 variation1bis, using the control model as patient simulator

second scenario, it can be seen that the controller does not lost too much of its performances in case of meal consumption and no bolus injection. This can be seen on fig.9.7 where the simulation results for the two variations of the scenario 2 on adult 10 are compared. As for the third variation of the second scenario, it has enabled to show that the controller provides robust control performances when used to control a time-varying process.

Now that it has been verified that the SPMPC controller can be efficiently used to control the modified minimal model of Bergman, we can envisage a more realistic series of virtual patients. Indeed, the retained control model is too simple to simulate a realistic metabolic behavior of a type 1 diabetic (see e.g. the non negligible difference between the measured and the simulated output on fig.9.3). That is why, in the next part, we will consider numerical simulation using a testing platform in which the Dalla-Man et al. model is implemented.

9.5 Simulation Result with the virtual testing platform

In this section we will be interested in testing the controller performances with the previously presented scenarios using a testing platform approved by the FDA [90]. The controller performances will be compared to the ones given by a classical NMPC controller (whose solution is computed using the numerical tools presented in chapter 4).

9.5.1 Scenario 1: Overnight

The table 9.7 sums up the simulation results for all adults. It can be seen that both the NMPC and the SPMPC controller can safely stabilize blood glucose in the sense that no hypoglycemia event has occurred. With this scenario, the performances of the SPMPC controller are comparable with the one

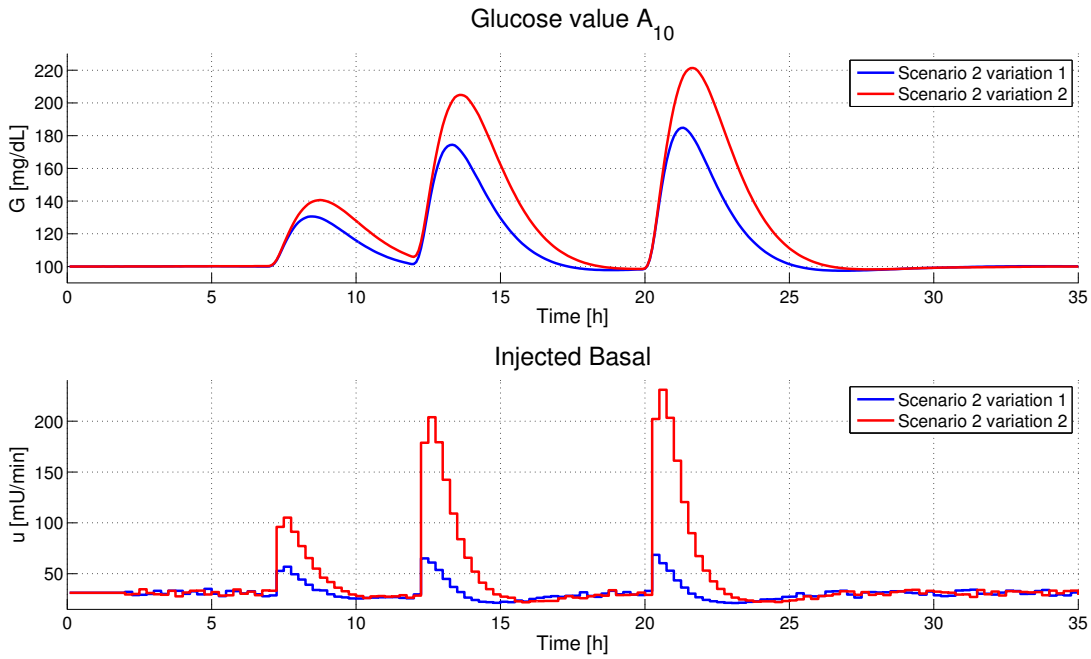

Figure 9.7: Simulation results for adult 10 with scenario 2 using the control model as patient simulator

given by a NMPC controller. This implies that it is certainly more interesting to consider the SPMPC approach because of the guaranteed robustness. Indeed, in this case, if the performances are comparable, it is also because the modified minimal model of Bergman is well adjusted, whereas with real patients, it will be more difficult to obtain such identification results. It is also interesting to see that the injected insulin profile consists in small variation around a given basal (see e.g. the simulation result for adult 7 on fig. 9.8).

9.5.2 Scenario 2: Classical day

Variation 1**:** 75% **of bolus injected**

The simulation results for all adults can be seen in table 9.8. The performances of both the NMPC and SPMPC controller are satisfactory. For all adults, no hypoglycemia and only a minor hyperglycemia for adult 9 can be seen. The performances of the NMPC controller are slightly better than the one of the SPMPC controller. This can be explained by the reduced conservatism of this approach. However, concretely, when dealing with artificial blood glucose control, it is preferable to be robust but conservative rather than being too optimistic in regards to the prediction given by the model (particularly in this application where it is hopeless to aim at good model).

The simulation results for the adult 9 using a SPMPC controller and a NMPC controller can be seen on fig. 9.9 and fig. 9.10 respectively. The first point that is worth mentioning is that the sensor noise is a real issue. The bias on the measure can be really large. This can be at the origin of a bad estimate of the current state value and in turn at the origin of bad control performances. The control input of the NMPC mainly differs from the control input of the SPMPC controller in terms of larger amplitude. Because it is safer to act carefully, this tends to suggest that a SPMPC control approach has to be favored.

Adult	% $G \in [70;140]$		% $G \in [80;120]$		$\min G$ mg.dL^{-1}	
	NMPC	SPMPC	NMPC	SPMPC	NMPC	SPMPC
1	89	89	87	86	82	82
2	86	83	60	61	106	106
3	89	89	76	75	97	92
4	90	91	87	88	95	90
5	87	86	83	81	95	96
6	88	87	80	83	94	90
7	90	92	91	90	91	81
8	91	90	88	88	82	83
9	88	84	82	71	103	108
10	88	87	84	83	90	90

Table 9.7: Simulation results for scenario 1, using the Dalla-Man et al. model as patient simulator

Adult	% $G \in [70;140]$		$\min G$ mg.dL^{-1}		$\max G$ mg.dL^{-1}	
	NMPC	SPMPC	NMPC	SPMPC	NMPC	SPMPC
1	92	91	75	74	155	155
2	100	84	88	96	131	152
3	100	96	79	77	135	149
4	93	92	80	77	177	178
5	100	100	74	78	130	137
6	93	85	83	81	150	158
7	100	100	79	70	127	127
8	100	100	79	79	132	132
9	74	71	66	76	174	183
10	90	85	74	76	157	164

Table 9.8: Simulation results for scenario 2 variation 1, using the Dalla-Man et al. model as patient simulator

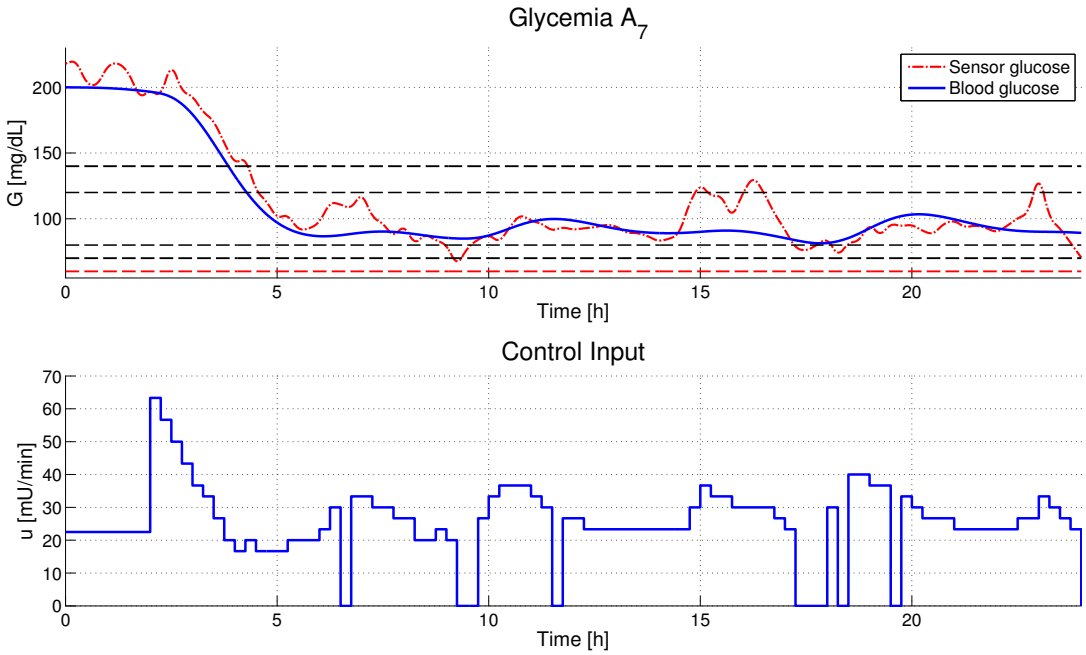

Figure 9.8: Simulation result using SPMPC controller for adult 7 with scenario 1, using the Dalla-Man et al. model as patient simulator

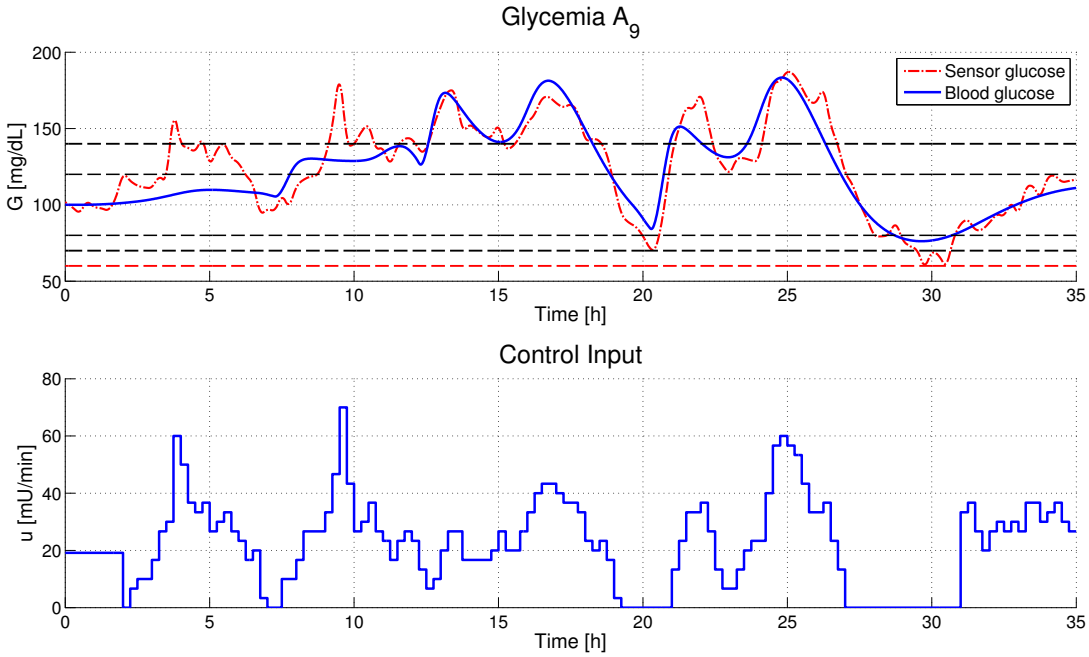

Figure 9.9: Simulation result using SPMPC controller for adult 9 with scenario 2 variation1, using the Dalla-Man et al. model as patient simulator

Variation 2: no bolus injected

The table 9.9 sums up the simulation results for all adults. Once again, for both controller, the results are satisfactory. The poorer results are than in the previous variation of the scenario can be explained by

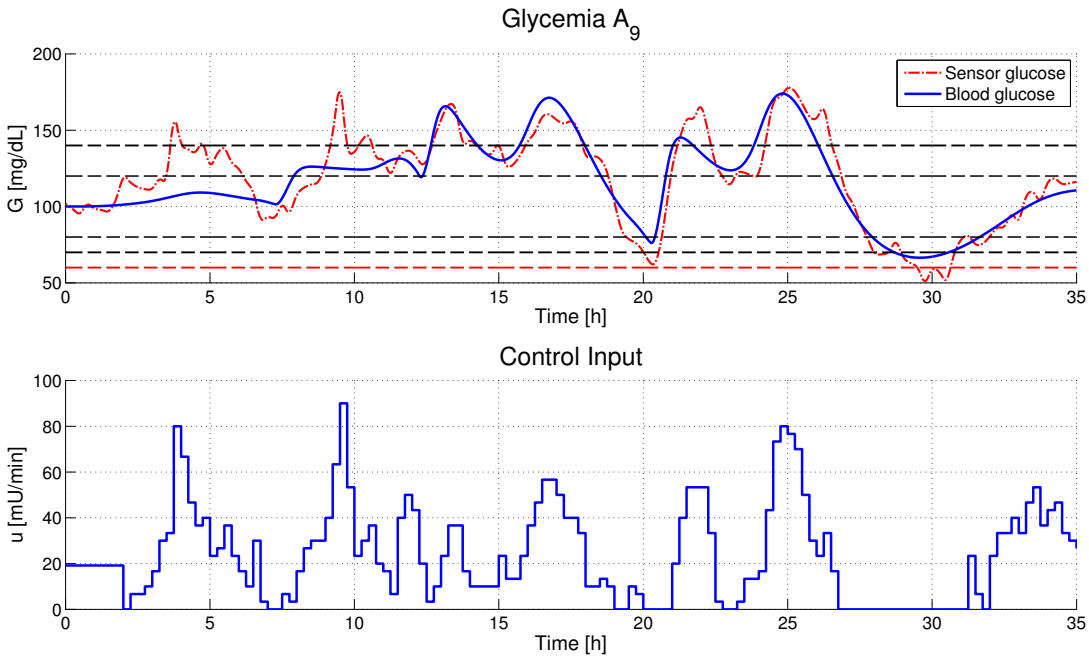

Figure 9.10: Simulation result using NMPC controller for adult 9 with scenario 2 variation1, using the Dalla-Man et al. model as patient simulator

the fact that the controller becomes more sensitive on the quality of the gastro-intestinal sub-model. It is certainly too simple to model a realistic digestion process.

9.5.3 Discussion

Using a more realistic patient model, the controller performances remain satisfactory. The blood glucose is still safely and robustly stabilized. Of course the results are poorer than in the previous part where the virtual patients were given by the control model. This was quite predictable as the Dalla-Man et al. model is a more realistic model of the glucose metabolism and so the predicted blood glucose trajectory were not as accurate as before.

The comparison with the NMPC controller tends to show that the intrinsic robustness of a *simple* predictive controller is sufficient for control purpose when using the testing platform as a virtual patient. However, it has to be noticed that despite the supplementary conservatism of the approach, the SPMPC controller provides nearly equivalent control performances. This motivates our interest in considering this robust approach. Indeed, it is well known that the gap between the testing platform and a real patient is still important. As an example, contrary to what is assumed in the testing platform, a real patient is a time-varying process (e.g. it is subject to the dawn phenomena) and it is not reduced to the sole glucose metabolism. Also, because the controller has to be safe in every circumstances, despite the supplementary complexity, this motivates to consider the design of the robust controller which can guarantee sufficient robustness.

Adult	% $G \in [70;140]$		$\min G$ mg.dL^{-1}		$\max G$ mg.dL^{-1}	
	NMPC	SPMPC	NMPC	SPMPC	NMPC	SPMPC
1	87	85	73	70	164	164
2	94	77	91	102	149	174
3	96	77	73	81	149	166
4	87	86	86	83	217	212
5	93	83	79	83	153	167
6	85	80	89	87	171	188
7	93	95	85	74	151	146
8	98	97	78	78	144	145
9	68	62	68	79	181	196
10	85	75	75	79	179	198

Table 9.9: Simulation results for scenario 2 variation 2, using the Dalla-Man et al. model as patient simulator

9.6 Conclusion

The problem of artificial blood glucose control has been tackled via the design of a SPMPC controller using a modified minimal model of Bergman. As the model possesses a few number of parameters, it has been possible to consider the inter-patient variability by identifying a set of parameters for each virtual patient. The performances of the controller have then been tested on two scenarios. The first one can be considered as an overnight scenario, *i.e.* the controller is only plug to control blood glucose during night. The idea was to test the controller performances against the potentially badly identified parameters, the neglected dynamics and the sensor noise. The second scenario has been used to test the controller performances during a classical day with three meals. The idea was to test if the controller can be combined with a bolus cure. In all cases the controller performances have shown to be satisfactory. Indeed, the blood glucose is safely and robustly stabilized.

These results are particularly interesting as it can be seen that in all cases no hypoglycemia event occurs. Also, the time spent in hyperglycemia is not hazardous for the patients. This tends to show that it is worth considering a SPMPC controller in order to dynamically adjust the basal component of a classical cure. However, this does not mean that the problem of artificial blood glucose control is solved. Indeed, as it has been previously mentioned, it is nearly impossible to model human metabolism, meaning that even the set of realistic virtual patient is not *real* enough. That is why these positive results have to be interpreted under the sole fact that it is worth considering this control approach for some clinical tests with real patients in the loop. It is only after these tests that we can finally conclude on the real interest of using this control methodology.

From a control point of view, because the controller performances are quite good, it is worth considering an extension of the SPMPC control approach to other control problem known to be challenging. This is the objective of the next chapter where it will be investigated, from a numerical point of view, the interest of extending this control approach to control process described by nonlinear uncertain delay differential equations.

Chapter 10

Further Extension on SPMPC

Contents

10.1 Introduction

In the previous chapters, we have considered, from a theoretical and a numerical point of view, the SPMPC controller. It consists in a variation of a classical MPC controller which has been designed to control systems described by nonlinear ordinary differential equation and that need robust control performances in a sampled-data framework. This controller has been tested to solve the problem of artificial blood glucose control and has shown satisfactory performances. This motivates us to consider an extension of this controller to the class of system which are described by nonlinear delay differential equations.

This extension is interesting as it is well known that many engineering phenomenon involve both nonlinearities and time delays, e.g. in the mass transport flow problem. For these systems it is of prime importance to explicitly consider the time delay in the design phase otherwise the time delay factors can lead to poor control performances (see e.g. [103]). On the other hand, in practical systems, uncertainties are really common. They can be caused either by the need to neglect some dynamics to obtain a model of a complex process or the difficulty to identify the parameters of a nonlinear process.

The control of time delay systems has been considered for a long time. This problem is known to be really complex. One reason is that the state belongs to an infinite dimensional space. The available results in this field strongly depend on the structure of the considered system. The field is quite mature for what deals with the problem of robust control of linear time delay system. Many controller originally designed for linear ordinary differential equation have been successfully transposed to control systems described by linear delay differential equation. Thus, it is possible to use, with robust guarantee on the control performances, a minimax approach (see e.g. [81]), a H^{∞} approach (see e.g. [42]) or a robust MPC approach (see e.g. [66] or [25]). These control techniques share the idea of using the LMI framework. As for the nonlinear case, the results are more sparse. This may be because in this case it is more intricate to find an adequate representation in order to *forget* the delay differential equations. Of course, it is always possible to make some assumptions on the system structure such that, by considering a robust design against a given nonlinearity, it becomes possible to use linear control techniques (see e.g. [158]). An other classical idea is to impose some assumptions on the system structure (either on the way the delay appears or on the model structure) in order to use some specific tools (see e.g. [149] or [67]). To consider the control of a more general structure of equations, the extension of the NMPC controller have been considered (see e.g. [44], [134] or [164]). The main issue with these approaches is that they do not ensure theoretical robustness against model uncertainties. Practically, the problem of designing a robust MPC controller for nonlinear time delay systems has rarely been considered. That is why we want to explore the possibility of extending the SPMPC controller to this class of problems.

The objective of this chapter is not to rigorously prove that when using a SPMPC controller it is possible to robustly stabilize a given system subject to delay. We will simply be interested in the numerical implementation of an adjusted version of the SPMPC controller. It is intended to question the interest of this extension in the framework of artificial blood glucose control. Depending on the obtained control performances, the relevance of theoretically extending this control approach will be assessed.

This chapter is organized as follows. First, in order to motivate our extension on a concrete example, we will search for a model of the glucose-insulin metabolism, based on a variation of the modified minimal model of Bergman (6.6), which makes use of nonlinear delay differential equations. The invariance property of this model is studied. Then, assuming that what has been done for NMPC controller for delay differential equation (see e.g. [134]) can be extended to a SPMPC controller, we will adjust the algorithm to compute an adequate final cost and an adequate terminal state constraint presented in chapter 3. Finally, numerical simulations are performed using both the control model and the virtual testing platform for simulation purpose.

10.2 Modeling a type 1 diabetic using delay differential equations

10.2.1 The delay minimal model of Bergman

The objective of this chapter is to formally explore the interest of extending the previously presented SPMPC controller to the control problem of time delay systems. To do so, let us consider the problem of artificial blood glucose control assuming that it is more interesting to model this process using nonlinear delay differential equations.

Let us recall that to describe the action of the blood insulin I on the blood glucose G, the fictitious state X has been introduced (see equation (6.3)). This state is assumed to model the fact that it is not insulin that ensures glucose storage but that insulin only initiates a sequence of action leading to glucose storage. From a control point of view, it may be advantageous to consider a different model to describe this phenomenon. As we are not really interested in modeling the biological phenomenon leading to glucose storage but rather in considering that there is a delay in the insulin action, a possibility is to model this phenomenon using delay differential equations. This leads to model the glucose sub-system as follows

$$\frac{dG}{dt} = -PG - k_0 GI(t-\tau) + D + k_{gr}R_2, \tag{10.1}$$

where P, k_0 and D are positive parameters and τ is a known positive and constant delay.

Also, as previously mentioned, the problem of artificial blood glucose control is concerned with delays in regards to various others aspects, e.g. because of the use of the sub-cutaneous route for both the insulin injection and the glucose measurement [72], [87]. However, practically it is not clear whether these are delays in the control sense or whether it is more some kind of filtering (as it has been assumed in the Dalla Man et al. model). That is why we will continue to model these phenomenon via first order filter. For what deals with the gastro-intestinal sub-model, because it is more difficult to evaluate the interest of introducing delay differential equations to model a digestion process, we will simply keep a simple second order filter.

Finally, the following model of a type 1 diabetic is deduced

$$\begin{aligned}
&\underline{\text{Glucose-insulin sub-model}}:\\
&\frac{dG}{dt} = -PG - k_0 GI(t-\tau) + D + k_{gr}R_2,\\
&\frac{dI}{dt} = -k_f I + b_f U_1,\\
&\frac{dU_1}{dt} = -k_s U_1 + u,\\
&(G,I,U_1)(s) = (G_0,I_0,U_{1,0})(s) \text{for all } s \in [t_0-\tau,t_0],
\end{aligned} \tag{10.2}$$

$$\begin{aligned}
&\underline{\text{Gastro-intestinal sub-model}}:\\
&\frac{dR_2}{dt} = -c_2(R_2 - R_1),\\
&\frac{dR_1}{dt} = -c_1(R_1 - d),\\
&(R_2,R_1)(s) = (R_{2,0},R_{1,0})(s) \text{for all } s \in [t_0-\tau,t_0],
\end{aligned} \tag{10.3}$$

where G_0, I_0, $U_{1,0}$, $R_{2,0}$, $R_{1,0}$ belong to $C([t_0-\tau,t_0],\mathbb{R})$.

In the sequel, we will call the combination of (10.2) and (10.3) the delay minimal model of Bergman

10.2.2 Invariance property

The delay minimal model of Bergman consists in 5 states which are all concentrations or quantities, and so have to remain positive for all time instant. Assuming that the differential equations (10.2) and (10.3) satisfy all the required properties to be integrated, let us find the condition on the parameters and on the control input such that the state of the model keeps their physiological meaning. To obtain the desired result, let us prove the following theorem.

Theorem 5. *Assume that the parameters of the model are given and positive, and for all $t \geq t_0$ the control input $u(t) \in [\underline{u}, \overline{u}]$, and the meal input $d(t) \in [\underline{d}, \overline{d}]$. Then, for a given data $(\underline{G}, \underline{I}, \underline{U}_1, \underline{R}_2, \underline{R}_1) \in \mathbb{R}^{+*} \times \mathbb{R}^+ \times \mathbb{R}^+ \times \mathbb{R}^+ \times \mathbb{R}^+$ and $(\overline{G}, \overline{I}, \overline{U}_1, \overline{R}_2, \overline{R}_1) \in \mathbb{R}^{+*} \times \mathbb{R}^+ \times \mathbb{R}^+ \times \mathbb{R}^+ \times \mathbb{R}^+$ such that*

$$
\begin{aligned}
&(\underline{G}, \underline{I}, \underline{U}_1, \underline{R}_2, \underline{R}_1) \leq (\overline{G}, \overline{I}, \overline{U}_1, \overline{R}_2, \overline{R}_1),\\
&\underline{u} = \frac{k_s k_f}{b_f} \max\left(\frac{b_f}{k_f}\underline{U}_1, \underline{I}, \frac{1}{k_0}\left(-P + \frac{D + k_{gr}\overline{R}_2}{\overline{G}}\right)\right),\\
&\overline{u} = \frac{k_s k_f}{b_f} \min\left(\frac{b_f}{k_f}\overline{U}_1, \overline{I}, \frac{1}{k_0}\left(-P + \frac{D + k_{gr}\underline{R}_2}{\underline{G}}\right)\right)\\
&\underline{d} = \max\left(\underline{R}_1, \underline{R}_2\right),\\
&\overline{d} = \min\left(\overline{R}_1, \overline{R}_2\right),\\
&0 \leq \underline{u} \leq \overline{u},\\
&0 \leq \underline{d} \leq \overline{d},\\
&\frac{1}{k_0}\left(-P + \frac{D + k_{gr}\overline{R}_2}{\overline{G}}\right) \leq \underline{I} \leq \overline{I} \leq \frac{1}{k_0}\left(-P + \frac{D + k_{gr}\underline{R}_2}{\underline{G}}\right)
\end{aligned}
$$

we have that, if for all $s \in [t_0 - \tau, t_0]$ $(\underline{G}, \underline{I}, \underline{U}_1, \underline{R}_2, \underline{R}_1) \leq (G, I, U_1, R_2, R_1)(s) \leq (\overline{G}, \overline{I}, \overline{U}_1, \overline{R}_2, \overline{R}_1)$ then for all $t \geq t_0$ $(\underline{G}, \underline{I}, \underline{U}_1, \underline{R}_2, \underline{R}_1) \leq (G, I, U_1, R_2, R_1)(t) \leq (\overline{G}, \overline{I}, \overline{U}_1, \overline{R}_2, \overline{R}_1)$.

Proof. The proof is the same as for the theorem 4. Thus let us simply consider the state G.

For this, let us consider $\tilde{G} = G - \underline{G}$ and $\tilde{G}^- = \max(0, -\tilde{G})$, using the differential equation on G we have:

$$
\int_{t_0}^{t} \frac{1}{2}\frac{d|\tilde{G}^-|^2}{dt} ds = \int_{t_0}^{t} -(P + k_0 I(s-\tau))|\tilde{G}^-|^2 - (-(P + k_0 I(s-\tau))\underline{G} + D + k_{gr} R_2)\tilde{G}^- ds. \tag{10.4}
$$

According to the positivity of the parameters and the assumptions on the initial condition $(\underline{I}, \underline{R}_2) \leq (I, R_2)(s)$ for all $s \in [t_0 - \tau, t_0]$, on the meal input $\underline{d} \leq d$ and on the control input $u \geq \frac{k_s k_f}{b_f}\underline{I}$, it is deduced that

$$
\int_{t_0}^{t} \frac{1}{2}\frac{d|\tilde{G}^-|^2}{dt} ds \leq \int_{t_0}^{t} -(-(P + k_0 I(s-\tau))\underline{G} + D + k_{gr}\underline{R}_2)\tilde{G}^- ds. \tag{10.5}
$$

Since $u \leq \frac{k_s k_f}{b_f k_0}\left(-P + \frac{D + k_{gr}\underline{R}_2}{\underline{G}}\right)$ and $\overline{I} \leq \frac{1}{k_0}\left(-P + \frac{D + k_{gr}\underline{R}_2}{\underline{G}}\right)$, as the parameters are positive, it is deduced for all $s \geq t_0$

$$
I(s-\tau) \leq \frac{1}{k_0}\left(-P + \frac{D + k_{gr}\underline{R}_2}{\underline{G}}\right). \tag{10.6}
$$

So, using inequality (10.5), we have

$$
\int_{t_0}^{t} \frac{1}{2}\frac{d|\tilde{G}_1^-|^2}{dt} ds \leq 0 \tag{10.7}
$$

and then

$$0 \leq |\tilde{G}_1^-|^2(t) \leq |\tilde{G}_1^-|^2(t_0). \tag{10.8}$$

As $G(t_0) \geq \underline{G}$, this implies that $|\tilde{G}^-|^2(t_0) = 0$ and then $G(t) \geq \underline{G}$ for all $t \geq t_0$. Using the same method we can deduce that $G(t) \leq \overline{G}$, for all $t \geq t_0$. □

Remark 11. Using this theorem it is straightforward to show that the states remain in $\mathbb{R}^{+*} \times \mathbb{R}^+ \times \mathbb{R}^+ \times \mathbb{R}^+ \times \mathbb{R}^+$ if the parameters of the model are positive and if the inputs are such that $d \geq 0$ and $u \geq 0$.

10.2.3 Control problem

In this part let us present the disturbed model that will be used for control purpose.

In order to consider the same control problem as for the ordinary differential case, in the sequel it is assumed that the meal consumption profile d and the initial condition $(R_2, R_1)(s)$ for all $s \in [t_0 - \tau, t_0]$ are known and given. So, as for what has been done in chapter 7, it is possible to integrate (10.3) to obtain the state trajectory $R_2(t)$. Let us call $R_a(t) = k_{gr} R_2(t)$ the rate of appearance. Then, for control purpose we consider the following model

$$\begin{aligned}
&\frac{dG}{dt} = -PG - k_0 GI(t-\tau) + D + R_a,\\
&\frac{dI}{dt} = -k_f I + b_f U_1,\\
&\frac{dU_1}{dt} = -k_s U_1 + u,\\
&(G, I, U_1)(s) = (G_0, I_0, U_{1,0})(s) \text{for all } t \in [t_0 - \tau, t_0],
\end{aligned} \tag{10.9}$$

The *nominal model* corresponds to (10.9) where all the parameters are assumed to be perfectly known. The trajectory generated by the nominal model for a given initial condition, a given rate of appearance profile $R_a(t)$ and a given insulin flow $u(t)$ is called *nominal trajectory*.

To obtain the variational problem, we begin to write the nominal model when disturbed both in states and parameters. This leads to the following disturbed system

$$\begin{aligned}
\frac{d(x_1+G)}{dt} &= -(\overline{p}+P)(x_1+G) - (\overline{k}_0 + k_0)(x_1+G)(x_2(t-\tau) + I(t-\tau))\\
&\quad + D + (R_a + r_a),\\
\frac{d(x_2+I)}{dt} &= -(\overline{k}_f + k_f)(x_2+I) + (\overline{b}_f + b_f)(x_3+U_1),\\
\frac{d(x_3+U_1)}{dt} &= -(\overline{k}_s + k_s)U_1 + (u+f),\\
(x_1+G, x_2+I, x_3+U_1)(s) &= \xi_s(s) + (G_0, I_0, U_{1,0})(s)\ \forall t \in [t_0 - \tau, t_0],
\end{aligned} \tag{10.10}$$

where $\xi_s \in \mathscr{C}([t_0 - \tau, t_0], \mathbb{R}^3)$. The control input f is a disturbance of the control input u. It has been introduced in order to reject the state disturbances $(x_i)_{i\in 1,2,3}$ despite the parameters disturbances $\overline{p}$, $\overline{k}_0$, $\overline{k}_f$, $\overline{b}_f$ and $\overline{k}_s$ and the disturbance of the rate of appearance r_a.

To obtain the control model, let us subtract the nominal model (10.9) from the previous disturbed

model

$$\begin{aligned}
\frac{dx_1}{dt} &= -\overline{p}(x_1+G) - \overline{k}_0(x_1+G)(x_2(t-\tau)+I(t-\tau)) \\
&\quad -(P+k_0I(t-\tau))x_1 - k_0Gx_2(t-\tau) - k_0x_1x_2(t-\tau) + r_a, \\
\frac{dx_2}{dt} &= -\overline{k}_f(x_2+I) + \overline{b}_f(x_3+U_1) - k_fx_2 + b_fx_3, \\
\frac{dx_3}{dt} &= -\overline{k}_s(x_3+U_1) - k_sx_3 + f, \\
(x_1,x_2,x_3)(s) &= \xi_s(s)\ \forall s \in [t_0-\tau, t_0].
\end{aligned} \tag{10.11}$$

In the sequel let us consider how the final cost and the terminal state constraint have to be adjusted in order to obtain a stable closed-loop when controlling time delay systems with a SPMPC controller.

10.3 On the final cost and the terminal state constraint

10.3.1 Context

As mentioned in [140], the control of time delay systems remains extremely challenging. This may explain the numerous issue when it comes to design a stable model predictive controller for nonlinear time delay systems despite the relative simple formulation of the corresponding control problem. Lately, it seems that it is possible to adjust the tools used for the usual NMPC (see e.g. [43] or [134]). The idea behind these results is to introduce a final cost and a terminal state constraint which share the same meanings as for the usual ordinary differential case. Namely the final cost is interpreted as a local Lyapunov function and the terminal set is a positive control invariant set. If the idea is simple, its application is more intricate. Indeed, in the delay differential case, there are several formulation of the Lyapunov theorem (e.g. we can use either Krasovskii or Razumikhin functional with a delay dependent or independent criteria, see e.g.[65]) leading to as many possibilities to express the final cost problem. This is at the origin of some difficulties as it is not easy to choose the representation which provides the best balance between simplicity and conservatism in the result. An other difficulty comes from the fact that, as we consider an infinite dimensional space, it is not straightforward to build the terminal state constraint. Indeed, classically in the ordinary differential case, the terminal state constraint is defined as a level set of the final cost. However for infinite dimensional system, we are not sure that a level set of the final cost provides a compact, closed and bounded subset, and so this means that this latter has to be defined cautiously.

In the sequel we consider time delay systems which are given as follows

$$\begin{aligned}
\frac{dx}{dt} &= \mathscr{G}(x, x(t-\tau), u, w), \\
x(s) &= \phi(s),\ \forall s \in [t_0-\tau, t_0],
\end{aligned} \tag{10.12}$$

where $\tau \in \mathbb{R}^{+*}$ is a known constant delay, $\mathscr{G}$ is assumed to satisfy all the necessary assumptions in order to provide forward complete trajectory and $\phi \in C([t_0-\tau, t_0])$ is the initial condition. The control input u and the disturbances w are such that

$$U(I) = \{u \in L^2(I),\ \|u(t)\| \leq u_M\ a.e.\ t \in I\}, \tag{10.13}$$

$$W(I) = \{w \in L^2(I),\ \|w(t)\| \leq w_M\ a.e.\ t \in I\}, \tag{10.14}$$

where u_M and w_M are known constants belonging to $\mathbb{R}^{+*}$ and I is an interval of length T.

For all $t \geq t_0$, for all $x \in C([t-\tau,t],\mathbb{R}^{n_x})$, in order to simplify the notation, we introduce the segment $x_t \in C([-\tau,0],\mathbb{R}^{n_x})$ which is defined by

$$x_t(s) = x(t+s) \text{ for all } s \in [-\tau,0]. \tag{10.15}$$

To solve the robust control problem, it is intended to design a SPMPC controller given by the solution of the following optimization problem

$$\begin{aligned}(u_0^*,w_0^*) = \arg\inf_{u\in U}\sup_{w\in W} J^{t_0}(u,w) = \arg\sup_{w\in W}\inf_{u\in U} J^{t_0}(u,w),\\ s.t.\ x_{t_0+T}(\phi,u,w,t_0;.) \in \Omega_a^{f_E}.\end{aligned} \tag{10.16}$$

where U and W denote $U([t_0;t_0+T])$ and $W([t_0;t_0+T])$ and $J^{t_0}(u,w)$ is defined as:

$$J^{t_0}(u,w) = E(x_{t_0+T}(\phi,u,w,t_i;.)) + \int_{t_0}^{t_0+T} F(x(\phi,u,w,t_0;s),u,w)ds, \tag{10.17}$$

where $E : C([-\tau,0],\mathbb{R}^{n_x}) \to \mathbb{R}^+$ and $F : \mathbb{R}^{n_x}\times\mathbb{R}^{n_u}\times\mathbb{R}^{n_w} \to \mathbb{R}$.

The objective of this chapter is not to prove that the SPMPC controller provides a stabilizing controller for time delay systems but only to present algorithms which can be used to compute an adequate final cost and terminal state constraint. The idea is to adjust assumptions 7 and 8, according to the assumptions needed to provide a stable NMPC controller for delay differential equation (DDE) (see e.g. [135]), to provide a *supposedly* stable SPMPC controller.

10.3.2 Conjecture on the adjustment of the assumptions

As previously mentioned, we assume that the SPMPC controller can provide a stable controller by simply extending the result of chapter 3 and what has been done for DDE with NMPC controller (see e.g. [135]). So, to formulate the problem of computing an adequate final cost and terminal state constraint which can be used to build a (supposedly) stable controller, we will consider the following adjusted assumptions.

Assumption 10. For all $t \geq t_0$, there exists $\Omega_a^{f_E}(t) \subset C([-\tau,0],\mathbb{R}^{n_x})$, a RCPI set associated with the feedback f_E, which is such that for all $y \in \Omega_a^{f_E}(t)$ we have $\|f_E(y)\| \leq u_M$.

Assumption 11. There exists a quadratic Lyapunov Krasovskii functional $E : C([-\tau,0],\mathbb{R}^{n_x}) \to \mathbb{R}^+$ (see e.g. [65])

$$\begin{aligned}E(y) = y(0)^T P y(0) + 2y(0)^T \int_{-\tau}^{0} Q(s)y(s)ds\\ + \int_{-\tau}^{0}\left(\int_{-\tau}^{0} y(s)^T R(s,\eta)y(\eta)d\eta\right)ds + \int_{-\tau}^{0} y(s)^T S(s)y(s)ds,\end{aligned}$$

where P, Q R and S are defined as in [65], such that for all $y \in \Omega_a^{f_E}(t)$ and for all $w \in W$ we have:

$$\begin{aligned}&2y(0)^T P\mathscr{G}(y(0),y(-\tau),f_E(y),w) + 2\mathscr{G}(y(0),y(-\tau),f_E(y),w)^T \int_{-\tau}^{0} Q(s)y(s)ds\\ &+2y(0)^T\left(Q(0)y(0) - Q(-\tau)y(-\tau) - \int_{-\tau}^{0}\frac{dQ}{ds}(s)y(s)ds\right)\\ &+2\left(y(0)^T\int_{-\tau}^{0} R(0,\eta)y(\eta)d\eta - y(-\tau)^T\int_{-\tau}^{0} R(-\tau,\eta)y(\eta)d\eta\right)\\ &-\int_{-\tau}^{0}\int_{-\tau}^{0} y(s)^T\left(\frac{\partial R}{\partial s}(s,\eta) + \frac{\partial R}{\partial \eta}(s,\eta)\right)y(\eta)d\eta ds\\ &+y(0)^T S(0)y(0) - y(-\tau)^T S(-\tau)y(-\tau) - \int_{-\tau}^{0} y(s)^T\frac{dS}{ds}(s)y(s)ds \leq -F(y(0),f_E(y),w).\end{aligned} \tag{10.18}$$

Remark 12. For simplicity reasons we have assumed that the final cost is given by a quadratic Lyapunov Krasovskii functional. It is also possible to use more general formulation. In this case the left hand side of (10.18) has to be understood as the derivatives of the final cost along a state trajectory.

10.3.3 Algorithm to compute a final cost and a terminal state constraint for DDE

Formulation of the final cost and terminal state constraint problem

To design a final cost and a terminal state constraint according to assumptions 10 and 11, we will formulate the final cost problem using a Lyapunov Krasovskii functional and then we will determine an adequate terminal state constraint problem using Razumikhin arguments.

As for the ordinary differential equation case, the stage cost F is assumed to be given quadratic (3.74). Furthermore we assume that a local PLDI embedding of (10.12) is possible, e.g. by assuming that $\mathscr{G}$ satisfies assumption 4.

The final cost and the final controller

To compute the final cost and the final controller, we will use a local polytopic linear differential inclusion embedding of (10.12). The final controller f_E will be chosen as a memory linear state feedback and the final cost E will be searched as a quadratic Lyapunov Krasovskii functional:

$$\begin{aligned} f_E(y) &= K_0 y(0) + K_1 y(-\tau), \\ E(y) &= y(0)^T S_1 y(0) + \int_{-\tau}^{0} y(s)^T S_2 y(s) ds, \end{aligned} \tag{10.19}$$

where $y \in C([-\tau,0],\mathbb{R}^{n_x})$, $K_0 \in \mathbb{R}^{n_x,n_u}$ and $K_1 \in \mathbb{R}^{n_x,n_u}$. The matrices $S_1 \in \mathbb{R}^{n_x,n_x}$ and $S_2 \in \mathbb{R}^{n_x,n_x}$ are symmetric definite positive.

Remark 13. From a theoretical point of view, it would have been more advantageous to express the final cost as a complete quadratic Lyapunov Krasovskii and to choose the following final controller $f_E(y) = K_0 y(0) + \int_{-\tau}^{0} K(s) y(s) ds$, however from a numerical point of view, the retained form are better. Also, as for the ordinary differential case, it is more desirable to work with a convex hull Lyapunov functional (see e.g. [21]). But, for simplicity reasons, we will focus on the problem of searching for a common Lyapunov functional which is valid on the complete PLDI.

The aim of this part is to use a PLDI embedding in order to formulate the problem of computing a final controller f_E and a final cost E which satisfy assumption 11 in the LMI framework. Let us assume that such an embedding is available. Then, we have that (10.12) is contained in the following differential inclusion

$$\frac{dx}{dt} \in \text{co}\{A_{0,i}x_t(0) + A_{1,i}x_t(-\tau) + B_{1,i}w + B_{2,i}u,\ i \in \{1,\dots,N\}\}, \tag{10.20}$$

where co$\{.\}$ denotes the convex hull of a set and $N > 0$ is the number of vertices of the PLDI. The matrices $A_{0,i}$, $A_{1,i}$, $B_{1,i}$ and $B_{2,i}$ are given and constant.

As we consider a PLDI it is possible to express $\dfrac{dx}{dt}$ as follows

$$\frac{dx}{dt} = \sum_{i=1}^{N} \beta_i(t) \left(A_{0,i}x_t(0) + A_{1,i}x_t(-\tau) + B_{1,i}w + B_{2,i}u\right), \tag{10.21}$$

where for all $t \geq t_0$ and for all i we have $\beta_i(t) \geq 0$ and $\sum_{i=1}^{N} \beta_i(t) = 1$.

According to the retain form of the final cost and of the final controller (10.19) and to the previous expression of the state derivative, we have the inequality (10.18) becomes

$$\begin{aligned}\sum_{i=1}^{N} \beta_i(t) &(2x_t(0)^T S_1((A_{0,i}+B_{2,i}K_0)x_t(0)+(A_{1,i}+B_{2,i}K_1)x_t(-\tau)+B_{1,i}w) \\ &+ x_t(0)^T S_2 x_t(0) - x_t(-\tau)^T S_2 x_t(-\tau) \\ &+ x_t(0)^T R x_t(0) + (K_0 x_t(0)+K_1 x_t(-\tau))^T \alpha (K_0 x_t(0)+K_1 x_t(-\tau)) - w^T Q w) \leq 0.\end{aligned} \tag{10.22}$$

Inequality (10.22) has to hold everywhere on the PLDI. This implies that this inequality holds if and only if it holds for all family of $(\beta_i)_{i\in\{1,\ldots,N\}}$. So for all $i \in \{1,\ldots,N\}$ we have to solve in S_1, S_2, K_0 and K_1 the following inequalities

$$\begin{aligned}2x_t(0)^T S_1&((A_{0,i}+B_{2,i}K_0)x_t(0)+(A_{1,i}+B_{2,i}K_1)x_t(-\tau)+B_{1,i}w) \\ &+ x_t(0)^T S_2 x_t(0) - x_t(-\tau)^T S_2 x_t(-\tau) \\ &+ x_t(0)^T R x_t(0) + (K_0 x_t(0)+K_1 x_t(-\tau))^T \alpha (K_0 x_t(0)+K_1 x_t(-\tau)) - w^T Q w \leq 0.\end{aligned} \tag{10.23}$$

Using matrix notation, the previous inequalities becomes:

$$\begin{pmatrix} x_t(0) \\ x_t(-\tau) \\ w \end{pmatrix}^T \left(\begin{pmatrix} 2S_1(A_{0,i}+B_{2,i}K_0)+S_2 & S_1(A_{1,i}+B_{2,i}K_1) & S_1B_{1,i} \\ \star & -S_2 & 0 \\ \star & \star & -Q \end{pmatrix} + \begin{pmatrix} K_0^T\alpha K_0+R & K_0^T\alpha K_1 & 0 \\ \star & K_1^T\alpha K_1 & 0 \\ \star & \star & 0 \end{pmatrix} \right) \begin{pmatrix} x_t(0) \\ x_t(-\tau) \\ w \end{pmatrix} \leq 0. \tag{10.24}$$

As for what has been done in chapter 3, in order to use the LMI framework, let us introduce the following factorization

$$\begin{pmatrix} K_0^T\alpha K_0+R & K_0^T\alpha K_1 \\ \star & K_1^T\alpha K_1 \end{pmatrix} = \begin{pmatrix} R^{\frac{1}{2}} & K_0^T\alpha^{\frac{1}{2}} \\ 0 & K_1^T\alpha^{\frac{1}{2}} \end{pmatrix} \begin{pmatrix} I_{n_x} & 0 \\ 0 & I_{n_u} \end{pmatrix} \begin{pmatrix} R^{\frac{1}{2}} & 0 \\ \alpha^{\frac{1}{2}}K_0 & \alpha^{\frac{1}{2}}K_1 \end{pmatrix}. \tag{10.25}$$

Using the Schur complement, inequality (10.24) can be rewritten as follows

$$D_i = \begin{pmatrix} 2A_{0,i}\overline{S}_1+2B_{2,i}Y_0+\overline{S}_2 & A_{1,i}\overline{S}_1+B_{2,i}Y_1 & B_{1,i} & \overline{S}_1R^{\frac{1}{2}} & Y_0^T\alpha^{\frac{1}{2}} \\ \star & -\overline{S}_2 & 0 & 0 & Y_1^T\alpha^{\frac{1}{2}} \\ \star & \star & -Q & 0 & 0 \\ \star & \star & \star & -I_{n_x} & 0 \\ \star & \star & \star & \star & -I_{n_u} \end{pmatrix} \leq 0, \tag{10.26}$$

where $\overline{S}_1 = S_1^{-1}$, $\overline{S}_2 = S_1^{-1}S_2S_1^{-1}$, $Y_0 = K_0S_1^{-1}$ and $Y_1 = K_1S_1^{-1}$.

Thus, the problem of computing a final cost and a final controller is solved if the following LMI admits a solution in S_1, S_2, K_0 and K_1

$$\operatorname{diag}(D_1,\ldots,D_N) \leq 0. \tag{10.27}$$

The terminal state constraint

At that point we have computed a final controller and a final cost which satisfy assumption 11. Now we can provide an algorithm to compute a robust control positive invariant set $\Omega_a^{f_E}(t)$ under the final controller f_E which satisfies assumption 10. This set will be expressed using Razumikhin like arguments. That is, we search for a terminal state constraint which can be expressed as follows

$$\Omega_a^{f_E}(t_0+T) = \{x_{t_0+T} \in C([-\tau,0],\mathbb{R}^{n_x}) / \max_{\theta\in[-\tau;0]} x_{t_0+T}(\theta)^T P_0 x_{t_0+T}(\theta) \leq \gamma\}. \tag{10.28}$$

For simplicity, in the sequel, we denote $\Omega_a^{f_E} = \Omega_a^{f_E}(t_0+T)$.

To determine an adequate terminal state constraint, we have to find a symmetric definite positive matrix P_0 and a positive constant γ such that the set $\Omega_a^{f_E}$ is robust control positive invariant when using the final controller f_E. To solve this problem, we will use a PLDI embedding and a first order transformation. The idea behind this transformation is to use an equivalent formulation of $x_t(-\tau)$. The positive invariant set is then searched on a system which use this new formulation. It is important to see that such an approach is valid because the terminal state constraint is determined independently of the initial condition of the differential equation. The interest of this transform is that we will consider a delay-dependent stability test meaning that the result is less conservative.

Before further proceeding, let us recall how this transformation works (for more details see e.g. [65] or [104] and the references therein). We have

$$x_t(-\tau) = x_t(0) - \int_{-\tau}^{0} \mathscr{G}(x_t(s), x_t(s-\tau), u_t(s), w_t(s))ds. \tag{10.29}$$

Using the previous equation to substitute the term $x_t(-\tau)$ in the system (10.12), we introduce the following system

$$\begin{aligned} &\frac{d\xi}{dt} = \mathscr{G}\left(\xi(t), \xi(t) - \int_{-\tau}^{0} \mathscr{G}(\xi(t+s), \xi(t+s-\tau), u(t+s), w(t+s))ds, u(t), w(t)\right), \\ &\xi(s) = \psi(s),\ \forall s \in [t_0-2\tau, t_0]. \end{aligned} \tag{10.30}$$

Then, the idea is to look for stability results on this new system independently of the initial condition ψ. Indeed, if conditions are found that prove stability on this system, then the original system is also stable. However, this is very important to see that the two systems are not equivalent. Practically, this implies that if we can not prove the stability of the transformed system then this does not imply that the original system is unstable.

Let us use the first order transformation on the PLDI embedding of the system (10.21). We have:

$$\begin{aligned} \frac{d\xi}{dt} = &\sum_{i=1}^{N} \beta_i(t)((A_{0k,i} + A_{1k,i})\xi(t) + B_{1,i}w(t) \\ &- A_{1k,i}\int_{-\tau}^{0} A_{0k,i}\xi(t+s) + A_{1k,i}\xi(t+s-\tau) + B_{1,i}w(t+s)ds), \\ \xi(s) = &\psi(s),\ \forall s \in [t_0-2\tau, t_0], \end{aligned} \tag{10.31}$$

where $A_{0k,i} = A_{0,i} + B_{2,i}K_0$ and $A_{1k,i} = A_{1,i} + B_{2,i}K_1$ where K_0 and K_1 are the previously computed gain and $w \in W$.

Let us define the following Razumikhin candidate:

$$V(\xi) = \xi^T P_0 \xi, \tag{10.32}$$

where P_0 is a symmetric definite positive matrix.

To solve the terminal state constraint problem, we have to find a matrix P_0 such that the previous candidate is a Lyapunov function (in the Razumikhin sense) everywhere on the PLDI. In particular, this implies that this candidate has to be a Lyapunov function at each vertex. Let us consider the i^{th} vertex of the PLDI. In this case, the derivative of V along a state trajectory is given as follows

$$\frac{d}{dt}(V(\xi)) = \begin{pmatrix}\xi(t)\\ w(t)\end{pmatrix}^T \begin{pmatrix}2P_0(A_{0k,i}+A_{1k,i}) & P_0B_{1,i}\\ B_{1,i}^TP_0 & 0\end{pmatrix}\begin{pmatrix}\xi(t)\\ w(t)\end{pmatrix} + \eta_1+\eta_2+\eta_3, \tag{10.33}$$

where

$$\begin{aligned}\eta_1 &= -2\xi(t)^TP_0A_{1k,i}\int_{-\tau}^0 A_{0k,i}\xi(t+s)ds,\\ \eta_2 &= -2\xi(t)^TP_0A_{1k,i}\int_{-\tau}^0 A_{1k,i}\xi(t+s-\tau)ds,\\ \eta_3 &= -2\xi(t)^TP_0A_{1k,i}\int_{-\tau}^0 B_{1,i}w(t+s)ds,\end{aligned} \tag{10.34}$$

We remind that for any symmetric definite positive matrix $S\in\mathbb{R}^{n,n}$ and for all $v_1,v_2\in\mathbb{R}^n$, we have:

$$-2v_1^Tv_2 \le v_1^TS^{-1}v_1 + v_2^TSv_2. \tag{10.35}$$

Using the previous inequality, it is deduced that η_1 can be upper-bounded

$$\eta_1 \le \tau\xi(t)^T\left(P_0(A_{1k,i}A_{0k,i})P_1^{-1}(A_{1k,i}A_{0k,i})^TP_0\right) + \int_{-\tau}^0 \xi(t+s)^TP_1\xi(t+s)ds, \tag{10.36}$$

where P_1 is chosen definite symmetric positive with the supplementary constraint that we have

$$P_1 - P_0 \le 0. \tag{10.37}$$

In particular, this implies that for all $v\in\mathbb{R}^{n_x}$ we have $v^TP_1v \le v^TP_0v$. So, it is deduced from (10.36) that

$$\eta_1 \le \tau\xi(t)^T\left(P_0(A_{1k,i}A_{0k,i})P_1^{-1}(A_{1k,i}A_{0k,i})^TP_0\right) + \int_{-\tau}^0 \xi(t+s)^TP_0\xi(t+s)ds. \tag{10.38}$$

Before further proceeding, let us recall that a function V is a Lyapunov Razumikhin function if it is such that (see e.g. [65])

$$\frac{d}{dt}(V(\xi)) \le 0 \tag{10.39}$$

whenever there exists $\rho\ge 1$ such that for all $\theta\in[-2\tau;0]$:

$$V(\xi(t+\theta)) \le \rho V(\xi(t)). \tag{10.40}$$

According to what is done in ([135]), let us consider the sign of $\frac{d}{dt}(V(\xi))$ in case the condition given by (10.40) holds. In this case, using (10.38), we have

$$\eta_1 \le \tau\xi(t)^T\left(P_0(A_{1k,i}A_{0k,i})P_1^{-1}(A_{1k,i}A_{0k,i})^TP_0 + \rho P_0\right)\xi(t). \tag{10.41}$$

Let us introduce $\gamma_1>0$ and $0<P_2\le P_0$. Then, using the same arguments as for η_1, we have

$$\begin{aligned}\eta_2 &\le \tau\xi(t)^T\left(P_0(A_{1k,i}A_{1k,i})P_2^{-1}(A_{1k,i}A_{1k,i})^TP_0 + \rho P_0\right)\xi(t),\\ \eta_3 &\le \tau\xi(t)^T\left(\frac{1}{\gamma_1}P_0(A_{1k,i}B_{1,i})(A_{1k,i}B_{1,i})^TP_0\right)\xi(t) + \gamma_1\int_{-\tau}^0 w(t+s)^Tw(t+s)ds,\end{aligned} \tag{10.42}$$

Since the disturbances are given bounded for all t, we have

$$\|w\|^2 \leq w_M^2.$$

Then, according to Razumikhin-like arguments (see e.g. [65] and [45]), a sufficient condition to formulate $\Omega_a^{f_E}$ is given by the following condition on V

$$\frac{d}{dt}\left(V(\xi)\right) \leq 0 \text{ if } V(\xi) \geq \gamma, \text{ and } \|w\|^2 \leq w_M^2. \tag{10.43}$$

To solve (10.43), we will use the S-procedure (see e.g. [19]). To do so, let us introduce the following variable:

$$\Delta\xi = \frac{d}{dt}\left(V(\xi)\right) + \lambda_1(V(\xi) - \gamma) + \lambda_2(w_M^2 - w^T w), \tag{10.44}$$

where λ_1 and λ_2 are positive chosen constants. The problem of interest admits a solution if we have $\Delta\xi \leq 0$.

Assume that for a given γ, it is possible to choose the constants λ_1 and λ_2 such that we have:

$$-\lambda_1\gamma + (\tau\gamma_1 + \lambda_2)w_M^2 \leq 0 \tag{10.45}$$

Then it is deduced that we have:

$$\begin{aligned}\Delta\xi \leq & \begin{pmatrix}\xi(t)\\ w(t)\end{pmatrix}^T \begin{pmatrix}2P_0(A_{0k,i}+A_{1k,i}) + (\lambda_1 + 2\tau\rho)P_0 & P_0B_{1,i}\\ B_{1,i}^T P_0 & -\lambda_2 I_{n_w}\end{pmatrix}\begin{pmatrix}\xi(t)\\ w(t)\end{pmatrix}\\ & + \tau\xi(t)^T(P_0(A_{1k,i}A_{0k,i})P_1^{-1}(A_{1k,i}A_{0k,i})^T P_0)\xi(t)\\ & + \tau\xi(t)^T(P_0(A_{1k,i}A_{1k,i})P_2^{-1}(A_{1k,i}A_{1k,i})^T P_0)\xi(t)\\ & + \tau\xi(t)^T\left(\frac{1}{\gamma_1}P_0(A_{1k,i}B_{1,i})(A_{1k,i}B_{1,i})^T P_0\right)\xi(t).\end{aligned} \tag{10.46}$$

Let us introduce the following factorization

$$\begin{aligned}&\tau P_0(A_{1k,i}A_{0k,i})P_1^{-1}(A_{1k,i}A_{0k,i})^T P_0 + \tau P_0(A_{1k,i}A_{1k,i})P_2^{-1}(A_{1k,i}A_{1k,i})^T P_0\\ &+ \frac{\tau}{\gamma_1}P_0(A_{1k,i}B_{1,i})(A_{1k,i}B_{1,i})^T P_0 = MN^{-1}M^T,\end{aligned} \tag{10.47}$$

where

$$\begin{aligned}M &= \begin{pmatrix}\tau P_0 A_{1k,i}A_{0k,i} & \tau P_0 A_{1k,i}A_{1k,i} & \tau P_0 A_{1k,i}B_{1,i}\end{pmatrix},\\ N^{-1} &= \begin{pmatrix}\frac{1}{\tau}P_1^{-1} & 0 & 0\\ 0 & \frac{1}{\tau}P_2^{-1} & 0\\ 0 & 0 & \frac{1}{\tau\gamma_1}I_{n_w}\end{pmatrix}.\end{aligned} \tag{10.48}$$

Using the Schur complement, it is finally deduced that we have $\Delta\xi \leq 0$, if there exist P_0, P_1, P_2 and γ_1 such that:

$$\begin{aligned}&N_i = \begin{pmatrix}\mathscr{M}_i(P_0) & P_0B_{1,i} & \tau P_0A_{1k,i}A_{0k,i} & \tau P_0A_{1k,i}A_{1k,i} & \tau P_0A_{1k,i}B_{1,i}\\ \star & -\lambda_2 I_{n_w} & 0 & 0 & 0\\ \star & \star & -\tau P_1 & 0 & 0\\ \star & \star & \star & -\tau P_2 & 0\\ \star & \star & \star & \star & -\tau\gamma_1 I_{n_w}\end{pmatrix} \leq 0,\\ &P_1 > 0,\ P_2 > 0,\ \gamma_1 > 0,\\ &P_1 \leq P_0,\ P_2 \leq P_0,\end{aligned} \tag{10.49}$$

where $\mathscr{M}_i(P_0) = 2P_0(A_{0k,i} + A_{1k,i}) + (\lambda_1 + 2\tau\rho)P_0$.

Finally, to solve the terminal state constraint problem, we have to solve the previous LMIs for all $i \in \{1,\dots,N\}$, that is

$$\begin{aligned} &\operatorname{diag}(N_1,\dots,N_N) \leq 0, \\ &P_1 > 0,\ P_2 > 0,\ \gamma_1 > 0, \\ &P_1 \leq P_0,\ P_2 \leq P_0, \end{aligned} \tag{10.50}$$

10.4 Numerical implementation

At that point, we have formally presented what has to be adjusted in order to use a SPMPC controller to control time delay systems. Also, in order to consider the delay in the insulin action, we have modeled the glucose metabolism using delay differential equations (10.2). The next step will consist in considering the numerical implementation issues (e.g. the issue of estimating the state value of the system). In order to integrate the various state trajectories we will use the *dde23* command in Matlab (see e.g. [88]).

This section will be organized as follows. First, we will present a state observer for DDE system whose aim is to estimate the value of the state of the system, for all $t \in [t_k - \tau, t_k]$, each time a new measure is made available. Then, in order to use the numerical methods presented in chapter 4, we will present the adjoint model and the derivatives of the criterion to solve both the identification problem and the control problem. Finally, numerical simulations, using both the control model and the virtual patient testing platform, will be performed.

10.4.1 Observer

An EKF filter for DDE

The problem of state estimation is of prime importance especially when considering predictive control technique. In the ODE case, this problem was not too much trouble as many observers exist. In the DDE case this problem is more intricate. One of the reason is that in this case the state evolves in a functional space.

In order to estimate the state value of (10.2) on the basis of the measurement of the blood glucose G, we will *extend* the work of [128]. This work deals with an adjustment of the classical Extended Kalman filter to design an observer for systems described by time continuous nonlinear delay differential equations using time continuous measurement. However, in our case, we work in a sampled-data framework. So, in order to use this filter, we propose to add a step in the observer which consists in pre-processing the measures thanks to an interpolation algorithm (e.g. using smoothing spline [138]). The main drawback of this approach is that the quality of the estimate and the convergence property of the complete observer scheme is correlated with the properties of the interpolation algorithm.

Let us consider the following nonlinear time-delay system for all $t \in [t_{k-1}, t_k]$

$$\begin{aligned} &\frac{dx}{dt} = \mathscr{G}(x, x(t-\tau), u) + w, \\ &y_k = Cx(\phi, u; t_k) + v_k, \\ &x(t) = \phi(t)\ \forall t \in [t_{k-1} - \tau; t_{k-1}], \end{aligned} \tag{10.51}$$

where y_k is the measured output, C is a known matrix, w is the noise on the system of variance Q and v_k is the noise on the measure of variance R. The objective is, given the discrete measure y_k, to estimate the function $x(\phi, u, 0; t)$ for all $t \in [t_k - \tau, t_k]$.

The vector field $\mathscr{G} : \mathbb{R}^{n_x} \times \mathbb{R}^{n_x} \times \mathbb{R}^{n_u} \to \mathbb{R}^{n_x}$ is assumed to be continuously differentiable with respect to its first two arguments. The observer is given as follows [128]

$$\begin{aligned} \frac{d\hat{x}}{dt} &= \mathscr{G}(\hat{x}, \hat{x}(t-\tau), u) + L(t)(\tilde{y}_k(t) - \hat{y}(t)), \\ \hat{y}(t) &= C\hat{x}(\hat{\phi}, u, 0; t), \\ \hat{x}(t) &= \hat{\phi}(t) \ \forall t \in [t_{k-1} - \tau; t_{k-1}], \end{aligned} \tag{10.52}$$

where $L(t)$ is a time varying observer matrix and $\tilde{y}_k(t)$ is defined for all $t \in [t_{k-1}, t_k]$. This latter signal is obtained by interpolating the m past measured data $(y_i)_{i \in \{k-m,\dots,k\}}$. The observer matrix $L(t)$ is computed as for the classical Extended Kalman filter (see e.g. [131]), that is

$$L(t) = \mathscr{P}(t) C^T R, \tag{10.53}$$

where $\mathscr{P}(t)$ is the solution of the following modified Riccati equation:

$$\frac{d\mathscr{P}}{dt} = \mathscr{P} A_0^T + A_0 \mathscr{P} - \mathscr{P} C^T R^{-1} C \mathscr{P} + Q + A_1^T A_1, \tag{10.54}$$

where

$$\begin{aligned} A_0 &= \nabla_x \mathscr{G}(\hat{x}, \hat{x}(t-\tau), u), \\ A_1 &= \nabla_h \mathscr{G}(\hat{x}, \hat{x}(t-\tau), u), \end{aligned} \tag{10.55}$$

where $\nabla_x \mathscr{G}$ stands for the derivative of $\mathscr{G}$ relatively to its first argument and $\nabla_h \mathscr{G}$ stands for the derivative of $\mathscr{G}$ relatively to its second argument.

In the case of time continuous measures, it is possible to prove that the observer is a local asymptotically stable observer [128]. In our case, to prove the good convergence property, the interaction between the interpolation error and the observer error should be studied.

Validation on the delay minimal model of Bergman

To test the good numerical implementation and performances of the observer, we consider the problem of estimating the state of the delay minimal of Bergman (10.9) when this latter is also used for simulation purpose. By doing so, we can check whether the observer converge toward the *true* state value. To do so let us consider the parameters given in table 10.1.

To test the observer performances, we simulate the model (10.9) where the initial condition is given by $[aG_{eq}, bI_{eq}, cU_{1,eq}, 0, 0]$ for all $t \in [t_0 - \tau, t_0]$ where $(a,b,c) \in (\mathbb{R}^{+*})^3$. The considered simulation scenario is given by

- $t = t_0$: the simulation begins,
- $t = t_0 + 7h$: the patient eats a meal of 25gCHO,
- $t = t_0 + 12h$: the patient eats a meal of 70gCHO,
- $t = t_0 + 20h$: the patient eats a meal of 80gCHO,
- $t = t_0 + 35h$: the simulation is ended.

Name	Value	Unit
P	6.25×10^{-4}	min^{-1}
k_0	1.06×10^{-4}	$\text{mU}^{-1}.\text{min}^{-1}$
D	0.27	$\text{mg.dL}^{-1}.\text{min}^{-1}$
k_f	3.85×10^{-2}	min^{-1}
b_f	1.77×10^{-4}	$\text{L}^{-1}\text{min}^{-1}$
k_s	6.5×10^{-3}	min^{-1}
c_1	9.95×10^{-2}	min^{-1}
c_2	2.39×10^{-2}	min^{-1}
k_{gr}	1.2×10^{-3}	$\text{dL}^{-1}.\text{min}^{-1}$
τ	105	min

Table 10.1: Parameters of the delay minimal model of Berman used for validation of the observer

To simulate that only sampled noisy measure are available, the output is given by $G(t_0 + kT_{ech}) + v_k$ where $T_{ech} = 5\text{min}$ and $v_k \approx \mathcal{N}(0,5)$. The interpolation is given by a simple linear interpolation between two successive measures.

The observer first estimate of the state is either set to the initial function

$$\phi_{EKFDDE}(s) = [G_{eq}, I_{eq}, U_{1,eq}, 0, 0]$$

for all $s \in [t_0 - \tau, t_0]$ or set to the true initial condition. In order to study the influence of the noise on the measure, the simulation is run 100 times. The observer performances are compared thanks to the computation of the mean RMS of the relative error between the estimated state and the true state according to the following formula

$$\text{RMS} = \sqrt{\sum_{k=0}^{420} \int_{t_k-\tau}^{t_k} \left(\frac{\|x(s) - \hat{x}(s)\|}{\|x(s)\|} \right)^2 ds}, \tag{10.56}$$

where x stands for the true value of the state and $\hat{x}$ stands for the estimated value of the state.

A simulation example when the observer initial condition is set to the equilibrium starting point can be seen on fig.10.1. In this figure, we have drawn the value of the estimated state function at each sampling instant. That is, at $t = t_k$, we have estimated $\hat{x}(\phi, u; t)$ for all $t \in [t_{k-1}, t_k]$ and we have plot the corresponding piece of trajectory. In this case, the mean RMS is equal to

$$RMS = 0.3142. \tag{10.57}$$

A simulation example when the observer initial condition is set to the exact initial condition can be seen on fig.10.2. The corresponding mean RMS is equal to

$$RMS = 0.1082. \tag{10.58}$$

It can be seen that for both initial condition, the observer converges toward the true state. The difference in the RMS between the equilibrium starting point and the exact starting point is mainly due to the needed convergence time which is naturally larger when the initial estimate is arbitrary chosen.

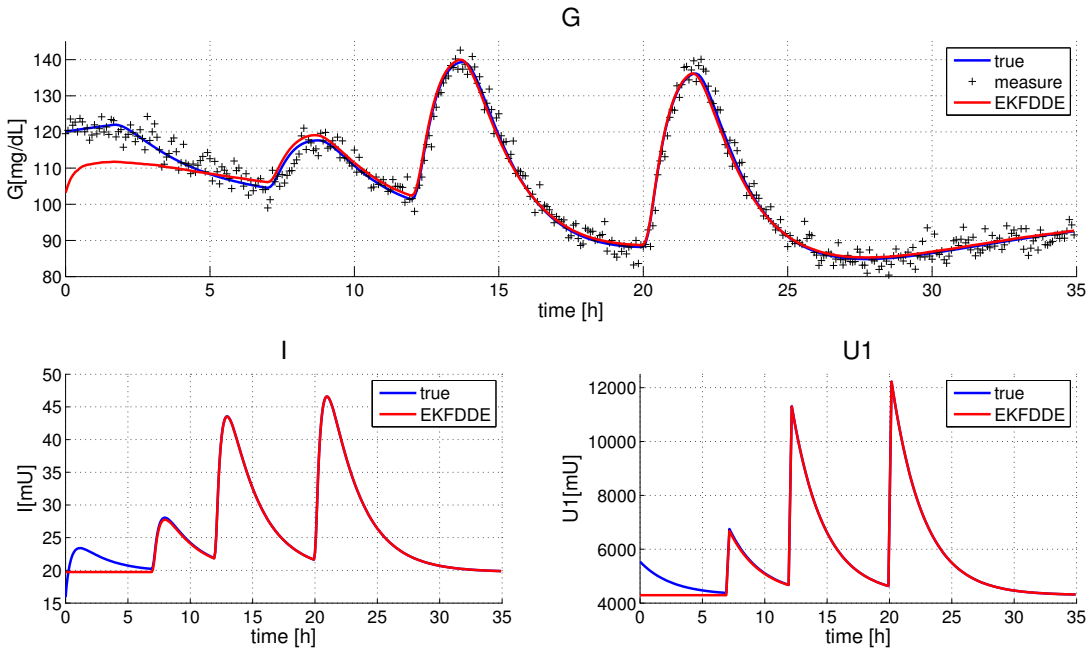

Figure 10.1: EKFDDE observer, equilibrium starting point

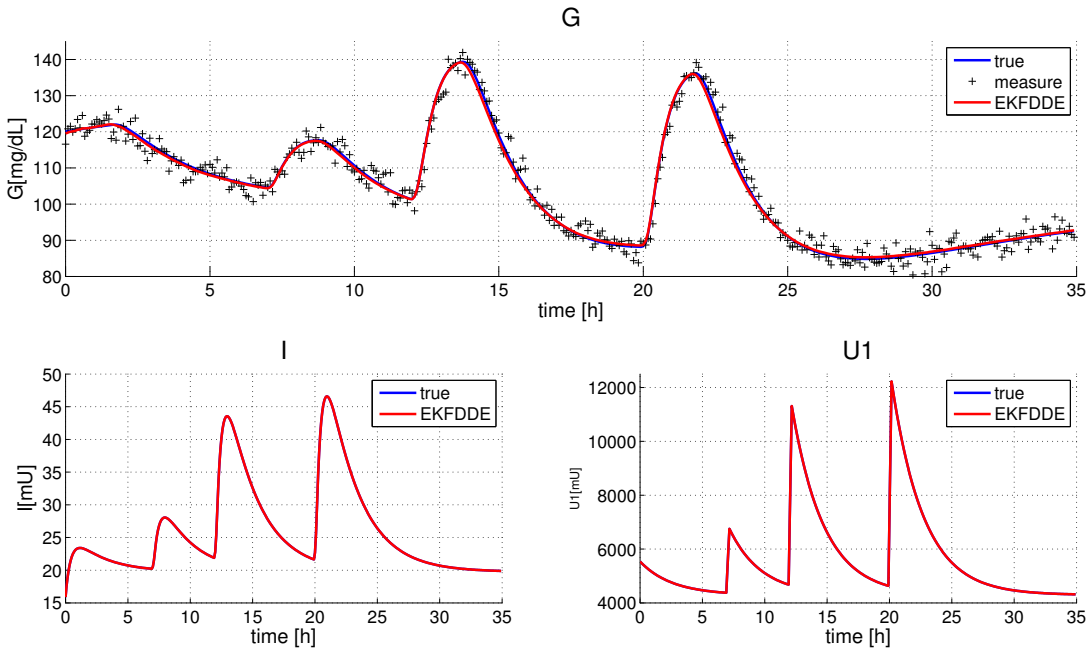

Figure 10.2: EKFDDE observer, exact starting point

10.4.2 Adjoint model and Gradient of the criterion

The control problem

The robust control problem is given by the solution of the optimization problem given by (10.16). Similarly to (4.29), to consider the terminal state constraint (10.28), we introduce the following modified

functional

$$\begin{aligned}\mathscr{L}_A^{t_0,\mu}(f,\tilde{w}) &= J^{t_0}(f,w)\\ &+\Psi^{\mu}(\gamma-\max_{\theta\in[-\tau;0]}x(t_0+T+\theta)^T P_0 x(t_0+T+\theta),\lambda_\Omega),\end{aligned} \tag{10.59}$$

where J^{t_0} is given by (10.17) with F quadratic (3.74) and E given by (10.19).

To solve this optimization problem, we will use the algorithms presented in chapter 4. To do so, let us introduce the adequate adjoint model and the corresponding value of the derivative of the criterion.

According to (4.35), to obtain the appropriate optimality system (necessary conditions), which corresponds to the identification of the gradient of $\mathscr{L}_A^{t_0,\mu}$ that is necessary to develop a numerical scheme in order to solve the saddle point problem, we introduce the adjoint system as follows

$$\begin{aligned}
-\frac{d\tilde{x}_1}{dt} &= -\left(P+\overline{p}+(k_0+\overline{k_0})(x_2(t-\tau)+I(t-\tau))\right)\tilde{x}_1+\sum_{i=1}^{3}\left(R^{1,i}+S_2^{1,i}\mathbb{1}_{[t_0+T-\tau;t_0+T]}(t)\right)x_i,\\
-\frac{d\tilde{x}_2}{dt} &= -(k_f+\overline{k}_f)\tilde{x}_2-(k_0+\overline{k}_0(t+\tau))(x_1(t+\tau)+G(t+\tau))\tilde{x}_1(t+\tau)\mathbb{1}_{[t_0;t_0+T-\tau]}(t)\\
&\quad+\sum_{i=1}^{3}\left(R^{2,i}+S_2^{1,i}\mathbb{1}_{[t_0+T-\tau;t_0+T]}(t)\right)x_i,\\
-\frac{d\tilde{x}_3}{dt} &= -(k_s+\overline{k}_s)\tilde{x}_3+(b_f+\overline{b}_f)\tilde{x}_2+\sum_{i=1}^{3}\left(R^{3,i}+S_2^{1,i}\mathbb{1}_{[t_0+T-\tau;t_0+T]}(t)\right)x_i,\\
\tilde{x}(t_0+T) &= 2S_1x(t_0+T)+\nabla_x\left(\Psi^{\mu}(\gamma-\max_{\theta\in[-\tau;0]}x(t_0+T+\theta)^T P_0 x(t_0+T+\theta),\lambda_\Omega)\right),
\end{aligned} \tag{10.60}$$

where $\mathbb{1}$ is the indicator function, $\nabla_x\left(\Psi^{\mu}(\gamma-\max_{\theta\in[-\tau;0]}x(t_0+T+\theta)^T P_0 x(t_0+T+\theta),\lambda_\Omega)\right)$ is defined according to (4.26).

According to (4.38), the following expression of the derivatives of $\mathscr{L}_A^{t_0,\mu}$ are deduced

$$\begin{aligned}
\frac{\partial\mathscr{L}_A^{t_0,\mu}}{\partial f}(f,\tilde{w}) &= \tilde{x}_3+\alpha f,\\
\frac{\partial\mathscr{L}_A^{t_0,\mu}}{\partial\tilde{w}}(f,\tilde{w}) &= \begin{pmatrix}
-\tilde{x}_1(x_1+G)-Q_{1,1}\overline{p}\\
-\tilde{x}_1(x_1+G)(x_2(t-\tau)+I(t-\tau))-Q_{2,2}\overline{k}_0\\
-\tilde{x}_2(x_2+I)-Q_{3,3}\overline{k}_f\\
\tilde{x}_2(x_3+U_1)-Q_{4,4}\overline{b}_f\\
-\tilde{x}_3(x_3+U_1)-Q_{5,5}\overline{k}_s\\
\dfrac{\partial\Psi^{\mu}}{\partial\lambda}(\gamma-\max_{\theta\in[-\tau;0]}x(t_0+T+\theta)^T P_0 x(t_0+T+\theta),\lambda_\Omega)
\end{pmatrix},
\end{aligned} \tag{10.61}$$

where x is the solution of (10.11) with initial condition ϕ under the influence of the couple control disturbances (f,w), $\tilde{x}$ is the solution of (10.60) and $\nabla_{\lambda_\Omega}\Psi^{\mu}$ is defined according to (4.27).

The identification problem

To test the controller performances using the virtual testing platform, we need to identify an adequate set of parameters for each adult of the simulator.

As the structure of the gastro-intestinal sub-model has remained unchanged, its parameters are assumed to remain unchanged and are given in table 9.2.

To identify the parameters of the glucose-insulin sub-model, we consider the methodology presented in chapter 9 where p given as follows

$$p = \begin{pmatrix} P & k_0 & D & k_f & b_f & k_s \end{pmatrix}^T. \tag{10.62}$$

According to (4.35), to obtain the appropriate optimality system (necessary conditions), which corresponds to the identification of the gradient of $J(p)$ that is necessary to develop a numerical scheme in order to solve the corresponding minimization problem, we introduce the adjoint system as follows

$$\begin{aligned}
-\frac{d\tilde{x}_1}{dt} &= -(P + k_0 x_2(t-\tau))\tilde{x}_1 + R(x_1 - x_{1,obs}),\\
-\frac{d\tilde{x}_2}{dt} &= -k_f\tilde{x}_2 - k_0 x_1(t+\tau)\tilde{x}_1(t+\tau)\mathbb{1}_{t\in[T_{start},T_{end}-\tau]},\\
-\frac{d\tilde{x}_3}{dt} &= b_f\tilde{x}_2 - k_s\tilde{x}_3,\\
-\frac{d\tilde{x}_4}{dt} &= k_{gr}\tilde{x}_1 - c_2\tilde{x}_4,\\
-\frac{d\tilde{x}_5}{dt} &= c_2\tilde{x}_4 - c_1\tilde{x}_5,\\
\tilde{x}(T_{end}) &= 0,
\end{aligned} \tag{10.63}$$

where $x_{1,obs}$ stands for the measured output and x_1 stands for the simulated output.

According to (4.38), the following expression of the derivative of $J(p)$ is deduced

$$\frac{\partial J}{\partial p}(p) = \begin{pmatrix} -\int_{T_{start}}^{T_{end}} \tilde{x}_1 x_1 ds + \alpha_{1,1}P \\ -\int_{T_{start}}^{T_{end}} \tilde{x}_1 x_1 x_2(s-\tau) ds + \alpha_{2,2}k_0 \\ \int_{T_{start}}^{T_{end}} \tilde{x}_1 ds + \alpha_{3,3}D \\ -\int_{T_{start}}^{T_{end}} \tilde{x}_2 x_2 ds + \alpha_{4,4}k_f \\ \int_{T_{start}}^{T_{end}} \tilde{x}_2 x_3 ds + \alpha_{5,5}b_f \\ -\int_{T_{start}}^{T_{end}} \tilde{x}_3 x_3 ds + \alpha_{6,6}k_s \end{pmatrix}. \tag{10.64}$$

Then, for a given set of parameters, to estimate the delay τ, we use the same methodology with $p = \tau$. The adjoint model is also given by (10.63). Similarly to (4.38), the derivative of the criterion is given by

$$\begin{aligned}
\frac{\partial J}{\partial p}(\tau) = &-\int_{T_{start}-\tau}^{T_{start}} k_0\tilde{x}_1(s+\tau)x_1(s+\tau)\frac{d\phi}{dt}(s)ds\\
&-\int_{T_{start}}^{T_{end}-\tau} k_0\tilde{x}_1(s+\tau)x_1(s+\tau)\left(-k_f x_2(s) + b_f x_3(s)\right)ds + \alpha\tau,
\end{aligned} \tag{10.65}$$

where ϕ is the initial condition of the system which is assumed to be sufficiently regular.

Finally, in order to converge to a set of parameters, the procedure is implemented recursively according to fig. 10.3.

The parameters obtained for the 10 adults with this methodology are resumed in table 10.2. The comparison between the measured output used to identify the parameters and the simulated output for

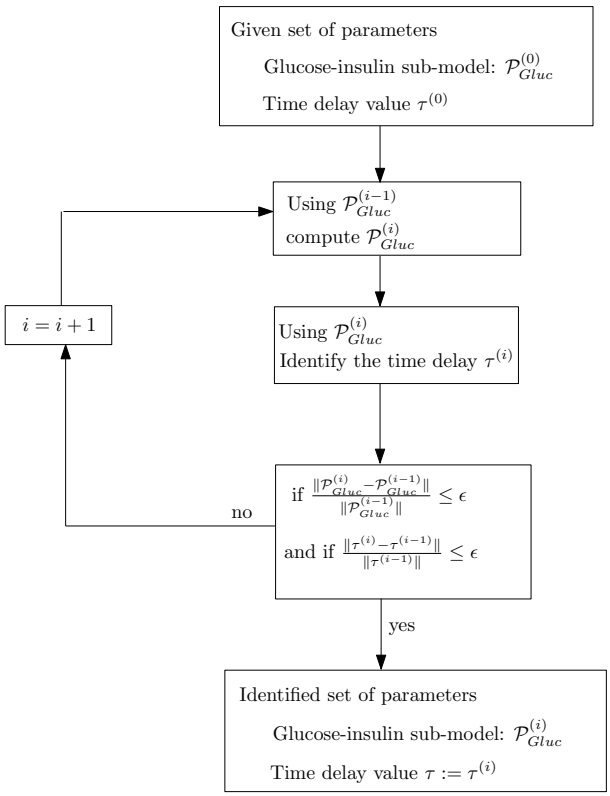

Figure 10.3: Identification procedure for time-delay system

adult 7 is shown on fig. 10.4 and for adult 10 on fig. 10.5. It can be seen that the global trend of the glucose metabolism is well represented. However, as for the ordinary differential case, the quality of the identification result strongly depends on the patient. Also, for adult 10, it can be observed that the simplicity of the gastro-intestinal sub-model can be at the origin of a poor fitting of the simulated output and so can be an issue when it comes to control.

10.4.3 Simulation scenario

To test the controller performances, we consider the following scenario (which corresponds to the first variation of scenario 2 in chapter 9)

$t = 0h$ The simulation is initialized. The initial blood glucose is set at 100mg.dl^{-1}. The observer (an EKF for DDE) is switched on.

$t = 2h$ The controller is switched on.

$t = 7h$ The patient eats a meal of 25g.

$t = 12h$ The patient eats a meal of 70g.

$t = 20h$ The patient eats a meal of 80g.

$t = 35h$ The simulation is ended.

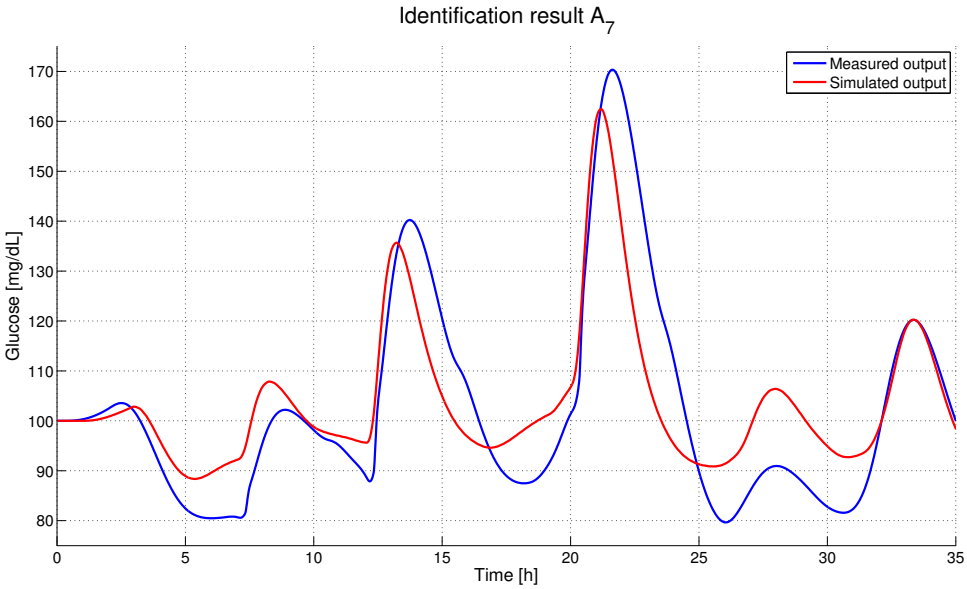

Figure 10.4: Comparison between the data used for identification purpose and simulated output for adult 7

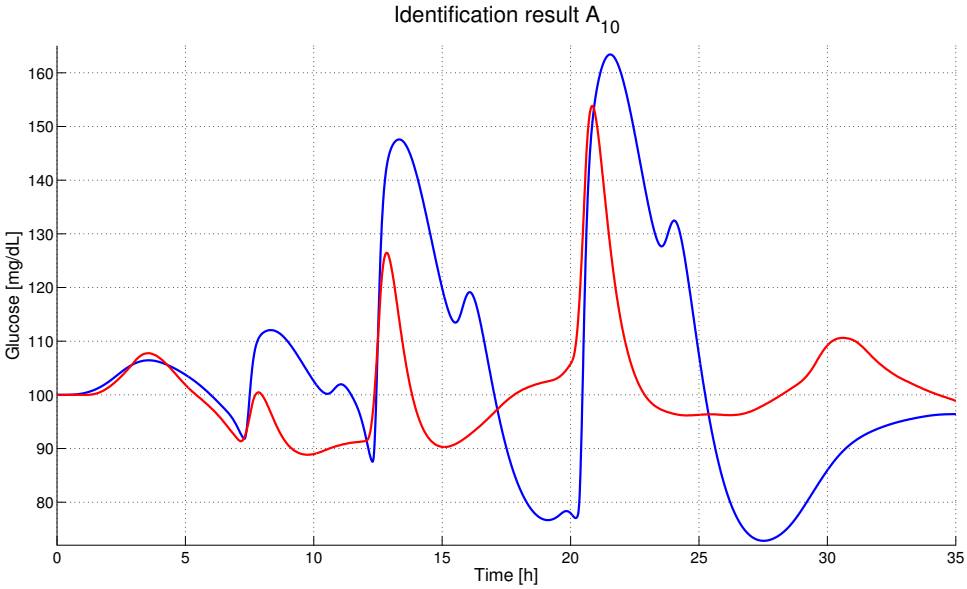

Figure 10.5: Comparison between the data used for identification purpose and simulated output for adult 10

It is assumed that each meals are regulated via injection of 75% of the optimal bolus (according to the insulin to carbohydrate ratio determined by the physician). The information concerning the meal size and the injected bolus are provided to the controller when the corresponding event occurs (no anticipatory behavior).

The prediction horizon has been set to 5τ. To consider the asymmetric control objective, the constraint $G \geq 80\text{mg.dL}^{-1}$ has been added in the optimization problem. The control objective is to robustly

Adult	P	k_0	D	k_f	b_f	k_s	τ
1	6.25×10^{-4}	1.06×10^{-4}	0.27	3.85×10^{-2}	1.77×10^{-4}	6.5×10^{-3}	105
2	1×10^{-3}	4.05×10^{-4}	1	1.1×10^{-2}	4.93×10^{-4}	5.64×10^{-2}	50
3	0	4.15×10^{-4}	1.2	1.04×10^{-2}	6.17×10^{-4}	6.42×10^{-2}	80
4	1.87×10^{-5}	7.09×10^{-4}	1.3	1.08×10^{-2}	5.67×10^{-4}	5.58×10^{-2}	73
5	3×10^{-3}	1.72×10^{-4}	0.72	5.80×10^{-2}	4.80×10^{-4}	1.06×10^{-2}	75
6	7.49×10^{-6}	5.93×10^{-4}	0.92	8.41×10^{-3}	1.58×10^{-4}	3.90×10^{-2}	78
7	1.55×10^{-7}	6.11×10^{-4}	1.37	4.22×10^{-2}	3.34×10^{-4}	9.1×10^{-3}	55
8	4.46×10^{-5}	1.06×10^{-4}	0.26	3.88×10^{-2}	4.49×10^{-4}	1.24×10^{-2}	101
9	3.78×10^{-5}	9.34×10^{-5}	0.22	6.65×10^{-2}	9.33×10^{-4}	1.37×10^{-2}	101
10	1.5×10^{-3}	1.93×10^{-4}	0.62	5.02×10^{-2}	4.78×10^{-4}	1.11×10^{-2}	63

Table 10.2: Parameters value for the adults of the simulator, glucose-insulin sub-model

stabilize the blood glucose at a value of $G_{eq} = 100\text{mg.dL}^{-1}$. The uncertainties on the parameters are given by variations of 10% around the nominal value of the corresponding parameters.

The stage cost F is chosen quadratic (see equation 3.74) with the following weight:

$$R = \text{diag}\left(\frac{1}{G_{eq}}, \frac{1}{I_{eq}}, 0\right),\ Q = \text{diag}\left(\frac{1}{P+10^{-10}}, \frac{1}{k_0}, \frac{1}{k_f}, \frac{1}{b_f}, \frac{1}{k_s}\right), \alpha = \frac{1}{u_{eq}}, \tag{10.66}$$

where $I_{eq} = \dfrac{D - PG_{eq}}{k_0 G_{eq}}$ and $u_{eq} = \dfrac{k_s k_f}{b_f} I_{eq}$.

The variational model, the adjoint model, the final cost and the terminal state constraint are defined according to the results of the previous sections.

10.4.4 Simulation with the delay minimal model of Bergman

In order to validate the implementation of the control methodology, let us consider the control of the delay minimal model of Bergman in case the model is also used to simulate a virtual patient.

The meals are assumed to be uniformly consumed in 15min. The sampling time on the input is set to 5min and on the output to 15min. For control purpose, a noisy blood glucose value is provided for the observer, *i.e.*

$$G_{sensor,k} = G_k + v_k, \tag{10.67}$$

where $v_k \approx \mathcal{N}(0,5)$. The remaining state of the system are estimated using the previously presented observer.

The simulation results for the 10 adults are summed up in table 10.3. The simulation results are good in the sense that no hypoglycemia and no hyperglycemia have to be deplored. In this case it is difficult to compare the results with the one given by the modified minimal model of Bergman (just see the difference between fig. 9.3 and fig. 10.5).

The simulation result for adult 9 on fig.10.6 is really interesting as it shows both the advantage and the inconvenient of using a SPMPC controller to stabilize a time delay system. In this case the system is indeed robustly stabilize despite the complexity of the control problem, but to do so, one of the only action of the controller has been to reduce the effect of the bolus (the basal input is decreased at meal time where a bolus was injected) leading to a very conservative control strategy.

Now that we have validated the controller implementation and performances, let us consider the control problem of blood glucose using realistic patient.

Adult	% $G \in [70;140]$	$\min G$ mg.dL^{-1}	$\max G$ mg.dL^{-1}
1	98	83	141
2	93	86	152
3	100	72	137
4	100	74	132
5	85	78	158
6	85	74	158
7	88	78	132
8	100	83	114
9	83	95	174
10	83	75	177

Table 10.3: Simulation results using the control model to simulate a patient

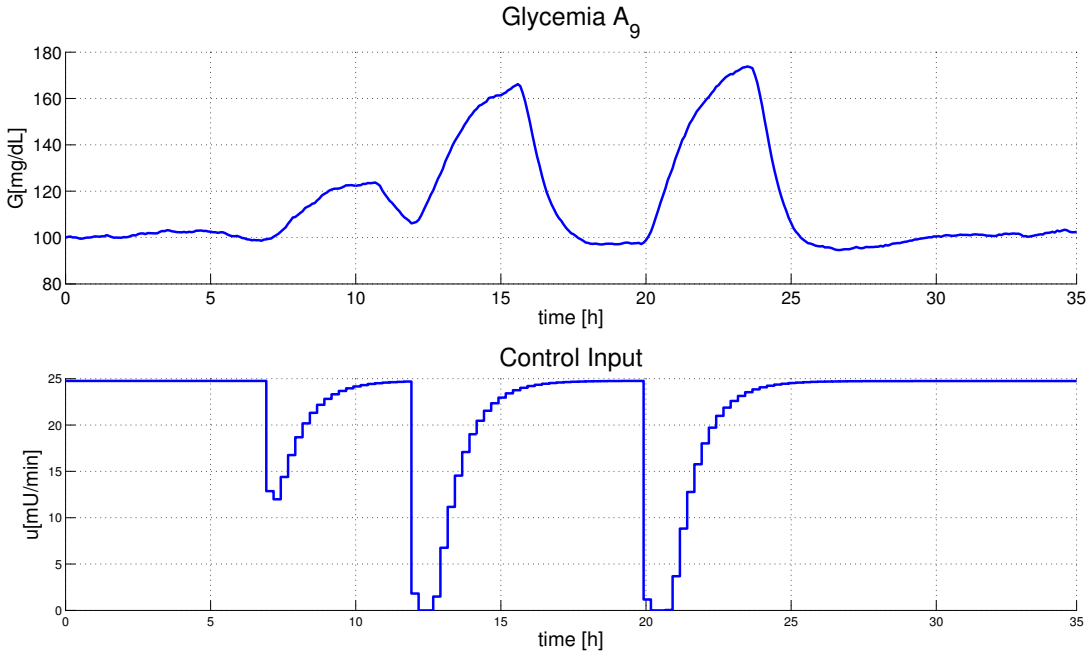

Figure 10.6: Simulation result for adult 9, using the control model as patient simulator

10.4.5 Simulation with the virtual testing platform

Then we are interested in testing the controller performances when using the testing platform approved by the FDA [90]. The table 10.4 sums up the simulation results for all adults. The simulation results are quite good and comparable to the one given by a SPMPC controller designed on the modified minimal model of Bergman (see table 9.8). For all adults the blood glucose is safely stabilized.

For all adults no hypoglycemia events occur and the time spent in hyperglycemia state is small enough such that it does not lead to heavy trauma. The percentage of time spent in the target is relatively good. Also, the control behavior is relatively safe in the sense that the control action consist in small variation of the insulin dose. This can be seen with the simulation results of adult 9 (see fig.10.7).

Adult	% $G \in [70;140]$	min G mg.dL^{-1}	max G mg.dL^{-1}
1	84	78	163
2	88	78	151
3	78	89	188
4	75	82	190
5	87	91	156
6	70	96	200
7	82	96	161
8	100	72	134
9	71	68	179
10	75	83	176

Table 10.4: Simulation results using the Dalla-Man et al. model as patient simulator

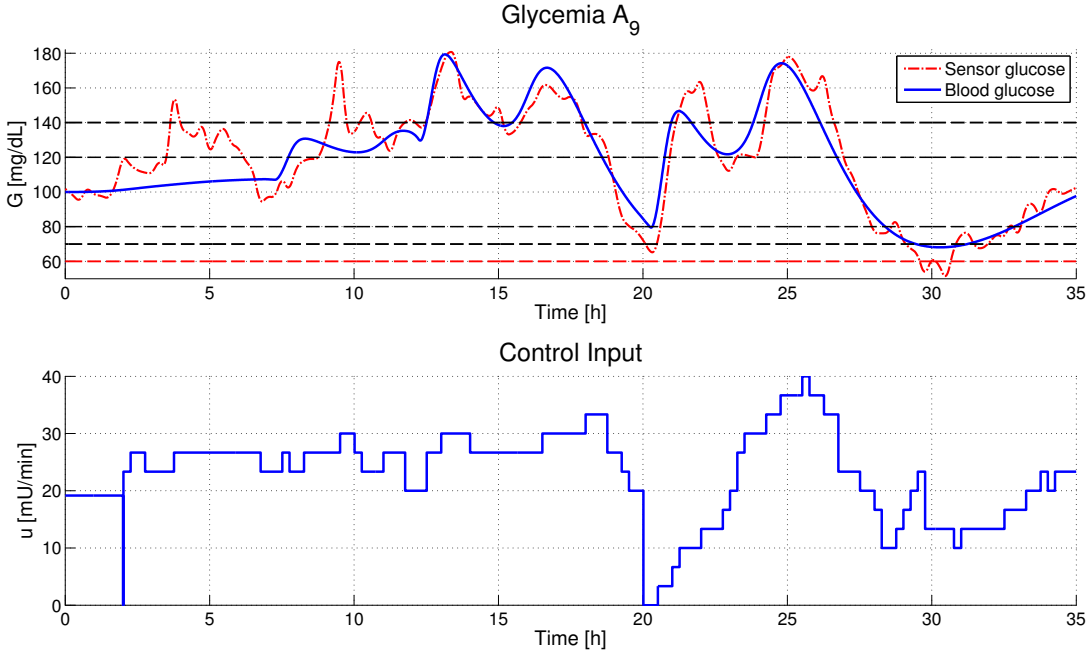

Figure 10.7: Simulation result for adult 9, using the Dalla-Man et al. model as patient simulator

10.5 Conclusion

In this chapter we have been interested in testing the possibility of extending the SPMPC control approach to the control problem of time delay systems. To do so, we have derived a model of the glucose metabolism using nonlinear delay differential equations. Then, we have considered a numerical implementation of an adjusted SPMPC controller. This has lead us to adjust the assumptions on the final cost and on the terminal state constraint similarly to what has been done in the NMPC case. Finally, numerical simulations have been performed using both the control model and the testing platform to simulate virtual patient.

It is worth noticing that from a numerical point of view the control problem is involved. First, to compute an adequate final cost and terminal state constraint, we have to use adjusted assumptions which

lead to more complex formulation. This has implied that to make the computation of the final cost and terminal state constraint tractable, we have made conservative choice (*i.e.* the final controller and the final cost have been chosen with a simple structure). This is at the origin of a deterioration of the expectable performances. Then, comes the problem of estimating the value of the state functional at each sampling instant. This task is quite complex because we have considered a sampled-data framework. Despite the lack of convergence guarantee, we have considered an extension of an adjusted extended Kalman filter. The idea has been to introduce an interpolation step in order to use a full time continuous observer. Finally, one last issue comes from the problem of estimating the parameters of the model. This issue is also of prime importance as it is not realistic to expect good control performances if the nominal model of the process is really too bad to explain the true process. To solve this issue we have considered optimal control techniques.

Despite all these difficulties, the obtained results were quite satisfactory in the sense that they are comparable to the one obtained in chapter 9. This motivates us to consider a more in depth study of this extension.

Chapter 11

Conclusion

11.1 Summary and Discussion

The main idea behind model predictive control is to solve on line, each time a control input has to be computed, an optimization problem. The resulting optimal control input is then applied in open-loop to the system for a small fraction of the prediction length. One problem is that to obtain this optimal trajectory, the control algorithm relies on a model of the process. Most of the time, this model is derived by neglecting some dynamics of the true process or that the real process is time-varying. Also, an other difficulty is that the control input can be applied in open-loop for a fraction of time which is not negligible compared to the system time constant leading to the need of working in a sampled-data framework. Therefore the design of a robust NMPC controller which ensures good control performances in a sampled-data framework is of prime importance.

In the first part of this thesis, we have focused on the presentation and analysis of a *saddle point MPC* controller (SPMPC). This controller has been designed to ensure robust control performances of systems described by nonlinear ordinary differential equations in a sampled-data framework. It has been proved that, under reasonable assumptions, this controller ensures that the system is ultimately bounded and, under supplementary assumptions, input-to-state practically stable. The interesting point is that to ensure these results, we use the same tools as for a usual NMPC controller, namely a final cost and a terminal state constraint. The problem of computing these elements for a SPMPC controller has then be formulated in the LMI framework using a local differential inclusion embedding.

One of the difficulty when it comes to design a SPMPC controller for a given control problem lies in the problem of solving an unusual optimization problem, namely a state-constrained saddle point optimization problem. That is why in this thesis we have proposed a numerical method based on the augmented Lagrangian techniques. That is, to solve a given state-constrained saddle point optimization problem, we consider the solution of a sequence of adequately penalized state-unconstrained saddle point optimization problem. Each unconstrained sub-problem has been solved using adjoint method. The numerical implementation and the controller performances have been validated on the problem of controlling a disturbed in parameters Van der Pol oscillator.

In the second part of this thesis, we were concerned with the application of the developed SPMPC controller to artificially control blood glucose of a type 1 diabetic. This controller choice is relevant in regards to many specificities of this control problem. Indeed, the problem of artificial blood glucose control is surrounded with uncertainties (to obtain a model of the glucose metabolism, we have neglected some dynamics, also the real process is time varying and the model is stationary, ...) thus robust performances are desired. Also the control problem is naturally set up in a sampled-data framework (the

glucose metabolism is time continuous and the measure are discrete) and so, to aim at the best control performances, it is needed to work in a sampled-data framework. More precisely, we have been interested in controlling the stabilizing part (basal) of the classical cure. Then, to validate the approach, we have considered numerical simulations on a testing platform validated by the FDA. We have considered two scenarios. The first one is an overnight type scenario and the second one consists in a classical day with three meals. In both cases, the numerical simulations have shown good results. Indeed, no hypoglycemia event occurs and the time spent in hyperglycemia does not lead to damageable consequences. Also, with the second scenario, it has been shown that our control approach can be efficiently combined with a given bolus cure. This means that the SPMPC controller can be considered as a viable solution to artificially control blood glucose.

Also, some exploratory works have been done by considering the potential extension of the SPMPC approach to control, in a sampled-data framework, nonlinear time delay systems. To do so, we have considered the modeling problem of the glucose metabolism using nonlinear delay differential equations. Then, assuming that the controller yields a stable closed-loop, we have presented what has to be adjusted from a numerical point of view. Numerical simulations have then been performed using the validated testing platform to simulate realistic virtual patients. It has been shown that the SPMPC controller provides satisfactory control performances, thus motivating a more in depth study of this extension.

Because of the good simulation results obtained when using the testing platform to simulate realistic virtual patients, it can be interesting to consider the control on real situation, using clinical data, with collaboration of medical staff. In particular, in the framework of an existing collaboration, it is planned to perform some clinical tests with the physicians of the University Hospital of Rennes to assess the behavior performances of the SPMPC controller when this latter is used to control the blood glucose of real patients.

11.2 Future work

Several results addressed in this thesis offer the opportunity for further research.

First of all, it can be worth considering the impact of the symmetry between the control input and the disturbances. Indeed, even if the controller has performed well in the framework of this thesis, it is natural to think that for some class of systems, the fact that the constraints are also imposed on the disturbances can lead to some difficulties. Hence a future work can be to define the class of systems for which the envisaged symmetry is not damageable in regards to the control performances and robustness guarantee. Afterwards, it can also be interesting to develop other assumptions for lemma 1 on recursive feasibility. Indeed, it is clear that the sufficient condition (3.11) is not so satisfying from a control point of view as it needs on line information. A possibility is to reformulate the notion of feasibility by requiring the existence of at least one control input such that for all admissible disturbances the terminal state constraint is satisfied. The problems of this choice come then from the difficulty to characterize the set of admissible initial condition or to compute an adequate control input.

An other obvious future work consists in considering the theoretical aspect of the extension of the SPMPC controller to control time delay systems.

Also, in order to apply the SPMPC controller for artificial blood glucose control, we have used a state observer. This situation is quite usual when it comes to practical problems. In our case we have implicitly assumed that a separation principle holds such that the combination of the observer and the SPMPC controller is stable. However, in the nonlinear case, no general separation principle exists. So, it can be interesting to consider the stability of the SPMPC controller from an output-feedback point of view (e.g. by adding a supplementary disturbance in the initial condition). It can also be interesting to

consider how the controller has to be adjusted when it is used to track time-varying trajectory.

Finally for what concerns the application to type 1 diabetes, because of the good performances of the controller, it is desirable to see in what extent enhancements are possible. To validate our approach we have considered that we have no control experience, and that in this case a default tuning has to be available. So, it can be interesting to see how we can use control experiences in order to change the weighting in the criterion to aim at better control performances. Also, as the controller only take care of the basal part of the cure, it can now be interesting to consider the bolus part of the cure.

It can also be interesting other applications where it can be advantageous to consider the design of a SPMPC controller. As an example, it can be more or less straightforward to consider other biological control problems, e.g. in thermal therapy, or to consider the control problem of some slow process, e.g. in building control.

Bibliography

[1] A. Abu-Rmileh and W. Garcia-Gabin. Feedforward-feedback multiple predictive controllers for glucose regulation in type 1 diabetes. *Computer Methods and Programs in Biomedicine*, 99:113–123, 2010.

[2] A. Abu-Rmileh and W. Garcia-Gabin. A gain-scheduling model predictive controller for blood glucose control in type 1 diabetes. *IEEE Transactions on Biomedical Engineering*, 57:2478–2484, 2010.

[3] A. Abu-Rmileh and W. Garcia-Gabin. Smith predictor sliding mode closed-loop glucose controller in type 1 diabetes. In *18th World IFAC congress*, 2011.

[4] A. Abu-Rmileh and W. Garcia-Gabin. Wiener sliding-mode control for artificial pancreas: a new nonlinear approach to glucose regulation. *Computer Methods and Programs in Biomedicine*, 107:327–340, 2012.

[5] A. Abu-Rmileh, W. Garcia-Gabin, and D. Zambrano. Internal model sliding mode control approach for glucose regulation in type 1 diabetes. *Biomedical Signal Processing and Control*, 5:94–102, 2010.

[6] T. Ahmed and D. Storey. Efficient generalized conjugate gradients, part 1: Theory. *J. Optim. Theorem. Appl.*, 71:399–405, 1991.

[7] T. Alamo, D.R. Ramirez, and D. Munoz de la Pena. Min-max MPC using a tractable qp problem. In *Proceedings of the 44th IEEE Conference on Decision and Control, and the European Control Conference*, 2005.

[8] A.M. Albisser, B.S. Leibel, T.G. Ewart, C.K. Botz Z. Davidovac, and W. Zingg. An artificial endocrine pancreas. *Diabetes*, 23:389–404, 1974.

[9] A. Alessandri, M. Baglietto, G. Battistelli, and V. Zavala. Advances in moving horizon estimation for nonlinear systems. In *49th IEEE Conference on Decision and Control*, 2010.

[10] A. Belmiloudi. *Stabilization, Optimal and Robust Control*. Springer Verlag London, 2008.

[11] A. Belmiloudi. *Thermal Therapy: Stabilization and Identification. In Edited Book: Heat Transfer-Mathematical Modelling, Numerical Methods and Information Technology*. Chapter 2, INTECH, Vienna, 2011.

[12] A. Bemporad and A. Morari. Robust model predictive control: a survey. *Lecture Notes in Control and Information Sciences*, 245:207–226, 1999.

[13] B.W. Bequette. Challenges and progress in the development of a closed-loop artificial pancreas. In *2012 American Control Conference, Fairmont Queen Elizabeth, Montréal, Canada*, 2012.

[14] R.N. Bergman, Y.Z. Ider, C.R. Bowden, and C. Cobelli. Quantitative estimation of insulin sensitivity. *Am. J. Physiol. Endocrinol. Metab.*, 236:667–677, 1979.

[15] R.N. Bergman, L.S. Phillips, and C. Cobelli. Physiologic evaluation of factors controlling glucose tolerance in man. *J. Clin. Invest. The American Society for Clinical Investigation*, 68:1456–1467, 1981.

[16] N. Bhitre and R. Padhi. An adaptive insulin infusion approach for customized blood glucose regulation of type i diabetic patients. In *2011 IEEE International Conference on Control Applications (CCA)*, 2011.

[17] M. Bichegkuev. On a weakened cauchy problem for a linear differential inclusion. *Math. Notes*, 79:449–453, 2006.

[18] F. Blanchini. Set invariance in control. *Automatica*, 35:1747–1767, 1999.

[19] S. Boyd. *Linear Matrix Inequalities in* S*ystem and* C*ontrol* T*heory*. SIAM, 1994.

[20] M. Breton and B. Kovatchev. Analysis, modeling, and simulation of the accuracy of continuous glucose sensors. *Journal of Diabetes Science and Technology*, 2:853–862, 2008.

[21] X. Cai, J. Huang, and L. Liu. Stability analysis of linear time-delay differential inclusion systems subject to input saturation. *IET Control Theory and Applications*, 4:2592–2602, 2010.

[22] E.F. Camacho and C. Bordons. *Model* P*redictive* C*ontrol*. Springer, 2005.

[23] F. Campos-Cornejo, D.U. Campos-Delgado, E. Dassau, H. Zisser, L. Jovanovic, and F.J. Doyle III. Adaptive control algorithm for a rapid and slow acting insulin therapy following run-to-run methodology. In *2010 American Control Conference*, 2010.

[24] D.U. Campos-Delgado, F. Campos-Cornejo, and M. Hernandez-Ordonez. Extension of the run-to-run control to multi-boluses schemes. In *17th IEEE International Conference on Control Applications Part of 2008 IEEE Multi-conference on Systems and Control*, 2008.

[25] B.D.O. Capron, M.T. Uchiyama, and D. Odloak. Linear matrix inequality-based robust model predictive control for time-delayed systems. *IET Control Theory and Applications*, 6:37–50, 2011.

[26] H. Chen and F. Allgöwer. A quasi-infinite horizon nonlinear model predictive control scheme with guaranteed stability. *Automatica*, 34:1205–1217, 1998.

[27] H. Chen, X. Gao, H. Wang, and R. Findeisen. On disturbance attenuation of nonlinear moving horizon control. *Assessment and Future Directions of Nonlinear Model Predictive Control, Lecture Notes in Control and Information Sciences*, 358:283–294, 2007.

[28] H. Chen, C.W. Scherer, and F. Allgöwer. A game theoretic approach to nonlinear robust receding horizon control of constrained systems. In *Proceedings of the American Control Conference*, 1997.

[29] W.-H. Chen, D.J. Ballance, and J. O'Reilly. Optimization of Attraction Domains of Nonlinear MPC via LMI Methods. In *Proceedings of the American Control Conference*, 2001.

[30] D. Chu, T. Chen, and H.J. Marquez. Offline robust model predictive control with rewinding prediction. In *Proceedings of the 2006 American Control Conference*, 2006.

[31] A. Cohen. Rate of convergence of several conjugate gradient algorithms. *SIAM J. Numer. Anal.*, 9:248–259, 1972.

[32] M. Crouzeix and A.L. Mignot. *Analyse numérique des équations différentielles*. Masson Paris, 1989.

[33] Y.H. Dai and Y. Yuan. Convergence properties of beale-powell restart algorithm. *Science in China Series A: Mathematics*, 41:1142–1150, 1998.

[34] Z. Dai and F. Wen. Global convergence of a modified hestenes-stiefel nonlinear conjugate gradient method with armijo line search. *Numer. Algor.*, 59:79–93, 2012.

[35] J.F. de Canetea, S. Gonzalez-Pereza, and J.C. Ramos-Diaz. Artificial neural networks for closed loop control of in silico and ad hoc type 1 diabetes. *Computer methods and programs in biomedicine*, 106:55–66, 2012.

[36] D. Munoz de la Pena, A. Bemporad, and C. Filippi. Robust explicit MPC based on approximate multiparametric convex programming. *IEEE Transactions on Automatic Control*, 51:1399–1403, 2006.

[37] The diabetes control and complications trial research group (DCCT). The effect of intensive treatment of diabetes on the development and progression of long-term complications in insulin-dependent diabetes mellitus. *N. Engl. J. Med.*, 329:977–986, 1993.

[38] A. Domahidi, M.N. Zeilinger, M. Morari, and C.N. Jones. Learning a feasible and stabilizing explicit model predictive control law by robust optimization. In *2011 50th IEEE Conference on Decision and Control and European Control Conference (CDC-ECC)*, 2011.

[39] J. Doyle, J.A. Primbs, B. Shapiro, and V. Nevistic. Nonlinear games: examples and counterexamples. In *35th Conference on Decision and Control*, 1996.

[40] F.J. DoyleIII. Zone model predictive control of an artificial pancreas. In *Proceedings of the 10th World Congress on Intelligent Control and Automation*, 2012.

[41] J. Dunik, M. Simandl, and O. Straka. Unscented kalman filter: Aspects and adaptive setting of scaling parameter. *IEEE Transactions on Automatic Control*, 57:2411–2416, 2012.

[42] C. Emharuethai and P. Niamsup. Robust h_∞ control of linear systems with interval non differentiable time-varying delays. In *10th World Congress on Intelligent Control and Automation*, 2012.

[43] R. Mahboobi Esfanjani and S.K. Nikravesh. Stabilizing model predictive control for constrained nonlinear distributed delay systems. *ISA Transactions*, 50:201–206, 2011.

[44] R. Mahboobi Esfanjani and S.K.Y. Nikravesh. Stabilizing predictive control of non-linear time-delay systems using control lyapunovkrasovskii functionals. *IET Control Theory and Applications*, 3:13951400, 2009.

[45] R.M. Esfanjani and S.K.Y. Mikravesh. Robust model predictive control for constrained distributed delay systems. In *International Symposium on Information, Communication and Automation Technologies*, 2009.

[46] M. Farina and R. Scattolini. Tube-based robust sampled-data MPC for linear continuous-time systems. *Automatica*, 48:14731476, 2012.

[47] R. Findeisen. *Nonlinear Model Predictive Control: A Sampled-Data Feedback Perspective*. PhD thesis, University of Stuttgart, 2004.

[48] R. Findeisen and F. Allgöwer. Robustness properties and output feedback of optimization based sampled-data open-loop feedback. In *Proceedings of the 44th IEEE Conference on Decision and Control, and the European Control Conference 2005*, 2005.

[49] M.E. Fisher. A semi closed-loop algorithm for the control of blood glucose levels in diabetics. *IEEE Transactions on Biomedical Engineering*, 38:57–61, 1991.

[50] F.A.C.C. Fontes. A general framework to design stabilizing nonlinear model predictive controllers. *Systems and Control Letters*, 42:127–143, 2001.

[51] F.A.C.C. Fontes and L. Magni. Min max model predictive control of nonlinear systems using discontinuous feedbacks. *IEEE Transactions on Automatic Control*, 43:1750–1755, 2003.

[52] Centers for Disease Control and (Atlanta GA) Prevention, National diabetes fact sheet, 2011.

[53] E. Fridman. A refined input delay approach to sampled data control. *Automatica*, 46:421–427, 2010.

[54] E. Fridman, U. Shaked, and V. Suplin. Input/output delay approach to robust sampled-data H_∞ control. *Systems and Control Letters*, 54:271–282, 2005.

[55] P. Gahinet, A. Nemirovski, A. J. Laub, and M. Chilali. LMI *Control Toolbox for use with* M*atlab*. The Math-Works, Inc., 1995.

[56] M. Gao, Z. He, and Y. Liu. Improved unscented kalman filter for bounded state estimation. In *International Conference on Electronics, Communications and Control*, 2011.

[57] X. Gao and Y. Wang. Closed-loop blood glucose control using dual subcutaneous infusion of insulin and glucagon based on switching pid controller. In *Proceedings of the 10th World Congress on Intelligent Control and Automation*, 2012.

[58] W. Garcia-Gabin, J. Vehi, J. Bondia, C. Tarin, and R. Calm. Robust sliding mode closed-loop glucose control with meal compensation in type 1 diabetes mellitus. In *Proceedings of the 17th World Congress The International Federation of Automatic Control*, 2008.

[59] L.C. Gatewood, E. Ackerman, J.W. Rosevear, and G.D. Molnar. Simulation studies of blood-glucose regulation: Effect of intestinal glucose absorption. *Computers and Biomedical Research*, 2:15–27, 1968.

[60] D. Gillbarg and N.S. Trudinger. *Elliptic partial differential equations of second order*. Springer Berlin, 1983.

[61] S. Gillijns and B. De Moor. Unbiased minimum-variance input and state estimation for linear discrete time systems. *Automatica*, 43:111–116, 2007.

[62] G. Grimm, M.J. Messina, S.E. Tuna, and A.R. Teel. Examples when nonlinear model predictive control is non robust. *Automatica*, 40:1729–1738, 2004.

[63] J.K. Gruber, D.R. Ramirez, T. Alamo, and E.F. Camacho. Minmax MPC based on an upper bound of the worst case cost with guaranteed stability. application to a pilot plant. *Journal of Process Control*, 21:194–204, 2011.

[64] L. Gruene, D. Nesic, and J. Pannek. Model predictive sampled data redesign for nonlinear systems. In *44th IEEE Conference on Decision and Control, and the European Control Conference 2005*, 2005.

[65] K. Gu, V.L. Kharitonov, and J. Chen. *Stability of Time-Delay Systems*. Birkhäuser, 2002.

[66] C. Han, X. Liu, and H. Zhang. Robust model predictive control for continuous uncertain systems with state delay. *J. Control Theory Appl.*, 6:189–194, 2008.

[67] X. Hao and Y. Wang. Guaranteed cost control of polynomial nonlinear uncertain systems with time-delay. *Practical Applications of Intelligent Systems Advances in Intelligent and Soft Computing*, 124:553–562, 2012.

[68] Y. Hao, Z. Xiong, F. Sun, and X. Wang. Comparisons of unscented kalman filters. In *IEEE International Conference on Mechatronics and Automation*, 2007.

[69] J. Hauser and A. Saccon. A barrier function method for the optimization of trajectory functionals with constraints. In *Proceedings of the 45th IEEE Conference on Decision & Control*, 2006.

[70] N. Haverbeke, M. Diehl, and B. De Moor. A structure exploiting interior-point method for moving horizon estimation. In *Join 48th IEEE Conference on Decision and Control and 28th Chinese Control Conference*, 2009.

[71] A.G. Gallardo Hernandez, L. Fridman, A. Levant, Y. Shtessel, R. Leder, C.R. Monsalve, and S. Andrade. High-order sliding-mode control for blood glucose: Practical relative degree approach. *Control Engineering Practice*, http://dx.doi.org/10.1016/j.conengprac.2012.11.015i: 2013.

[72] R. Hovorka. Continuous glucose monitoring and closed-loop systems. *Diabetic Med.*, 23:1–12, 2006.

[73] R. Hovorka, V. Canonico, L.J. Chassin, U. Haueter, M. Massi-Benedetti, M.O. Federici, T.R. Pieber, H.C. Schaller, L. Schaupp, T. Vering, and M.E. Wilinska. Nonlinear model predictive control of glucose concentration in subjects with type 1 diabetes. *Physiol. Meas.*, 25:905–920, 2004.

[74] T. Hu and Z. Lin. Composite quadratic lyapunov functions for constrained control system. *IEEE Transaction on Automatic Control*, 48:440–450, 2003.

[75] J. Huang, Z. Han, X. Cai, and L. Liu. Robust stabilization of linear differential inclusions with affine uncertainty. *Circuits Syst. Signal Process.*, 30:1369–1382, 2011.

[76] F.J. Doyle III, B.W. Bequette, R. Middleton, B. Ogunnaike, B. paden, R.S. Parker, and M. Vidyasagar. Control in biological system. *The impact of Control Technology*, www.ieeecs.org:[online], 2011.

[77] S. Ishihara and M. Yamakita. Constrained state estimation for nonlinear systems with non-gaussian noise. In *48th IEEE Conference on Decision and Control and 28th Chinese Control Conference*, 2009.

[78] A. Isidori. *Nonlinear Control Systems, third edition*. Springer Verlag London, 1995.

[79] G.E. Ivanov and V.A. Kazeev. Minimax algorithm for constructing an optimal control strategy in differential games with a lipschitz payoff. *Computational Mathematics and Mathematical Physics*, 51:550–574, 2011.

[80] M.A. Jaradat and Y. Sardahi. Optimal pid-fuzzy logic controller for type 1 diabetic patients. In *8th International Symposium on Mechatronics and its Applications (ISMA)*, 2012.

[81] N. Jiang, B. Liu, Y. jing, and G.M. Dimirovski. Minimax robust control of structured uncertain time-delay systems. In *2008 American Control Conference*, 2008.

[82] S. Julier and K. Uhlmann. Reduced sigma point filters for the propagation of means and covariances through nonlinear transformation. In *Proceedings of tha American Control Conference*, 2002.

[83] R.E. Kalman. A new approach to linear filtering and prediction problems. *Transaction of the ASME, Journal of Basic Engineering*, .:35–45, 1960.

[84] H. Katayama and A. Ichikawa. Receding horizon H_∞ control for time-varying sampled-data systems. In *Proceedings of the 44th IEEE Conference on Decision and Control, and the European Control Conference 2005*, 2005.

[85] H. Katayama and A. Ichikawa. Receding horizon H_∞ control for nonlinear sampled data systems. In *Proceedings of the 17th International Symposium on Mathematical Theory of Networks and Systems*, 2006.

[86] H. Katayama and A. Ichikawa. Robust model predictive control for sampled-data systems. In *SICE-ICASE International Joint Conference 2006*, 2006.

[87] D. Barry Keenan, J.J. Mastrototaro, S.A. Weinzimmer, and G.M. Steil. Interstitial fluid glucose time-lag correction for real-time continuous glucose monitoring. *Biomedical Signal Processing and Control*, 8:81–89, 2012.

[88] J. Kierzenka, L.F. Shampine, and S. Thompson. Solving delay differential equations with DDE23. Technical report, Mathworks, 2000.

[89] H. Kirchsteiger and L. del Re. Reduced hypoglycemia risk in insulin bolus therapy using asymmetric cost functions. In *Proceedings of the 7th Asian Control Conference, Hong Kong, China*, 2009.

[90] B.P. Kovatchev, M. Breton, C. Dalla Man, and C. Cobelli. In silico preclinical trials: A proof of concept in closed-loop control of type 1 diabetes. *Journal of Diabetes Science and Technology*, 3:44–55, 2009.

[91] R. Kuiava, R.A. Ramos, and H.R. Pota. A new procedure for modeling nonlinear systems via norm bounded linear differential inclusions. In *Australian Control Conference*, 2011.

[92] M. Lazar, D. Munoz de la Pena, W.P.M.H. Heemels, and T. Alamo. On input-to-state stability of min-max nonlinear model predictive control. *Systems and Control Letters*, 57:39–48, 2008.

[93] B.S. Leon, A.Y. Alanis, E.N. Sanchez, F. Ornelas, and E. Ruiz-Velazquez. Subcutaneous blood glucose neural inverse optimal control for type 1 diabetes mellitus patients. In *World Automation Congress (WAC)*, 2012.

[94] D. Limon, T. Alamo, and E.F. Camacho. Robust stability of min-max MPC controllers for nonlinear systems with bounded uncertainties. In *16th Symposium on Mathematical Theory of Networks and Systems*, 2004.

[95] D. Limon, T. Alamo, F. Salas, and E.F. Camacho. Input to state stability of min-max MPC controllers for nonlinear systems with bounded uncertainties. *Automatica*, 42:797–803, 2006.

[96] K. Lunze, T. Singh, M. Walter, M.D. Brendel, and S. Leonhardt. Blood glucose control algorithms for type 1 diabetic patients: A methodological review. *Biomedical Signal Processing and Control*, 8:107–119, 2013.

[97] C. Magnan. Production and secretion of insulin by the pancreatic β-cell. *EMC-Endocrinologie*, 2:241–264, 2005.

[98] L. Magni, H. Nijmeijer, and A.J. van der Schaft. A receding horizon approach to the nonlinear H_∞ control problem. *Automatica*, 37:429–435, 2001.

[99] L. Magni, D.M. Raimondo, G. De Nicolao, B. Kovatchev, and C. Cobelli. Model predictive control of glucose concentration in subjects with type 1 diabetes: an in silico trial. In *Proceedings of the 17th World Congress the International Federation of Automatic Control*, 2008.

[100] L. Magni, D.M. Raimondo, and R. Scattolini. Regional input-to-state stability for nonlinear model predictive control. *IEEE Transactions on Automatic Control*, 51:1548–1553, 2006.

[101] L. Magni and R. Scattolini. Model Predictive Control of Continuous-Time Nonlinear Systems with Piecewise Constant Control. *IEEE Transactions on Automatic Control*, 49:900–906, 2004.

[102] L. Magni, C. Toffanin, C. Dalla Man, B. Kovatchev, C. Cobelli, and G. De Nicolao. Model predictive control of type 1 diabetes added to conventional therapy. In *18th IFAC World Congress*, 2011.

[103] M.S. Mahmoud. *Robust control and filtering for time-delay systems*. Control Engineering (Marcel Dekker), 2000.

[104] M.S. Mahmoud. *Switched Time-Delay Systems*. Springer, 2010.

[105] A. Makroglou, J. Li, and Y. Kuang. Mathematical models and software tools for the glucose-insulin regulatory system and diabetes: an overview. *Applied Numerical Mathematics*, 56:559–573, 2006.

[106] C. Dalla Man, R.A. Rizza, and C. Cobelli. Meal simulation model of the glucose-insulin system. *IEEE Transactions on Biomedical Engineering*, 54:1740–1749, 2007.

[107] Z. Mao, B. Jiang, and P. Shi. Fault-tolerant control for a class of nonlinear sampled-data systems via a euler approximate observer. *Automatica*, 46:1852–1859, 2010.

[108] N. Marchand and A. Alamir. From open loop trajectories to stabilizing state feedback - application to a CSTR. In *IFAC Symposium on System Structure and Control*, 1998.

[109] G. Marchetti, M. Barolo, L. Jovanovic, H. Zisser, and D.E. Seborg. An improved pid switching control strategy for type 1 diabetes. *IEEE Transactions on Biomedical Engineering*, 55:857–865, 2008.

[110] D. Mayne, J.B. Rawling, C. Rao, and P. Scokaert. Constrained model predictive control: Stability and optimality. *Automatica*, 36:789–814, 2000.

[111] D.Q. Mayne, S.V. Rakovic, R.B. Vinter, and E.C. Kerrigan. Characterization of the solution to a constrained H_∞ optimal control problem. *Automatica*, 42:371–382, 2006.

[112] H. Michalska and D.Q. Mayne. Robust receding horizon control of constrained nonlinear systems. *IEEE Transactions on Automatic Control*, 38:1623–1633, 1993.

[113] B.S.N. Murty and A. Husain. Orthogonality correction in the conjugate gradient method. *Journal of Computational and Applied Mathematics*, 9:299–304, 1983.

[114] D. Nesic and L. Gruene. A receding horizon control approach to sampled-data implementation of continuous-time controllers. *Systems and Control Letters*, 55:660–672, 2006.

[115] G. De Nicolao, L. Magni, C. Dalla Man, and C. Cobelli. Modeling and control of diabetes: Towards the artificial pancreas. In *18th IFAC World Congress, Milano*, 2011.

[116] J. Nocedal and S.J. Wright. *Numerical Optimization*. Springer, 1999.

[117] C. Owens, H. Zisser, L. Jovanovic, B. Srinivasan, D. Bonvin, and F.J. Doyle III. Run-to-run control of blood glucose concentrations for people with type 1 diabetes mellitus. *IEEE Transactions on Biomedical Engineering*, 53:996–1005, 2006.

[118] M.M. Ozyetkin, N. Nath, E. Tatlicioglu, and D.M. Dawson. A new robust nonlinear control algorithm for the regulation of blood glucose in diabetic patients. In *IEEE International Conference on Control Applications*, 2012.

[119] C.C. Palerm, H. Zisser, L. Jovanovic, and F.J. DoyleIII. A run-to-run control strategy to adjust basal insulin infusion rates in type 1 diabetes. *Journal of Process Control*, 18:258–265, 2008.

[120] R.S. Parker, F.J. Doyle III, J.H. Ward, and N.A. Peppas. Robust H_∞ glucose control in diabetes using a physiological model. *AIChE*, 46:2537–2549, 2000.

[121] S.D. Patek, L. Magni, E.Dassau, C. Hughes-Karvetski, C. Toffanin, G. De Nicolao, S. Del Favero, M. Breton, C. Dalla Man, E. Renard, H. Zisser, III F.J. Doyle, C. Cobelli, B.P. Kovatchev, and International Artificial Pancreas (iAP) Study Group. Modular closed-loop control of diabetes. *IEEE Transactions on Biomedical Engineering*, 59:2986–2999, 2012.

[122] M.W. Percival, Y. Wang, B. Grosman, E. Dassau, H. Zisser, L. Jovanovic, and F.J. DoyleIII. Development of a multi-parametric model predictive control algorithm for insulin delivery in type 1 diabetes mellitus using clinical parameters. *Journal of Process Control*, 21:391–404, 2011.

[123] E.M. Pfeiffer, C. Thum, and A.H. Clemens. The artificial beta cell, a continuous control of blood sugar by external regulation of insulin infusion. *Horm. Metab. Res.*, 6:339–342, 1974.

[124] P. Philipp. Structure exploiting derivative computation for moving horizon estimation. In *American Control Conference*, 2011.

[125] B. Picasso, D. Desiderio, and R. Scattolini. Robust stability analysis of nonlinear discrete-time systems with application to MPC. *IEEE Transactions on Automatic Control*, 57:185–191, 2012.

[126] S.J. Qin and T.A. Badgwell. A survey of industrial model predictive control technology. *Control Engineering Practice*, 11:733–764, 2003.

[127] C. Qu. *Nonlinear Estimation for Model Based Fault Diagnosis of Nonlinear Chemical Systems*. PhD thesis, Texas A and M University, 2009.

[128] T. Raff and F. Allgöwer. An ekf-based observer for nonlinear time-delay systems. In *Proceedings of the 2006 American Control Conference*, 2006.

[129] D.M. Raimondo. *Nonlinear Model Predictive Control Stability, Robustness and Applications*. PhD thesis, University of Pavia, 2008.

[130] D.M. Raimondo, D. Limon, M. Lazar, L. Magni, and E.F. Camacho. Min-max model predictive control of nonlinear systems : a unifying overview on stability. *European Journal of Control*, 15:528, 2009.

[131] R. Rajamani. Observers for lipschitz nonlinear systems. *IEEE Transaction on Automatic Control*, 43:397–401, 1998.

[132] D.R. Ramirez, T. Alamo, E.F. Camacho, and D. Munoz de la Pena. Min-Max MPC based on a computationally efficient upper bound of the worst case cost. *Journal of Process Control*, 16:511519, 2006.

[133] C.V. Rao, J.B. Rawlings, and D.Q. Mayne. Constrained state estimation for nonlinear discrete-time systems: Stability and moving horizon approximations. *IEEE Transactions on Automatic Control*, 48:246–258, 2003.

[134] M. Reble and F. Allgöwer. General design parameters of model predictive control for nonlinear time-delay systems. In *49th IEEE Conference on Decision and Control*, 2010.

[135] M. Reble and F. Allgöwer. Design of terminal cost functionals and terminal regions for model predictive control of nonlinear time-delay systems. *Time Delay Systems: Methods, Applications and New Trends Lecture Notes in Control and Information Sciences*, 423:355–366, 2012.

[136] K. Reif, S. Guenther, and R. Unbehauen. Stochastic stability of the discrete-time extended kalman filter. *IEEE Transactions on Automatic Control*, 44:714–728, 1999.

[137] K. Reif, S. Guenther, and R. Unbehauen. Stochastic stability of the continuous-time extended kalman filter. *IEE Proceedings- Control Theory and Applications*, 147:45–52, 2000.

[138] C.H. Reinsch. Smoothing by spline functions. *Numerische Mathematik*, 10:177–183, 1967.

[139] E. Renard. Insulin delivery route for the artificial pancreas: Subcutaneous, intraperitoneal, or intravenous? pros and cons. *Journal of Diabetes Science and Technology*, 2:735–738, 2008.

[140] J.P. Richard. Time-delay systems: an overview of some recent advances and open problems. *Automatica*, 39:1667–1694, 2003.

[141] E. Rocha-Cozatl, J.A. Moreno, and A. Vandle Wouwer. Application of a continuous-discrete unknown input observer to estimation in phytoplanktonic cultures. In *8th IFAC Symposium on Advanced Control of Chemical Processes*, 2012.

[142] M. Rubagotti, D.M. Raimondo, A. Ferrara, and L. Magni. Robust Model Predictive Control with Integral Sliding Mode in Continuous-Time Sampled-Data Nonlinear Systems. *IEEE Transactions on Automatic Control*, 56:556–570, 2011.

[143] L.O. Santos and L.T. Biegler. A tool to analyze robust stability for model predictive controllers. *Journal of Process Control*, 9:233–246, 1999.

[144] S. Sarkka. On unscented kalman filtering for state estimation of continuous-time nonlinear systems. *IEEE Transactions on Automatic Control*, 52:1631–1641, 2007.

[145] L. Schwartz. *Calcul différentiel et* E*quations différentielles, tome II :* A*nalyse*. Hermann, 1997.

[146] P.O.M. Scokaert, D.Q. Mayne, and J.B. Rawlings. Suboptimal model predictive control (feasibility implies stability). *IEEE Transactions on Automatic Control*, 44:648–654, 1999.

[147] Z. Shen, J. Zhao, J. Xu, and X. Gu. Nonlinear unknown input observer design by LMI for lipschitz nonlinear systems. In *8th World Congress on Intelligent Control and Automation*, 2010.

[148] J.R. Shewchuk. *An introduction to the conjugate gradient method without the agonizing pain*. Citeseer, 1994.

[149] S. Shi and L. Yu. Adaptive robust control for uncertain nonlinear systems with time-delay. *Recent Advances in Computer Science and Information Engineering, Lecture Notes in Electrical Engineering*, 129:135–140, 2012.

[150] C.A. Silva. On sampled-data models for model predictive control. In *IECON. 2010 - 36th Annual Conference on IEEE Industrial Electronics Society*, 2010.

[151] J.T. Sorensen. *A Physiologic Model of Glucose Metabolism in Man and its Use to Design and Assess Improved Insulin Therapies for Diabetes*. PhD thesis, MIT, 1985.

[152] J. Stecha and V. Havlena. Unscented kalman filter revisited - hermite-gauss quadrature approach. In *15th International Conference on Information Fusion*, 2012.

[153] G.M. Steil, A.E. Panteleon, and K. Rebrin. Closed-loop insulin deliverythe path to physiological glucose control. *Advanced Drug Delivery Reviews*, 56:125–144, 2004.

[154] J. Styskal, H. Van Remmen, A. Richardson, and A.B. Salmon. Oxidative stress and diabetes: What can we learn about insulin resistance from antioxidant mutant mouse models? *Free Radical Biology & Medicine*, 52:46–58, 2012.

[155] P.S. Teh. Observer-based residual design for nonlinear systems with unknown inputs. In *Australian Control Conference*, 2011.

[156] K. van Heusden, E. Dassau, H.C. Zisser, D.E. Seborg, and F.J. Doyle III. Control-relevant models for glucose control using a priori patient characteristics. *IEEE Transactions on Biomedical Engineering*, 59:1839–1849, 2012.

[157] A. Voelker, K. Kouramas, and E.N. Pistikopulos. Simultaneous constrained moving horizon state estimation and model predictive control by multi-parametric programming. In *49th IEEE Conference on Decision and Control*, 2010.

[158] C. Wang and Y. Chen. Robust h_∞ control for stochastic systems with nonlinearity, uncertainty and time-varying-delay. *Computers and Mathematics with Applications*, 63:985–998, 2012.

[159] Y. Wang, E. Dassau, and F.J. Doyle III. Closed-loop control of artificial pancreatic β-cell in type 1 diabetes mellitus using model predictive iterative learning control. *IEEE Transactions on Biomedical Engineering*, 57:211–219, 2010.

[160] C.L. Wei, J.S.H. Tsai, S.M. Guo, and L.S. Sieh. Universal predictive kalman filter-based fault estimator and tracker for sampled-data non-linear time-varying system. *IET Control Theory and Applications*, 5:203–220, 2011.

[161] Q. Weiwei, Z. Zhiqiang, L. Peng, and L. Gang. Improved off-line formulation of robust model predictive control for a discrete time uncertain system. In *Proceedings ofthe 2009 IEEE International Conference on Mechatronics and Automation*, 2009.

[162] M.E. Wilinska and R. Hovorka. Simulation models for in silico testing of closed-loop glucose controllers in type 1 diabetes. *Drug Discovery Today: Disease Models*, 5:289–298, 2008.

[163] D.R. Worthington. Minimal model of food absorption in the gut. *Med. Inform.*, 22:35–45, 1997.

[164] H. Yoo, Y.S. Lee, and S. Han. Constrained receding horizon controls for nonlinear time-delay systems. *Nonlinear Dyn.*, 69:149158, 2012.

[165] J. El Youssef and W.K. Ward J. Castle. A review of closed-loop algorithms for glycaemic control in the treatment of type 1 diabetes. *Algorithms*, 2:518–532, 2009.

[166] S. Yu, H. Chen, and F. Allgöwer. Tube MPC scheme based on robust control invariant set with application to lipschitz nonlinear systems. In *2011 50th IEEE Conference on Decision and Control and European Control Conference (CDC-ECC)*, 2011.

[167] S. Yu, M. Reble, H. Chen, and F. Allgöwer. Inherent robustness properties of quasi-infinite horizon MPC. In *18th IFAC World Congress, Milano*, 2011.

[168] K. Zarkogianni, A. Vazeou, S.G. Mougiakakou, A. Prountzou, and K.S. Nikita. An insulin infusion advisory system based on auto tuning nonlinear model-predictive control. *IEEE Transactions on Biomedical Engineering*, 58:2467–2477, 2011.

[169] V. Zavala, C.D. Laid, and L.T. Biegler. A fast moving horizon estimation algorithm based on nonlinear programming sensitivity. *Journal of Process Control*, 18:876–884, 2008.

Chapter 12

Appendix

12.1 $\mathcal{K}$, $\mathcal{K}^\infty$, $\mathcal{KL}$ functions

Let us remind the definition and various properties on $\mathcal{K}$, $\mathcal{K}^\infty$ and $\mathcal{KL}$ functions (see e.g. [94]):

Definition 6. *a) A function $\alpha : \mathbb{R}^+ \to \mathbb{R}^+$ is of class $\mathcal{K}$ if it is continuous, strictly increasing and $\alpha(0) = 0$,*

b) A function $\alpha : \mathbb{R}^+ \to \mathbb{R}^+$ is of class $\mathcal{K}^\infty$ if it is of class $\mathcal{K}$ and is unbounded,

c) A continuous function $\beta : \mathbb{R}^+ \times \mathbb{R}^+ \to \mathbb{R}^+$ is of class $\mathcal{KL}$ if $s \to \beta(s,\tau)$ is of class $\mathcal{K}$ for each $\tau \geq 0$ and $\tau \to \beta(s,\tau)$ is decreasing to zero for each s.

The following proposition recall some properties of $\mathcal{K}$, $\mathcal{K}^\infty$ and $\mathcal{KL}$ functions (see e.g. [94]).

Proposition 2. *Let $\theta_1 : \mathbb{R}^+ \to \mathbb{R}^+$ and $\theta_2 : \mathbb{R}^+ \to \mathbb{R}^+$ be $\mathcal{K}$ functions, let $\alpha_1 : \mathbb{R}^+ \to \mathbb{R}^+$ and $\alpha_2 : \mathbb{R}^+ \to \mathbb{R}^+$ be $\mathcal{K}^\infty$ functions and $\beta : \mathbb{R}^+ \times \mathbb{N} \to \mathbb{R}^+$ be a $\mathcal{KL}$ function, then:*

1) θ_1^{-1} *is a $\mathcal{K}$ function,*

2) $\theta_1 \circ \theta_2$ *is a $\mathcal{K}$ function,*

3) $\alpha_1^{-1}(.)$ *is a $\mathcal{K}^\infty$ function,*

4) $\alpha_1 \circ \alpha_2$ *is a $\mathcal{K}^\infty$ function,*

5) $\theta_1 \circ \beta$ *is a $\mathcal{KL}$ function,*

6) $\max(\theta_1, \theta_2)$ *is a $\mathcal{K}$ function,*

7) $\max(\alpha_1, \alpha_2)$ *is a $\mathcal{K}^\infty$ function,*

8) $\min(\theta_1, \theta_2)$ *is a $\mathcal{K}$ function,*

9) $\min(\alpha_1, \alpha_2)$ *is a $\mathcal{K}^\infty$ function,*

10) $\theta_1(s_1 + s_2) \leq \theta_1(s_1) + \theta_1(s_2)$,

11) $\theta_1(s_1) + \theta_1(s_2) \leq \theta_3(s_1 + s_2)$ *where* $\theta_3(s) = \theta_1(s) + \theta_2(s)$,

12) $\theta_1(s_1) + \theta_1(s_2) \geq \theta_4(s_1 + s_2)$ *where* $\theta_4(s) = \min\left(\theta_1\left(\frac{s}{2}\right), \theta_2\left(\frac{s}{2}\right)\right)$.

Finally, let us recall a last property related to the existence of a $\mathscr{K}$ function:

Proposition 3. *13) For all $\alpha \in \mathscr{K}^{\infty}$ there exists $\theta_5 \in \mathscr{K}^{\infty}$ such that $\theta_5(s) \leq \alpha_1(s)$ for all $s \geq 0$ and $\theta_6(s) = s - \theta_5(s)$ is a $\mathscr{K}$ function*

12.2 Gronwall-Bellman inequality

Let us recall the Gronwall inequality (see e.g. [10]):

Lemma 7 (Gronwall inequality)**.** *Be given three continuous functions ϕ, ψ and y:$[a;b] \to \mathbb{R}^+$ satisfying:*

$$\forall t \in [a;b],\ y(t) \leq \phi(t) + \int_a^t \psi(s)y(s)ds,$$

then for all $t \in [a;b]$

$$y(t) \leq \int_a^t \phi(s)\psi(s)\exp\left(\int_s^t \psi(u)du\right)ds + \phi(t).$$

If the function ϕ is equal to a constant $C \in \mathbb{R}^+$ then Gronwall inequality can be expressed as follows

$$\forall t \in [a;b],\ y(t) \leq C\exp\left(\int_a^t \psi(s)ds\right).$$

12.3 Schur complement

Let us recall the results concerning the Schur complement.

Theorem 6 (Schur complement)**.** *Be given three matrices R, Q and S where R and Q are symmetric then we have:*

$$\begin{cases} R < 0, \\ Q - SR^{-1}S^T < 0. \end{cases} \quad \textit{iff} \quad \begin{pmatrix} Q & S \\ \star & R \end{pmatrix} < 0. \tag{12.1}$$

12.4 Computation of the observation matrix Ω

In order to prove the observability of the model (6.6), we have to consider the computation of various Lie derivatives which are given as follows

$$h(x) = x_1. \tag{12.2}$$

$$L_G h(x) = a_1^{(0)}x_1 + a_5^{(0)}x_5 + a_{12}^{(0)}x_1x_2 + d^{(0)}, \tag{12.3}$$

where $a_1^{(0)} = -P_1$, $a_5^{(0)} = k_{gr}$, $a_{12}^{(0)} = -1$ and $d^{(0)} = P_1G_b$.

$$L_G^2 h(x) = a_1^{(1)}x_1 + a_2^{(1)}x_2 + a_5^{(1)}x_5 + a_6^{(1)}x_6 + a_{12}^{(1)}x_1x_2 + a_{13}^{(1)}x_1x_3 + a_{25}^{(1)}x_2x_5 + a_{122}^{(1)}x_1x_2^2 + d^{(1)}, \tag{12.4}$$

where $a_1^{(1)} = -P_1a_1^{(0)} - a_{12}^{(0)}P_3I_b$, $a_2^{(1)} = a_{12}^{(0)}P_1G_b$, $a_5^{(1)} = a_1^{(0)}k_{gr} - a_5^{(0)}c_2$, $a_6^{(1)} = a_5^{(0)}c_2$, $a_{12}^{(1)} = -a_1^{(0)} - a_{12}^{(0)}P_1 - a_{12}^{(0)}P_2$, $a_{13}^{(1)} = a_{12}^{(0)}P_3$, $a_{25}^{(1)} = a_{12}^{(0)}k_{gr}$, $a_{122}^{(1)} = -a_{12}^{(0)}$ and $d^{(1)} = a_1^{(0)}P_1G_b$

$$\begin{aligned}L_G^3 h(x) = {} & a_1^{(2)}x_1 + a_2^{(2)}x_2 + a_3^{(2)}x_3 + a_5^{(2)}x_5 + a_6^{(2)}x_6 + a_{12}^{(2)}x_1x_2 + a_{13}^{(2)}x_1x_3 + a_{14}^{(2)}x_1x_4 \\ & + a_{22}^{(2)}x_2^2 + a_{23}^{(2)}x_2x_3 + a_{25}^{(2)}x_2x_5 + a_{26}^{(2)}x_2x_6 + a_{35}^{(2)}x_3x_5 + a_{122}^{(2)}x_1x_2^2 + a_{123}^{(2)}x_1x_2x_3 \\ & + a_{225}^{(2)}x_2^2x_5 + a_{1222}^{(2)}x_1x_2^3 + d^{(2)},\end{aligned} \tag{12.5}$$

where $a_1^{(2)} = -a_1^{(1)}P_1 - P_3I_ba_{12}^{(1)}$, $a_2^{(2)} = a_{12}^{(1)}P_1G_b - a_2^{(1)}P_2 - 2P_3I_ba_{122}^{(1)}$, $a_3^{(2)} = a_{13}^{(1)}P_1G_b + a_2^{(1)}P_3$, $a_5^{(2)} = a_1^{(1)}k_{gr} - P_3I_ba_{25}^{(1)} - c_2a_5^{(1)}$, $a_6^{(2)} = c_2a_5^{(1)} - c_1a_6^{(1)}$, $a_{12}^{(2)} = -a_1^{(1)} - a_{12}^{(1)}P_1 - a_{12}^{(1)}P_2$, $a_{13}^{(2)} = -a_{13}^{(1)}P_1 + a_{12}^{(1)}P_3 - a_{13}^{(1)}k_f$, $a_{14}^{(2)} = b_fa_{13}^{(1)}$, $a_{22}^{(2)} = a_{122}^{(1)}P_1G_b - 2P_2a_{122}^{(1)}$, $a_{23}^{(2)} = 2a_{122}^{(1)}P_3$, $a_{25}^{(2)} = a_{12}^{(1)}k_{gr} - P_2a_{25}^{(1)} - c_2a_{25}^{(1)}$, $a_{26}^{(2)} = c_2a_{25}^{(1)}$, $a_{35}^{(2)} = a_{13}^{(1)}k_{gr} + P_3a_{25}^{(1)}$, $a_{122}^{(2)} = -a_{122}^{(1)}P_1 - a_{12}^{(1)}$, $a_{123}^{(2)} = -a_{13}^{(1)}$, $a_{225}^{(2)} = a_{122}^{(1)}k_{gr}$, $a_{1222}^{(2)} = -a_{122}^{(1)}$ and $d^{(2)} = a_1^{(1)}P_1G_b - a_2^{(1)}P_3 + a_6^{(1)}c_1d$.

$$\begin{aligned}L_G^4 h(x) = {} & a_1^{(3)}x_1 + a_2^{(3)}x_2 + a_3^{(3)}x_3 + a_4^{(3)}x_4 + a_5^{(3)}x_5 + a_6^{(3)}x_6 + a_{12}^{(3)}x_1x_2 + a_{13}^{(3)}x_1x_3 + a_{14}^{(3)}x_1x_4 \\ & + a_{22}^{(3)}x_2^2 + a_{23}^{(3)}x_2x_3 + a_{24}^{(3)}x_2x_4 + a_{25}^{(3)}x_2x_5 + a_{26}^{(3)}x_2x_6 + a_{33}^{(3)}x_3^2 + a_{35}^{(3)}x_3x_5 + a_{36}^{(3)}x_3x_6 + a_{45}^{(3)}x_4x_5 \\ & + a_{122}^{(3)}x_1x_2^2 + a_{123}^{(3)}x_1x_2x_3 + a_{124}^{(3)}x_1x_2x_4 + a_{133}^{(3)}x_1x_3^2 + a_{222}^{(3)}x_2^3 + a_{225}^{(3)}x_2^2x_5 + a_{226}^{(3)}x_2^2x_6 \\ & + a_{235}^{(3)}x_2x_3x_5 + a_{1222}^{(3)}x_1x_2^3 + a_{1223}^{(3)}x_1x_2^2x_3 + a_{2225}^{(3)}x_2^3x_5 + a_{12222}^{(3)}x_1x_2^4 + d^{(3)},\end{aligned} \tag{12.6}$$

where $a_1^{(3)} = -P_1a_1^{(2)} - P_3I_ba_{12}^{(2)}$, $a_2^{(3)} = P_1G_ba_{12}^{(2)} - P_2a_2^{(2)} - 2P_3I_ba_{22}^{(2)} + c_1da_{26}^{(2)}$, $a_3^{(3)} = P_1G_ba_{13}^{(2)} + P_3a_2^{(2)} - k_fa_3^{(2)}$, $a_4^{(3)} = P_1G_ba_{14}^{(2)} - P_3I_ba_{23}^{(2)} + b_fa_3^{(2)}$, $a_5^{(3)} = k_{gr}a_1^{(2)} - P_3I_ba_{25}^{(2)} - c_2a_5^{(2)}$, $a_6^{(3)} = -P_3I_ba_{26}^{(2)} + c_2a_5^{(2)} - c_1a_6^{(2)}$, $a_{12}^{(3)} = -a_1^{(2)} - P_1a_{12}^{(2)} - P_2a_{12}^{(2)} - 2P_3I_ba_{122}^{(2)}$, $a_{13}^{(3)} = -P_1a_{13}^{(2)} + P_3a_{12}^{(2)} - P_3I_ba_{123}^{(2)} - k_fa_{13}^{(2)}$, $a_{14}^{(3)} = -P_1a_{14}^{(2)} + b_fa_{13}^{(2)} - k_sa_{14}^{(2)}$, $a_{22}^{(3)} = P_1G_ba_{122}^{(2)} - P_22a_{22}^{(2)}$, $a_{23}^{(3)} = P_1G_ba_{123}^{(2)} + P_32a_{22}^{(2)} - P_2a_{23}^{(2)} - k_fa_{23}^{(2)}$, $a_{24}^{(3)} = b_fa_{23}^{(2)}$, $a_{25}^{(3)} = k_{gr}a_{12}^{(2)} - P_2a_{25}^{(2)} - 2P_3I_ba_{225}^{(2)} - c_2a_{25}^{(2)}$, $a_{26}^{(3)} = -P_2a_{26}^{(2)} + c_2a_{25}^{(2)} - c_1a_{26}^{(2)}$, $a_{33}^{(3)} = P_3a_{23}^{(2)}$, $a_{35}^{(3)} = k_{gr}a_{13}^{(2)} + P_3a_{25}^{(2)} - k_fa_{35}^{(2)} - c_2a_{35}^{(2)}$, $a_{36}^{(3)} = P_3a_{26}^{(2)} + c_2a_{35}^{(2)}$, $a_{45}^{(3)} = k_{gr}a_{14}^{(2)} + b_fa_{35}^{(2)}$, $a_{122}^{(3)} = -a_{12}^{(2)} - P_1a_{122}^{(2)} - 2P_2a_{122}^{(2)} - 3P_3I_ba_{1222}^{(2)}$, $a_{123}^{(3)} = -a_{13}^{(2)} - P_1a_{123}^{(2)} + 2P_3a_{122}^{(2)} - P_2a_{123}^{(2)} - k_fa_{123}^{(2)}$, $a_{124}^{(3)} = -a_{14}^{(2)} + b_fa_{123}^{(2)}$, $a_{133}^{(3)} = P_3a_{123}^{(2)}$, $a_{222}^{(3)} = P_1G_ba_{1222}^{(2)}$, $a_{225}^{(3)} = k_{gr}a_{122}^{(2)} - 2P_2a_{225}^{(2)} - c_2a_{225}^{(2)}$, $a_{226}^{(3)} = c_2a_{225}^{(2)}$, $a_{235}^{(3)} = k_{gr}a_{123}^{(2)} + 2P_3a_{225}^{(2)}$, $a_{1222}^{(3)} = -a_{122}^{(2)} - P_1a_{1222}^{(2)} - 3P_2a_{1222}^{(2)}$, $a_{1223}^{(3)} = -a_{123}^{(2)} + 3P_3a_{1222}^{(2)}$, $a_{2225}^{(3)} = k_{gr}a_{1222}^{(2)}$, $a_{12222}^{(3)} = -a_{1222}^{(2)}$ and $d^{(3)} = P_1G_ba_1^{(2)} - P_3I_ba_2^{(2)} + ua_{14}^{(2)} + c_1da_6^{(2)}$.

$$\begin{aligned}L_G^5 h(x) = {} & a_1^{(4)}x_1 + a_2^{(4)}x_2 + a_3^{(4)}x_3 + a_4^{(4)}x_4 + a_5^{(4)}x_5 + a_6^{(4)}x_6 + a_{12}^{(4)}x_1x_2 + a_{13}^{(4)}x_1x_3 + a_{14}^{(4)}x_1x_4 + a_{22}^{(4)}x_2^2 \\ & + a_{23}^{(4)}x_2x_3 + a_{24}^{(4)}x_2x_4 + a_{25}^{(4)}x_2x_5 + a_{26}^{(4)}x_2x_6 + a_{33}^{(4)}x_3^2 + a_{34}^{(4)}x_3x_4 + a_{35}^{(4)}x_3x_5 + a_{36}^{(4)}x_3x_6 \\ & + a_{45}^{(4)}x_4x_5 + a_{46}^{(4)}x_4x_6 + a_{122}^{(4)}x_1x_2^2 + a_{123}^{(4)}x_1x_2x_3 + a_{124}^{(4)}x_1x_2x_4 + a_{133}^{(4)}x_1x_3^2 + a_{134}^{(4)}x_1x_3x_4 \\ & + a_{222}^{(4)}x_2^3 + a_{223}^{(4)}x_2^2x_3 + a_{225}^{(4)}x_2^2x_5 + a_{226}^{(4)}x_2^2x_6 + a_{235}^{(4)}x_2x_3x_5 + a_{236}^{(4)}x_2x_3x_6 \\ & + a_{245}^{(4)}x_2x_4x_5 + a_{335}^{(4)}x_3^2x_5 + a_{1222}^{(4)}x_1x_2^3 + a_{1223}^{(4)}x_1x_2^2x_3 + a_{1224}^{(4)}x_1x_2^2x_4 \\ & + a_{1233}^{(4)}x_1x_2x_3^2 + a_{2222}^{(4)}x_2^4 + a_{2225}^{(4)}x_2^3x_5 + a_{2226}^{(4)}x_2^3x_6 + a_{2235}^{(4)}x_2^2x_3x_5 + a_{12222}^{(4)}x_1x_2^4 \\ & + a_{12223}^{(4)}x_1x_2^3x_3 + a_{22225}^{(4)}x_2^4x_5 + a_{122222}^{(4)}x_1x_2^5 + d^{(4)},\end{aligned} \tag{12.7}$$

where $a_1^{(4)} = -P_1a_1^{(3)} - P_3I_ba_{12}^{(3)} + ua_{14}^{(3)}$, $a_2^{(4)} = P_1G_ba_{12}^{(3)} - P_2a_2^{(3)} - 2P_3I_ba_{22}^{(3)} + ua_{24}^{(3)} + c_1da_{26}^{(3)}$, $a_3^{(4)} = P_1G_ba_{13}^{(3)} + P_3a_2^{(3)} - P_3I_ba_{23}^{(3)} - k_fa_3^{(3)} + c_1da_{36}^{(3)}$, $a_4^{(4)} = P_1G_ba_{14}^{(3)} - P_3I_ba_{24}^{(3)} + b_fa_3^{(3)} - k_sa_4^{(3)}$, $a_5^{(4)} = k_{gr}a_1^{(3)} -$

$P_1a_{12}^{(3)} - P_3I_ba_{25}^{(3)} + ua_{45}^{(3)} - c_2a_5^{(3)}$, $a_6^{(4)} = -P_3I_ba_{26}^{(3)} + c_2a_5^{(3)} - c_1a_6^{(3)}$, $a_{12}^{(4)} = -a_1^{(3)} - P_2a_{12}^{(3)} - 2P_3I_ba_{122}^{(3)} + ua_{124}^{(3)}$, $a_{13}^{(4)} = -P_1a_{13}^{(3)} + P_3a_{12}^{(3)} - P_3I_ba_{123}^{(3)} - k_fa_{13}^{(3)}$, $a_{14}^{(4)} = -P_1a_{14}^{(3)} - P_3I_ba_{124}^{(3)} + b_fa_{13}^{(3)} - k_sa_{14}^{(3)}$, $a_{22}^{(4)} = P_1G_ba_{122}^{(3)} - 2P_2a_{22}^{(3)} - 3P_3I_ba_{222}^{(3)} + c_1da_{226}^{(3)}$, $a_{23}^{(4)} = P_1G_ba_{123}^{(3)} + 2P_3a_{22}^{(3)} - P_2a_{23}^{(3)} - k_fa_{23}^{(3)}$, $a_{24}^{(4)} = P_1G_ba_{124}^{(3)} - P_2a_{24}^{(3)} + b_fa_{23}^{(3)} - k_sa_{24}^{(3)}$, $a_{25}^{(4)} = k_{gr}a_{12}^{(3)} - P_2a_{25}^{(3)} - 2P_3I_ba_{225}^{(3)} - c_2a_{25}^{(3)}$, $a_{26}^{(4)} = -P_2a_{26}^{(3)} - 2P_3I_ba_{226}^{(3)} + c_2a_{25}^{(3)} - c_1a_{26}^{(3)}$, $a_{33}^{(4)} = P_1G_ba_{133}^{(3)} + P_3a_{23}^{(3)} - 2k_fa_{33}^{(3)}$, $a_{34}^{(4)} = P_3a_{24}^{(3)} + 2b_fa_{33}^{(3)}$, $a_{35}^{(4)} = k_{gr}a_{13}^{(3)} + P_3a_{25}^{(3)} - P_3I_ba_{235}^{(3)} - k_fa_{35}^{(3)} - c_2a_{35}^{(3)}$, $a_{36}^{(4)} = P_3a_{26}^{(3)} - k_fa_{36}^{(3)} + c_2a_{35}^{(3)} - c_1a_{36}^{(3)}$, $a_{45}^{(4)} = k_{gr}a_{14}^{(3)} + b_fa_{35}^{(3)} - k_sa_{45}^{(3)} - c_2a_{45}^{(3)}$, $a_{46}^{(4)} = b_fa_{36}^{(3)} + c_2a_{45}^{(3)}$, $a_{122}^{(4)} = -a_{12}^{(3)} - P_1a_{122}^{(3)} - 2P_2a_{122}^{(3)} - 3P_3I_ba_{1222}^{(3)}$, $a_{123}^{(4)} = -a_{13}^{(3)} - P_1a_{123}^{(3)} + 2P_3a_{122}^{(3)} - P_2a_{123}^{(3)} - 2P_3I_ba_{1223}^{(3)} - k_fa_{123}^{(3)}$, $a_{124}^{(4)} = -a_{14}^{(3)} - P_1a_{124}^{(3)} - P_2a_{124}^{(3)} + b_fa_{123}^{(3)} - k_sa_{124}^{(3)}$, $a_{133}^{(4)} = -P_1a_{133}^{(3)} + P_3a_{123}^{(3)} - 2k_fa_{133}^{(3)}$, $a_{134}^{(4)} = P_3a_{124}^{(3)} + 2b_fa_{133}^{(3)}$, $a_{222} = P_1G_ba_{1222}^{(3)} - 3P_2a_{222}^{(3)}$, $a_{223} = P_1G_ba_{1223}^{(3)} + 3P_3a_{222}^{(3)}$, $a_{225}^{(4)} = k_{gr}a_{122}^{(3)} - 2P_2a_{225}^{(3)} - 3P_3I_ba_{2225}^{(3)} - c_2a_{225}^{(3)}$, $a_{226}^{(4)} = -2P_2a_{226}^{(3)} + c_2a_{225}^{(3)} - c_1a_{226}^{(3)}$, $a_{235}^{(4)} = k_{gr}a_{123}^{(3)} + 2P_3a_{225}^{(3)} - P_2a_{235}^{(3)} - k_fa_{235}^{(3)} - c_2a_{235}^{(3)}$, $a_{236}^{(4)} = 2P_3a_{226}^{(3)} + c_2a_{235}^{(3)}$, $a_{245}^{(4)} = k_{gr}a_{124}^{(3)} + b_fa_{235}^{(3)}$, $a_{335}^{(4)} = k_{gr}a_{133}^{(3)} + P_3a_{235}^{(3)}$, $a_{1222}^{(4)} = -a_{122}^{(3)} - P_1a_{1222}^{(3)} - 3P_2a_{1222}^{(3)} - 4P_3I_ba_{12222}^{(3)}$, $a_{1223}^{(4)} = -a_{123}^{(3)} - P_1a_{1223}^{(3)} + 3P_3a_{1222}^{(3)} - 2P_2a_{1223}^{(3)} - k_fa_{1223}^{(3)}$, $a_{1224}^{(4)} = -a_{124}^{(3)} + b_fa_{1223}^{(3)}$, $a_{1233}^{(4)} = -a_{133}^{(3)} + 2P_3a_{1223}^{(3)}$, $a_{2222}^{(4)} = P_1G_ba_{12222}^{(3)}$, $a_{2225}^{(4)} = k_{gr}a_{1222}^{(3)} - 3P_2a_{2225}^{(3)} - c_2a_{2225}^{(3)}$, $a_{2226}^{(4)} = c_2a_{2225}^{(3)}$, $a_{2235}^{(4)} = k_{gr}a_{1223}^{(3)} + 3P_3a_{2225}^{(3)}$, $a_{12222}^{(4)} = -a_{1222}^{(3)} - P_1a_{12222}^{(3)} - 4P_2a_{12222}^{(3)}$, $a_{12223}^{(4)} = -a_{1223}^{(3)} + 4P_3a_{12222}^{(3)}$, $a_{22225}^{(4)} = k_{gr}a_{12222}^{(3)}$, $a_{122222}^{(4)} = -a_{12222}^{(3)}$ and $d^{(4)} = P_1G_ba_1^{(3)} - P_3I_ba_2^{(3)} + ua_4^{(3)} + c_1da_6^{(3)}$.

It is deduced that the lines of Ω are given by

$$\nabla_x h(x) = \begin{pmatrix} 1 & 0 & 0 & 0 & 0 & 0 \end{pmatrix}, \tag{12.8}$$

$$\nabla_x L_G h(x) = \begin{pmatrix} a_1^{(0)} + a_{12}^{(0)}x_2 & a_{12}^{(0)}x_1 & 0 & 0 & 0 & 0 \end{pmatrix}, \tag{12.9}$$

$$\nabla_x L_G^2 h(x) = \begin{pmatrix} T_{3,1} & \begin{pmatrix} a_2^{(1)} + a_{12}^{(1)}x_1 + a_{25}^{(1)}x_5 \\ +2a_{122}^{(1)}x_1x_2 \end{pmatrix} & a_{13}^{(1)}x_1 & 0 & a_5^{(1)} + a_{25}^{(1)}x_2 & a_6^{(1)} \end{pmatrix} \tag{12.10}$$

where

$$T_{3,1} = \left(a_1^{(1)} + a_{12}^{(1)}x_2 + a_{13}^{(1)}x_3 + a_{122}^{(1)}x_2^2 \right),$$

$$\nabla_x L_G^3 h(x) = \begin{pmatrix} T_{4,1} & T_{4,2} & \begin{pmatrix} a_3^{(2)} + a_{13}^{(2)}x_1 \\ +a_{23}^{(2)}x_2 + a_{35}^{(2)}x_5 \\ +a_{123}^{(2)}x_1x_3 \end{pmatrix} & a_{14}^{(2)}x_1 & \begin{pmatrix} a_5^{(2)} + a_{25}^{(2)}x_2 \\ +a_{35}^{(2)}x_3 + a_{225}^{(2)}x_2^2 \end{pmatrix} & a_6^{(2)} + a_{26}^{(2)}x_2 \end{pmatrix}, \tag{12.11}$$

where

$$T_{4,1} = \left(a_1^{(2)} + a_{12}^{(2)}x_2 + a_{13}^{(2)}x_3 + a_{14}^{(2)}x_4 + a_{122}^{(2)}x_2^2 + a_{123}^{(2)}x_2x_3 + a_{1222}^{(2)}x_2^3 \right),$$

$$T_{4,2} = \begin{pmatrix} a_2^{(2)} + a_{12}^{(2)}x_1 + 2a_{22}^{(2)}x_2 + a_{23}^{(2)}x_3 + a_{25}^{(2)}x_5 + a_{26}^{(2)}x_6 + 2a_{122}^{(2)}x_1x_2 + a_{123}^{(2)}x_1x_3 \\ +2a_{225}^{(2)}x_2x_5 + 3a_{1222}^{(2)}x_1x_2^2 \end{pmatrix}$$

$$\nabla_x L_G^4 h(x) \begin{pmatrix} T_{5,1} & T_{5,2} & T_{5,3} & T_{5,4} & \begin{pmatrix} a_5^{(3)} + a_{25}^{(3)}x_2 \\ +a_{35}^{(3)}x_3 + a_{45}^{(3)}x_4 \\ +a_{225}^{(3)}x_2^2 + a_{235}^{(3)}x_2x_3 \\ +a_{2225}^{(3)}x_2^3 \end{pmatrix} & \begin{pmatrix} a_6^{(3)} + a_{26}^{(3)}x_2 \\ +a_{36}^{(3)}x_3 + a_{226}^{(3)}x_2^2 \end{pmatrix} \end{pmatrix}, \tag{12.12}$$

where

$$T_{5,1} = \begin{pmatrix} a_1^{(3)} + a_{12}^{(3)} x_2 + a_{13}^{(3)} x_3 + a_{14}^{(3)} x_4 + a_{122}^{(3)} x_2^2 + a_{123}^{(3)} x_2 x_3 + a_{124}^{(3)} x_2 x_4 + a_{133}^{(3)} x_3^2 \\ + a_{1222}^{(3)} x_2^3 + a_{1223}^{(3)} x_2^2 x_3 + a_{12222}^{(3)} x_2^4 \end{pmatrix},$$

$$T_{5,2} = \begin{pmatrix} a_2^{(3)} + a_{12}^{(3)} x_1 + 2a_{22}^{(3)} x_2 + a_{23}^{(3)} x_3 + a_{24}^{(3)} x_4 + a_{25}^{(3)} x_5 + a_{26}^{(3)} x_6 + 2a_{122}^{(3)} x_1 x_2 \\ + a_{123}^{(3)} x_1 x_3 + a_{124}^{(3)} x_1 x_4 + 3a_{222}^{(3)} x_2^2 + 2a_{225}^{(3)} x_2 x_5 + 2a_{226}^{(3)} x_2 x_6 + a_{235}^{(3)} x_3 x_5 \\ + 3a_{1222}^{(3)} x_1 x_2^2 + 2a_{1223}^{(3)} x_1 x_2 x_3 + 3a_{2225}^{(3)} x_2^2 x_5 + 4a_{12222}^{(3)} x_1 x_2^3 \end{pmatrix},$$

$$T_{5,3} = \begin{pmatrix} a_3^{(3)} + a_{13}^{(3)} x_1 + a_{23}^{(3)} x_2 + 2a_{33}^{(3)} x_3 + a_{35}^{(3)} x_5 + a_{36}^{(3)} x_6 + a_{123}^{(3)} x_1 x_2 + 2a_{133}^{(3)} x_1 x_3 \\ + a_{235}^{(3)} x_2 x_5 + a_{1223}^{(3)} x_1 x_2^2 \end{pmatrix},$$

$$T_{5,4} = \left(a_4^{(3)} + a_{14}^{(3)} x_1 + a_{24}^{(3)} x_2 + a_{45}^{(3)} x_5 + a_{124}^{(3)} x_1 x_2 \right).$$

and

$$\nabla_x L_G^5 h(x) = \begin{pmatrix} & & & & \begin{pmatrix} a_5^{(4)} + a_{25}^{(4)} x_2 \\ + a_{35}^{(4)} x_3 + a_{45}^{(4)} x_4 \\ + a_{225}^{(4)} x_2^2 + a_{235}^{(4)} x_2 x_3 \\ + a_{245}^{(4)} x_2 x_4 + a_{335}^{(4)} x_3^2 \\ + a_{2225}^{(4)} x_2^3 + a_{2235}^{(4)} x_2^2 x_3 \\ + a_{22225}^{(4)} x_2^4 \end{pmatrix} & \begin{pmatrix} a_6^{(4)} + a_{26}^{(4)} x_2 \\ + a_{36}^{(4)} x_3 + a_{46}^{(4)} x_4 \\ + a_{226}^{(4)} x_2^2 + a_{236}^{(4)} x_2 x_3 \\ + a_{2226}^{(4)} x_2^3 \end{pmatrix} \\ T_{6,1} & T_{6,2} & T_{6,3} & T_{6,4} & & \end{pmatrix}, \quad (12.13)$$

where

$$T_{6,1} = \begin{pmatrix} a_1^{(4)} + a_{12}^{(4)} x_2 + a_{13}^{(4)} x_3 + a_{14}^{(4)} x_4 + a_{122}^{(4)} x_2^2 + a_{123}^{(4)} x_2 x_3 + a_{124}^{(4)} x_2 x_4 + a_{133}^{(4)} x_3^2 + a_{134}^{(4)} x_3 x_4 \\ + a_{1222}^{(4)} x_2^3 + a_{1223}^{(4)} x_2^2 x_3 + a_{1224}^{(4)} x_2^2 x_4 + a_{1233}^{(4)} x_2 x_3^2 + a_{12222}^{(4)} x_2^4 + a_{12223}^{(4)} x_2^3 x_3 + a_{122222}^{(4)} x_2^5 \end{pmatrix},$$

$$T_{6,2} = \begin{pmatrix} a_2^{(4)} + a_{12}^{(4)} x_1 + 2a_{22}^{(4)} x_2 + a_{23}^{(4)} x_3 + a_{24}^{(4)} x_4 + a_{25}^{(4)} x_5 + a_{26}^{(4)} x_6 + 2a_{122}^{(4)} x_1 x_2 + a_{123}^{(4)} x_1 x_3 + a_{124}^{(4)} x_1 x_4 \\ + 3a_{222}^{(4)} x_2^2 + 2a_{223}^{(4)} x_2 x_3 + 2a_{225}^{(4)} x_2 x_5 + 2a_{226}^{(4)} x_2 x_6 + a_{235}^{(4)} x_3 x_5 + a_{236}^{(4)} x_3 x_6 + a_{245}^{(4)} x_4 x_5 \\ + 3a_{1222}^{(4)} x_1 x_2^2 + 2a_{1223}^{(4)} x_1 x_2 x_3 + 2a_{1224}^{(4)} x_1 x_2 x_4 + a_{1233}^{(4)} x_1 x_3^2 + 4a_{2222}^{(4)} x_2^3 + 3a_{2225}^{(4)} x_2^2 x_5 + 3a_{2226}^{(4)} x_2^2 x_6 \\ + 2a_{2235}^{(4)} x_2 x_3 x_5 + 4a_{12222}^{(4)} x_1 x_2^3 + 3a_{12223}^{(4)} x_1 x_2^2 x_3 + 4a_{22225}^{(4)} x_2^3 x_5 + 5a_{122222}^{(4)} x_1 x_2^4 \end{pmatrix},$$

$$T_{6,3} = \begin{pmatrix} a_3^{(4)} + a_{13}^{(4)} x_1 + a_{23}^{(4)} x_2 + 2a_{33}^{(4)} x_3 + a_{34}^{(4)} x_4 + a_{35}^{(4)} x_5 + a_{36}^{(4)} x_6 + a_{123}^{(4)} x_1 x_2 \\ + 2a_{133}^{(4)} x_1 x_3 + a_{134}^{(4)} x_1 x_4 + a_{223}^{(4)} x_2^2 + a_{235}^{(4)} x_2 x_5 + a_{236}^{(4)} x_2 x_6 + 2a_{335}^{(4)} x_3 x_5 + a_{1223}^{(4)} x_1 x_2^2 + 2a_{1233}^{(4)} x_1 x_2 x_3 \\ + a_{2235}^{(4)} x_2^2 x_5 + a_{12223}^{(4)} x_1 x_2^3 \end{pmatrix},$$

$$T_{6,4} = \left(a_4^{(4)} + a_{14}^{(4)} x_1 + a_{24}^{(4)} x_2 + a_{34}^{(4)} x_3 + a_{45}^{(4)} x_5 + a_{46}^{(4)} x_6 + a_{124}^{(4)} x_1 x_2 + a_{134}^{(4)} x_1 x_3 + a_{245}^{(4)} x_2 x_5 + a_{1224}^{(4)} x_1 x_2^2 \right).$$

It can then be verified that the matrix Ω is almost everywhere full rank.